Tampere University

ALESSIO D'AQUINO

Denitrification Under Salinity Stress in Biofilm Reactors

Tampere University Dissertations 1349

Tampere University Dissertations 1349

ALESSIO D'AQUINO

Denitrification Under Salinity Stress in Biofilm Reactors

Tampere University

Doctoral Programme in Engineering and Natural Sciences

COTUTELLE

UNIVERSITÀ DI TRENTO

PhD Course in Civil, Environmental and Mechanical Engineering

ACADEMIC DISSERTATION
To be presented, with the permission of
the Faculty of Engineering and Natural Sciences
of Tampere University,
and the Department of Civil, Environmental and Mechanical Engineering
of the University of Trento
for public discussion in Pieni Sali 1 auditorium
of the Festia Building, Korkeakoulunkatu 8, 33014, Tampere,
on 14th of November 2025, at 12 o'clock.

ACADEMIC DISSERTATION
Tampere University, Faculty of Engineering and Natural Sciences, Finland
University of Trento, Department of Civil, Environmental and Mechanical Engineering, Italy

Responsible supervisor and Custos	Docent Marja R.T. Palmroth Tampere University, Finland	
Supervisors	Professor Gianni Andreottola University of Trento, Italy	Professor Emeritus Jaakko A. Puhakka Tampere University, Finland
	University lecturer Hannele Auvinen Tampere University, Finland	
Pre-examiners	Assistant Professor Anna Mikola Aalto University, Finland	Associate Professor Stefano Papirio University of Naples Federico II, Italy
Opponents	Assistant Professor Anna Mikola Aalto University, Finland	Senior Research Fellow Elisangela Heiderscheidt University of Oulu, Finland
	Associate Professor Stefano Papirio University of Naples Federico II, Italy	

The originality of this thesis has been checked using the Turnitin Originality service.

Cover design: Roihu Inc.

ISBN 978-952-03-4179-4 (print)
ISBN 978-952-03-4180-0 (pdf)
ISSN 2489-9860 (print)
ISSN 2490-0028 (pdf)
http://urn.fi/URN:ISBN:978-952-03-4180-0

Carbon dioxide emissions from printing Tampere University dissertations have been compensated.

PunaMusta Oy – Yliopistopaino
Joensuu 2025

Life is life

ACKNOWLEDGMENTS

The origins of this journey date back to the first Covid-19 lockdown, with an e-mail to Prof. Jaakko Puhakka asking for a possible PhD research topic, after my master thesis experience at Tampere University. Few weeks later, another email was sent to Prof. Gianni Andreottola at the University of Trento, who was eager to join the project. I am profoundly grateful to these two professors for giving me the chance to pursue this PhD, for what I have gained from their expertise and guidance, and for being always positively minded and having great ideas. Then, also Engineer Niko Kalinainen from Valmet Oy started collaborating with our team, adding practical relevance to the project. I truly appreciate his commitment. With their invaluable help, all the pieces of the research plan were together and, finally, the realization of the project was made possible by Maa- ja vesitekniikan tuki funding (grant 4301).

The project started in August 2021 in the laboratories of the Bio and Circular Economy Unit in the Faculty of Engineering and Natural Sciences at Tampere University. Here, docent Marja Palmroth was the main supervisor of this work. I am deeply thankful to her for being always available to help, for her guidance and precious advice that enriched my doctoral experience, and for finding answers to my questions. Under her supervision, we secured fundings for the research material acquisition (Emil Aaltosen Säätiö, grant 220015KO), for the last year of the PhD (Maa- ja vesitekniikan tuki, grant 4758), and arranged an agreement to pursue a double PhD degree with the University of Trento supported by ECIU SMART-ER Co-tutelle programme (funded by the European Union's Horizon 2020 research and innovation pro-gramme under Grant Agreement #101016888). I would like to thank also university lecturer Hannele Auvinen for her contribution to this project as well as for giving me the chance to take part in teaching activities, which were a great learning experience.

During the two years in Tampere, we had good times with Roy, Markus, Ramita and Kant on adventurous trips, gourmet home dinners and analytical procedures, while with Stefano and Placido we had constructive weekend night dialogues "concerning the two

chief world systems". Thank to Réka, I learned how to survive in the lab, while Dr. Susanna Maanoja was of great help with her expertise in the analytical equipment.

In September 2023, the research and I moved to the laboratories of the DICAM at the University of Trento, my alma mater, supported also by Tutkijat Maailmalle Programme (Walter Ahlström Foundation, project 20220036). Here, Prof. Gianni Andreottola gave me a unique opportunity to work in his lab, to meet other researchers and to contemplate the mountains once again. In the office, we had important working days with Sajid the wise and Simone, always available to collaborate and to eat at Onto. My acknowledgments go also to the faculty staff of both universities, who always made sure everything was working smoothly.

Sincere thanks go to Prof. Marja Tiirola from the University of Jyväskylä, for her contribution and willingness to share her expertise in microbiology, which were invaluable to this project.

I also acknowledge the precious feedback provided on this thesis by the pre-examiners, Assistant Professor Anna Mikola from Aalto University (FIN) and Associate Professor Stefano Papirio from the University of Naples Federico II (ITA).

Finally, I owe a special thought to my family, for always being there, Kia and her family, for their support, and my friends, who made a long pilgrimage to the north to visit me.

This journey has been made of science, meetings, work, travelling, funding, bacteria, and, most importantly, people, all essential in accomplishing this thesis and in shaping the memories of this experience.

Helsinki, October 2025

Alessio D'Aquino

ABSTRACT

Denitrification represents a sustainable solution to remove nitrate from saline wastewaters generated by many industrial activities such as food processing, aquaculture, flue gas washing, etc. To improve the process' performance under salinity inhibition, biofilm reactors could represent an elegant strategy, but a systematic analysis focusing on the reactor system under salinity stress is needed for their optimisation. Moreover, since the electron donors available for the process may vary, the comparison between autotrophic and heterotrophic denitrification is relevant.

The aim of this study was to investigate the potential and inhibition tolerance of methanol-driven and thiosulphate-driven denitrifying bacteria from non-saline sources for the treatment of saline wastewaters. Also, their denitrification performance in fluidised bed biofilm reactors (FBBR) and in moving bed biofilm reactors (MBBR) were studied, optimizing the process via reactor and biofilm carrier selection, and a salinity inhibition modelling strategy was proposed for the biofilm.

Methanol-driven denitrification showed higher tolerance to inorganic ions than thiosulphate-driven, and for both, chloride had the most inhibitory role. This was also observed in the FBBRs, where the former showed higher removal rates (2.4 vs. 1.2 gN/L/d) at higher salinities (6.8 vs 5.6%), with stable denitrifying communities at increasing salinities, than the latter, dependent on *Thiobacillus denitrificans* activity. In the MBBR, where hollow- and porous- body carriers were compared for methanol-driven denitrification, a more exposed biofilm in the hollows showed higher removal rates at salinities <7.5%, while the less exposed biofilm in the pores had more stable nitrogen removal up to 9.5% salinity. With both carriers, an inhibition factor was implemented in an existing biofilm model and successfully reproduced denitrification kinetics under salinity stress. Eventually, the potential of denitrification for the pre-treatment of NO_x-SO_2 scrubber saline wastewater was confirmed, and pulp mill foul condensate as electron donor promoted nitrogen removal under salinity stress.

Overall, this study showed that methanol- and thiosulphate- driven denitrification have potential for the treatment of industrial saline wastewaters, whose salinity tolerance and nitrogen removal performance can be improved by selecting biofilm reactors and optimised with suitable biofilm carriers.

TIIVISTELMÄ

Biologinen denitrifikaatio on kestävä ratkaisu nitraatin poistamiseen teollisuuden suolapitoisista jätevesistä, jotka ovat peräisin esimerkiksi elintarvikejalostuksesta, vesiviljelystä ja savukaasupesureista. Biofilmireaktorit ovat mahdollinen vaihtoehto prosessin suorituskyvyn ja suolojen sietokyvyn parantamiseksi, mutta biofilmireaktorien optimointi suolapitoisille jätevesille vaatii systemaattista tutkimusta. Lisäksi jätevedet voivat sisältää orgaanisia ja/tai epäorgaanisia elektronien luovuttajia, jotka mahdollistavat autotrofisen ja/tai heterotrofisen denitrifikaation.

Tutkimuksen tavoitteena oli tutkia metanoli- ja tiosulfaattipohjaisen denitrifikaation potentiaalia ja inhibition sietokykyä suolapitoisten jätevesien käsittelyssä, ilman mikrobien aiempaa altistusta suolaisille olosuhteille. Lisäksi typenpoiston suorituskykyä leijupetibiofilmireaktoreissa (Fluidised Bed Biofilm Reactor, FBBR) ja kantoainereaktoreissa (Moving Bed Biofilm Reactor, MBBR) tutkittiin. Prosesseja optimoitiin reaktorityypin ja biofilmin kantoaineen valinnan avulla. Lisäksi mallinnettiin biofilmille suolainhibitiokinetiikat kantoainereaktoreissa.

Metanolilla hapettamiseen perustuva denitrifikaatio sieti paremmin epäorgaanisia ioneja kuin tiosulfaatille perustuva denitrifikaatio, ja kloridilla oli molemmille suurin inhiboiva rooli. Myös FBBR:ssä metanolipohjainen denitrifikaatio osoitti korkeampia poistonopeuksia kuin tiosulfaattipohjainen (2.4 vs. 1.2 gN/l/d) korkeammilla suolapitoisuuksilla (6.8% vs. 5.6%). Metanoliin perustuvat denitrifioivat mikrobiyhteisöt olivat vakaampia kuin tiosulfaattiin perustuvat.

Kahden eri kantoaineella kasvavan biofilmin metanolin syöttöön perustuvaa denitrifikaatiota verrattiin MBBR:ssä ja altistuneempi biofilmi kantoaineen onteloissa osoitti korkeampia poistonopeuksia suolapitoisuuksilla <7.5%, kun taas suojatumpi biofilmi kantoaineen huokosissa saavutti vakaan typenpoiston jopa 9.5%:n suolapitoisuudella. Olemassa olevaa biofilmimallia täydennettiin inhibitiokertoimella, ja stabiilin metanolia käyttävän mikrobiyhteisön denitrifikaatiokinetiikka mallinnettiin onnistuneesti. Denitrifikaation toimivuus NO_x-SO_2-pesurijätevesille osoitettiin käyttäen useita orgaanisia yhdisteitä sisältävää sellutehtaan lauhdevettä elektronien lähteenä.

Metanoli- ja tiosulfaattipohjaisella denitrifikaatiolla on potentiaalia teollisuuden suolapitoisten jätevesien käsittelyyn. Inhibitiosietokykyä ja typenpoistokykyä voidaan parantaa valitsemalla biofilmireaktoreita ja sopivia biofilmin kantajia

CONTENTS

List of Figures

List of Tables

ABBREVIATIONS

AD	Autotrophic Denitrification
ATS and AVS	Attached Total Solids and Attached Volatile Solids
CFPP	Coal Fired Power Plant
COD	Chemical Oxygen Demand
DNRA	Dissimilatory nitrate reduction to ammonium
DOC	Dissolved Organic Carbon
EPS	Extracellular Polymeric Substance
FBBR	Fluidised Bed Biofilm Reactor
FGD	Flue Gas Desulphurisation
GAC	Granular Activated Carbon
HD	Heterotrophic Denitrification
HRT	Hydraulic Retention Time
K_I or IC_{50}	Half Inhibition Constant
K_{NO2}	Nitrite Half Saturation Constant
L	Biofilm Thickness
MD	Mixotrophic Denitrification
MBBR	Moving Bed Biofilm Reactor
NO_3-RR	Nitrate Removal Rate (volumetric)
NRE	Nitrogen Removal Efficiency
NSLR	Nitrogen Surface Loading Rate
NSRR	Nitrogen Surface Removal Rate
NUR	Nitrogen Uptake Rate
NVLR	Nitrogen Volumetric Loading Rate
NVRR	Nitrogen Volumetric Removal Rate
OP	Osmotic Pressure
PE	Polyethylene
PCoA	Principal Coordinate Analysis
PP	Polypropylene
PSA	Protected Surface Area
S-K	Stover-Kincannon (model)
SSA	Specific Surface Area
U_{max}	Maximum Nitrogen Removal Rate
VS and VSS	Volatile Solids and Volatile Suspended Solids
WWTP	Waste Water Treatment Plant
Y	Biomass Yield

LIST OF ORIGINAL PUBLICATIONS

This thesis is based on the following original publications which are referred to in the text as I-III. The publications are reproduced under the CC BY license.

Publication I D'Aquino, A., Kalinainen, N., Auvinen, H., Andreottola, G., Puhakka, J.A., Palmroth, M.R.T., 2023. Effects of inorganic ions on autotrophic denitrification by *Thiobacillus denitrificans* and on heterotrophic denitrification by an enrichment culture. Science of The Total Environment, 901, 165940.

Publication II D'Aquino, A., Maanoja, S.T., Auvinen, H., Tiirola, M., Andreottola, G., Puhakka, J.A., Palmroth, M.R.T., 2024. Methanol and thiosulphate from pulp mill waste streams support denitrification under salinity stress. Chemical Engineering Journal, 502, 158131.

Publication III D'Aquino, A., Tiirola M., Puhakka J.A., Palmroth M.R.T. and Andreottola G., 2025. Inhibition-level-based carrier selection and kinetic insights for optimised denitrification of saline wastewaters in MBBR. Journal of Environmental Management, 394, 127288.

AUTHOR'S CONTRIBUTION

Publication I	**AD**: Planned and performed the experiments and the analyses, elaborated the data and wrote the original draft, is the corresponding author. NK: participated in planning and editing of the manuscript, provided research material. HA, GA, JAP, MRTP: supervised and participated in planning the work, edited and reviewed the manuscript.
Publication II	**AD**: Planned and performed the experiments and most of the analyses, elaborated the data and wrote the original draft, is the corresponding author. STM: Performed GC-MS and part of IC analyses, participated in writing the manuscript. MT: Performed microbial analyses, participated in writing the manuscript. HA, GA, JAP, MRTP: supervised and participated in planning the work, edited and reviewed the manuscript.
Publication III	**AD**: Planned and performed the experiments and the analyses as well as the modelling, elaborated the data and wrote the original draft, is the corresponding author. MT: Performed microbial analyses, participated in editing and reviewing the manuscript. JA, MRTP, GA: supervised and participated in planning the work, edited and reviewed the manuscript.

1 INTRODUCTION

The global wastewater production for the year 2030 is estimated to reach 470 billion m^3, with an increasing trend towards year 2050, without considering streams that do not end up in the municipal sewage system (Qadir et al., 2020). One of the main pollutants found in the effluents is nitrogen (N), amounting to 17 billion kg per year (Qadir et al., 2020) and requiring removal prior their discharge, but only around 50% of the polluted global wastewater is treated (Jones et al., 2021). The high percentage of untreated wastewaters discharged to the environment represents a worldwide water pollution issue that necessitates urgent intervention.

1.1 Challenges in the biological treatment of saline wastewaters

Among the countless typologies of wastewaters, saline effluents represent around 5% of the yearly treated wastewaters (Lefebvre et al., 2007). These are generated by many industrial activities (desalination plants, textile industries, flue gas washing systems, food industry, aquaculture industry, etc.), with salinities up to 150 g/L (15% m/v) (Panagopoulos, 2022). Inorganic ions (as Cl^-, Na^+, SO_4^{2-}, K^+ up to several tens of g/L), nitrogen (as NO_3^-/NO_2^- and NH_4^+), organic recalcitrant compounds and heavy metals are commonly found in saline wastewaters, which can cause eutrophication, fluctuations in water bodies' salinity, have detrimental effects on aquatic ecosystem and soils if released untreated (S. Chen et al., 2024; Z. Huang et al., 2024; Panagopoulos, 2022; Song et al., 2023).

Currently, physical-chemical methods are commonly used to treat saline wastewaters. Membrane filtration, evaporation and crystallisation methods are employed in many sectors to recover valuable salts and water, but are accompanied by high energy and management costs (Z. Huang et al., 2024; Lefebvre and Moletta, 2006; Panagopoulos, 2022; Song et al., 2023). Pre-treatments assume a key role in making the abovementioned methods more effective and less costly, by removing organics and unwanted ions that negatively affect the treatment techniques (Z.

Huang et al., 2024; Song et al., 2023). For example, ion exchange is used to remove anions, but is characterised by secondary waste production and its resins require periodical regeneration (Lefebvre and Moletta, 2006; Park and Yoo, 2009).

Biological treatments can represent a sustainable and economically feasible solution as pretreatment for saline wastewaters (He et al., 2017; Lefebvre and Moletta, 2006), like denitrification for the removal of NO_3^-/NO_2^- (S. Chen et al., 2024). They can reduce energy requirements and fouling in the downstream physical-chemical techniques, and have usually low capital and maintenance costs (Z. Huang et al., 2024). However, the microorganisms involved in the biological treatments are negatively affected by the saline conditions in the effluents, which cause their inhibition and reduced effectiveness of the process. Moreover, often industrial waste streams lack suitable electron donors needed for the microorganisms' catabolism, such as for nitrate reduction, requiring costly chemical addition (De Lucas et al., 2005; Park and Yoo, 2009).

To improve the bioprocess tolerance to salinity, some effective techniques have been engineered, such as the use of salt-tolerant bacteria, adaptation of the microbial communities to saline conditions and the addition of compatible solutes (S. Chen et al., 2024; Z. Huang et al., 2024). However, often these strategies require long startup times or costly chemical additions on large scale plants (S. Chen et al., 2024; Song et al., 2023; Vyrides and Stuckey, 2017). An important approach to increase the process' salinity tolerance is the bioreactor initial design. Since biofilm structures protect the microorganisms from external stress and inhibition (Parrilli et al., 2022), biofilm reactors, where a carrier retains the microorganisms as biofilm, represent an optimal choice, considering their additional benefits including high volumetric rates and low sludge production (Di Capua et al., 2015; Huang et al., 2019; Z. Huang et al., 2024). Then, to enhance both the cost-effectiveness and sustainability of the biological treatment, chemical compounds found in other waste streams could serve as supplement for the microorganisms. Thus, the optimal condition from an operational point of view would consist in a biofilm reactor inoculated with easily available microorganisms characterised by fast startup times and resilience to salinity changes, while adding an almost costless chemical supplement.

In view of this, the biological removal of nitrate in biofilm technologies represents a solution of interest for the pre-treatment of saline wastewaters. To date, successful denitrification under salinity stress is widely reported, but the tolerated salinity range

observed for activated sludge process, commonly applied in wastewater treatment, is usually between 2 and 5% (He et al., 2017; Lefebvre and Moletta, 2006), while industrial wastewaters can easily exceed these values. In addition, many studies have focused on NaCl salinity, as also noted by Macêdo et al. (2019), but industrial wastewaters can contain different Na^+/Cl^- ratios as well as K^+ and SO_4^{2-} ions (Panagopoulos, 2022) that may contribute to the inhibition. Different typologies of biofilm reactors have been used in denitrification studies but a systematic analysis reviewing as well as experimentally comparing the reactor designs and their performances under salinity stress is missing. Considering the potential of biofilm-based systems in enhancing the salinity tolerance of the process, such analysis is relevant for the optimisation of denitrification of saline wastewaters, in terms of reactor typology and biofilm carrier choice, as well as of modelling of the salt inhibition on the biofilm. Moreover, based on the most easily available electron donor, a specific type of metabolism for nitrate reduction (heterotrophic or autotrophic) may be most suitable for the treatment. However, a comparative analysis between heterotrophic and autotrophic denitrification tolerances and performances under salinity stress is missing.

Addressing these research gaps could be useful for implementing denitrification in biofilm reactors for the pre-treatment of saline wastewater from wet scrubbers removing simultaneously NO_x and SO_2 from flue gases in pulp mills. The use of this flue gas treatment technology is advantageous if compared to single-pollutant purification methods in series, in terms of simpler operating conditions, lower operation and capital costs, heat recovery, as well as smaller volume-area (Chen et al., 2021; Johansson et al., 2021b; J. Zhao et al., 2021). On the other hand, one of the main drawbacks is the generation of a complex-matrix saline wastewater (Córdoba, 2015; J. Zhao et al., 2021; M. Zhao et al., 2021), which contains dissolved NO_x^- that require removal. However, the common wastewater treatment processes in pulp mills are not optimised for denitrification (Ashrafi et al., 2015). Thus, the potential of denitrification in treating such wastewater must be explored, for example by supplementing electron donors easily available in the mill, to achieve an air-water integrated NO_x emission control technology.

1.2 Research goals and structure of the thesis

The aim of this thesis was to develop heterotrophic and autotrophic denitrification in biofilm reactors for the treatment of saline industrial wastewaters. A systematic analysis including salinity toxicity studies, evaluation of biofilm reactors performance under salinity stress, salinity inhibition modelling in biofilms and studies on the potential applicability of denitrification to NO_x-SO_2 scrubber wastewater was conducted. The inhibition caused by the wastewaters' multi-ionic salinity stress was investigated and compared for both heterotrophs and autotrophs. Their nitrogen removal capacity in biofilm systems were explored and the denitrification process optimised via reactor, biofilm carrier as well as electron donor selection, and a strategy to model the inhibition effect on denitrification kinetic in biofilms was proposed. Specifically, this study aimed at investigating the following:

- **Tolerance of denitrification to specific inorganic ions (Publication I)**. Inhibition by salinity was studied in a series of batch tests in terms of inorganic ions commonly found in industrial wastewaters (Cl^-, Na^+, SO_4^{2-}, K^+), simulated with different salts. The purpose was to reveal the most inhibitory ones in wastewaters with different ionic compositions than NaCl, such as those produced by NO_x-SO_2 wet scrubbers for flue gas cleaning.

- **Performance of methanol-driven and thiosulphate-driven denitrification under salinity stress (Publication I, II, III)**. Methanol and thiosulphate were selected as electron donors, given their availability in pulp mills, for heterotrophic and autotrophic denitrifying cultures with non-saline history. First, batch tests with different inorganic ions pairs at increasing concentrations revealed the salinity tolerance of the microorganisms. Then, heterotrophic and autotrophic denitrification were compared in terms of nitrogen removal performance and biofilm dynamics in continuous flow lab-scale biofilm reactors under increasing multi-ionic salinity. The aim was to investigate the potential enhancement of salinity tolerance in biofilm systems.

- **Analyse and compare the denitrification performance in two high-rate treatment biofilm reactors, with focus on the role of biofilm carriers, and reveal their optimisation (Publication II, III)**. Lab-scale fluidised bed biofilm reactor (FBBR) and moving bed biofilm reactor (MBBR), with their respective carriers, were compared for heterotrophic denitrification at

increasing salinities and various HRTs, to understand their potential in removing nitrogen from saline wastewaters. The MBBR denitrification process was further studied by comparing two different types (hollow- and porous- body) of biofilm carriers to pursue its optimisation via carrier selection at different salinity concentrations.

- **Modelling of denitrification salinity inhibition kinetics in biofilm with a hollow- and a porous-body MBBR carrier.** The apparent effect of salinity inhibition on the MBBR's denitrification rate was implemented in a complex existing biofilm model (Sumo©22), introducing a simplified modelling approach for the prediction of denitrification kinetics under salinity stress in MBBRs.

- **Potential of denitrification for the pre-treatment of NO_x-SO_2 scrubber wastewater in pulp mills (Publication I, II, III)**. Real scrubber wastewater denitrification potential was studied with both suspended flocs and biofilm in batch and semi-batch tests, by using methanol and thiosulphate as electron donors. Moreover, foul condensate, a waste stream rich in organics produced in pulp mills, was tested as an alternative source of electrons and compared with pure methanol for heterotrophic denitrification under salinity stress in the lab-scale FBBR.

The state-of-the-art of denitrification and biofilm reactors under salinity stress is presented in Chapter 2, together with an overview of the challenges for the denitrification of flue gas scrubber wastewaters. Chapter 3 summarises the experiments and analyses performed to achieve the above-mentioned research goals, while the results obtained are presented and discussed in Chapter 4. Eventually, the conclusions of this work are drawn in Chapter 5.

2 THEORETICAL BACKGROUND

In this chapter, first, heterotrophic and autotrophic denitrification are described from the point of view of the electron donor, followed by the effects of salinity inhibition on denitrification process. Then, the main strategies to improve the process' salinity tolerance are briefly introduced, with the focus on biofilm reactors. The studies on denitrifying biofilm reactors are reviewed, outlining the key factors and research gaps for the optimisation of the reactor technology, highlighting the important aspects of carrier selection and the challenges in mathematical modelling of biofilm systems. Eventually, the challenges of saline scrubber wastewater denitrification are introduced and the case of NO_x-SO_2 scrubber wastewater in pulp mills illustrated.

2.1 Denitrification under salinity stress

Denitrification is a known process for nitrate removal in wastewater treatment in which bacteria reduce dissolved oxidised forms of nitrogen (usually NO_3^-) to gaseous N_2. The reduction reaction is accomplished through four reductive steps each catalysed by specific enzymes (Zumft, 1997), as shown in Figure 1. When the reduction is not complete, due for example to environmental factors (pH, oxygen, electron donor, etc.) disturbing the reaction, the intermediary products (e.g., NO_2^- or N_2O) accumulate. Moreover, only some denitrifying microorganisms are capable of complete denitrification of nitrate ("true denitrifiers"), while others are classified as "nitrate respirators" or "incomplete denitrifiers", when they can only reduce nitrate to nitrite, or only nitrogen oxides to other nitrogen oxides, and the "exclusive nitrite reducers" (Lu et al., 2014; Philips et al., 2002). Furthermore, denitrifying bacteria usually need anoxic environments, with the exception of some capable of denitrification in aerobic conditions (for a review Hao et al. (2022)), where they use nitrate for respiration and an electron donor for nitrate reduction. Based on the electron donor, denitrification can be sorted into heterotrophic and autotrophic.

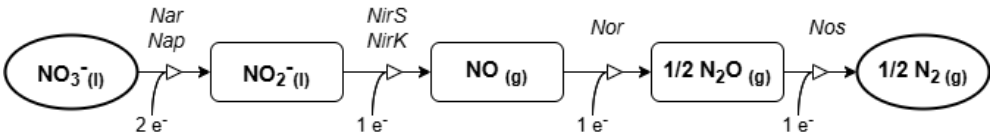

Figure 1. Denitrification reductive steps from nitrate to nitrogen gas and the enzymes involved. Nar and Nap: nitrate reductases, NirS and NirK: nitrite reductases, Nor: nitric oxide reductase, Nos: nitrous oxide reductase. Modified from Di Capua et al. (2019).

2.1.1 Heterotrophic and autotrophic denitrification

Heterotrophic denitrification is carried out by chemoorganoheterotrophic bacteria, like genera *Hyphomicrobium*, *Paracoccus*, *Pseudomonas, Comamonas*, *Thauera*, *Azoarcus* spp., commonly found in denitrifying reactors (Lu et al., 2014). These bacteria use organic compounds (methanol, ethanol, glucose, organic acids etc.) both as electron donor for nitrate respiration and carbon source for growth. In addition to N_2, other denitrification reaction products are CO_2 and OH^-, which result in pH and alkalinity increase, as showed in the methanol driven denitrification reaction (eq.1) (Foglar and Briški, 2003):

$$1.08\ CH_3OH + NO_3^- + H^+ \rightarrow 0.06\ C_5H_7O_2N + 0.48\ N_2 + 0.76\ CO_2 + 2.44\ H_2O \qquad \text{(eq.1)}$$

Industrial wastewater lacking suitable electron donors usually require the addition of organics for heterotrophic denitrification process, resulting in added costs and possible secondary organic pollution (Pang and Wang, 2021; Park and Yoo, 2009). Methanol is one of the most used soluble organic compounds due to is lower cost and sludge production than other organics (Lu et al., 2014), despite it requiring careful handling due to its toxicity to the environment and high flammability. Moreover, only a limited number of heterotrophic bacterial genera (e.g., *Paracoccus*, *Hyphomicrobium*, *Methylophilus*, *Methyloversatilis* spp.) is known of being capable of methanol oxidation (methylotrophs) (Lu et al., 2014), which would require the selection of specific microorganisms especially for industrial wastewater treatment. For denitrification of saline wastewaters, the use of complex electron donor mixtures found in other waste streams, like sludge fermentation liquid (Zhang et al., 2020), has shown promising results, by improving the response of the process to salinity changes, with beneficial effects on the diversity of the denitrifying community. The use of organic waste streams, such as food and agro-industry wastewaters (De Lucas et al., 2005; Fernández-Nava et al., 2010), provided they are easily accessible, can

promote the circularity of the process and reduce the chemical addition costs, but their beneficial effects on denitrification under salinity stress need further research.

Autotrophic denitrification is performed by chemolithoautotrophic bacteria, with *Thiobacillus denitrificans*, *Sulfurimonas* spp., *Thiomicrospira CVO* among the most known (Di Capua et al., 2019). These bacteria can use inorganic electron donors like reduced sulphur compounds, hydrogen and ferrous iron to reduce nitrate and carbon dioxide for biomass growth. The products of the reaction depend on the electron donor, as shown for the thiosulphate driven denitrification reaction (eq.2) (Mora et al., 2014):

$$S_2O_3^{2-} + 1.16NO_3^- + 0.03CO_2 + 0.52HCO_3^- + 0.12H_2O + 0.11NH_4^+ \rightarrow 0.11C_5H_7O_2N + 0.58N_2 + 0.43H^+ + 2SO_4^{2-} \quad \text{(eq.2)}$$

As a result, the pH decreases, contrarily to heterotrophic denitrification, and sulphate is one of the main products of the reaction, which is not toxic but is regulated by water quality standards. Usually, autotrophic bacteria have lower growth rates than heterotrophic, resulting, on one hand, in lower denitrification rates, but on the other, in lower excess sludge production and related handling costs (Pang and Wang, 2021). Moreover, inorganic electron donors, including H_2 and depending on its production process (Acar and Dincer, 2019), are usually cheaper than organic ones (Di Capua et al., 2019), leading to lower chemical addition costs when suitable electron donors are lacking from the industrial wastewater. S^0 is the most used electron donor, being easy to handle and inexpensive, but has usually low denitrification rates due to its low solubility. On the other hand, soluble $S_2O_3^{2-}$ guarantees the highest denitrification rates among S-compounds, but results in high sulphate production and its residuals in the effluent are unwanted, due to its potential toxicity under certain environmental conditions (Di Capua et al., 2019; Miranda-Trevino et al., 2013). Due to the limited number of suitable electron donors for autotrophic denitrification, their mixtures in industrial waste streams are difficult to find, contrarily to heterotrophic denitrification, and usually contain one to two electron donors (such as thiosulphate or pyrite from mining activities, thiosulphate or sulphide from petrochemical industries, elemental sulphur from gas biological treatment (Di Capua et al., 2019)).

To improve the autotrophic process performance, an organic electron source could be added. This results in the mixotrophic denitrification process, which consists in simultaneous heterotrophic and autotrophic denitrification, with some bacteria capable of using both electron donors (e.g., *Paracoccus denitrificans*), favouring a

more diverse community that could respond more readily to salinity changes. Moreover, mixotrophic denitrification could offer several advantages, namely higher nitrogen removal rates and lower SO_4^{2-} production than the only autotrophic denitrification, pH buffering, lower effluent organics, N_2O accumulation and excess sludge production than the sole heterotrophic process (Sahinkaya et al., 2011).

2.1.2 Effects of salinity on denitrification

Inhibition by salinity on microorganisms acts via osmotic stress (Bremer and Krämer, 2019) and ions' specific toxicity (Zhao, 2005). At macroscopic level, this results in the deterioration of the denitrification treatment process. The most important aspects are discussed in the following paragraphs.

Denitrification rate. Increasing salinity causes a gradual decrease in denitrification rate (Chen et al., 2022; Dinçer and Kargi, 1999; Glass and Silverstein, 1999; Koenig and Liu, 2004; Mariángel et al., 2008). In continuous flow processes, this results in the decrease in nitrogen removal efficiency. Such decline in the denitrification rate is a direct effect of the functional enzymes' inhibition by ions and of the osmotic stress, as well as of the protective response to salinity. For example, high concentrations of Na^+ adversely affect denitrification functional enzymes by substituting metal ions or binding to non-active sites of the enzymes, resulting in a non-competitive inhibition, which does not compete with the substrate for the active site but still reduces the catalysis of the reaction (S. Chen et al., 2024). Not only each inorganic ion species has a different toxicity level (B. Chen et al., 2024; Chen et al., 2022; Lin et al., 2021; Macêdo et al., 2019), but the presence of different inorganic ions at the same time can also result in added or antagonistic effect on microbial activity (Lin et al., 2021; Macêdo et al., 2019). Furthermore, when the osmotic pressure (OP) is excessive, the cells lose their turgor pressure by expelling the internal water and dehydrating, reducing their metabolic activity (e.g., enzyme production), and consequently the denitrification activity, and eventually leading to cell lysis (Bremer and Krämer (2019), S. Chen et al. (2024)). A common defence strategy used by microorganisms against high OP is the increased production of extracellular polymeric substances (EPS) to form a protective layer (Costa et al., 2018; Song et al., 2023). As EPS production is an energy demanding process (Costa et al., 2018), microbes allocate metabolic energy to it (Cortés-Lorenzo et al., 2012; He et al., 2017; Rillig et al., 2015), which can result in higher carbon demand (Wang et al., 2020), lower living cell synthesis

(Corsino et al., 2019) and eventually lower enzymatic activity (Cortés-Lorenzo et al., 2012) that leads to lower denitrification rates.

Nitrite accumulation. NO_2^- is an intermediate of denitrification reaction, whose accumulation is unwanted because of its toxicity to the environment and the same denitrifying bacteria (Philips et al., 2002). NO_2^- accumulation is often observed under non-saline conditions triggered by environmental factors (like temperature, pH, e-donor:N ratio and concentrations, dissolved oxygen) and different explanations for it have been proposed over time in the literature (Philips et al., 2002). NO_2^- is produced within the cell from NO_3^- reduction and transported out of the cell via special pores in the cell membrane, leading to accumulation of extracellular NO_2^- (Glass and Silverstein, 1998; Zumft, 1997). If the microbial community is unbalanced towards nitrate respirators, such extracellular NO_2^- is an end product and accumulates with little or no reduction to N_2 (Dhamole et al., 2007; Glass and Silverstein, 1998; Philips et al., 2002). If the community is capable of the nitrite reducing step, then the extracellular NO_2^- is eventually taken up by the bacterial cells and further reduced. However, NO_3^- is preferred as electron acceptor, while nitrite reductases can be repressed as long as NO_3^- is present and by environmental factors like oxygen, resulting in slower nitrite reduction rates than nitrate and temporary NO_2^- accumulation (Betlach and Tiedje, 1981; Cao et al., 2013; Dhamole et al., 2007; Di Capua et al., 2019; Glass and Silverstein, 1998; Lu et al., 2014).

Under saline conditions, NO_2^- accumulation is widely reported as an effect of salinity inhibition (Feng et al., 2023; Glass and Silverstein, 1999; Jiang et al., 2024; R. Li et al., 2024; Li et al., 2018, 2023; Miao et al., 2020; Yang et al., 1995; Zhai et al., 2020, 2018). Similarly to NO_2^- accumulation under non saline conditions, one of the underlaying mechanisms can be identified in the selection of nitrate respirators by salinity (Jiang et al., 2024; Li et al., 2018). Then, nitrite reductase activity has been reported of being more inhibited than nitrate reductase (Feng et al., 2023; Jiang et al., 2024; Li et al., 2023; Miao et al., 2020), at different intensities depending on the main enzymes involved (Li et al., 2023; Miao et al., 2015), explaining the NO_2^- accumulation. Some other reports (Chen et al., 2022; Mariángel et al., 2008; Zeng et al., 2020; Zhao et al., 2013) showed the opposite, with nitrate reduction step being more affected by salinity than nitrite reduction, despite nitrite temporarily accumulating. These contrasting observations might depend on the microbial community composition and history, but further investigations are needed especially to quantify NO_2^- accumulation under salinity stress.

Nitrous oxide accumulation. N_2O is another intermediate in denitrification reaction, whose accumulation and consequent release in atmosphere are unwanted due to it being a strong greenhouse gas. Its release, commonly observed in municipal WWTP (Kosonen et al., 2016), is due for example to the presence of oxygen (Kornaros and Lyberatos, 1998) or to low pH, low COD/N ratio as well as to the carbon source typology, as listed by Pan et al. (2012), that disturb the denitrification reaction steps. Salinity has shown to increase N_2O accumulation (B. Chen et al., 2024; Ma et al., 2023; Yang et al., 1995; Zhao et al., 2013). The reason of the increased accumulation is possibly linked to the higher sensitiveness to salinity of nitrous oxide reduction rather than nitrate or nitrite reduction steps (B. Chen et al., 2024; Zhao et al., 2013). Further research is required to describe quantitatively the correlation between salinity and nitrous oxide production and related inhibition kinetics.

Increased dissimilatory nitrate reduction to ammonium (DNRA). DNRA process is an alternative nitrate reduction pathway, that reduces nitrate to NH_4^+ instead of N_2, with NO_2^- as intermediate, performed by bacteria possessing multiple nitrite reductase enzymes (Philips et al., 2002). DNRA activity is usually favoured by limiting electron acceptor conditions, but salinity has been reported of increasing this process, resulting in NH_4^+ accumulation in the effluent (Ma et al., 2023; Zhai et al., 2020, 2018; Zhu et al., 2015). Such accumulation is usually unwanted in industrial wastewaters, especially if no ammonium removal technologies follow denitrification.

Community changes. Salinity inhibition leads to a selection of the most tolerant genera in the microbial community while the less tolerant are outcompeted, resulting in decreased diversity (S. Chen et al., 2024; Jiang et al., 2024; R. Li et al., 2024; Li et al., 2023; Miao et al., 2015; Osaka et al., 2008; Zhai et al., 2020). This often causes the decline of the denitrification process, in terms of decreased rate and efficiency, if the main denitrifying genera disappear. Overall, community changes can partially explain many of the abovementioned aspects of denitrification performance decline. For instance, the shift of the community towards incomplete denitrifiers could result in NO_2^- or N_2O accumulation (Jiang et al., 2024; Li et al., 2018).

In summary, the choice of the electron donor for heterotrophic and autotrophic denitrification processes can influence their nitrogen removal capacity and response to salinity. Similarly, salinity inhibition affects denitrification efficiency and stability, requiring engineered strategies to partially overcome these detrimental effects.

2.1.3 Strategies to enhance denitrification process' salinity tolerance

Engineered strategies, based on promoting the natural responses of microorganisms to salinity, have been studied to enhance the biological process under salinity stress. The most known methods and their main characteristics are reported in Table 1.

Table 1. Summary of the main strategies used to enhance the process' salinity tolerance.

Strategy	Main mechanism	Advantages	Disadvantages	References
Sludge "acclimation or domestication"	Gradual exposure of a common sludge to process salinity. Leads to selection of the salt-tolerant bacteria in the sludge.	Useful when only inoculum available has a non-saline history.	Unpredictability of times required. Limited tolerance to salinity (2- 5%) and to its fluctuations.	Vyrides and Stuckey (2017), S. Chen et al. (2024), Ji et al. (2021), Li et al. (2019), Zhang et al. (2020).
Start-up with salt-tolerant bacteria	Microorganisms with a saline history (e.g., from marine sediments or existing saline wastewater treatments) are selected to startup the process.	Provides higher tolerance than a culture with non-saline history. Valid choice when biomass is autochthonous to the wastewater or easily obtainable.	Process-specific microorganisms not always easily available.	Corsino et al. (2019), Mallick and Chakraborty (2020), Miao et al. (2020), Panswad and Anan (1999), Wang et al. (2020)
Bioaugmentation	Inoculation of halophilic bacteria that participate in substrate removal and produce and share protective biomolecules for other bacteria in the community.	Improved process performance	Biosecurity risks (e.g. aquaculture systems). Possible competition for substrate. Substantial amount of the inoculum and long times to settle in real scale reactors.	Li et al. (2019), W. Chen et al. (2024), Huang et al. (2024), Vyrides and Stuckey (2017), Xiang et al. (2023)
Compatible solutes addition	Compatible solutes (ectoine, glycine betaine etc.) are used by bacteria to balance OP and limit dehydration.	Improved salinity tolerance. Simple operation.	Selectivity of different microorganisms towards different solutes. Solute used as electron donor by heterotrophic activity. Secondary organic pollution. Amount of solute needed at real scale is costly.	Bremer and Krämer (2019), Cyplik et al. (2012), Huang et al. (2024), Li et al. (2024), Vyrides and Stuckey (2017)

The choice of the best strategy is strongly case specific, and needs to consider technical aspects (e.g., timescale, suitability, secondary pollution) as well as

economy and sustainability criteria. The combination of some of the strategies could balance costs and time and improve the removal performance of the biological process at the same times, but further studies, especially on real scale reactors, are still needed. In addition to the techniques reported in Table 1, the amendment of the process via reactor selection is an easily implementable strategy and thus, the optimisation of the reactor technology for the treatment of saline wastewaters is crucial.

2.2 Biofilm reactors optimisation for high denitrification performance under salinity inhibition

Biofilms are dynamic and complex ecosystems of microorganisms attached to a surface (Parrilli et al., 2022). In these systems, the EPS secreted by the cell, mainly consisting of polysaccharides, structural proteins, enzymes, nucleic acids and lipids (Costa et al., 2018), generates a matrix for microorganisms favouring the adhesion and cohesion of cells and the trapping of water and nutrients. Not only do biofilm systems create a protective environment from the external salinity, but they also facilitate microbial interactions (Costa et al., 2018; Parrilli et al., 2022) via signalling molecules (quorum sensing) that can coordinate the activity of cells in response to salinity (for a review Huang et al. (2024), Shrout and Nerenberg (2012)). This co-operation, important in saline conditions where the microbial diversity is limited, results, for instance, in synthesis and sharing of fundamental and protective biomolecules (e.g., vitamins or compatible solutes) among the microorganisms, or promotion of EPS production (B. Chen et al., 2024; García-Roldán et al., 2024; Li et al., 2023; Shrout and Nerenberg, 2012; Wang et al., 2024; Zhou et al., 2024). Therefore, biofilm reactors represent an optimal choice for the denitrification of saline wastewaters, creating a protective environment, retaining the microorganisms in the system and ensuring stable process performances (Z. Huang et al., 2024; Zhao et al., 2019).

2.2.1 Biofilm reactor designs used for denitrification under salinity stress

In general, biofilm reactors adopt different types of high surface materials, also called biofilm carriers, to facilitate the growth of biofilm. Biofilm reactors present some advantages if compared to conventional activated sludge processes, such as high

removal rates and low hydraulic retention times (HRT), i.e., lower volume requirements, high biomass retention and concentration, and low excess sludge production (Di Capua et al., 2015; Huang et al., 2019; Zhao et al., 2019). On the other hand, some of the disadvantages associated with biofilm reactors are prolonged start-up times for biofilm development, risk of limited mass transfer, as well as high operational costs to control the hydrodynamics for optimal conditions (Di Capua et al., 2015; Rittmann et al., 2018; Wu et al., 2021). Such aspects need careful attention during the selection of a biofilm technology, especially from an economic perspective.

Heterotrophic, autotrophic and mixotrophic denitrification (Table 2), have been studied in various type of biofilm reactors under salinity stress showing different performances in terms of nitrogen volumetric loading rate (NVLR) capacity and removal efficiency (NRE) at different salinity levels. The highest NVLR (13.2 gN/L/d) and lowest HRT (~0.7 h) were reached for heterotrophic denitrification with a FBBR (Vredenbregt et al., 1997), proving its high-rate treatment capacity and high (>90%) removal efficiency. Also, MBBRs enabled generally higher NVLR (1.4-3.5 gN/L/d) with NRE >70% for heterotrophic denitrification (Dupla et al., 2006; Labelle et al., 2005; Shelly et al., 2021), if compared to the majority of the other studies. For autotrophic denitrification under salinity stress, the most used reactors have been the S^0 packed bed and up flow columns. The highest NVLR reached was 1.2 gN/L/d with low HRTs (1-4 h), but NRE was around 20% (Y. Li et al., 2024). The studies using mixotrophic denitrification with S^0 as carrier and addition of organics showed improved NREs, if compared to the sole autotrophic denitrification, at NVLR up to 1.9 gN/L/d (Aminzadeh et al., 2010).

In general (Table 2), when the source of microorganisms was a municipal WWTP sludge, the best denitrification performances were obtained in the salinity range 1-3.5%. Contrarily, when the biomass had a saline history, NRE above 70% were obtained at salinities of 6-7% for heterotrophic denitrification, with high (24 h) HRT at low NVLR (0.02-0.15 gN/L/d) in sequencing batch biofilm reactors (Feng et al., 2023; Wang et al., 2020). For autotrophic and mixotrophic denitrification, the best denitrification performances were obtained when salinity ≤3.5% even with biomass with a saline history, showing the higher tolerance to salinity of heterotrophic denitrifying biofilms. Nevertheless, the highest salinities tested for denitrification have been reported for reactors without biofilm carriers. For example, in expanded granular sludge bed reactor studies, tested salinities reached 11.6 and 14.5%, with NREs>95%, high NVLRs but also high (22-24 h) HRTs (Liao et al., 2013; Miao et al.,

2015). The highest salinity tolerance (14.5%) (Liao et al., 2013) was obtained mainly with $NaNO_3$ and CH_3COONa, indicating that inhibition by chloride and sulphate was not present, while the study with the second highest salinity (11.6% NaCl) used biomass from a reactor treating highly toxic wastewater (Miao et al., 2015). Nonetheless, granular sludge has been shown of forming a protective environment for bacteria from salinity stress (Corsino et al., 2018), thus representing an interesting option for saline wastewater treatment but with long startup times for the granules formation that need improvements (Han et al., 2022). Also, in a study using a continuously stirred tank reactor with a biomass coming from a municipal WWTP (Osaka et al., 2008), a NRE of 99% was reached at salinity (NaCl) of 10%, with an HRT of 48 h and after a gradual salinity increase lasted for more than 200 days of operation.

Overall, the main difference between biofilm and floc/granular sludge reactor studies here reported can be found in the lower HRTs tested for biofilm reactors. Regardless of the reactor type, the inorganic ions forming salinity and the source of the microorganisms are crucial aspects in saline wastewater treatment that need to be considered for the process design. Further research is needed to investigate the best performing reactor designs and the carrier typology to optimise the process under salinity stress.

Table 2. Performance of biofilm reactors for denitrification under salinity stress in anoxic conditions. Nitrogen Volumetric Loading Rate (NVLR) is in gNO_x^--N/L/d, hydraulic retention time (HRT) in h, T in ºC. If not reported, operational parameters were estimated from the data available in the references. (p 1/2)

Reactor	Process	Biofilm carrier, filling	Salinity %	Biomass' source	NVLR	NRE (%)	Conditions (HRT, T, pH)	Reference
MBBR	HD with CH_3OH	spherical PE, 25%	2.8 (seawater)	Seawater	1.5	88 (NO_x^-)	>24, 19, NA	Labelle et al. (2005)
MBBR	HD with CH_3OH	spherical PE, 30%	2.8 (seawater)	Seawater	3.5	75 (NO_x^-)	1.6, 14, NA	Dupla et al. (2006)
MBBR	HD with phenol	PE hollow-body (Hel-X)	1.4 (RO concentrate)	*Acinetobacter* culture	1.4	98 (NO_3^-)	4, 32, neut.	Shelly et al. (2021)
FBBR	HD with CH_3COOH	Sand	3.8 (Cl^- in FGD wastewater)	WWTP sludge	13.2	>90 (NO_3^-)	~0.7, 30, neut.	Vredenbregt et al. (1997)
SBBR	HD with mustard tuber industry water	polyacrylonitrile disk and fibre threads, 60%	7 (NaCl)	Reactor treating saline wastewater	0.02	>90 (NO_3^-)	24, 30, 5.5	Wang et al. (2020)
SBBR	HD with CH_3OH	Biological rope, 35%	6 (Na_2SO_4, NaCl)	Saline enrichment from sludge	0.15	<80 (TN)	24, NA, NA	Feng et al. (2023)
UAFB	HD with PBS	PBS granules	2.5 (seasalt)	Intertidal zone	0.7	99 (NO_3^-)	2, room, NA	Zhu et al. (2015)
FBB-MR	HD with CH_3COONa	NA	3 (NaCl)	WWTP sludge	0.06	43 (NO_3^-)	12, room, neut.	An et al. (2024)
PBR	HD with PBS and bamboo powder	PBS and bamboo powder pellets, 60%	2.5 (seasalt)	NA	0.48	70 (NO_3^-)	4, room, NA	Qi et al. (2020)
CRB	HD with catechol	polyurethane foam cubes, 30%	2 (NaCl)	Reactor removing catechol	0.27	99 (NO_3^-)	10, room, neut.	Jafari et al. (2015)

Table 2. (p 2/2)

Reactor	Process	Biofilm carrier, filling	Salinity %	Biomass' source	NVLR	NRE (%)	Conditions (HRT, T, pH)	Reference
BES	HD with CH_3OH	plastic fibres	3.5 (NaCl)	WWTP sludge	0.06	55 (NO_3^-)	8, NA, neut.	Zhai et al. (2020)
UPC	MD with S^0 and CH_3OH	S^0	3.5 (NaCl)	WWTP sludge	1.9	99 (NO_3^-)	8*, room, neut.	Aminzadeh et al. (2010)
UPC	MD with CH_3COONa and S^{2-}	Sand	3 (seawater)	Seawater denitrifying reactor	0.07	99 (NO_2^-)	24, 17, 8	Li et al. (2021)
PBR	MD with S^0 and glucose	S^0 and $CaCO_3$	1.5 (NaCl)	WWTP sludge	0.18	96 (NO_3^-)	4, room, neut.	X. Huang et al. (2024)
PBR	AD with S^0	S^0	3 (NaCl)	WWTP sludge	0.6	~80 (NO_3^-)	1*, room, NA	Li et al. (2023)
PBR	AD with S^{2-}	Generic PE, 70%	3 (Na_2SO_4)	Intertidal sediments	0.02	>80 (NO_3^-)	24, 30, NA	Feng et al. (2024)
PBR	PAD with S^0	S^0	1.5 (NaCl)	Lab-scale reactor	1.2	20 (NO_3^-)	2*, room, NA	Y. Li et al. (2024)
UPC	AD with S^0	S^0	3.1 (seawater)	Marine sediments, mariculture tank and anaerobic WWTP sludge	1	55 (NO_3^-)	1, 20, NA	Wang et al. (2023)
UPC	AD with S^0	S^0	2.5 (NaCl)	WWTP sludge	0.18	34 (NO_3^-)	4, room, neut.	Fan et al. (2024)

HD: Heterotrophic Denitrification, AD: Autotrophic Denitrification, MD: Mixotrophic Denitrification, PE: Polyethylene, PBS: Polybutylene succinate, WWTP: Wastewater Treatment Plant, RO: reverse osmosis, FGD: Flue Gas Desulphurisation, MBBR: Moving Bed Biofilm Reactor, FBBR: Fluidised Bed Biofilm Reactor, SBBR: Sequencing Batch Biofilm Reactor, UAFB: Upflow Anaerobic Sludge Blanket, FBB-MR: Fixed Bed Biofilm Membrane Reactor, PBR: Packed Bed Reactor, CRB: Cycling rotating bed, BES: Bioelectrochemical Biofilm System, UPC: Upflow Packed Column. *refers to empty bed contact time, NA: not available.

2.2.2 Biofilm carrier selection for saline conditions

An important aspect of biofilm reactors is the selection of the biofilm carrier. Its material and surface properties (surface area, roughness, porosity, hydrophobicity, charge), as well as the filling fraction in the reactor affect the biofilm formation, growth and process performance (Morgan-Sagastume, 2018). To date, many materials are being used and studied as carriers, such as inert inorganic (granular activated carbon (GAC), sand, zeolite) or organic (polypropylene (PP), polyethylene (PE) etc.), reactive inorganic (S^0) and organic (vegetal wastes, polybutylene succinate) that act also as electron donor, as well as with chemically modified surfaces, with their related strengths and weaknesses in terms of microbial attachment, mechanical resistance and protected surface area (Zhao et al., 2019). Ideally, a biofilm carrier should have a large specific area for the biofilm attachment but at the same time limit clogging due to excessive biofilm growth, to guarantee an adequate biofilm-liquid interface and efficient mass transfer, as well as presenting resistance to abrasion, mechanical stress and biodegradation together with affordable costs (Morgan-Sagastume, 2018). Therefore, the active biofilm surface area and the biofilm thickness, both determined also by the carrier structure, play key roles for the process performance (Morgan-Sagastume, 2018; Zhao et al., 2019).

Under saline conditions, carriers favouring thick biofilms could improve the tolerance to salinity. Thick biofilms have shown higher tolerance to inhibition than thin biofilms (Piculell et al., 2016). In a thick biofilm, the inner layers are less exposed to inhibitors, making the biomass resilient to sudden changes in the external conditions (Piculell, 2016). On one hand, thick dense biofilms provide more protection and more biomass with a higher removal potential than thinner biofilms, on the other, however, the substrate diffusion is limited for the deeper layers (Piculell, 2016). The latter can cause endogenous activity and lower adhesion capacity of the microorganisms in these layers, reduce the biofilm surface area resulting in lower removal performance and biofilm detachment (Boltz and Daigger, 2010; Huang et al., 2019). Nonetheless, thick biofilms can also present a porous structure, which could favour the substrate mass transfer from the liquid to the deeper layers but also the penetration of inhibitors. To control the biofilm thickness and density the adjustment of the hydraulic shear forces, e.g., via mixing velocity, and of the organic loading rate are effective strategies (Dupla et al., 2006; Morgan-Sagastume, 2018), while the biofilm porosity

has been reported of depending on the microorganisms' biomass yield (Van Loosdrecht et al., 1997).

Also, the carrier's structure should be considered. For instance, carriers with a porous structure could represent an option, given their high surface area (>1000 m^2/m^3), where the biofilm can grow in the pores protected from external stressors and inhibitors (Raj Deena et al., 2022; Zhang et al., 2009). Moreover, such carriers have usually the advantage of quick biofilm formation. Nonetheless, due to the clogging of the pores by the biofilm during the reactor operations, the active surface area is usually lower than the initial one, resulting in lower biofilm-liquid interface and thus, lower mass transfer than expected (Morgan-Sagastume, 2018).

As for the carriers used in denitrification studies under salinity stress (Table 2), no direct conclusions can be drawn for the best performing ones. On one hand, carriers used for MBBRs that present thick biofilms and high biomass quantity per single carrier have shown high removal rates. On the other hand, sand, with a lower surface area than many MBBR carriers, was used in the best performing reactor (FBBR) (Vredenbregt et al., 1997), possibly suggesting that other factors rather than the carrier played a more important role. S^0 is the most used carrier for autotrophic denitrification under salinity stress and present the advantage of acting also as electron donor, but the denitrification rates could be improved with $S_2O_3^{2-}$ as electron donor (Di Capua et al., 2019).

Research focusing on biofilm carrier optimisation for denitrification under salinity stress is limited. An optimal carrier should provide a protected environment for a thick and microbially diverse biofilm, whose thickness should be controlled to guarantee an effective substrate removal, and be characterised by a suitable material density to avoid the effect of salinity increased buoyancy. Thus, further research is needed about the carrier selection under salinity stress.

2.2.3 Biofilm reactors for denitrification: MBBR vs FBBR

MBBR and FBBR are among the most used biofilm reactors for denitrification (Di Capua et al., 2015; Ødegaard, 2006; Wu et al., 2021). Their comparison is reported in Table 3, where their operational differences are summarised.

Table 3. Comparison of MBBR and FBBR technologies.

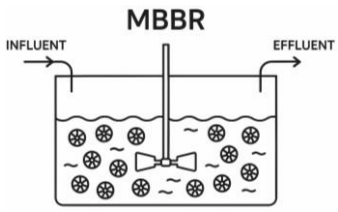

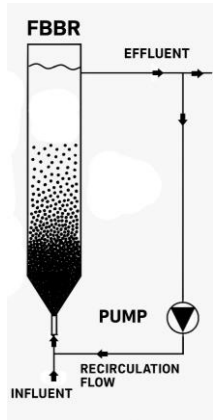

Operating mode	Biofilm carriers suspended and moved by a mechanical mixer	Fine carrier material bed fluidised by a high recirculation flow
Common carriers	Plastic or foam, various dimensions (0.5-5 cm) and shapes (chips, cylindrical, cubes or disk), hollow or porous (Morgan-Sagastume, 2018; Raj Deena et al., 2022).	GAC, zeolite, sand, lava rock, plastic, in fine grains (<1 cm), porous or not (Eldyasti et al., 2012; Papirio et al., 2013).
Benefits	Simple operating conditions, compactness and flexibility, high biomass quantity retention, no recirculation, fully mixed conditions, low excess sludge production, no backwash (McQuarrie and Boltz, 2011; Ødegaard, 2006).	Low HRTs and small reactor volume, biofouling control, substrate toxicity dilution, (semi)fully mixed conditions, low excess sludge production, no backwash (Di Capua et al., 2015; Özkaya et al., 2019).
Limitations	Substrate diffusion limitations for thick biofilms, biofouling and clogging of carriers, necessity to control biofilm thickness (McQuarrie and Boltz, 2011; Ødegaard, 2006).	Pumping energy cost for fluidisation, reactor size limitations (height:diameter ratio constraint), carrier deterioration due to strong friction forces, challenging biomass monitoring (Di Capua et al., 2015; Özkaya et al., 2019).

As seen from Table 2 and 3, FBBRs can guarantee high removal rates and low HRTs. The dilution of the influent created by the internal recirculation makes the FBBR a suitable reactor for reducing the toxicity of the influent, such as metals in mining wastewaters (Papirio et al., 2013). Therefore, it could also provide a high-rate denitrification technology for saline wastewater. Moreover, the FBBR is suitable for slow growing biomass, such as autotrophic denitrifiers (for a review Özkaya et al. (2019)). High nitrogen removal rates have been achieved with both non-porous sand (12 gN/L/d) for heterotrophic (Rabah and Dahab, 2004) and porous GAC (3.2 gN/L/d) for autotrophic (Zou et al., 2016) denitrification, respectively. Carriers with different surface areas (blast plastics, zeolite and lava rock), have shown similar nitrogen

removal performances, suggesting that the large surface area of porous carriers decreases due to the clogging of the pores by the biofilm (Eldyasti et al., 2012). An advantage of using porous carriers like GAC is given by its adsorption capacity of toxic pollutants or substrate for the attached microbes (Dutta et al., 2014), but the possible inhibition of the carrier on the microorganisms (Kowalski et al., 2019; Morgan-Sagastume, 2018), as well as their abrasion due to high friction (Özkaya et al., 2019) should also be considered. Eventually, the carrier material determines the recirculation flow required for fluidisation, and, hence, influences the cost of the process (Papirio et al., 2013). Overall, the FBBR carrier selection has shown of affecting the reactor operation more than the denitrification rate, but the choice of the carrier needs further investigation due to the limited literature about the use of FBBR in saline conditions.

The MBBR is a well-known reactor technology used to treat many wastewaters from different industrial sectors like textile, pharmaceutical, pulp and paper etc. (Gupta et al., 2022). The MBBR presents an easier and cheaper operation mode than the FBBR, with mixing provided by a mechanical mixer, but it requires more control for the clogging of the carriers and the biofilm thickness. The larger dimensions, compared to FBBR carriers, should enable higher biomass retention and thicker biofilms, but are also more prone to clogging due to the lower shear stress present in the MBBR. For denitrification under non-inhibitory conditions, PE carriers have shown higher denitrification rates than other polymeric material carriers (Yuan et al., 2015), possibly due to their shape, surface area and efficient mass transfer, while under toxic conditions (naphthalene removal), porous polyurethane foam carriers showed faster removal kinetics than PE or PP carriers (Sonwani et al., 2019). Therefore, the best performing carrier selection strongly depends on the wastewater treated as well as on the biological process employed. Under saline conditions, different MBBR carriers have been compared for nitrogen removal at constant 1% (Zan et al., 2022), 2.8% (Dupla et al., 2006) and 3% salinity (Tadda et al., 2021), but knowledge about carriers at higher salinities characterizing industrial wastewaters is needed.

In summary, MBBR and FBBR are known high-rate treatment technologies that could provide improved salinity tolerance. Both reactors have been used for denitrification under salinity stress (Table 2), but a systematic analysis of the optimal reactor design as well as of the optimal carrier selection under salinity stress is missing, requiring further investigation.

2.2.4 Salinity inhibition modelling in biofilm reactors

Modelling is an important aspect not only for the operation and prediction of the bioprocess, but also for its optimisation (Rittmann et al., 2018). The inclusion of salinity inhibition on denitrification in biofilm models would enable, for example, prediction of its behaviour at a certain salinity concentration and its optimisation accordingly.

Biofilm models are characterised by higher complexity than activated suspended sludge models, since they need to include mass transport phenomena, such as diffusion of dissolved matter from the bulk phase to the biofilm layer. Usually, 1D models represent sufficiently well biofilm dynamics, enabling shorter computational times and requiring less input parameters to be determined (Rittmann et al., 2018). A further simplification consists in considering apparent kinetics for the biofilm process, which are based only on observed macro-measurements in the bulk phase, and include phenomena like diffusion in adapted kinetic parameters (μ_{max}, K_s etc.) (Plattes et al., 2006; Y. Wang et al., 2016).

Salinity inhibition on nitrogen removal rate is usually represented by non-competitive inhibition functions, like Hill's (Carrera et al., 2023; Lin et al., 2021; Mariángel et al., 2008; Zuo et al., 2021), which correlates the salinity concentration with the decrease in nitrogen removal rate. This function can then be implemented in a time-dependent biokinetic model to reproduce the kinetics of nitrogen removal and intermediates accumulation, as done for granular sludge (Carrera et al., 2023) and sludge flocs (Zuo et al., 2021). Nevertheless, there are no reports about modelling salinity inhibition on biofilms, possibly because of its complexity.

Biofilm inhibition modelling has been reported for some substances, such as aniline, by using a model that considers the diffusion mechanism (Gheewala et al., 2004). Such approach, which represents more accurately the real phenomena but is also complex to be implemented in time dependent models, is challenging for the simulation of salinity inhibition, considering the possible formation of salinity gradients in the biofilm, the possible precipitation of salts on the carrier surface and the specific toxicity of different ions. Simplified approaches that include the mass transfer in apparent parameters (half-saturation and half-inhibition constants) has also been used for substrate inhibition on attached biomass nitrification (Carrera et al., 2004). This method would simplify the inclusion of salinity inhibition in biofilm models, starting from simulating the inhibition kinetics, and is, therefore, relevant for the reactor optimisation under salinity stress.

2.3 Denitrification of wet flue gas scrubber wastewater

Wet scrubbing is one of the most established and flexible post-combustion technologies used in many industrial sectors to remove harmful pollutants from flue gases, like SO_2, known as flue gas desulphurisation (FGD) process (Córdoba, 2015; J. Zhao et al., 2021; M. Zhao et al., 2021), or simultaneously NO_x and SO_2 (M. Zhao et al., 2021). In these systems, flue gases are washed with a solution, such as CaO, seawater, NaOH or $Mg(OH)_2$, which adsorbs the pollutants from the gaseous to the liquid phase, generating a wastewater (Córdoba, 2015; Lecomte et al., 2017).

2.3.1 Scrubber wastewater and common treatment methods

Wet scrubber wastewater has a complex matrix characterised by high salinity and the frequent presence of nitrogenous and sulphurous compounds, heavy metals and polyaromatic hydrocarbons (Córdoba, 2015; Gingerich and Mauter, 2020; Hu et al., 2023). The volume and composition of scrubber wastewater depends on flue gas composition, on the scrubber type (scrubbing solution, source of water, operation mode, heat recovery) and on the flue gas treatments before the scrubber (Gingerich and Mauter, 2020; Hu et al., 2023; Parsons et al., 2016; Pöyry, 2016). For instance, in 2014 in only the United States, 210 million m^3 of FGD wastewater was generated by coal fired power plants (Gingerich et al., 2017), even though the transition to other forms of energy indicates a possible decreasing trend of FGD wastewater production. In marine transportation sector, it is estimated that ships equipped with scrubbers discharge worldwide around 10 billion m^3 of scrubber wastewater in a year (Osipova et al., 2021). Therefore, scrubber wastewaters need proper treatment before discharge, as they do pose risks for human health and the aquatic environment (Córdoba, 2015; Gingerich et al., 2017; Osipova et al., 2021; Teuchies et al., 2020; Ytreberg et al., 2022).

Currently, physical-chemical treatments (e.g., oxidation, flocculation, sedimentation) are the most employed for scrubber wastewater (Córdoba, 2015; EPA, 2011; Gingerich et al., 2018; Hu et al., 2023; Lecomte et al., 2017; Shuangchen et al., 2016). Alternatives to the treatment have also been reported, such as the recirculation of the effluent in the same scrubber after solids separation or injection to the boiler (Cordoba and Staicu, 2018; Gall et al., 2022). These methods would notably reduce the amount of wastewater to be managed, but could cause technical

problems to the scrubber operation, as the scrubbing solution becomes more concentrated, or to the boiler, where it could cause fouling and corrosion. In smaller power plants as well as in other sectors (e.g., municipal sludge incineration), where the scrubber wastewater volumes are small, it is common to convey the wastewater directly to an existing WWTP (Pöyry, 2016). This choice mainly depends on the scrubber effluent composition, effectiveness of the existing treatment plant in removing the pollutants in the flue gas scrubbing wastewater and environmental requirements.

2.3.2 Biological nitrogen removal under saline conditions

Nitrate and nitrite, known contributors to eutrophication of water bodies, are commonly present in scrubber wastewaters from many industrial sectors, with increased concentrations in the case of NO_x-SO_2 scrubbers. To reduce the overall NO_x emission load to the environment, their removal from the water phase is important.

The common physical-chemical treatment-chains for scrubber wastewaters seldom target dissolved pollutants, such as nitrate. To improve their removal, biological treatments, also suggested by the US Environmental Protection Agency (EPA, 2020, 2015), could play an important role in complying with the emission regulations, representing cost-effective and sustainable solutions (Z. Huang et al., 2024). Multiple biological approaches for scrubber wastewater can be found in literature, such as biological S^0 recovery (Blázquez et al., 2019; Mora et al., 2020) and Se^0 recovery (Cordoba and Staicu, 2018; Gingerich et al., 2018), or as a sulphur source for the treatment of municipal sewage in the Sulphate Reduction, Autotrophic Denitrification and Nitrification Integrated process (Jiang et al., 2013).

Usually, as showed in Figure 2, NO_3^-/NO_2^- co-occur with high concentrations of inorganic ions like chloride, sodium or magnesium, and sulphate, which contribute to the salinity of the wastewater. Thus, bioprocess inhibition, due to the composition of the wastewater, and the lack of suitable energy sources for the biological treatments represent the two main challenges (Cordoba and Staicu, 2018; Gingerich et al., 2018, 2017), also for denitrification.

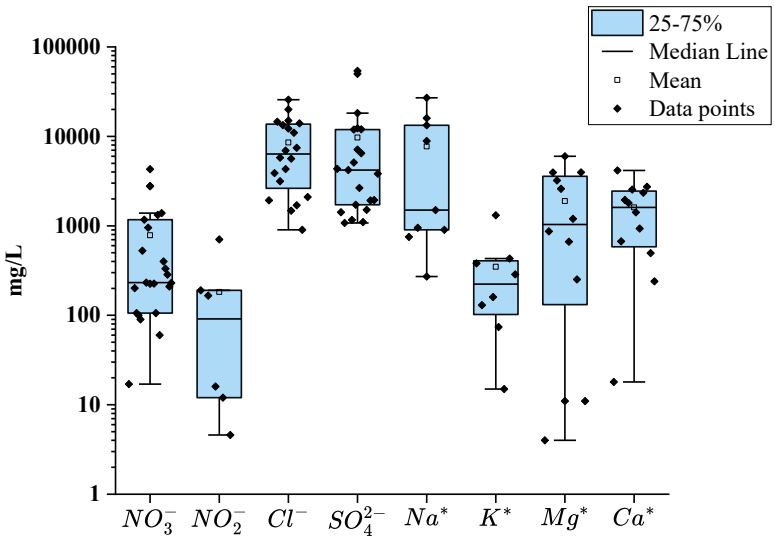

Figure 2. Nitrate and nitrite concentrations found in wet flue gas scrubber wastewaters and co-occurring concentrations of other ions. Number of datasets: 23, of which 18 are from FGD (wet lime-gypsum) scrubbers, 4 from NO_x-SO_2 scrubbers and 1 not specified. When a range of the concentration values was reported, the mean value of that range is shown in the table. * Refers to the element. References: (This study; Ahmed et al., 2024; Bogacki et al., 2018; Brown et al., 2012; Chen et al., 2023; Chin et al., 2023; Fang et al., 2018; Galkaduwa et al., 2017; Gall et al., 2022; Huang et al., 2013, 2012; Iskra et al., 2020; Jo et al., 2016; Koenig and Liu, 2004; Ma et al., 2019b, 2019a; Martin et al., 2021; Morita et al., 2007; Riffe et al., 2008; Solińska and Bajda, 2022; Vendrup and Sund, 1994; Wei et al., 2017).

The co-presence of heavy metals as Cr, Hg or V could have adverse effects on microbial metabolism, while other trace metals (e.g. Co, Fe, Ni, Zn) could be beneficial to microorganisms' activity (Cordoba and Staicu, 2018). Nonetheless, at real scale, when the biological treatment is located after chemical precipitation, where most of the heavy metals are removed, the main inhibitor is considered to be salinity (Yan et al., 2019). Table 4 shows denitrification studies, both autotrophic and heterotrophic, on scrubber wastewater reported in literature, where the majority focused on FGD wastewater. All of them were performed under high salinity stress, with high concentrations of chloride, sulphate and sodium. Moreover, most of them needed to add a suitable electron donor for denitrification. Alternatively, some of them used electron donors internal to the process (S^{2-}), whose production, however, required the addition of an external organic. Similarly, in real applications like the Envirogen FBBR Technology (Togna, n.d.) and ABMet technology by Veolia (Veolia Water Technologies, n.d.), where both nitrate and selenate are removed, carbon addition is required.

Table 4. Overview of flue gas scrubber wastewater denitrification studies in literature.

Type of scrubber wastewater	Max salinity g/L	e-donor for denitrification	Process studied	Reference
FGD (wet lime-gypsum) in CFPP	45 (Cl^-)	Acetate (added)	NO_3^- removal via heterotrophic denitrification in pilot scale FBBR	Vredenbregt et al. (1997)
FGD (wet lime-gypsum) in CFPP	20 (Cl^-)	Acetate (added)	NO_3^- removal via heterotrophic denitrification in pilot scale CSTR	Dahl et al. (1997)
FGD (wet lime-gypsum) in CFPP	36 (TDS)	S^0 particles (added)	Wastewater inhibition on autotrophic denitrification in lab-scale batch reactor	Koenig and Liu (2004)
FGD (wet lime-gypsum) in CFPP	3.2 (SO_4^{2-})	Ethanol (added)	NO_3^- removal via heterotrophic denitrification in pilot-scale packed gel reactor	Morita et al. (2007)
FGD in petrochemical industry	1.5 (SO_4^{2-})	S^{2-} produced in anaerobic reactor with COD in municipal sewage	SO_4^{2-} conversion, NO_3^- and NH_4^+ removal via integrated sulphate reduction, autotrophic denitrification, nitrification in lab scale reactor	Wei et al. (2017)
Lab-scale NO_x scrubber	30 (SO_4^{2-})	S^{2-} produced in anaerobic reactor with added crude glycerol	SO_3^{2-} conversion, NO_3^- removal, S^0 recovery via Integrated sulphite reduction, autotrophic denitrification and settling in lab-scale UASB and CSTR	Guimerà et al. (2021)
FGD (wet lime-gypsum) in CFPP	22 (Cl^-)	Not specified (added)	NO_3^- removal via heterotrophic denitrification in lab-scale packed bed reactor	Iskra et al. (2020)
FGD in petrochemical industry	27 (SO_4^{2-})	Methanol (added)	NO_3^- removal via heterotrophic denitrification in lab-scale reactor filled with plastic carriers	Wu et al. (2023)
FGD in refining and chemical industry	60 (Na_2SO_4)	Acetate (added)	NH_4^+ and NO_3^- removal via nitrification and heterotrophic denitrification in lab-scale SBR	Ren et al. (2024)

FGD: Flue Gas Desulphurisation, CFPP: Coal Fired Power Plant, COD: Chemical Oxygen Demand, TDS: Total Dissolved Solids, FBBR: Fluidised Bed Bioreactor; CSTR: Continuously Stirred Tank Reactor; UASB: Up-flow Anaerobic Sludge Blanket; SBR: Sequencing Batch Reactor.

2.3.3 Scrubber wastewater denitrification in pulp mills

Pulp industry must deal with SO_2 and NO_x emissions control in flue gases (Suhr et al., 2015), especially from the recovery boiler where the process' chemical solution (white liquor) is recovered from the spent one (black liquor). The flue gases are characterised by high SO_2 and dust content, and by temperatures <250 °C, often making the use of selective catalytic reduction for NO_x removal challenging (Valmet, 2017). For this reason, scrubbers removing simultaneously NO_x and SO_2 are an attractive solution. In these systems, NO solubility is increased by adding oxidisers as ClO_2 (Johansson et al., 2021a) or NaClO (Flagiello et al., 2023), as well as compounds like Na_2SO_3 (Schmid et al., 2022), while $Na_2S_2O_3$ addition can prevent the fast oxidation of SO_3^- to SO_4^{2-} (Schmid et al., 2023). Moreover, these chemicals are employed in the pulping and bleaching processes and, hence, easily available on site (Johansson et al., 2021b). Eventually, the generated wastewater is high in NO_3^-/NO_2^-, SO_4^{2-}, Na^+ and Cl^-, while it is low in heavy metals, since wood contains low amounts of them. A possible solution proposed for managing this wastewater is to treat it at the existing WWTP of the pulp mill (Gall et al., 2022). As a pretreatment, a case study (Myrberg, 2024) suggested that SO_4^{2-} should be removed, for example via precipitation with lime, to avoid possible settling issues in the activated sludge basin.

In general, the overall pulp mill wastewater is low in nutrients (N and P), with common BOD:N:P ratios of 100:(1-2):(0.15-0.3) (Cabrera, 2017). Thus, NH_4^+ and PO_4^{3-} are usually added to support the biological treatment, which typically consists of an aerobic activated sludge process (Ashrafi et al., 2015; Cabrera, 2017). Therefore, the existing WWTP is not optimised for the reduction of NO_3^-/NO_2^- that are introduced with the scrubber wastewater. Moreover, the daily scrubber wastewater production is estimated to be 100-1000 times lower than the overall pulp mill wastewater, which is around 10^4-10^5 m^3/day (Suhr et al., 2015), indicating that it would not fulfil the N requirement of the existing aerobic biological treatment. In support of this, a lab-scale study showed that NO_3^- and NO_2^- could only partially replace conventional N supplements (e.g., urea) to support aerobic COD removal (Keskinen, 2021). Hence, a pre-denitrification treatment could represent a sustainable option to remove NO_3^-/NO_2^- from the scrubber wastewater prior to the mill's WWTP, avoiding modifications to the existing plant or dilution of NO_x^-.

To support the denitrification process, some waste streams rich in organic compounds generated in pulp mills could be potentially suitable as inexpensive electron donors. For instance, evaporator foul condensate is produced during the chemical recovery process (Figure 3), when black liquor is concentrated in evaporators, prior to the recovery boiler, and the resulting vapour is condensed (Tran and Vakkilainen, 2008). Such stream is rich in methanol and other organics, as well as NH_4^+ (Badshah et al., 2012; Rintala and Puhakka, 1994). Given the high impurity of the methanol and to reduce the organic load in the WWTP, foul condensate is usually treated by stripping and burning (Suhr et al., 2015), but some studies have successfully treated it with biological methods for COD removal (Dias et al., 2005), volatile fatty acid (Eregowda et al., 2021) or methane production (Badshah et al., 2012). Thus, foul condensate could potentially serve as electron donor for heterotrophic denitrification. Similarly, autotrophic denitrification could be facilitated by the S-compounds in the same scrubber wastewater, such as exceeding SO_3^{2-} and $S_2O_3^{2-}$ from the scrubbing process, also easily available in the mill. Therefore, the potential of denitrification in biofilm reactors for saline pulp mill streams treatment, supported by electron donors found on site, requires further investigation.

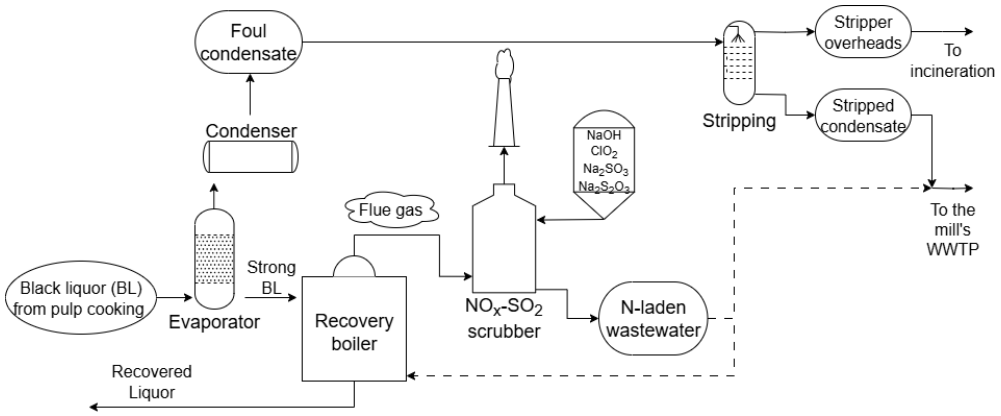

Figure 3. Simplified process flow diagram of foul condensate treatment and possible fates of scrubber wastewater in pulp mills.

3 MATERIALS AND METHODS

In this chapter, a summary of the designs, calculations, modelling and analytical methods of the experiments is presented. More detailed descriptions of the materials and methods used are reported in Publications I, II, III and their related supplementary materials.

3.1 Source of denitrifying microorganisms

All the microorganisms used in this work had a non-saline history. The heterotrophic biomass used in the experiments of Publication I was enriched from the denitrification compartment sludge of a Finnish municipal WWTP (Helsinki). The autotrophic microorganism used in Publication I (*T. denitrificans* DSM12475) was purchased from Leibniz-Institute DSMZ (Germany) and originated from domestic sewage lagoons. Both heterotrophic enrichment and autotrophic pure cultures were maintained as reported in Publication I, with methanol and thiosulphate as electron donors, respectively. The same cultures were used in Publication II as inocula for the heterotrophic FBBR and the autotrophic FBBR. In Publication III, the heterotrophic biomass was enriched from a denitrifying sludge of an Italian municipal WWTP (Lavis, Italy) and maintained as in Publication I prior to be inoculated in the MBBRs.

3.2 Experimental overview

The summary of the experimental designs conducted in this work is shown in Figure 4. In the first set of experiments (Publication I), a series of batch tests were performed to study the effects of inorganic ions (Na^+, Cl^-, SO_4^{2-} and K^+), commonly present in saline industrial wastewaters, on both methanol-driven heterotrophic (enriched mixed culture) and thiosulphate-driven autotrophic denitrification (*T. denitrificans*). Pairs of ions were added as salts at increasing concentrations and the inhibitory effects were observed on nitrate removal rate and nitrite accumulation. Modified Hill's inhibition

function was fitted for each salt to compare the inhibition levels, and the data were analysed to identify the ion with the highest effect on denitrification.

Next, the performance and tolerance of methanol-driven (HD) and thiosulphate-driven (AD) denitrification were studied in two continuous flow FBBRs filled with GAC (Publication II) by evaluating nitrogen removal rates and efficiency, denitrification kinetics and biomass quantity and microbial community changes. Nitrogen loading rate and salinity, given by multiple inorganic ions, were gradually increased in a simulated saline wastewater and, once inhibition was met, the reactors were recovered by decreasing salinity concentration. Then, in the methanol-driven FBBR, the suitability of pulp mill foul condensate as energy and carbon source was investigated, aiming at evaluating its potential as supplement for denitrification.

The denitrification process showing the highest nitrate removal rate at the highest salinity in FBBRs (heterotrophic) was then tested in two MBBRs (Publication III). Methanol-driven denitrification was studied with a hollow-body (K5) and a porous-body (M30) carrier, by observing nitrogen removal rates and efficiencies, denitrification kinetics, biofilm quantity, development and microbial community dynamics under increasing nitrogen loading rates and multi-ionic salinity in a simulated wastewater. The aim was to obtain the highest nitrogen removal efficiency in the MBBR process under salinity stress via carrier selection at different salinities. Eventually, the performances of FBBRs and MBBRs, as well as the carriers used, were compared to outline the differences of the two biofilm reactor systems for denitrification of saline wastewaters. Also, the salinity inhibition effect on denitrification kinetics in the MBBRs biofilm was introduced in an existing biofilm model in Sumo©22 software, as described in Section 3.3.

To assess the potential of denitrification in removing nitrogen from scrubber wastewater, real NO_x-SO_2 scrubber wastewater from pulp mill was chemically characterised and tested. First (Publication I), batch tests with suspended biomass were run both for heterotrophic and autotrophic denitrification, and methanol and thiosulphate were added as electron donors, respectively. Then (Publication III), heterotrophic denitrification was tested in two lab-scale MBBRs (carrier filling fraction 25%), one with K5 and the other with M30 colonised carriers, in a semi-batch mode.

In all the tests, pH was maintained in neutral range, temperature was controlled at 30 or 35 °C and anoxic conditions were created by N_2 purging.

I. Ions inhibition in denitrification batch bioassays:

- Methanol-driven and thiosulphate-driven
- 1-35 g/L Na^+ (as NaCl), Na^+ (as Na_2SO_4), Cl^- (as KCl) and K^+ (as K_2SO_4)
- Real NO_x-SO_2 scrubber wastewater inhibition

II. Denitrification FBBR studies:

- Methanol-driven (HDFBBR) and thiosulphate-driven (ADFBBR)
- Salinity 1.1-8.1% (Na_2SO_4+KCl)
- HRT: 13.4-1.1 h
- Carrier: GAC
- Bed filling and fluidization: 44% and 17%

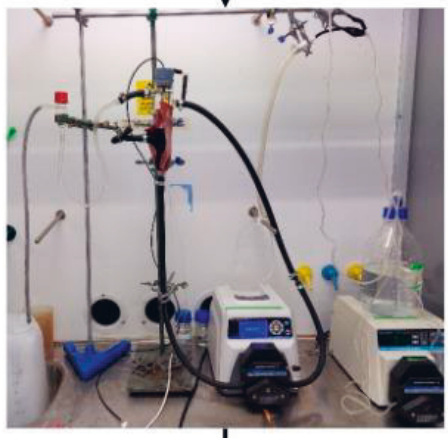

Filtrasorb 200
(Calgon Carbon Corp., USA)
PSA: 850 m^2/g, d: 0.55-0.75 mm
vol.: 75 mL
(GAC)

Pulp mill foul condensate as energy source in HDFBBR

III. Denitrification MBBR studies:

- Methanol-driven with two carriers (K5-MBBR and M30-MBBR) (a)
- Salinity 1-9.5% (Na_2SO_4+KCl)
- HRT: 12-4 h
- Carriers: hollow- and porous- body
- Carrier filling ratio: 25%
- Semi-batch test with real NO_x-SO_2 scrubber wastewater (b, c)
- Biofilm inhibition kinetics modelling

Hollow-body AnoxK™ 5
(AnoxKaldnes, Sweden)
PSA: 800 m^2/m^3, d: 25 mm,
pieces: 191
(K5)

Porous-body Mutag BioChip 30™
(Mutag, Denmark)
PSA: 5500 m^2/m^3, d: 30mm
pieces: 285
(M30)

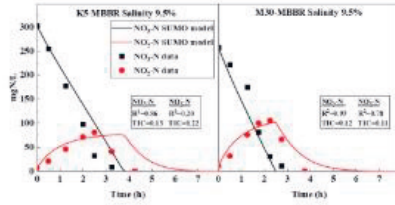

Figure 4. Summary of the experiments performed in this work.

3.3 Modelling of salinity effect on denitrification kinetics in MBBR

At each salinity concentration tested in the MBBRs, the reactors were temporarily operated in batch mode to perform a nitrogen uptake rate (NUR) test. The specific denitrification rates (NO_x^--N/gVS/d) calculated for the whole reactor (attached+suspended biomass) were then fitted with modified Hill's inhibition function, to obtain the salinity parameters (K_I and n) to be used in the modelling, for each of the MBBRs. The existing biofilm model for MBBR in Sumo©22 (Dynamita, France) software was used to simulate the denitrification kinetics in the two MBBRs (K5-MBBR and M30-MBBR) in the NUR tests. Only methanol-driven denitrification process was considered in the model. To include the inhibitory effect of salinity on the denitrification kinetics an inhibition factor ($\mu_{S\text{-}inhib}$) was implemented in the nitrate removal rate of the biokinetic model "SUMO 4N", which incorporates the four steps of denitrification, allowing the heterotrophic biomass to grow with NO_3^-, NO_2^-, NO and N_2O as electron acceptors (Hiatt and Grady, 2008). The resulting equation system is:

$$\begin{cases} \dfrac{d(NO_3^-\text{-}N)}{dt} = -\dfrac{(1\text{-}Y)}{Y\cdot f_{COD,2}}\left(\mu_{S\text{-}inhib}\cdot X\cdot\dfrac{NO_3^-}{K_{NO3}+NO_3^-}\cdot\dfrac{K_{NO2}}{K_{NO2}+NO_2^-}\right) \\ \dfrac{d(NO_2^-\text{-}N)}{dt} = -\dfrac{(1\text{-}Y)}{Y\cdot f_{COD,1}}\left(\mu_T\cdot X\cdot\dfrac{NO_2^-}{K_{NO2}+NO_2^-}\right) - \dfrac{d(NO_3^-\text{-}N)}{dt} \\ \mu_{S\text{-}inhib} = \mu_T\cdot\dfrac{K_I^n}{K_I^n+I^n} \end{cases}$$

where μ_T (1/d) is the specific growth rate determined at 30 °C, X (gCOD/L) is the active biomass, $f_{COD,1}$ and $f_{COD,2}$ are COD-N conversion coefficients, K_{NO3} and K_{NO2} (mgN/L) are the half-saturation constants for nitrate and nitrite, respectively. I (salinity concentration, g/L) was a new input parameter.

To simulate nitrite accumulation, K_{NO2} was calibrated accordingly. The initial conditions of biofilm thickness (L) and specific surface area (SSA) in the carriers were estimated by microscopy and visual observations or calibrated. Other parameters were set as described in Publication III.

To verify the consistency of the model under different biofilm conditions, each salinity concentration was simulated under the initial conditions of each NUR test, by modifying I to the simulated salinity concentration and inserting the K_{NO2} value calibrated for that salinity concentration. This resulted in five calculated denitrification rates, one for each initial conditions of the NURs, for each salinity concentration.

Eventually, a sensitivity analysis of the parameters (L, SSA, K_I and n) on the model output was conducted.

3.4 Analytical methods

The main analytical methods used are summarised in Table 5.

Biomass quantity measurements and microbial community characterisation were conducted for both suspended and attached biomass in FBBRs and MBBRs. The detailed sampling, detachment and analytical procedures are reported in subsection 2.4.3 and 2.5 (Publication II) and 2.5.2 and 2.7 (Publication III).

Table 5. Main analytical methods used in the experimental part of this work.

Analyses	Instrument/Method	Publication
NO_3^-, NO_2^-,	Ion chromatography (Dionex Integrion, Thermo Fisher Scientific Inc., USA); Hach cuvette tests (LCK339, LCK340, LCK343)+ spectrophotometer (HACH LANGE DR 3900, Hach Company, USA).	I and II; III
SO_4^{2-}, $S_2O_3^{2-}$	Ion chromatography (Dionex Integrion, Thermo Fisher Scientific Inc., USA)	I and II
NH_4^+	HACH cuvette test (LCK 303)+ spectrophotometer (HACH LANGE DR 3900, Hach Company, USA).	II and III
CH_3OH	Gas chromatograph equipped with a flame ionisation detector (GC-2010, Shimadzu Co., Japan)	I and II
Dissolved organic Carbon (DOC)	TOC-VCPH/CPN analyser (Shimadzu Co., Japan); TOC/TN analyser (FORMACS™ HT-I, Model 2CA17910, Skalar, Netherlands).	I and II; III
Biomass as $C_5H_7O_2N$	Digestion+ NO_3^--N measurement with HACH LCK 339+ spectrophotometer (HACH LANGE DR 2800, Hach Company, USA).	II
Biomass as volatile solids (VS)	Gravimetric analysis after heating at 550 ºC.	III
Biofilm observation	Optical microscopy (Biostar BM 45, Optech, UK) with Plan 40x/0.65 objective	III
Microbial community	DNA extraction and 16S rRNA gene sequencing	II and III

3.5 Calculations and data analyses

Calculations, models and analyses performed with the data of the experiments are summarised in Table 6.

Table 6. Summary of calculations, models and data analyses used in this work. Unit conversion factors are not included in the equation/method.

Parameter/model	Equation/method	Publication
Nitrate removal rate (NO_3^-RR) (mg/L/h)	Linear regression of steepest part in NO_3^- concentration time profile	I and III
Osmotic pressure (OP) (atm)	$OP = i \cdot M \cdot R \cdot T$ i: van't Hoff factor, M: conc of the salt (mol/L), R: ideal gas constant (0.082 $L \cdot atm \cdot mol^{-1} \cdot K^{-1}$), T: temperature (K)	I, II and III
Modified Hill's inhibition function	$NO_3^-RR = NO_3^-RR_{max} \cdot \frac{K_I^n}{K_I^n + I^n}$ NO_3^-RR: nitrate removal rate (mg/L/h), K_I (or IC_{50}): half-inhibition constant (g/L), n: tuning parameter (-)	I and III
Hydraulic retention time (HRT) (h)	$HRT_{FBBR} = \frac{V_{FB}}{Q_{in}}$; $HRT_{MBBR} = \frac{V_{MBBR}}{Q_{in}}$ Q_{in}: inflow (L/h), V_{FB}: volume of fluidised bed (L), V_{MBBR}: Volume of the MBBR (L)	II; III
Nitrogen volumetric loading rate (NVLR) for FBBR and MBBR (gN/L/d)	$NVLR_{FBBR}, NVLR_{MBBR} = \frac{[NO_{3\,in}^- - N]}{HRT_{FB} \text{ or } HRT_{MBBR}}$	II; III
Nitrogen surface loading rate (NSLR) for MBBR ($g/m^2/d$)	$\frac{NVLR_{MBBR}}{f \cdot PSA}$ f: carrier volumetric filling fraction (25%), PSA: protected surface area of the carrier (m^2/m^3)	III
Nitrogen removal efficiency (NRE) (%)	$NRE = \frac{[NO_{3\,in}^- - N] - ([NO_{3\,out}^- - N] + [NO_{2\,out}^- - N])}{[NO_{3\,in}^- - N]} \cdot 100$	II and III
Nitrogen removal rate, volumetric (NVRR, gN/L/d) or surface (NSRR, $g/m^2/d$)	$NVRR, NSRR = NVLR \text{ or } NSLR \cdot NRE$	II and III
Modified Stover-Kincannon (S-K) kinetic model	$\frac{HRT}{N_{in} - N_{out}} = \frac{K_B}{U_{max}} \cdot \frac{HRT}{N_{in}} + \frac{1}{U_{max}}$ U_{max}: maximum nitrogen removal rate (g N/L/d); K_B: saturation constant (g N/L/d)	II and III
Analysis	**Method**	**Publication**
Goodness of fitting	Coefficient of Determination (R^2); Thiel's inequality coefficient (TIC)	I, II and III; III
Variable importance	Partial Least Square Regression and Random Forest Regression	I
Reactor performance difference significance	Mann-Whitney U test (α=0.05)	III
Sensitivity of the model	Sensitivity Analysis	III
Microbial community changes	Principal coordinate analysis (PCoA) and Permutational analysis of variance (PERMANOVA) (α=0.05), Spearman Correlation	II and III

4 RESULTS AND DISCUSSION

This work revealed the inhibition of inorganic ions and the potential of biofilm reactors in providing improved tolerance to multi-ionic stress for high-rate denitrification, such as for the treatment of NO_x-SO_2 scrubber wastewater. The optimisation of the biofilm process can be achieved via carrier selection as well as suitable electron donor addition, based on the salinity concentration. Moreover, the successful implementation of an apparent inhibition factor to an existing biofilm model lays the foundation for a simplified approach in biofilm process inhibition modelling.

4.1 Tolerance of heterotrophic and autotrophic denitrification to inorganic ions

In the first step of the research (Publication I), the inhibition of inorganic ions on denitrification activity, added in pairs as salts (NaCl, KCl, Na_2SO_4 and K_2SO_4), was investigated in batch tests to identify the most inhibitory ones, among those characterizing industrial saline wastewaters. Previous reports have mainly used NaCl to study salinity inhibition on denitrification, as also noted by Macêdo et al. (2019), and few used Na_2SO_4 or Na_3PO_4 (Koenig and Liu, 2004; R. Wang et al., 2016), while the knowledge about single ions inhibition, like chloride, is limited. Then, in the FBBR (Publication II) and MBBR (Publication III) studies, a mix of salts (KCl and Na_2SO_4) was tested on both heterotrophic and autotrophic denitrifying biofilms to simulate industrial streams rich in sodium and sulphate, with the presence of chloride.

4.1.1 Inorganic ions inhibition in batch bioassays

For each ion pair tested, methanol-driven denitrification by an enriched mixed culture showed higher tolerance than thiosulphate-driven denitrification by the pure culture of *T. denitrificans* (Figure 5). This can be explained by the likely presence of various salt-tolerant genera in the mixed culture, as reported by Macêdo et al. (2019), while in the pure culture, denitrification activity ceased when the salinity tolerance threshold

of *T. denitrificans* was reached. For heterotrophic denitrification, the IC_{50} observed in this study for Na^+ as NaCl (4.3±0.3 g/L) and Na^+ as Na_2SO_4 (7.9±0.5 g/L) were comparable to other studies using mixed cultures with non-saline history (R. Wang et al., 2016; Zhao et al., 2013). On the other hand, Mariángel et al. (2008) obtained 50% inhibition at 18 g/L Na^+(as NaCl) with a culture from a long-term enrichment under saline conditions. For autotrophic denitrification by the strain *T. denitrificans* (DSM12475), inhibition by inorganic ions was studied for the first time in this work. For a general comparison, Claus and Kutzner (1985) and Koenig and Liu (2004) observed higher salinity tolerance for *T. denitrificans* enriched from soil (35% inhibition at 12 g/L Na^+(as NaCl)) and tidal flats (10% inhibition at 12 g/L Na^+(as Na_2SO_4)), respectively, while Na^+ IC_{50} of both salts was <5 g/L in this study. Thus, in closed batch systems, the history of the biomass is the key factor in the observed salinity tolerance of the process.

The same inhibition level was caused by different concentrations of the ion pairs and OP levels, indicating that both the specific toxicity of the salt ions and the osmotic pressure played roles in denitrification inhibition (Figure 5). It was observed that the tested chloride salts were more inhibitory than sulphate salts (Publication I), and when discerning the effects with variable importance analyses, Cl^- resulted the most inhibitory for both heterotrophic and autotrophic nitrate removal among the ions (Publication I). Such results were promising for the treatment of saline wastewaters where Na^+ and SO_4^{2-} are the main inorganic ions. Therefore, when dealing with inhibition by salinity, the identification of the main inorganic ions is of key importance for predicting the limits of the selected process.

Nitrite accumulation differed between the methanol-driven mixed culture and the *T. denitrificans* culture, with NO_2^- concentration peak decreasing with increasing ions concentrations in the heterotrophic process, while in the autotrophic process it rather had a downward opening parabola-like trend (Publication I). Eventually, in almost all the cases with accumulation, nitrite was consumed by more than 95%. Therefore, by observing overall nitrite accumulation and removal, it can be inferred that nitrite reduction step was less affected by salinity than nitrate reduction step, as in other reports (Chen et al., 2022; Mariángel et al., 2008; Zeng et al., 2020; Zhao et al., 2013). Moreover, it can be speculated that different accumulation mechanisms underlay in the two cultures. In the *T. denitrificans* pure culture, nitrite reduction step was inhibited at the low concentrations of ions resulting in NO_2^- accumulation. At increasing concentrations of the ions, nitrate reduction step became more inhibited

than nitrite reduction, resulting in lower accumulation of NO_2^- but slower nitrate removal. Thus, the whole denitrification process was inhibited. In the heterotrophic mixed culture, the tolerance of certain microorganisms might be the reason for NO_2^- accumulation decrease. Under non-inhibitory conditions, nitrate respirators grew faster than the true denitrifiers resulting in NO_2^- accumulation (Glass and Silverstein, 1998). At increasing salinity concentrations, the true denitrifiers were likely less inhibited than nitrate respirators and grew during the extended lag-phase, resulting in slower nitrate removal rates but also lower NO_2^- peaks. Despite the high accumulation (850-1000 mg NO_2^-/L), denitrification inhibition by NO_2^- (Philips et al., 2002) was low or absent, considering also that it was eventually consumed in the tests. Such outcomes are favourable for the treatment of saline wastewaters, where NO_2^- usually accumulates with increasing salinity (Section 2.1.2).

4.1.2 Improved salinity tolerance in biofilm reactors

In biofilm reactors, methanol-driven denitrification was active at 8.1% salinity (OP ~44 atm) in the FBBR (Publication II) and 9.5% (OP ~51 atm) in the MBBR (Publication III). Thiosulphate-driven denitrification showed lower tolerance, being strongly inhibited at 6.9% salinity in the FBBR (Publication II). Nonetheless, in the batch bioassays (Publication I), autotrophic denitrification activity ceased at 4.7% salinity and OP 24 atm (Na_2SO_4), while it was still active in the FBBR at 5.6% and OP 30 atm, showing the improved tolerance in a continuous flow biofilm reactor system. The biofilm system provides a protective environment that allows the attached microorganisms to tolerate higher salinities than the suspended ones. In particular, the EPS matrix plays a key role in this, forming a gel-like diffusion barrier that protects from the high osmotic pressure and the toxicity of the ions. Not only does the EPS matrix hinder diffusion of salt ions in the biofilm (Siegrist and Gujer, 1985), but it also repels (e.g., Cl^-) and adsorbs (e.g., Na^+) some ions (Sudmalis et al., 2020), ensuring a less saline and more stable microenvironment with less fluctuations in ions concentrations than the liquid phase. This resistance of biofilm systems, if compared to suspended biomass reactors, can be extended also to other biological processes under salinity stress (e.g., COD removal (Hasanzadeh et al., 2020)) as well as to different inhibitors, such as toxic organic compounds (Zhang et al., 1995).

The salinities tolerated in this study, at which denitrification was still active, were among the highest reported in literature for methanol-driven and thiosulphate-driven denitrification (Table 7). This comparison demonstrates that MBBR and FBBR could

provide improved salinity tolerance to the process, considering also that the microorganisms in this work did not have a saline history. Moreover, it also suggested that when treating saline wastewaters dominated by Na^+ and SO_4^{2-} (>10 g/L), with lower concentrations of the highly toxic Cl^- (<10 g/L), higher overall salinities can be tolerated by the microorganisms.

As a result of partial salinity inhibition, NO_2^- started to accumulate in the effluent of the continuous flow biofilm reactors, contrarily to what observed in the batch bioassays, especially for methanol-driven denitrification. Such behaviour is possibly due to the enrichment of a stable community in the biofilm (see Section 4.2.3), capable of nitrite reduction, which was inhibited by the increasing salinity.

Overall, the selection of heterotrophic or autotrophic denitrification for the treatment of saline wastewaters depends on the salinity concentration of the process and on the most easily available electron donor. In general, heterotrophic tolerates higher salinities (Table 2, 7) than autotrophic, whose tolerance can be improved by using biofilm reactors. When available, $S_2O_3^{2-}$ guarantees higher rates to autotrophic denitrification as electron donor, but S^0 and S^{2-} seems to be more common, given also their presence in industries generating saline wastewaters (e.g., oil and gas industries) as well as elemental sulphur being environmentally and operationally safe (Di Capua et al., 2019; Panagopoulos, 2022). For heterotrophic denitrification, mixtures of organics as electron sources seems preferable to single electron donors, as they could further improve the process tolerance to salinity stress (Choi et al., 2025; Zhang et al., 2020).

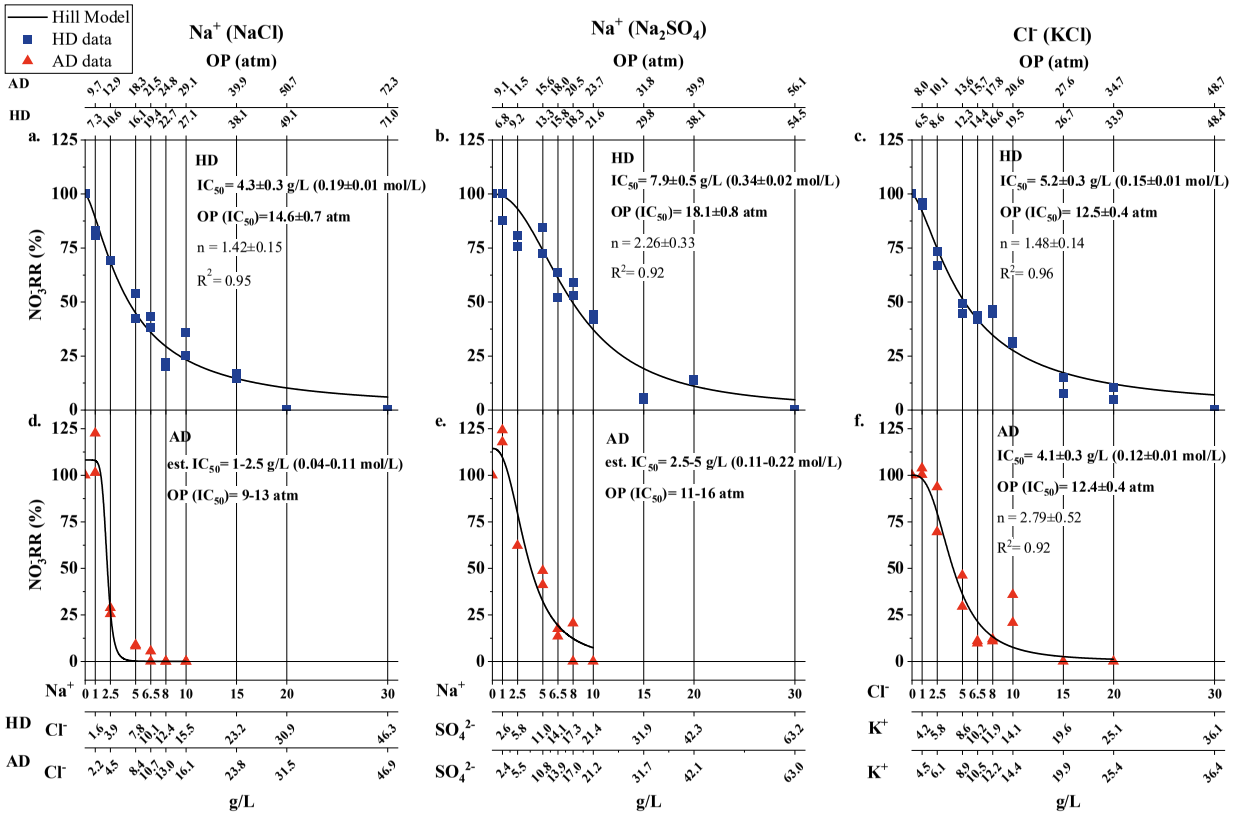

Figure 5. Nitrate removal rate (NO_3^-RR) inhibition at increasing ions concentrations and osmotic pressure (OP) for heterotrophic denitrification (HD) (a, b, c), autotrophic denitrification (AD) (d, e, f). Each column reports the effect of one salt on NO_3^-RR for both HD (1st row) and AD (2nd row). The top x-axis reports the OP condition associated to the ions' concentrations reported on the bottom x-axis for both HD and AD. Modified from Publication I.

Table 7. Methanol-driven and sulphur-driven denitrification performance under saline conditions for different reactor systems in terms of salinity concentration, hydraulic retention time (HRT), nitrogen volumetric loading rate (NVLR) and Nitrogen Removal Efficiency (NRE). If not reported, operational parameters were estimated from the data available in the references. Modified from Publication II.

	Microorganisms' source, influent	Reactor type	Salinity %	HRT (h)	NVLR (gN/L/d)	NRE %	Reference
HD	WWTP sludge, synthetic	MBBR	9.5 (Na_2SO_4+KCl)	4	1.5	≥70 (NO_x^-)	Publication III
	WWTP sludge, synthetic	FBBR	6.8 (Na_2SO_4+KCl)	2.2	2.5	>97(NO_x^-)	Publication II
	WWTP sludge, synthetic	CSTR	≤3; 4 (NaCl)	48	0.75	99 (NO_x^-); inhib.	Osaka et al. (2008)
	Seawater, marine mesocosm wastewater	MBBR	2.8 (seawater)	>24	1.5	88 (NO_x^-)	Labelle et al. (2005)
	WWTP sludge+soil, synthetic	EMCI	3 (NaCl)	3	8.4	60 (NO_3^-)	Yang et al. (1995)
	Saline enrichment of sludge, synthetic	SBBR	6 (Na_2SO_4+NaCl)	24	0.11	<80 (TN)	Feng et al. (2023)
	WWTP sludge, synthetic	BES	3.5 (NaCl)	8	0.06	55 (NO_3^-)	Zhai et al. (2020)
	Seawater, marine mesocosm wastewater	MBBR	2.8 (seawater)	1.6	3.5	75 (NO_x^-)	Dupla et al. (2006)
	Sea aquarium, aquarium water	FBBR	3 (seawater)	NA	0.33	86 (NO_x^-)	Rissanen et al. (2016)
AD	T. denitrificans culture, synthetic	FBBR	5.6 (Na_2SO_4+KCl)	4.1	1.2	>98 (NO_x^-)	Publication II
	WWTP sludge, synthetic	S-PBR	3 (NaCl)	1	0.6	~80 (NO_3^-)	Li et al. (2023)
	WWTP sludge, synthetic	UASB	3.2 (NaCl)	8	0.3	56 (NO_3^-)	B. Chen et al. (2024)
	marine sediments, mariculture tank and anaerobic sludge, synthetic	UPC	3.1 (seawater)	1-4	1	55 (NO_3^-)	Wang et al. (2023)

WWTP: Wastewater Treatment Plant; FBBR: Fluidised Bed Bioreactor; CSTR: Continuous Stirred Tank Reactor; MBBR: Moving Bed Biofilm Reactor; EMCI: Entrapped Microbial Cell Immobilisation reactor, SBBR: Sequencing Batch Biofilm Reactor; BES: Biofilm Electrochemical System, S-PBR: Sulphur Packed Bed Reactor, UPC: Upflow Packed Column, UASB: Upflow Anaerobic Sludge Blanket, NA: not available.

4.2 Denitrification under salinity stress in biofilm reactors: FBBR vs MBBR

The performance of denitrification under salinity stress in FBBR and MBBR was compared. Methanol-driven heterotrophic (HDFBBR) and thiosulphate-driven autotrophic denitrification (ADFBBR) were tested separately in FBBRs filled with GAC (Publication II). Then, methanol-driven denitrification, which had an overall better performance in FBBR than autotrophic, was also tested in MBBRs by comparing two different plastic biofilm carriers (hollow-body (K5-MBBR) and porous-body (M30-MBBR)) (Publication III).

4.2.1 Reactors' denitrification performances

In FBBRs (Publication II), methanol-driven denitrification showed higher nitrogen removal performance at higher salinities than thiosulphate driven (Figure 6a and b), as can also be extrapolated from Table 7 for other studies. Nevertheless, thiosulphate-driven denitrification showed the highest denitrification capacity among other S-driven denitrification reactor studies. When using foul condensate as electron donor in the HDFBBR, its denitrification performance improved and achieved NRE >97% at NVLR around 2.5 gN/L/d and 6.8% salinity. After inhibition at 6.9% salinity for autotrophic and at 8.1% for heterotrophic denitrification, it required 17 and 5 days to recover NRE to >90%, respectively, facilitated by the biomass stored in the biofilm.

In methanol-driven denitrification in MBBRs (Publication III), both K5-MBBR with hollow-body carrier and M30-MBBR with porous-body carrier showed NRE>96% at 5.5% salinity (Figure 6c and d). In the K5-MBBR, volumetric nitrogen removal rate and surface removal rate were higher than in M30-MBBR, as also showed for the specific denitrification rate in the NUR batch tests (Figure 10). At 7.5% and 9.5% salinity, M30-MBBR had significantly ($p<0.05$) higher NRE than K5-MBBR and responded faster to the salinity increment. At the highest salinity (9.5%), M30-MBBR had also more stable NRE (89.5±1.6%) than K5-MBBR (80.9±6.5%) at NVLR up to 1.4 and 1.6 gN/L/d, respectively.

When comparing the MBBRs' nitrogen removal performances with the HDFBBR (Figure 6), higher volumetric rates were reached when using the FBBR, possibly due to the enhanced contact area between biofilm growing on the GAC and the liquid phase (Nelson et al., 2017). On the other hand, higher salinity tolerance was shown by the MBBRs and was likely linked to the thick biofilm structure, with differences in the removal rates and stability of the process based on the biofilm carrier, as explained later in Section 4.2.2.

S-K model returned the highest maximum denitrification rate (U_{max}) for K5-MBBR at 5.5% salinity (Figure 7a), while at 9.5%, M30-MBBR showed a higher removal rate potential. U_{max} for HDFBBR at 6.8% salinity was comparable to the MBBRs at 9.5% salinity, suggesting that its potential was not yet reached at the tested NVLR, while the ADFBBR's denitrification capacity was close to the tested conditions and the lowest among the reactors. Thus, it was shown that both MBBR and FBBR could provide high-rate treatment technologies for denitrification of saline wastewaters.

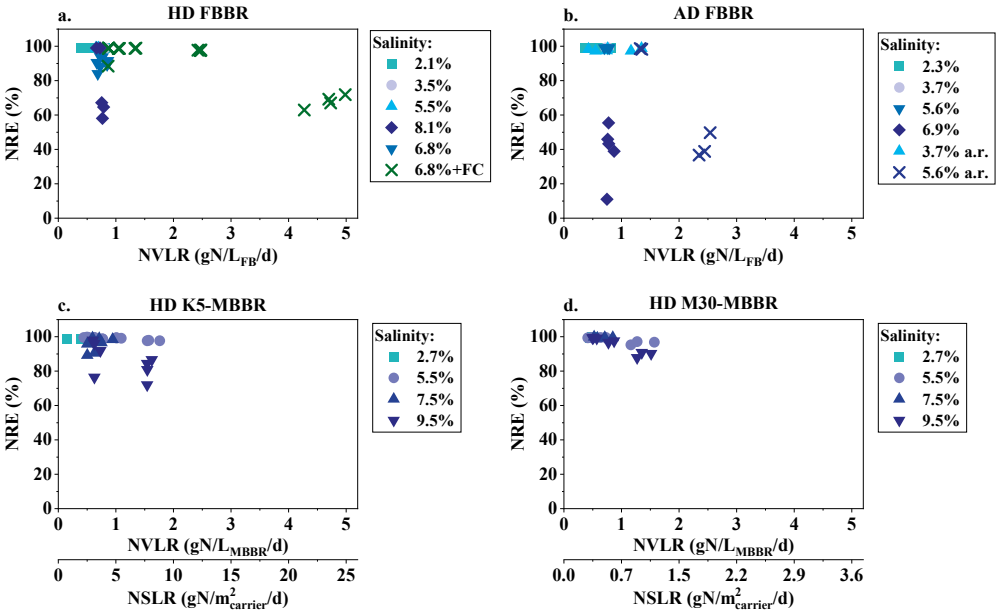

Figure 6. FBBRs and MBBRs nitrogen removal performances comparison at different salinities. a.) Heterotrophic FBBR (HDFBBR), b.) Autotrophic MBBR (ADFBBR), c.) Heterotrophic MBBR with hollow-body carrier (HD K5-MBBR), d.) Heterotrophic MBBR with porous-body carrier (HD M30-MBBR). The legends show the salinity conditions in the tested temporal order. Periods of recovery were not included.

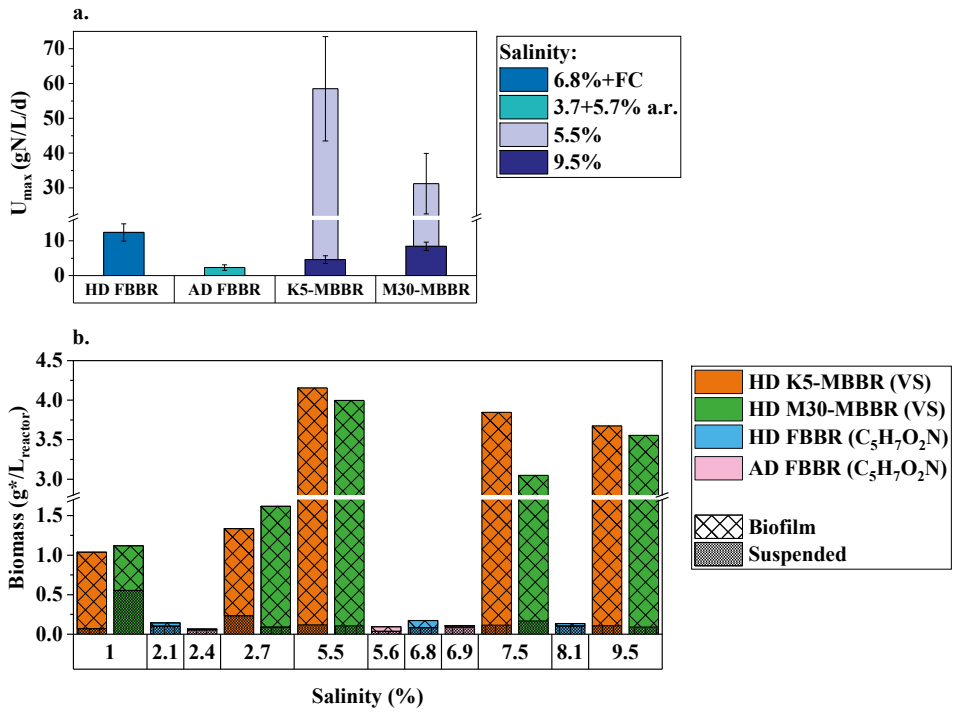

Figure 7. Maximum denitrification rate from the S-K model (U_{max}) (a) and biomass concentration (b) for all the biofilm reactors tested. a) error bars represent standard error resulting from the model fitting, b.) only the highest concentration for each salinity condition is shown. *gVS or $gC_5H_7O_2N$.

4.2.2 Role of biofilm carriers in reactor performance and biomass protection

Biomass retainment was considerably different in the FBBRs and MBBRs (Figure 7b). Considering the conditions with the highest biofilm biomass concentrations, the values in the MBBR (gVS/L) were around 45 times those in the FBBR ($gC_5H_7O_2N/L$), explaining the superior performance of MBBRs. The concentration difference was such that it indicated the higher biomass retention capacity as biofilm for the MBBR, despite the different biomass determination method used for the reactors and the difficulty in detaching all the biofilm from GAC. For instance, when calculating the heterotrophic biomass quantity per protected surface area of the reactor carriers, this resulted in biofilm densities of $8 \cdot 10^{-7}$ $gC_5H_7O_2N/m^2$, 20 gVS/m^2, 2.8 gVS/m^2 for the HDFBBR, K5-MBBR and M30-MBBR, respectively. Hence, the hollow-body carrier in

the MBBR showed the highest biofilm density, resulting also in the highest denitrification rate capacity and activity per single carrier.

At 7.5% salinity, in the K5-MBBR with the hollow-body carrier, the biofilm started to visually detach as regular segments from the plastic (Figure 8a), possibly due to biofilm shrinkage and expansion caused by osmotic pressure variations (Liu et al., 2020) as well as salts electrostatic interferences with biofilm-surface cohesion (Chen and Stewart, 2000; Simões et al., 2005). The biofilm growing in the large hollows of the hollow-body carriers was more exposed not only to substrate, showing higher removal rates at 5.5% salinity, as reported at 2.8% salinity by Dupla et al. (2006), but also to salinity, resulting in higher inhibition (lower NRE) and detachment. In the porous-body carrier, the detachment was not microscopically so evident and possibly involved mainly the outer layer of biofilm, while the biofilm growing in the pores remained mostly undisturbed and less exposed to substrate and salinity (Figure 8b), resulting in lower inhibition and a more stable removal efficiency at 9.5% salinity.

Therefore, the exposure of the biofilm to the inhibitors in the liquid phase becomes a crucial aspect for the choice of the carrier. Such exposure depends on the biofilm structure (density, porosity and thickness) as well as on the carrier structure and shear stress. In the porous GAC used in the FBBR, the micropores could store and provide a protective environment for the microorganisms against salinity, but the amount and thickness of the biofilm is limited by the small-sized grains as well as the high friction forces (Özkaya et al., 2019). GAC had also two side effects in the FBBRs. First, it interfered with the activity of the autotrophic biomass before the attachment (Publication II, Supplementary Materials), resulting in a longer startup time for ADFBBR than HDFBBR. Then, in both FBBRs, GAC adsorbed some $S_2O_3^{2-}$ from the liquid phase, which could have a beneficial effect for the removal of other pollutants than N compounds from industrial wastewaters.

The PE carriers used in MBBRs, had a visually thicker biofilm than GAC, enabling higher denitrification rates but also protection against salinity, with higher protection in the pores of M30-MBBR carriers. Such observations lay the foundation for the optimisation of denitrification in MBBRs under salinity stress via carrier selection based on the salinity concentration, with hollow-body carriers showing more suitability for high-rate denitrification at salinities <7.5%, and porous-body carriers providing more stable removal performance at higher salinities.

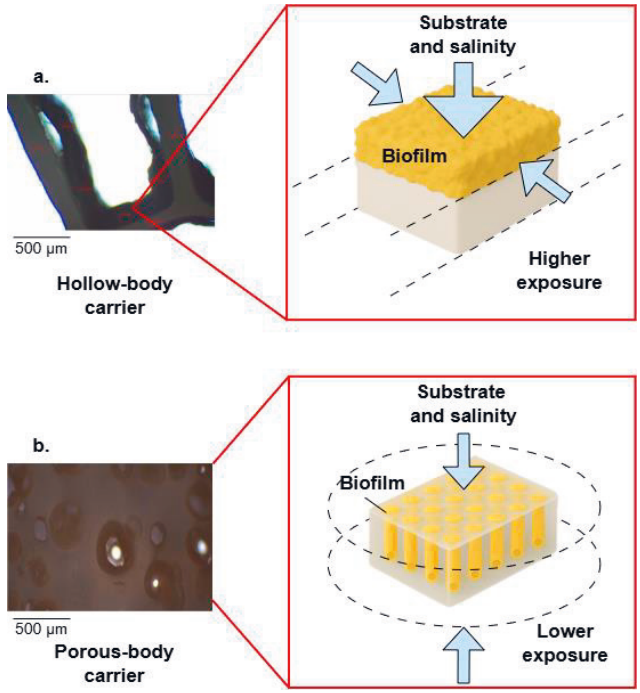

Figure 8. Differences in biofilm detachment and exposure to substrate and salinity in the hollow-body biofilm carrier (a.) and the porous-body biofilm carrier (b.). On the left, microscopic pictures (40x) of the two carriers at 7.5% salinity, on the right a scheme illustrating the exposure of the biofilm to salinity and substrate.

Part of the biomass in the reactor was also suspended in the liquid phase. In both MBBRs with a mature biofilm, the suspended biomass was <6% of the total biomass, and the main denitrification activity was demonstrated to be mainly in the biofilm (Publication III, Supplementary materials). For the HDFBBR, the suspended biomass was in all the measurements ≥49% of the total biomass in the reactor, indicating that it likely played an important role in denitrification. Such observation would require considering also the liquid phase volume in the rate calculation of the FBBR, which is usually calculated based on the volume of the fluidised bed. For example, in the best removal performance of HDFBBR at 6.8% salinity, this would result in a reactor HRT of 6.2 h and a volumetric removal rate of 0.9±0.1 gN/L/d, against the fluidised-bed-based values of 2.2 h and 2.4±0.1 gN/L/d. Thus, in this study, the MBBR would outperform the FBBR for denitrification under salinity stress.

4.2.3 Microbial community dynamics with salinity changes

Methanol-driven denitrifying communities were characterised by a certain stability in both MBBRs and FBBR (Figure 9a, c and d). Despite the loss of some genera at 5.5% salinity in the MBBRs, the main denitrifying genera (*Methylovorus*, *Paracoccus*, *Hyphomicrobium*, *Proteiniphilum* etc.) continued to dominate the biofilm community up to 9.5% salinity, and the changes were due to other less abundant genera. Similarly, in the HDFBBR, no major changes due to salinity were observed in the biofilm methanol-driven community (*Methylovorus*, *Paracoccus*, *Aquamicrobium*, *Proteiniphilum* etc.). Possibly, the higher presence in the MBBRs of *Hyphomicrobium* and *Paracoccus*, both salt-tolerant genera (Labbé et al., 2003; Osaka et al., 2008; Rissanen et al., 2016), contributed to the higher salinity tolerance than in HDFBBR, together with the higher biomass retention. When foul condensate was used as electron donor in the HDFBBR, resulting in improved NRE, *Pseudomonas* and *Paracoccus* relative abundances increased. Interestingly, no microbial genera present in the foul condensate were enriched, and, in addition to methanol, other organic compounds in the foul condensate (acetone, dimethyl sulphide, dimethyl disulphide, methanethiol and ethanol) were also consumed (Publication II, Supplementary materials). Therefore, the complex mixture of electron donors in the foul condensate stimulated the community and promoted denitrification under salinity stress, similarly to what observed for sludge fermentation liquid (Zhang et al., 2020). Overall, the stability of methanol-driven denitrification, reported also by others and likely due to the limited number of methylotrophs tolerant to hypersaline conditions (Labbé et al., 2003; Osaka et al., 2008; Rissanen et al., 2016), is a possible advantage for the stability of the process in industrial applications.

In ADFBBR, after the inoculation of a pure culture of *T. denitrificans*, more genera became enriched, likely from tap-water, during the operations (Figure 9b). Despite the presence of other S-utilising capable genera like *Paracoccus* and *Pseudomonas* (Chen et al., 2013; Cui et al., 2019), *T. denitrificans* had the main role in autotrophic denitrification, and when it was inhibited at 6.9% salinity, the whole process declined. The denitrification activity was then recovered, showing the resilience of the system, but the central role in denitrification of only one microorganism (*T. denitrificans*) is a disadvantage in terms of process performance and stability.

In the suspended phase, microbial communities were similar to those in the biofilm (Figure 9). Therefore, biofilm acted as a source of biomass for the liquid phase,

facilitating also the recovery of the ADFBBR by retaining and protecting *T. denitrificans.* Such protection of the community in the biofilm was also seen in the MBBRs, where the quantity of suspended biomass was considerably lower than in the biofilm (Figure 7b).

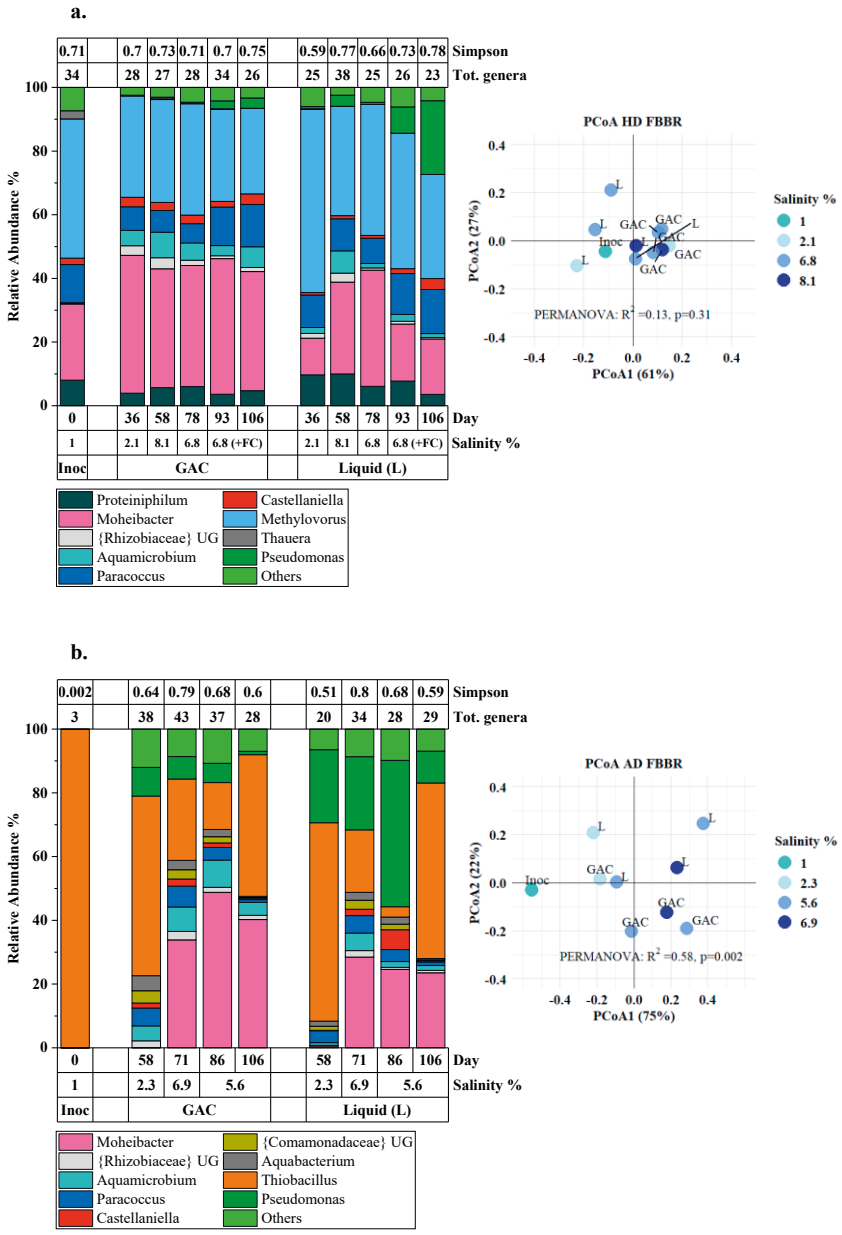

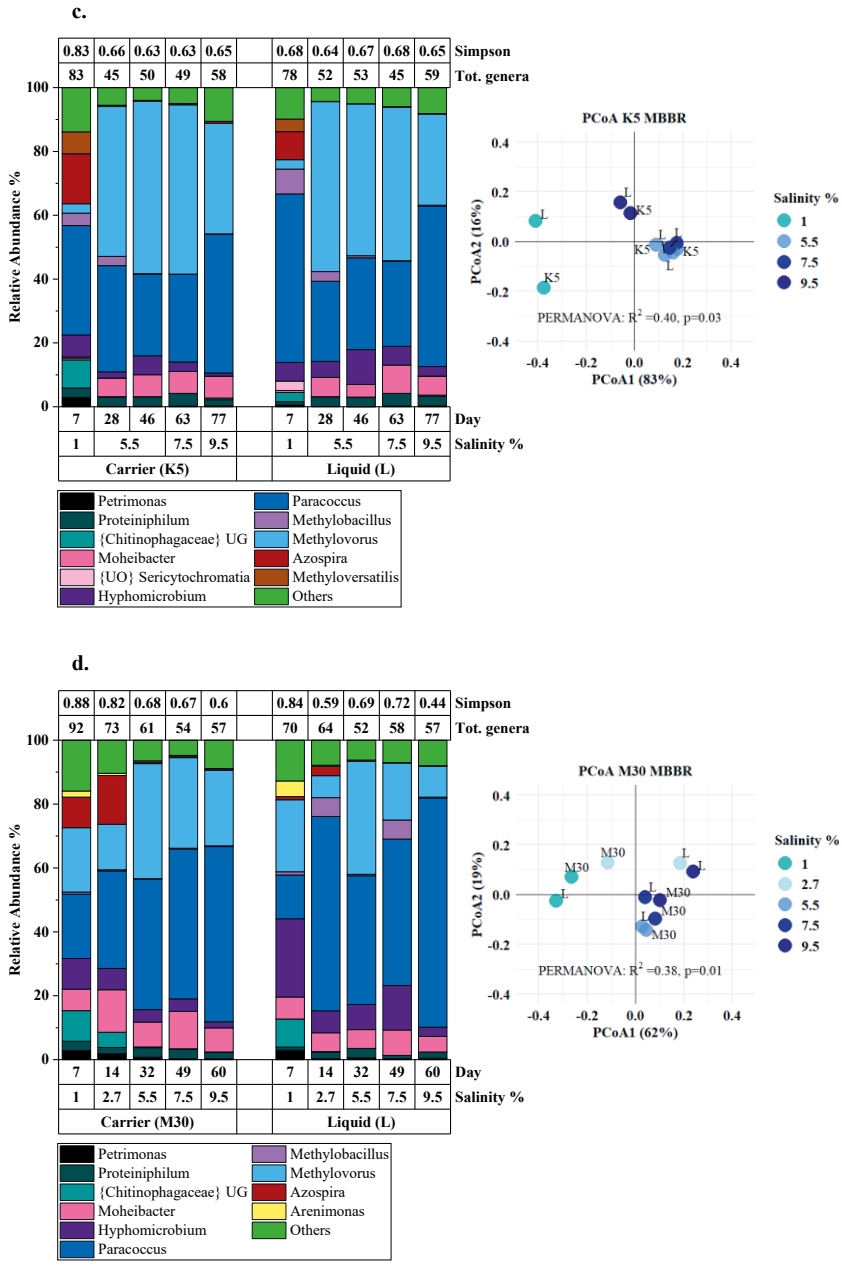

Figure 9. Microbial community dynamics in terms of relative abundance changes at different salinity conditions in the biofilm reactors. a.) Heterotrophic FBBR (HDFBBR), b.) Autotrophic MBBR (ADFBBR), c.) Heterotrophic MBBR with hollow-body carrier (HD K5-MBBR), d.) Heterotrophic MBBR with porous-body carrier (HD M30-MBBR). The genus "Others" refer to the sum of genera below 2.5% relative abundance. Modified from Publications II and III.

4.2.4 Modelling of salinity inhibition on denitrification kinetics in biofilm

The inhibited denitrification rate, measured in the NUR batch tests at different salinities with the two MBBRs, was modelled by adding an apparent inhibition factor μ_{inhib} for nitrate removal rate, which incorporates mass diffusion phenomena but is based on bulk concentration measurements (Plattes et al., 2006). Similarly, nitrite accumulation was simulated by calibrating an apparent K_{NO2}, as done by Y. Wang et al. (2016).

The model reproduced well the denitrification rates observed in the tests when the biofilm was mature (5.5-9.5% salinity) (Figure 10). In the tests at 1 and 2.7% salinity, the suspended biomass had still an important role in denitrification and the model showed its limits in discerning between biofilm and biomass contribution and inhibition, as suggested by the consistency test. The sensitivity analysis (Figure 10) showed that the half-inhibition constant K_I had significant influence (S>0.25) in both reactors at 9.5% salinity. With the porous-body carrier (M30-MBBR), the influence of biofilm thickness (L) and specific surface area (SSA) were higher than K_I, suggesting that in the modelling of high surface area carriers these parameters play a more important role. The determination of these parameters was possible for the hollow-body carrier also considering the detachment of biofilm due to salinity. However, for the porous carrier, the values were assumed (SSA) and calibrated (L) due to the challenge in their determination. (Publication III)

The half-inhibition constant K_I, obtained from the modified Hill's model from the NUR tests, includes also the protective effect of the biofilm, resulting in overall higher values (Figure 10) than observed for the suspended biomass tests (Figure 5), where it depended only on the microorganisms. The stability of the methanol-driven denitrifying community made possible to assume that kinetic and salinity parameters did not change during the reactors' operation, and hence, the same values were adopted in all the NUR tests simulations.

Overall, this is the first report of salinity inhibition modelling in biofilm reactors with different carrier typologies. The implementation of an apparent inhibition factor and an apparent half-saturation constant showed promising results for predicting salinity inhibition on an established denitrifying biofilm on MBBR carriers. Limits of such approach are the difficulty of discerning between biofilm and suspended biomass inhibition and representing inhibitory processes internal to the biofilm. Further

research is required to develop inhibition functions targeted to NO_2^- and N_2O reduction steps, as well as biomass detachment due to salinity, before modelling continuous flow operation.

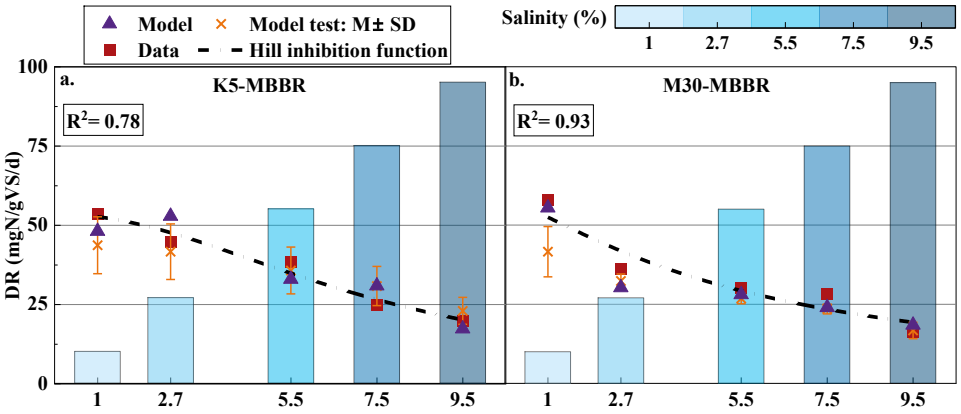

Input		K5-MBBR					M30-MBBR				
Parameter	**Determ. method**	**1**	**2.7**	**5.5**	**7.5**	**9.5**	**1**	**2.7**	**5.5**	**7.5**	**9.5**
μ_{max} (1/d)	Experimental	2.04					1.33				
Y (mgCOD/mgCOD)	Experimental	0.1					0.2				
K_I (g salt/L), n(-)	Experimental	74.4, 2.06					55.6, 1.3				
K_{NO2} (mgN/L)	Calibrated	4	4	4	4	250	70	4	20	25	550
AVS (g)	Measured	2.4	2.7	9.8	7.3	8.7	1.4	3.7	9.5	7	8.4
SSA (m^2/m^3)	Calib./Est./Assum.	800	800	800	600	600	5500				
L (μm)	Calib./Est.	200	200	350	250	275	100	150	200	175	200

S	Sensitivity Analysis K5-MBBR					Sensitivity Analysis M30-MBBR				
Salinity (%)	L	SSA	K_I	μ_{max}	Y	L	SSA	K_I	μ_{max}	Y
2.7	0.14	0.14	0.14	1.01	1.22	0.73	0.73	0.21	1.02	1.37
9.5	0.56	0.59	0.77	1	1.19	0.91	0.92	0.42	1	1.44

Figure 10. Results of the denitrification rate (DR) inhibition modelling with Sumo©22 software, input parameters and sensitivity analysis results for the two reactors (K5-MBBR and M30-MBBR). "Model test" refers to the consistency test. Modified from Publication III.

4.3 Potential of pre-denitrification of saline wastewaters: case of NO_x-SO_2 scrubber wastewater in pulp mills

The potential of autotrophic and heterotrophic denitrification for the treatment of scrubber wastewater in pulp mills was evaluated by testing real NO_x-SO_2 scrubber wastewater for both suspended and attached biomass.

In the batch test with suspended biomass, both autotrophic and heterotrophic denitrification were initially inhibited by the scrubber wastewater, if compared to the control conditions, but eventually removed all the nitrate (Figure 11a). In the semi-batch test for heterotrophic denitrification in the MBBRs (Publication III), the biofilm was gradually exposed to wastewaters coming from the three different stages of the NO_x-SO_2, starting from the less concentrated (stage III) and ending with the most concentrated (stage II). Regardless of the carrier (K5 or M30), stage II wastewater (1.9 Cl^-, 27 Na^+, 50 SO_4^{2-}, 0.4 K^+ g/L) was the most inhibitory, but the biomass remained active and eventually NO_x^--N was removed in all the wastewaters (Figure 11b). The main inhibitor, as reported by Koenig and Liu (2004) for FGD scrubber wastewater, was likely salinity, given the low concentration of metals (Publications I, III). In a real case, the effluents from the scrubber stages would be mixed and stage II wastewater share would be the highest. Unexpectedly high concentrations of DOC (~2 g/L) were measured in stage II wastewater (Publication III), possibly coming from impure scrubbing chemicals rather than the flue gases. These could provide a multi electron donor source in addition to methanol, but their presence is unpredictable and the affinity and possible inhibition of the organic compounds for denitrification were not investigated separately.

In both suspended biomass and biofilm tests with the real scrubber wastewater, methanol or thiosulphate were added as external electron donors and supported denitrification. In view of a more sustainable approach that could enable savings on chemical addition costs, evaporator foul condensate was added (12-15% v/v), replacing pure methanol, as electron donor in the influent of the HDFBBR test with simulated scrubber wastewater (Publication II). Not only foul condensate supported denitrification, but it also promoted it (Section 4.2.3), reducing NO_2^- accumulation in the effluent (Figure 11c). Moreover, in the same system, also $S_2O_3^{2-}$ was partially removed via adsorption and bio-oxidation, thus achieving the removal of multiple pollutants (Publication II).

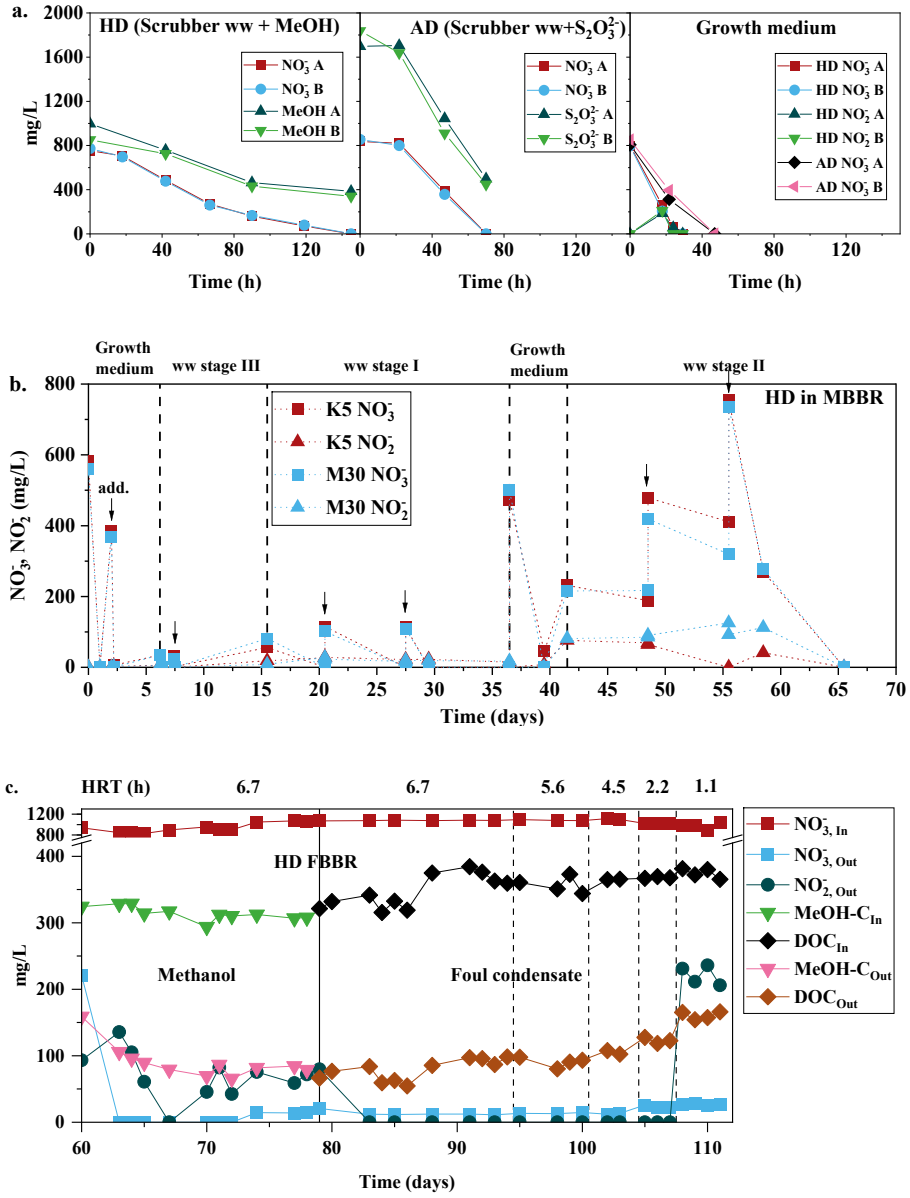

Figure 11. Potential of scrubber wastewater denitrification in pulp mills: a.) Real scrubber wastewater batch test with suspended biomass for both heterotrophic (HD) and autotrophic (AD) denitrification with addition of electron donor, b.) Real scrubber wastewater semi-batch test with attached biomass on two different carriers (K5 and M30) in MBBRs for HD (arrows indicate re-addition of substrates), c.) Results of denitrification of simulated scrubber wastewater with real foul condensate supplementation as electron donor from the heterotrophic FBBR at 6.8% salinity. Modified from Publications I, II and III.

The results obtained are promising for an integrated NO_x removal system from flue gases (scrubber) produced by the recovery boiler and the consequently generated wastewater (pre-denitrification reactor). The foul condensate generated by the evaporation of the black liquor, during the same chemical recovery process, could act as electron donor for the denitrification of the scrubber wastewater (Figure 12). The implementation of a specific pre-denitrification system for the N-laden scrubber wastewater prior to the overall pulp mill wastewater treatment, not optimised for NO_x^- removal (Ashrafi et al., 2015), could present a more favourable solution than modifying the existing plant or just diluting the NO_x^- concentration with the overall wastewater (Publication II). As demonstrated in this study, a high rate treatment performance providing improved tolerance to inhibition could be achieved for example by an MBBR, a known technology in pulp mills (Matheus et al., 2021). The NH_4^+ present in the foul condensate (and occasionally in the same scrubber wastewater depending on urea addition in the recovery boiler) would serve as assimilatory N source for the biomass in the pre-denitrification treatment, while P would need to be supplemented. Eventually, based on the salinity level expected in the scrubber wastewater, the biofilm carrier could be selected accordingly, but further research at pilot scale is required to assess the technical and economic feasibility of the NO_x-SO_2 scrubber wastewater pre-treatment process.

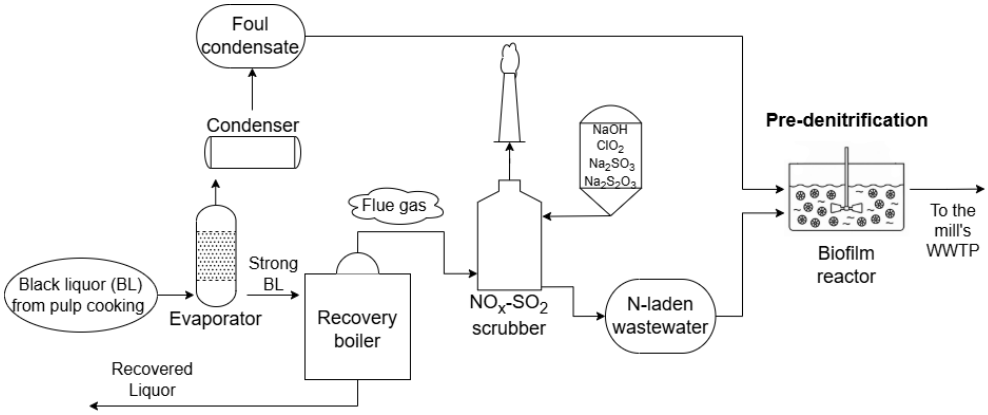

Figure 12. Simplified process flow diagram of a possible NO_x air-water integrated treatment in pulp mills.

4.4 Operational implications for biofilm reactors and potential limitations of this study

The potential of the FBBR and MBBR in treating saline wastewaters was demonstrated in this study, in terms of tolerated salinity, loading rates and stability of the process. In general, salinity inhibition causes a predictable decrease in the denitrification rate (Hill's function). Thus, when the inhibition causes the accumulation of NO_x^- in the effluent, increasing the reactor's HRT could represent a stabilization measure to obtain complete nitrogen removal, requiring, in turn, controlling the influent flow rate and increasing the treatment system space footprint, e.g. with equalisation tanks.

The knowledge of the influent wastewater's salinity range becomes a key factor for the selection of the biofilm carrier typology in MBBRs and its optimisation. Hollow-body carriers could be optimal for wastewaters with moderate salinity and high substrate loading rates (e.g., food and mariculture industries), while porous-body carriers could guarantee protection against higher salinities with more stable substrate removal (e.g., petrochemical, oil and gas industries, desalination plants) (Publication III). Despite demonstrating the high-rate treatment solution offered by biofilm reactors in this study, the potential deterioration of the process' denitrification performance remains to be determined on the long term (6-12 months) prior to real scale application. Key aspects like the phenomena of biofilm detachment and denitrification intermediates accumulation due to salinity require mechanistic and mathematical formulations for the comprehensive understanding, modelling and prediction of the process.

Moreover, the selection of the carrier affects also the operational parameters such as the number of pieces as well as mixing velocity (i.e., material costs and energy consumption) to keep the carriers adequately distributed in the reactor volume. For example, to achieve similar volumetric removal rates, more pieces of the porous-body carrier were needed if compared to the hollow-body carrier. On the other hand, the movement of the hollow-body carriers was more affected by the highly saline (9.5%) water buoyancy, which caused the carriers to distribute mainly in the upper part of the reactor. In this case, the use of an increased density plastic represents a possible solution for adequate mobility (Publication III). Nonetheless, regardless of the carrier, to guarantee a sufficient nitrogen removal performance together with adequate

salinity tolerance, the amount and thickness of the biofilm should be controlled at an optimal value, for example via mixing velocity.

As for the attached biomass determination, in Publication III, the AVS/ATS ratio in both MBBR carriers was averagely 0.32-0.35, indicating the high presence of inorganic precipitates, such as calcium carbonate and phosphate (Gonzalez-Martinez et al., 2015; Goode and Allen, 2011). Thus, to avoid large overestimations of the biomass, it is suggested that in multi-ionic hypersaline wastewaters, AVS should be preferred to ATS, which is commonly used with biofilm carriers. However, the challenges of this approach became most evident in this study when detaching the biofilm from the pores of the porous-body carrier, leaving room for some uncertainty in the AVS determination (Publication III, Supplementary Materials).

In the case of the FBBR, high removal rates and a compact volume are among the main strengths. Theoretically, at the same influent flow rate, the FBBR requires lower reactor volumes than the MBBR, given the highly efficient mass transfer in a smaller volume. However, in this study, the suspended biomass quantity was comparable with the attached one in the FBBR, possibly playing an important role in the removal process. Thus, the role of the suspended biomass should always be determined for more accurate rate calculations and consequent dimensioning. Also, given the difficulty in detaching the whole biofilm from the pores, the determination of the attached biomass quantity on the GAC was subjected to uncertainty (Publication II). The possible underestimation of attached biomass is crucial to be addressed for accurate biofilm specific activity and salinity inhibition function determination, especially when dealing with highly porous carriers.

The functional but limited biofilm quantity and thickness, if compared to MBBR, might restrain the FBBR process' tolerance to salinity, but, in turn, the clogging problem of the carriers is better controlled. On the other hand, to guarantee the fluidisation of the carrier bed, a high recirculation flow rate is required. For instance, in this study, the recirculation flow was >100 times the influent flow rate, highlighting the pumps' energy requirement for real scale applications. Moreover, abrasion of GAC, as suggested by the blackish residue in the effluent, was observed in the FBBR (Publication II). This aspect must be considered on the long term for real scale reactors where the recirculation flow is considerable, as the GAC might require replacement and the effluent purification from the solid residue.

Eventually, methanol-driven denitrification demonstrated a certain stability in the process of both FBBR and MBBR, showing stable NREs under moderate salinity inhibition and in many cases recovering promptly after stronger inhibition with all the carriers tested (Publication II and III). On one hand, as suggested by Kruglova (2018), possible overlooked changes in the microbial community due to salinity could result in a misinterpretation of the data, such as in the linkage carrier-salinity-NRE or the stability of denitrification in this study. On the other, although the continuous flow reactors tests were not duplicated in this study, the denitrifying microbial community composition at genus level, as also indicated by PCoA and Permanova analyses, did not change significantly during the reactor operations (HDFBBR or MBBRs) and among different reactors (K5-MBBR and M30-MBBR). Therefore, it can be assumed that the different reactor performances were likely due to operational factors, such as the carrier typology, rather than shifts in the microbial community. Such community stability can be beneficial for the stability of the process itself and an advantage of using methanol-driven denitrification. Thus, in real scale applications, where the environmental conditions might fluctuate more than in a controlled laboratory-scale reactor, the stability of the denitrifying community under salinity stress should be monitored to better understand the causes of a possible deterioration in denitrification performance.

5 CONCLUSIONS

This study performed a systematic analysis on autotrophic and heterotrophic denitrification under salinity stress to develop biofilm reactors for the treatment of saline wastewaters. The tolerance of methanol-driven and of thiosulphate-driven denitrification to single ions and to multi-ionic stress was revealed on suspended microorganisms and biofilm. FBBR and MBBR were studied for an improved salinity tolerance and their denitrification performance compared to achieve the process optimisation via reactor, biofilm carrier and electron donor selection. Also, a possible strategy to model denitrification kinetics under salinity inhibition in biofilms was proposed.

Methanol-driven denitrification by an enriched mixed culture shows higher tolerance to all the pairs of ions tested (NaCl, Na_2SO_4, KCl and K_2SO_4) than thiosulphate-driven denitrification dominated by *T. denitrificans*, with both the specific toxicity of the salt ions and the osmotic pressure playing roles in inhibition. Chloride ion has the highest inhibitory effect on denitrification, demonstrating potential for treatment of saline wastewaters where Na^+ and SO_4^{2-} are the main inorganic ions.

In the biofilm reactors, heterotrophic denitrification shows superior removal rates at higher salinity (2.4 gN/L/d at 6.8%) than autotrophic (1.2 gN/L/d at 5.6%). Thiosulphate-driven denitrification has potential for the treatment of saline wastewaters, also recovering from inhibition, but the stability of the process should be improved, for example by testing mixotrophic denitrification in MBBR. Thus, a methanol-driven nitrogen removal process is preferrable to a thiosulphate-driven one, when methanol is easily available. Nevertheless, the salinities tolerated by the process in both FBBR and MBBR are among the highest reported in literature for both methanol- (up to 9.5%) and thiosulphate- (5.6%) driven denitrification, showing that biofilm reactors provide a protective environment for the microorganisms and represent a valid strategy for improved process' tolerance, enabling a startup with microorganisms with non-saline history.

For methanol-driven denitrification, the MBBR provides higher salinity tolerance, reaching ≥70% nitrogen removal efficiency at 9.5% salinity, while it remains ≥58% in the FBBR at 8.1% salinity. The FBBR has higher volumetric nitrogen removal rates (2.4 gN/L/d) than the MBBR (up to 1.6 gN/L/d), but the potential denitrification capacity of the MBBR is higher, due to higher biomass retention. Eventually, in both reactors, the main methanol-driven denitrifying community remains stable in the biofilm even at the higher salinities, providing stability to the process. Overall, considering also the simpler operational mode, the MBBR provides a more robust design for denitrification under salinity stress than the FBBR.

The GAC in FBBR provides protection to the biofilm within the pores, but the retained biomass quantity and biofilm thickness are limited, and the abrasion of the carrier must be considered on the long-term. The PE carriers in the MBBRs enable higher biofilm quantity and thickness than GAC. The hollow-body carrier allows high-rate denitrification at salinity <7.5%, with a more exposed biofilm in the large cavities, while the porous-body carrier enables more stable nitrogen removal at salinity ≥7.5%, with a less exposed biofilm within the pores. Such findings outline the potential of an optimised denitrification performance in MBBR by selecting a suitable carrier based on the salinity concentration.

The implementation of apparent kinetic inhibition factor and half-saturation constant to include salinity inhibition in an existing biofilm model, as proposed in this work, is a potential strategy for a simplified approach that enables prediction of denitrification process tolerance to salinity. The model reproduced well the denitrification rates at different salinities and with both hollow- and porous-body carriers, but to comprehensively simulate a continuous flow denitrification process, inhibitory functions describing nitrite and nitrous oxide accumulation and reduction, as well as the effect of salinity on biofilm detachment need to be included in the model.

In practice, biofilm reactors can be optimised by a suitable carrier selection, and thus, can provide a high-rate denitrification technology for saline industrial wastewater treatment, such as NO_x-SO_2 scrubber wastewater in pulp mills. The potential of denitrification in treating this wastewater is demonstrated, pointing towards continuous flow tests in biofilm reactors as the next research step. Moreover, the use of a non-inhibitory waste stream containing a mixture of organic compounds, like pulp mill foul condensate, as electron donor for heterotrophic denitrification, enhances the

denitrification performance under salinity stress, while achieving a multi pollutants removal technology.

In conclusion, this study contributes to the optimisation of biological treatments to reduce the nitrogenous emissions from industries to the environment. Methanol-driven and thiosulphate-driven denitrification have potential for nitrate removal under multi-ionic salinity stress, and biofilm reactors represent a valid strategy for their improved performance. The observations on biofilm reactors made in this study are useful also when dealing with other inhibitors of biological processes. Future investigations towards a pilot scale pre-denitrification biofilm reactor should be performed on the long-term, focusing on biofilm detachment caused by salinity, which could negatively affect the process, and harmful N_2O emissions possibly resulting from denitrification inhibition, as well as on testing carriers with both pores and hollows for a balanced performance in the presence of salinity fluctuations. A cost-benefit analysis is also required to evaluate the economic feasibility of the pre-denitrification step, including the benefit offered by using other waste streams as supplement, not only in pulp mills but also in other industrial sectors. This would enable the cost-effectiveness of the optimised technology for a sustainable mitigation of environmental pollution from human activities.

REFERENCES

Acar, C., Dincer, I., 2019. Review and evaluation of hydrogen production options for better environment. Journal of Cleaner Production 218, 835–849. https://doi.org/10.1016/j.jclepro.2019.02.046

Ahmed, M.H., Buzby, K., Finklea, H., Hodges, C., Amos, M., Seats, P., White, N., Rutnik, C., Siefert, N., Lin, L.-S., 2024. Co-treating flue gas desulfurized effluent and produced water enables novel waste management and recovery of critical minerals. Desalination 585, 117782. https://doi.org/10.1016/j.desal.2024.117782

Aminzadeh, B., Torabian, A., Azimi, A.A., Nabi Bidhendi, G.R., Mehrdadi, N., 2010. Salt inhibition effects on simultaneous heterotrophic/ autotrophic denitrification of high nitrate wastewater. International Journal of Environmental Research 4, 255–262. https://doi.org/10.22059/ijer.2010.17

An, N., Ma, L., Lian, D., Wang, S., 2024. Effect of salinity on denitrification, membrane fouling and bacterial community in a fixed-bed biofilm membrane reactor. Water Science and Technology 89, 1124–1141. https://doi.org/10.2166/wst.2024.050

Ashrafi, O., Yerushalmi, L., Haghighat, F., 2015. Wastewater treatment in the pulp-and-paper industry: A review of treatment processes and the associated greenhouse gas emission. Journal of Environmental Management 158, 146–157. https://doi.org/10.1016/j.jenvman.2015.05.010

Badshah, M., Parawira, W., Mattiasson, B., 2012. Anaerobic treatment of methanol condensate from pulp mill compared with anaerobic treatment of methanol using mesophilic UASB reactors. Bioresource Technology 125, 318–327. https://doi.org/10.1016/j.biortech.2012.08.109

Betlach, M.R., Tiedje, J.M., 1981. Kinetic Explanation for Accumulation of Nitrite, Nitric Oxide, and Nitrous Oxide During Bacterial Denitrification. Appl Environ Microbiol 42, 1074–1084. https://doi.org/10.1128/aem.42.6.1074-1084.1981

Blázquez, E., Baeza, J.A., Gabriel, D., Guisasola, A., 2019. Treatment of real flue gas desulfurization wastewater in an autotrophic biocathode in view of elemental sulfur recovery: Microbial communities involved. Science of the Total Environment 657, 945–952. https://doi.org/10.1016/j.scitotenv.2018.12.037

Bogacki, J., Marcinowski, P., Majewski, M., Zawadzki, J., Sivakumar, S., 2018. Alternative approach to current EU BAT recommendation for coal-fired power plant flue gas desulfurization wastewater treatment. Processes 6, 9–13. https://doi.org/10.3390/pr6110229

Boltz, J.P., Daigger, G.T., 2010. Uncertainty in bulk-liquid hydrodynamics and biofilm dynamics creates uncertainties in biofilm reactor design. Water Science and Technology 61, 307–316. https://doi.org/10.2166/wst.2010.829

Bremer, E., Krämer, R., 2019. Responses of Microorganisms to Osmotic Stress. Annual Review of Microbiology 73, 313–334. https://doi.org/10.1146/annurev-micro-020518-115504

Brown, B.P., Brown, S.R., Senko, J.M., 2012. Microbial communities associated with wet flue gas desulfurization systems. Front. Microbiol. 3. https://doi.org/10.3389/fmicb.2012.00412

Cabrera, M.N., 2017. Pulp Mill Wastewater: Characteristics and Treatment, in: Biological Wastewater Treatment and Resource Recovery. IntechOpen. https://doi.org/10.5772/67537

Cang, Y., Roberts, D.J., Clifford, D.A., 2004. Development of cultures capable of reducing perchlorate and nitrate in high salt solutions. Water Research 38, 3322–3330. https://doi.org/10.1016/j.watres.2004.04.020

Cao, X., Qian, D., Meng, X., 2013. Effects of pH on nitrite accumulation during wastewater denitrification. Environmental Technology (United Kingdom) 34, 45–51. https://doi.org/10.1080/09593330.2012.679700

Carrera, J., Jubany, I., Carvallo, L., Chamy, R., Lafuente, J., 2004. Kinetic models for nitrification inhibition by ammonium and nitrite in a suspended and an immobilised biomass systems. Process Biochemistry 39, 1159–1165. https://doi.org/10.1016/S0032-9592(03)00214-0

Carrera, P., Strubbe, L., Río, A.V. del, Mosquera-Corral, A., Volcke, E.I.P., 2023. Modelling salinity effects on aerobic granular sludge treating fish-canning wastewater. Environ. Sci.: Water Res. Technol. 9, 747–755. https://doi.org/10.1039/D2EW00874B

Chen, B., Qaisar, M., Wang, K., Li, W., Cai, J., 2022. Response of simultaneous sulfide and nitrate removal process on acute toxicity of substrate concentration and salinity: Single toxicity and combined toxicity. Science of The Total Environment 836, 155639. https://doi.org/10.1016/j.scitotenv.2022.155639

Chen, B., Qaisar, M., Xiao, J., Li, W., Li, J., Cai, J., 2024. Strategy to mitigate salinization of sulfide-autotrophic denitrification: Sodium ion uptake from the environment and mutualistic symbiosis among microorganisms. Desalination 573, 117228. https://doi.org/10.1016/j.desal.2023.117228

Chen, C., Ho, K.-L., Liu, F.-C., Ho, M., Wang, A., Ren, N., Lee, D.-J., 2013. Autotrophic and heterotrophic denitrification by a newly isolated strain *Pseudomonas sp.* C27. Bioresource Technology, Special Issue: IBS 2012 & IFIBiop 145, 351–356. https://doi.org/10.1016/j.biortech.2012.12.027

Chen, Heng, Hou, D., Zhan, L., Li, Z., Zheng, S., Li, F., Chen, Haijie, Wu, H., Yang, L., 2023. A demonstration project for desulfurization wastewater evaporation technology: Field test and performance analysis. Journal of Water Process Engineering 53, 103874. https://doi.org/10.1016/j.jwpe.2023.103874

Chen, R., Zhang, T., Guo, Y., Wang, J., Wei, J., Yu, Q., 2021. Recent advances in simultaneous removal of SO_2 and NO_x from exhaust gases: Removal process, mechanism and kinetics. Chemical Engineering Journal 420. https://doi.org/10.1016/j.cej.2020.127588

Chen, S., Liu, C., Cao, G., Li, K., Huang, J., 2024. Effect of salinity on biological nitrogen removal from wastewater and its mechanism. Environ Sci Pollut Res 31, 24713–24723. https://doi.org/10.1007/s11356-024-32417-8

Chen, W., Qin, S., Yang, C., Long, K., Liang, S., Liu, H., Tan, S., Zhang, Q., 2024. Bioaugmentation using salt-tolerant bacteria in a dual-stage process for high-salinity wastewater treatment: Performance, microbial community, and salt-tolerance mechanism. Journal of Water Process Engineering 57, 104620. https://doi.org/10.1016/j.jwpe.2023.104620

Chin, T., Tam, I., Yin, C.-Y., 2023. Wet scrubbing process with oxidation and reduction in series for removal of SO_2 and NO from marine diesel engine exhaust. Chemical Engineering Journal 464, 142299. https://doi.org/10.1016/j.cej.2023.142299

Choi, M., Jeon, J., Park, S., Choi, D., Kwon, S., Bae, H., 2025. Impact of mixed carbon sources on microbial function and network structure in hypersaline denitrification. Bioresource Technology 426, 132366. https://doi.org/10.1016/j.biortech.2025.132366

Claus, G., Kutzner, H., 1985. Physiology and kinetics of autotrophic denitrification by *Thiobacillus denitrificans*. Applied Microbiology and Biotechnology 22, 283–288. https://doi.org/10.1007/BF00252031

Córdoba, P., 2015. Status of Flue Gas Desulphurisation (FGD) systems from coal-fired power plants: Overview of the physic-chemical control processes of wet limestone FGDs. Fuel 144, 274–286. https://doi.org/10.1016/J.FUEL.2014.12.065

Cordoba, P., Staicu, L.C., 2018. Flue gas desulfurization effluents: An unexploited selenium resource. Fuel 223, 268–276. https://doi.org/10.1016/j.fuel.2018.03.052

Corsino, S.F., Capodici, M., Di Pippo, F., Tandoi, V., Torregrossa, M., 2019. Comparison between kinetics of autochthonous marine bacteria in activated sludge and granular sludge systems at different salinity and SRTs. Water Research 148, 425–437. https://doi.org/10.1016/j.watres.2018.10.086

Corsino, S.F., Capodici, M., Torregrossa, M., Viviani, G., 2018. A comprehensive comparison between halophilic granular and flocculent sludge in withstanding short and long-term salinity fluctuations. Journal of Water Process Engineering 22, 265–275. https://doi.org/10.1016/j.jwpe.2018.02.013

Cortés-Lorenzo, C., Rodríguez-Díaz, M., López-Lopez, C., Sánchez-Peinado, M., Rodelas, B., González-López, J., 2012. Effect of salinity on enzymatic activities in a submerged fixed bed biofilm reactor for municipal sewage treatment. Bioresource Technology 121, 312–319. https://doi.org/10.1016/j.biortech.2012.06.083

Costa, O.Y.A., Raaijmakers, J.M., Kuramae, E.E., 2018. Microbial Extracellular Polymeric Substances: Ecological Function and Impact on Soil Aggregation. Front. Microbiol. 9. https://doi.org/10.3389/fmicb.2018.01636

Cui, Y.-X., Biswal, B.K., van Loosdrecht, M.C.M., Chen, G.-H., Wu, D., 2019. Long term performance and dynamics of microbial biofilm communities performing sulfur-oxidizing autotrophic denitrification in a moving-bed biofilm reactor. Water Research 166, 115038. https://doi.org/10.1016/j.watres.2019.115038

Cyplik, P., Piotrowska-Cyplik, A., Marecik, R., Czarny, J., Drożdżyńska, A., Chrzanowski, Ł., 2012. Biological denitrification of brine: the effect of compatible solutes on enzyme activities and fatty acid degradation. Biodegradation 23, 663–672. https://doi.org/10.1007/s10532-012-9542-0

Dahl, C., Sund, C., Kristensen, G.H., Vredenbregt, L., 1997. Combined biological nitrification and denitrification of high-salinity wastewater. Water Science and Technology 36, 345–352. https://doi.org/10.1016/S0273-1223(97)00407-1

De Lucas, A., Rodríguez, L., Villaseñor, J., Fernández, F.J., 2005. Denitrification potential of industrial wastewaters. Water Research 39, 3715–3726. https://doi.org/10.1016/j.watres.2005.06.024

Dhamole, P.B., Nair, R.R., D'Souza, S.F., Lele, S.S., 2007. Denitrification of high strength nitrate waste. Bioresource Technology 98, 247–252. https://doi.org/10.1016/j.biortech.2006.01.019

Di Capua, F., Papirio, S., Lens, P.N.L., Esposito, G., 2015. Chemolithotrophic denitrification in biofilm reactors. Chemical Engineering Journal 280, 643–657. https://doi.org/10.1016/j.cej.2015.05.131

Di Capua, F., Pirozzi, F., Lens, P.N.L., Esposito, G., 2019. Electron donors for autotrophic denitrification. Chemical Engineering Journal 362, 922–937. https://doi.org/10.1016/j.cej.2019.01.069

Dias, J.C.T., Rezende, R.P., Silva, C.M., Linardi, V.R., 2005. Biological treatment of kraft pulp mill foul condensates at high temperatures using a membrane bioreactor. Process Biochemistry 40, 1125–1129. https://doi.org/10.1016/j.procbio.2004.03.015

Dinçer, A.R., Kargi, F., 1999. Salt inhibition of nitrification and denitrification in saline wastewater. Environmental Technology (United Kingdom) 20, 1147–1153. https://doi.org/10.1080/09593332008616912

Dupla, M., Comeau, Y., Parent, S., Villemur, R., Jolicoeur, M., 2006. Design optimization of a self-cleaning moving-bed bioreactor for seawater denitrification. Water Research 40, 249–258. https://doi.org/10.1016/j.watres.2005.10.029

Dutta, K., Tsai, C.-Y., Chen, W.-H., Lin, J.-G., 2014. Effect of carriers on the performance of anaerobic sequencing batch biofilm reactor treating synthetic municipal wastewater. International Biodeterioration & Biodegradation, Challenges in Environmental Science and Engineering, CESE-2013 95, 84–88. https://doi.org/10.1016/j.ibiod.2014.04.021

Eldyasti, A., Nakhla, G., Zhu, J., 2012. Influence of particles properties on biofilm structure and energy consumption in denitrifying fluidized bed bioreactors (DFBBRs). Bioresource Technology, Advances in Biological Waste Treatment and Bioconversion Technologies 126, 162–171. https://doi.org/10.1016/j.biortech.2012.07.113

EPA, 2020. Federal Register: Steam electric reconsideration rule by environmental protection agency (EPA) [WWW Document]. URL https://www.federalregister.gov/documents/2020/10/13/2020-19542/steam-electric-reconsideration-rule (accessed 7.15.21).

EPA, 2015. Federal Register: Effluent limitations guidelines and standards for the steam electric power generating point source category [WWW Document]. URL https://www.federalregister.gov/documents/2015/11/03/2015-25663/effluent-limitations-guidelines-and-standards-for-the-steam-electric-power-generating-point-source (accessed 7.15.21).

EPA, 2011. Exhaust Gas Scrubber Washwater Effluent-800R11006. [WWW Document]. URL https://nepis.epa.gov/Exe/ZyPDF.cgi/P100DCMY.PDF?Dockey=P100DCMY.PDF

Eregowda, T., Kokko, M.E., Rene, E.R., Rintala, J., Lens, P.N.L., 2021. Volatile fatty acid production from Kraft mill foul condensate in upflow anaerobic sludge blanket reactors. Environmental Technology 42, 2447–2460. https://doi.org/10.1080/09593330.2019.1703823

Fan, W., Huang, X., Xiong, J., Wang, S., 2024. Salinity stress results in ammonium and nitrite accumulation during the elemental sulfur-driven autotrophic denitrification process. Front. Microbiol. 15. https://doi.org/10.3389/fmicb.2024.1353965

Fang, P., Tang, Z.J., Chen, X.B., Huang, J.H., Tang, Z.X., Cen, C.P., 2018. Chloride Ion Removal from the Wet Flue Gas Desulfurization and Denitrification Wastewater Using Friedel's Salt Precipitation Method. Journal of Chemistry 2018. https://doi.org/10.1155/2018/5461060

Feng, L., Sun, X., Wang, J., Xie, T., Wu, Z., Xu, J., Wang, Z., Yang, G., 2024. Performance and microbial mechanism in sulfide-driven autotrophic denitrification by different inoculation sources in face of various sulfide and sulfate stress. Bioresource Technology 413, 131443. https://doi.org/10.1016/j.biortech.2024.131443

Feng, L., Wu, G., Zhang, Z., Tian, Z., Li, B., Cheng, J., Yang, G., 2023. Improving denitrification performance of biofilm technology with salt-tolerant denitrifying bacteria agent for treating high-strength nitrate and sulfate wastewater from lab-scale to pilot-scale. Bioresource Technology 387, 129696. https://doi.org/10.1016/j.biortech.2023.129696

Fernández-Nava, Y., Marañón, E., Soons, J., Castrillón, L., 2010. Denitrification of high nitrate concentration wastewater using alternative carbon sources. Journal of Hazardous Materials 173, 682–688. https://doi.org/10.1016/j.jhazmat.2009.08.140

Flagiello, D., Erto, A., Lancia, A., Di Natale, F., 2023. Advanced exhaust-gas scrubbing for simultaneous de-SO_x/NO_x using a wet oxidative process with integrated washwater treatment. Chemical Engineering Research and Design 194, 731–741. https://doi.org/10.1016/j.cherd.2023.05.014

Foglar, L., Briški, F., 2003. Wastewater denitrification process - The influence of methanol and kinetic analysis. Process Biochemistry 39, 95–103. https://doi.org/10.1016/S0032-9592(02)00318-7

Galkaduwa, M.B., Hettiarachchi, G.M., Kluitenberg, G.J., Hutchinson, S.L., Davis, L., Erickson, L.E., 2017. Transport and Transformation of Selenium and Other Constituents of Flue-Gas Desulfurization Wastewater in Water-Saturated Soil Materials. Journal of Environmental Quality 46, 384–392. https://doi.org/10.2134/jeq2016.09.0335

Gall, D., Allgurén, T., Johansson, J., Normann, F., Hultén, A.H., Gunnarsson, A., Andersson, K., 2022. Recirculation of NO_x and SO_x Scrubber Effluent to an Industrial Grate Fired MSW Boiler─Influence on Combustion Performance, Deposition Behavior, and Flue Gas Composition. Energy & Fuels 36, 5868–5877. https://doi.org/10.1021/acs.energyfuels.2c00293

García-Roldán, A., de la Haba, R.R., Sánchez-Porro, C., Ventosa, A., 2024. 'Altruistic' cooperation among the prokaryotic community of Atlantic salterns assessed by metagenomics. Microbiological Research 288, 127869. https://doi.org/10.1016/j.micres.2024.127869

Gheewala, S.H., Pole, R.K., Annachhatre, A.P., 2004. Nitrification modelling in biofilms under inhibitory conditions. Water Research 38, 3179–3188. https://doi.org/10.1016/j.watres.2004.04.018

Gingerich, D.B., Grol, E., Mauter, M.S., 2018. Fundamental challenges and engineering opportunities in flue gas desulfurization wastewater treatment at coal fired power plants. Environmental Science: Water Research & Technology 4, 909–925. https://doi.org/10.1039/C8EW00264A

Gingerich, D.B., Mauter, M.S., 2020. Flue gas desulfurization wastewater composition and implications for regulatory and treatment train design. Environmental Science and Technology 54, 3783–3792. https://doi.org/10.1021/acs.est.9b07433

Gingerich, D.B., Sun, X., Behrer, A.P., Azevedo, I.L., Mauter, M.S., 2017. Spatially resolved air-water emissions tradeoffs improve regulatory impact analyses for electricity generation. Proceedings of the National Academy of Sciences of the United States of America 114, 1862–1867. https://doi.org/10.1073/PNAS.1524396114

Glass, C., Silverstein, J., 1999. Denitrification of high-nitrate, high-salinity wastewater. Water Research 33, 223–229. https://doi.org/10.1016/S0043-1354(98)00177-8

Glass, C., Silverstein, J., 1998. Denitrification kinetics of high nitrate concentration water: pH effect on inhibition and nitrite accumulation. Water Research 32, 831–839. https://doi.org/10.1016/S0043-1354(97)00260-1

Gonzalez-Martinez, A., Leyva-Díaz, J.C., Rodriguez-Sanchez, A., Muñoz-Palazon, B., Rivadeneyra, A., Poyatos, J.M., Rivadeneyra, M.A., Martinez-Toledo, M.V., 2015. Isolation and metagenomic characterization of bacteria associated with calcium carbonate and struvite precipitation in a pure moving bed biofilm reactor-membrane bioreactor. Biofouling 31, 333–348. https://doi.org/10.1080/08927014.2015.1040006

Goode, C., Allen, D.G., 2011. Effect of Calcium on Moving-Bed Biofilm Reactor Biofilms. Water Environment Research 83, 220–232. https://doi.org/10.2175/106143010X12780288628255

Guimerà, X., Mora, M., Dorado, A.D., Bonsfills, A., Gabriel, D., Gamisans, X., 2021. Optimization of SO_2 and NO_x sequential wet absorption in a two-stage bioscrubber for elemental sulphur valorisation. Environ Sci Pollut Res 28, 24605–24617. https://doi.org/10.1007/s11356-020-09607-1

Gupta, B., Gupta, A.K., Ghosal, P.S., Lal, S., Saidulu, D., Srivastava, A., Upadhyay, M., 2022. Recent advances in application of moving bed biofilm reactor for wastewater treatment: Insights into critical operational parameters, modifications, field-scale performance, and sustainable aspects. Journal of Environmental Chemical Engineering 10, 107742. https://doi.org/10.1016/j.jece.2022.107742

Han, X., Jin, Y., Yu, J., 2022. Rapid formation of aerobic granular sludge by bioaugmentation technology: A review. Chemical Engineering Journal 437, 134971. https://doi.org/10.1016/j.cej.2022.134971

Hao, Z.-L., Ali, A., Ren, Y., Su, J.-F., Wang, Z., 2022. A mechanistic review on aerobic denitrification for nitrogen removal in water treatment. Science of The Total Environment 847, 157452. https://doi.org/10.1016/j.scitotenv.2022.157452

Hasanzadeh, R., Abbasi Souraki, B., Pendashteh, A., Khayati, G., Ahmadun, F.-R., 2020. Application of isolated halophilic microorganisms suspended and immobilized on walnut shell as biocarrier for treatment of oilfield produced water. Journal of Hazardous Materials 400, 123197. https://doi.org/10.1016/j.jhazmat.2020.123197

He, H., Chen, Y., Li, X., Cheng, Y., Yang, C., Zeng, G., 2017. International Biodeterioration & Biodegradation In fl uence of salinity on microorganisms in activated sludge processes: A review. International Biodeterioration & Biodegradation 119, 520–527. https://doi.org/10.1016/j.ibiod.2016.10.007

Hiatt, W.C., Grady, C.P.L., 2008. An Updated Process Model for Carbon Oxidation, Nitrification, and Denitrification. Water Environment Research 80, 2145–2156. https://doi.org/10.2175/106143008X304776

Hu, X., Ji, Z., Gu, S., Ma, Z., Yan, Z., Liang, Y., Chang, H., Liang, H., 2023. Mapping the research on desulfurization wastewater: Insights from a bibliometric review (1991–2021). Chemosphere 314, 137678. https://doi.org/10.1016/j.chemosphere.2022.137678

Huang, H., Peng, C., Peng, P., Lin, Y., Zhang, X., Ren, H., 2019. Towards the biofilm characterization and regulation in biological wastewater treatment. Appl

Microbiol Biotechnol 103, 1115–1129. https://doi.org/10.1007/s00253-018-9511-6

Huang, X., Fan, W., Wang, S., Xiong, J., Chen, Y., Xie, C., 2024. Highly effective removal of nitrate from saline wastewater by glucose-enhanced sulfur autotrophic system. Journal of Water Process Engineering 63, 105439. https://doi.org/10.1016/j.jwpe.2024.105439

Huang, Y.H., Peddi, P.K., Tang, C., Zeng, H., Teng, X., 2013. Hybrid zero-valent iron process for removing heavy metals and nitrate from flue-gas-desulfurization wastewater. Separation and Purification Technology 118, 690–698. https://doi.org/10.1016/j.seppur.2013.07.009

Huang, Y.H., Peddi, P.K., Zeng, H., Tang, C.-L., Teng, X., 2012. Pilot-scale demonstration of the hybrid zero-valent iron process for treating flue-gas-desulfurization wastewater: Part I. Water Science and Technology 67, 16–23. https://doi.org/10.2166/wst.2012.446

Huang, Z., Yi, G., Wang, Q., Wang, S., Xu, Q., Huan, C., Wang, Y., Zhang, W., Wang, A., Liu, W., 2024. Improving microbial activity in high-salt wastewater: A review of innovative approaches. Science of The Total Environment 954, 176278. https://doi.org/10.1016/j.scitotenv.2024.176278

Iskra, K., Krawczyk, Ł., Miodoński, J.M., Wierzbicka-Kopertowska, D., 2020. Nitrate removal from wastewater generated in wet flue gas desulphurisation systems (FGD) in coal-fired power generation using the heterotrophic denitrification method. Ochrona Srodowiska i Zasobow Naturalnych 31, 27–34. https://doi.org/10.2478/oszn-2020-0012

Jafari, S.J., Moussavi, G., Yaghmaeian, K., 2015. High-rate biological denitrification in the cyclic rotating-bed biological reactor: Effect of COD/NO_3^-, nitrate concentration and salinity and the phylogenetic analysis of denitrifiers. Bioresource Technology 197, 482–488. https://doi.org/10.1016/J.BIORTECH.2015.08.047

Ji, B., Zhang, H., Zhou, L., Yang, J., Zhang, K., Yuan, X., Ma, J., Qian, Y., 2021. Effect of the rapid increase of salinity on anoxic-oxic biofilm reactor for treatment of high-salt and high-ammonia–nitrogen wastewater. Bioresource Technology 337, 125363. https://doi.org/10.1016/j.biortech.2021.125363

Jiang, F., Zhang, L., Peng, G.L., Liang, S.Y., Qian, J., Wei, L., Chen, G.H., 2013. A novel approach to realize SANI process in freshwater sewage treatment – Use of wet flue gas desulfurization waste streams as sulfur source. Water Research 47, 5773–5782. https://doi.org/10.1016/J.WATRES.2013.06.051

Jiang, X., Wang, H., Wu, P., Lei, Y., Deng, L., Wang, W., 2024. Enhanced narH gene expression contributing to nitrite accumulation in simultaneous nitrification and denitrification under Na^+ stress instead of K^+ stress. Chemical Engineering Journal 479, 147637. https://doi.org/10.1016/j.cej.2023.147637

Jo, E.Y., Park, S.M., Yeo, I.S., Cha, J.D., Lee, J.Y., Kim, Y.H., Lee, T.K., Park, C.G., 2016. A study on the removal of sulfate and nitrate from the wet scrubber wastewater using electrocoagulation. Desalination and Water Treatment 57, 7833–7840. https://doi.org/10.1080/19443994.2015.1028461

Johansson, J., Heijnesson Hultén, A., Normann, F., Andersson, K., 2021a. Simultaneous Removal of NO_x and SO_x from Flue Gases Using ClO_2: Process Scaling and Modeling Simulations. Ind. Eng. Chem. Res. 60, 1774–1783. https://doi.org/10.1021/acs.iecr.0c05828

Johansson, J., Normann, F., Andersson, K., 2021b. Techno-Economic Evaluation of Co-Removal of NO_x and SO_x Species from Flue Gases via Enhanced Oxidation of NO by ClO_2—Case Studies of Implementation at a Pulp and Paper Mill, Waste-to-Heat Plant and a Cruise Ship. Energies 14, 8512. https://doi.org/10.3390/en14248512

Jones, E.R., van Vliet, M.T.H., Qadir, M., Bierkens, M.F.P., 2021. Country-level and gridded estimates of wastewater production, collection, treatment and reuse. Earth System Science Data 13, 237–254. https://doi.org/10.5194/essd-13-237-2021

Keskinen, P., 2021. Flue gas scrubber water for nitrogen supply in biological pulp and paper mill wastewater treatment (M.Sc. (Tech) Thesis). Tampere University. https://urn.fi/URN:NBN:fi:tuni-202109287315

Koenig, A., Liu, L., 2004. Autotrophic Denitrification of High-Salinity Wastewater Using Elemental Sulfur: Batch Tests. Water Environment Research 76, 37–46. https://doi.org/10.2175/106143004x141564

Kornaros, M., Lyberatos, G., 1998. Kinetic modelling of *Pseudomonas denitrificans* growth and denitrification under aerobic, anoxic and transient operating conditions. Water Research 32, 1912–1922. https://doi.org/10.1016/S0043-1354(97)00403-X

Kosonen, H., Heinonen, M., Mikola, A., Haimi, H., Mulas, M., Corona, F., Vahala, R., 2016. Nitrous Oxide Production at a Fully Covered Wastewater Treatment Plant: Results of a Long-Term Online Monitoring Campaign. Environ. Sci. Technol. 50, 5547–5554. https://doi.org/10.1021/acs.est.5b04466

Kowalski, M.S., Devlin ,Tanner R., and Oleszkiewicz, J.A., 2019. Attachment of anaerobic ammonium-oxidizing bacteria to augmented carrier material. Environmental Technology 40, 576–583. https://doi.org/10.1080/09593330.2017.1397770

Kruglova, A., 2018. Biological removal of emerging micropollutants in nitrifying activated sludge at low temperatures (PhD thesis). Aalto University. https://urn.fi/URN:ISBN:978-952-60-3755-4

Labbé, N., Juteau, P., Parent, S., Villemur, R., 2003. Bacterial Diversity in a Marine Methanol-Fed Denitrification Reactor at the Montreal Biodome, Canada. Microb Ecol 46, 12–21. https://doi.org/10.1007/s00248-002-1056-6

Labelle, M.-A., Juteau, P., Jolicoeur, M., Villemur, R., Parent, S., Comeau, Y., 2005. Seawater denitrification in a closed mesocosm by a submerged moving bed biofilm reactor. Water Research 39, 3409–3417. https://doi.org/10.1016/j.watres.2005.06.001

Lecomte, T., Félix Ferrería de la Fuente, J., Neuwahl, F., Canova, M., Pinasseau, A., Jankov, I., Brinkmann, T., Roudier, S., Delgado Sancho, L., 2017. Best

Available Techniques (BAT) Reference Document for Large Combustion Plants - Industrial Emissions Directive 2010/75/EU (Integrated Pollution Prevention and Control). https://doi.org/10.2760/949

Lefebvre, O., Moletta, R., 2006. Treatment of organic pollution in industrial saline wastewater: A literature review. Water Research 40, 3671–3682. https://doi.org/10.1016/j.watres.2006.08.027

Lefebvre, O., Quentin, S., Torrijos, M., Godon, J.J., Delgenès, J.P., Moletta, R., 2007. Impact of increasing NaCl concentrations on the performance and community composition of two anaerobic reactors. Appl Microbiol Biotechnol 75, 61–69. https://doi.org/10.1007/s00253-006-0799-2

Li, C., Liang, J., Lin, X., Xu, H., Tadda, M.A., Lan, L., Liu, D., 2019. Fast start-up strategies of MBBR for mariculture wastewater treatment. Journal of Environmental Management 248, 109267. https://doi.org/10.1016/j.jenvman.2019.109267

Li, R., Hou, Y.-N., Li, H., Han, Y., Zhang, D., Song, Y., Huang, C., Guo, J., Liu, Z., Wei, W., Ni, B.-J., 2024. Salinity responsive mechanisms of sulfur-based mixotrophic denitrification and ectoine induced tolerance enhancement. Chemical Engineering Journal 496, 154266. https://doi.org/10.1016/j.cej.2024.154266

Li, W., Li, H., Liu, Y., Zheng, P., Shapleigh, J.P., 2018. Salinity-Aided Selection of Progressive Onset Denitrifiers as a Means of Providing Nitrite for Anammox. Environ. Sci. Technol. 52, 10665–10672. https://doi.org/10.1021/acs.est.8b02314

Li, W., Liu, J., Zhen, Y., Lin, M., Sui, X., Zhao, W., Bing, X., Lin, J., Zhai, L., 2021. Simultaneous removal of nitrite and organics in a biofilm-enhanced high-salt wastewater treatment system via mixotrophic denitrification coupled with sulfate reduction. Journal of Water Process Engineering 40, 101976. https://doi.org/10.1016/j.jwpe.2021.101976

Li, Y., Chen, B., Zhang, X., Luo, Z., Lei, M., Song, T., Wei, Y., Li, J., Long, Z., Ma, J., 2024. Effect of High Salinity on Elemental Sulfur Autotrophic Partial Denitrification and Feasibility Evaluation of an Enhanced Strategy with Glycine Betaine Addition: Performance, Microorganisms, and Mechanisms. ACS EST Eng. 4, 831–841. https://doi.org/10.1021/acsestengg.3c00477

Li, Z.-R., Zhang, X.-N., Wang, H.-C., Cheng, H.-Y., Wang, A.-J., Zhang, Y.-Q., Cui, C.-W., Sun, Y.-L., 2023. Effects of salinity on sulfur-dominated autotrophic denitrification microorganisms: Microbial community succession, key microorganisms and response mechanisms. Chemical Engineering Journal 478, 147308. https://doi.org/10.1016/j.cej.2023.147308

Liao, R., Shen, K., Li, A.-M., Shi, P., Li, Y., Shi, Q., Wang, Z., 2013. High-nitrate wastewater treatment in an expanded granular sludge bed reactor and microbial diversity using 454 pyrosequencing analysis. Bioresource Technology 134, 190–197. https://doi.org/10.1016/j.biortech.2012.12.057

Lin, L., Pratt, S., Crick, O., Xia, J., Duan, H., Ye, L., 2021. Salinity effect on freshwater Anammox bacteria: Ionic stress and ion composition. Water Research 188, 116432. https://doi.org/10.1016/j.watres.2020.116432

Liu, N., Dopffel, N., Hovland, B., Alagic, E., Vik, B.F., Bødtker, G., 2020. High osmotic stress initiates expansion and detachment of *Thalassospira sp.* biofilms in glass microchannels. Journal of Environmental Chemical Engineering 8, 104525. https://doi.org/10.1016/j.jece.2020.104525

Lu, H., Chandran, K., Stensel, D., 2014. Microbial ecology of denitrification in biological wastewater treatment. Water Research 64, 237–254. https://doi.org/10.1016/j.watres.2014.06.042

Ma, S., Chai, J., Wu, K., Xiang, Y., Jia, S., Li, Q., 2019a. Experimental research on bypass evaporation tower technology for zero liquid discharge of desulfurization wastewater. Environmental Technology 40, 2715–2725. https://doi.org/10.1080/09593330.2018.1449901

Ma, S., Liu, C., Sun, Y., Gong, C., Qu, B., Ma, L., Tang, R., 2019b. Advanced treatment technology for fgd wastewater in coal-fired power plantcurrent situation and future prospects. Desalination and Water Treatment 167, 122–132. https://doi.org/10.5004/dwt.2019.24630

Ma, X., Wang, K., Li, X., Liu, G., Chen, H., Piao, C., You, S., 2023. Elucidating the elevated salinity effect on removal of carbon and nitrogen in coupling aromatic degradation to anaerobic denitrification. Chemical Engineering Journal 471, 143999. https://doi.org/10.1016/j.cej.2023.143999

Macêdo, W.V., Sakamoto, I.K., Azevedo, E.B., Damianovic, M.H.R.Z., 2019. The effect of cations (Na^+, Mg^{2+}, and Ca^{2+}) on the activity and structure of nitrifying and denitrifying bacterial communities. Science of The Total Environment 679, 279–287. https://doi.org/10.1016/J.SCITOTENV.2019.04.397

Mariángel, L., Aspé, E., Cristina Martí, M., Roeckel, M., 2008. The effect of sodium chloride on the denitrification of saline fishery wastewaters. Environmental Technology 29, 871–879. https://doi.org/10.1080/09593330802015318

Martin, G., Sharma, S., Ryan, W., Srinivasan, N.K., Senko, J.M., 2021. Identification of Microbiological Activities in Wet Flue Gas Desulfurization Systems. Front. Microbiol. 12. https://doi.org/10.3389/fmicb.2021.675628

Matheus, M.C., Ekenberg, M., Bassin, J.P., Dezotti, M.W.C., Piculell, M., 2021. High loaded moving bed biofilm reactors treating pulp & paper industry wastewater: Effect of hydraulic retention time, filling degree and nutrients availability on performance, biomass fractions and nutrients utilization. Journal of Environmental Chemical Engineering 9, 104944. https://doi.org/10.1016/j.jece.2020.104944

McQuarrie, J.P., Boltz, J.P., 2011. Moving Bed Biofilm Reactor Technology: Process Applications, Design, and Performance. Water Environment Research 83, 560–575. https://doi.org/10.2175/106143010X12851009156286

Miao, S., Jin, C., Liu, R., Bai, Y., Liu, H., Hu, C., Qu, J., 2020. Microbial community structures and functions of hypersaline heterotrophic denitrifying process: Lab-

scale and pilot-scale studies. Bioresource Technology 310, 123244. https://doi.org/10.1016/j.biortech.2020.123244

Miao, Y., Liao, R., Zhang, X.-X., Liu, B., Li, Y., Wu, B., Li, A., 2015. Metagenomic insights into salinity effect on diversity and abundance of denitrifying bacteria and genes in an expanded granular sludge bed reactor treating high-nitrate wastewater. Chemical Engineering Journal 277, 116–123. https://doi.org/10.1016/j.cej.2015.04.125

Miranda-Trevino, J.C., Pappoe, M., Hawboldt, K., Bottaro, C., 2013. The Importance of Thiosalts Speciation: Review of Analytical Methods, Kinetics, and Treatment. Critical Reviews in Environmental Science and Technology 43, 2013–2070. https://doi.org/10.1080/10643389.2012.672047

Mora, M., Fernández-Palacios, E., Guimerà, X., Lafuente, J., Gamisans, X., Gabriel, D., 2020. Feasibility of S-rich streams valorization through a two-step biosulfur production process. Chemosphere 253, 126734. https://doi.org/10.1016/j.chemosphere.2020.126734

Mora, M., López, L.R., Gamisans, X., Gabriel, D., 2014. Coupling respirometry and titrimetry for the characterization of the biological activity of a SO-NR consortium. Chemical Engineering Journal 251, 111–115. https://doi.org/10.1016/J.CEJ.2014.04.024

Morgan-Sagastume, F., 2018. Biofilm development, activity and the modification of carrier material surface properties in moving-bed biofilm reactors (MBBRs) for wastewater treatment. Critical Reviews in Environmental Science and Technology 48, 439–470. https://doi.org/10.1080/10643389.2018.1465759

Morita, M., Uemoto, H., Watanabe, A., 2007. An additional simple denitrification bioreactor using packed gel envelopes applicable to industrial wastewater treatment. Biotechnology and Bioengineering 97, 1439–1447. https://doi.org/10.1002/bit.21349

Myrberg, S., 2024. Emissions control at pulp mills: A case study on the implementation of combined SO_x and NO_x removal technology (M.Sc. thesis). Chalmers University of Technology. http://hdl.handle.net/20.500.12380/307931

Nelson, M.J., Nakhla, G., Zhu, J., 2017. Fluidized-Bed Bioreactor Applications for Biological Wastewater Treatment: A Review of Research and Developments. Engineering 3, 330–342. https://doi.org/10.1016/J.ENG.2017.03.021

Ødegaard, H., 2006. Innovations in wastewater treatment: the moving bed biofilm process. Water Science and Technology 53, 17–33. https://doi.org/10.2166/wst.2006.284

Osaka, T., Shirotani, K., Yoshie, S., Tsuneda, S., 2008. Effects of carbon source on denitrification efficiency and microbial community structure in a saline wastewater treatment process. Water Research 42, 3709–3718. https://doi.org/10.1016/j.watres.2008.06.007

Osipova, L., Georgeff, E., Comer, Bryan, 2021. Global scrubber washwater discharges under IMO's 2020 fuel sulfur limit - ICCT. https://theicct.org/wp-content/uploads/2021/06/scrubber-discharges-Apr2021.pdf

Özkaya, B., Kaksonen, A.H., Sahinkaya, E., Puhakka, J.A., 2019. Fluidized bed bioreactor for multiple environmental engineering solutions. Water Research 150, 452–465. https://doi.org/10.1016/j.watres.2018.11.061

Pan, Y., Ye, L., Ni, B.-J., Yuan, Z., 2012. Effect of pH on N_2O reduction and accumulation during denitrification by methanol utilizing denitrifiers. Water Research 46, 4832–4840. https://doi.org/10.1016/j.watres.2012.06.003

Panagopoulos, A., 2022. Study and evaluation of the characteristics of saline wastewater (brine) produced by desalination and industrial plants. Environ Sci Pollut Res 29, 23736–23749. https://doi.org/10.1007/s11356-021-17694-x

Pang, Y., Wang, J., 2021. Various electron donors for biological nitrate removal: A review. Science of The Total Environment 794, 148699. https://doi.org/10.1016/j.scitotenv.2021.148699

Panswad, T., Anan, C., 1999. Impact of high chloride wastewater on an anaerobic/anoxic/aerobic process with and without inoculation of chloride acclimated seeds. Water Research 33, 1165–1172. https://doi.org/10.1016/S0043-1354(98)00314-5

Papirio, S., Villa-Gomez ,D. K., Esposito ,G., Pirozzi ,F., and Lens, P.N.L., 2013. Acid Mine Drainage Treatment in Fluidized-Bed Bioreactors by Sulfate-Reducing Bacteria: A Critical Review. Critical Reviews in Environmental Science and Technology 43, 2545–2580. https://doi.org/10.1080/10643389.2012.694328

Park, J.Y., Yoo, Y.J., 2009. Biological nitrate removal in industrial wastewater treatment: Which electron donor we can choose. Applied Microbiology and Biotechnology 82, 415–429. https://doi.org/10.1007/s00253-008-1799-1

Parrilli, E., Tutino, M.L., Marino, G., 2022. Biofilm as an adaptation strategy to extreme conditions. Rend. Fis. Acc. Lincei 33, 527–536. https://doi.org/10.1007/s12210-022-01083-8

Parsons, T.R., Brown, S.R., De Vault, R.F., Chenevey, J., 2016. Wet FGD effluent characterization in preparation for WWT technology selection. Air and Waste Management Association - Power Plant Pollutant Control "MEGA" Symposium, MEGA 2016.

Philips, S., Laanbroek, H.J., Verstraete, W., 2002. Origin, causes and effects of increased nitrite concentrations in aquatic environments. Reviews in Environmental Science and Bio/Technology 1, 115–141. https://doi.org/10.1023/A:1020892826575

Piculell, M., 2016. New Dimensions of Moving Bed Biofilm Carriers: Influence of biofilm thickness and control possibilities (PhD thesis). Lund University. https://lucris.lub.lu.se/ws/portalfiles/portal/7673290/Maria_Piculell_Webb_kappa.pdf

Piculell, M., Suarez, C., Li, C., Christensson, M., Persson, F., Wagner, M., Hermansson, M., Jönsson, K., Welander, T., 2016. The inhibitory effects of

reject water on nitrifying populations grown at different biofilm thickness. Water Research 104, 292–302. https://doi.org/10.1016/j.watres.2016.08.027

Plattes, M., Henry, E., Schosseler, P.M., Weidenhaupt, A., 2006. Modelling and dynamic simulation of a moving bed bioreactor for the treatment of municipal wastewater. Biochemical Engineering Journal 32, 61–68. https://doi.org/10.1016/j.bej.2006.07.009

Pöyry, 2016. Energiateollisuuden ympäristöpooli - Selvitys polttolaitosten savukaasupesureiden jätevesien ja lietteiden laadusta, hyötykäytöstä ja siihen liittyvästä luvituksesta. Pöyry Finland Oy. https://energia.fi/wp-content/uploads/2023/08/Savukaasupesurit_raportti_201216.pdf

Qadir, M., Drechsel, P., Jiménez Cisneros, B., Kim, Y., Pramanik, A., Mehta, P., Olaniyan, O., 2020. Global and regional potential of wastewater as a water, nutrient and energy source. Natural Resources Forum 44, 40–51. https://doi.org/10.1111/1477-8947.12187

Qi, W., Taherzadeh, M.J., Ruan, Y., Deng, Y., Chen, J.-S., Lu, H.-F., Xu, X.-Y., 2020. Denitrification performance and microbial communities of solid-phase denitrifying reactors using poly (butylene succinate)/bamboo powder composite. Bioresource Technology 305, 123033. https://doi.org/10.1016/j.biortech.2020.123033

Rabah, F.K.J., Dahab, M.F., 2004. Nitrate removal characteristics of high performance fluidized-bed biofilm reactors. Water Research 38, 3719–3728. https://doi.org/10.1016/j.watres.2004.07.002

Raj Deena, S., Kumar, G., Vickram, A.S., Rani Singhania, R., Dong, C., Rohini, K., Anbarasu, K., Thanigaivel, S., Ponnusamy, V.K., 2022. Efficiency of various biofilm carriers and microbial interactions with substrate in moving bed-biofilm reactor for environmental wastewater treatment. Bioresource Technology 359, 127421. https://doi.org/10.1016/j.biortech.2022.127421

Ren, M., Wang, Y., Zhang, H., Li, Y., Sun, K., 2024. Investigation of Nitrogen Removal in Flue Gas Desulfurization and Denitrification Wastewater Utilizing Halophilic Activated Sludge. Toxics 12, 742. https://doi.org/10.3390/toxics12100742

Riffe, M.R., Heimbigner, B.E., Kutzora, P.G., Braunstein, K.A., 2008. Wastewater treatment for FGD purge streams. MEGA Symposium, Baltimore. https://www3.epa.gov/region1/npdes/merrimackstation/pdfs/ar/AR-24.pdf

Rillig, M.C., Rolff, J., Tietjen, B., Wehner, J., Andrade-Linares, D.R., 2015. Community priming - effects of sequential stressors on microbial assemblages. FEMS Microbiology Ecology 91, fiv040. https://doi.org/10.1093/femsec/fiv040

Rintala, J.A., Puhakka, J.A., 1994. Anaerobic treatment in pulp- and paper-mill waste management: A review. Bioresource Technology 47, 1–18. https://doi.org/10.1016/0960-8524(94)90022-1

Rissanen, A.J., Ojala, A., Dernjatin, M., Jaakkola, J., Tiirola, M., 2016. *Methylophaga* and *Hyphomicrobium* can be used as target genera in monitoring saline water

methanol-utilizing denitrification. J Ind Microbiol Biotechnol 43, 1647–1657. https://doi.org/10.1007/s10295-016-1839-2

Rittmann, B.E., Boltz, J.P., Brockmann, D., Daigger, G.T., Morgenroth, E., Sørensen, K.H., Takács, I., van Loosdrecht, M., Vanrolleghem, P.A., 2018. A framework for good biofilm reactor modeling practice (GBRMP). Water Science and Technology 77, 1149–1164. https://doi.org/10.2166/wst.2018.021

Sahinkaya, E., Dursun, N., Kilic, A., Demirel, S., Uyanik, S., Cinar, O., 2011. Simultaneous heterotrophic and sulfur-oxidizing autotrophic denitrification process for drinking water treatment: Control of sulfate production. Water Research 45, 6661–6667. https://doi.org/10.1016/j.watres.2011.09.056

Schmid, D., Hupa, M., Paavola, M., Vuorinen, I., Lehikoinen, A., Karlström, O., 2023. Role of Thiosulfate in NO_2 Absorption in Aqueous Sulfite Solutions. Ind. Eng. Chem. Res. 62, 105–110. https://doi.org/10.1021/acs.iecr.2c04299

Schmid, D., Karlström, O., Kuvaja, V., Vuorinen, I., Paavola, M., Hupa, M., 2022. Role of Sulfite Oxidation in NO_2 Absorption in a pH-Neutral Scrubber Solution. Energy & Fuels 36, 2666–2672. https://doi.org/10.1021/acs.energyfuels.1c03914

Shelly, Y., Kuk, M., Menashe, O., Zeira, G., Azerrad, S., Kurzbaum, E., 2021. Nitrate removal from a nitrate-rich reverse osmosis concentrate: Superior efficiency using the bioaugmentation of an Acinetobacter biofilm. Journal of Water Process Engineering 44, 102425. https://doi.org/10.1016/j.jwpe.2021.102425

Shrout, J.D., Nerenberg, R., 2012. Monitoring Bacterial Twitter: Does Quorum Sensing Determine the Behavior of Water and Wastewater Treatment Biofilms? Environ. Sci. Technol. 46, 1995–2005. https://doi.org/10.1021/es203933h

Shuangchen, M., Jin, C., Gongda, C., Weijing, Y., Sijie, Z., 2016. Research on desulfurization wastewater evaporation: Present and future perspectives. Renewable and Sustainable Energy Reviews 58, 1143–1151. https://doi.org/10.1016/j.rser.2015.12.252

Siegrist, H., Gujer, W., 1985. Mass transfer mechanisms in a heterotrophic biofilm. Water Research 19, 1369–1378. https://doi.org/10.1016/0043-1354(85)90303-3

Solińska, A., Bajda, T., 2022. Modified zeolite as a sorbent for removal of contaminants from wet flue gas desulphurization wastewater. Chemosphere 286, 131772. https://doi.org/10.1016/j.chemosphere.2021.131772

Song, Q., Chen, X., Hua, Y., Chen, S., Ren, L., Dai, X., 2023. Biological treatment processes for saline organic wastewater and related inhibition mechanisms and facilitation techniques: A comprehensive review. Environmental Research 239, 117404. https://doi.org/10.1016/j.envres.2023.117404

Sonwani, R.K., Swain, G., Giri, B.S., Singh, R.S., Rai, B.N., 2019. A novel comparative study of modified carriers in moving bed biofilm reactor for the treatment of wastewater: Process optimization and kinetic study. Bioresource Technology 281, 335–342. https://doi.org/10.1016/j.biortech.2019.02.121

Sudmalis, D., Mubita, T.M., Gagliano, M.C., Dinis, E., Zeeman, G., Rijnaarts, H.H.M., Temmink, H., 2020. Cation exchange membrane behaviour of extracellular polymeric substances (EPS) in salt adapted granular sludge. Water Research 178, 115855. https://doi.org/10.1016/j.watres.2020.115855

Suhr, M., Roudier, S., Kourti, I., Delgado Sancho, L., Rodrigo Gonzalo, M., Giner Santonja, G., Klein, G., 2015. Best Available Techniques (BAT) reference document for the production of pulp, paper and board. Publications Office of the European Union. https://op.europa.eu/en/publication-detail/-/publication/fcaab1a5-d287-40af-b21c-115e529685fc/language-en

Tadda, M.A., Altaf, R., Gouda, M., Rout, P.R., Shitu, A., Ye, Z., Zhu, S., Liu, D., 2021. Impact of Saddle-Chips biocarrier on treating mariculture wastewater by moving bed biofilm reactor (MBBR): Mechanism and kinetic study. Journal of Environmental Chemical Engineering 9, 106710. https://doi.org/10.1016/j.jece.2021.106710

Teuchies, J., Cox, T.J.S., Van Itterbeeck, K., Meysman, F.J.R., Blust, R., 2020. The impact of scrubber discharge on the water quality in estuaries and ports. Environmental Sciences Europe 32, 103. https://doi.org/10.1186/s12302-020-00380-z

Togna, P., n.d. Managing the new FGD wastewater regulations. Technology options for biological treatment: maximum treatment reliability with lowest lifecycle cost. Envirogen Technologies.

Tran, H., Vakkilainnen, E.K., 2008. The Kraft Chemical Recovery Process. Tappi Kraft Pulping Short Course 1–8. https://www.tappi.org/content/events/08kros/manuscripts/1-1.pdf

Valmet, 2017. Technical paper series: Recovery Boiler SCR-Retrofit challenge and opportunity in Retrofit Cases. https://www.valmet.com/globalassets/media/downloads/white-papers/power-and-recovery/recovery_boiler_scr_whitepaper.pdf

Van Loosdrecht, M.C.M., Picioreanu, C., Heijnen, J.J., 1997. A more unifying hypothesis for biofilm structures. FEMS Microbiology Ecology 24, 181–183. https://doi.org/10.1016/S0168-6496(97)00064-0

Vendrup, M., Sund, C., 1994. Treatment of Wastewater from Flue Gas Cleaning. Water Science and Technology 29, 307–312. https://doi.org/10.2166/wst.1994.0498

Veolia Water Technologies, n.d. Selenium Removal from Wastewater [WWW Document]. URL https://www.watertechnologies.com/products/wastewater-treatments/wastewater-selenium-removal (accessed 1.24.25).

Vredenbregt, L.H.J., Nielsen, K., Potma, A.A., Kristensen, G.H., Sund, C., 1997. Fluid bed biological nitrification and denitrification in high salinity wastewater. Water Science and Technology 36, 93–100. https://doi.org/10.1016/S0273-1223(97)00341-7

Vyrides, I., Stuckey, D.C., 2017. Compatible solute addition to biological systems treating waste/wastewater to counteract osmotic and other environmental

stresses: a review. Critical Reviews in Biotechnology 37, 865–879. https://doi.org/10.1080/07388551.2016.1266460

Wang, J., Zhou, J., Wang, Y., Wen, Y., He, L., He, Q., 2020. Efficient nitrogen removal in a modified sequencing batch biofilm reactor treating hypersaline mustard tuber wastewater: The potential multiple pathways and key microorganisms. Water Research 177, 115734. https://doi.org/10.1016/j.watres.2020.115734

Wang, L., Liu, J., Li, Y., Liu, Z., Zhang, L., Che, H., Cui, H., Zhang, Y., 2023. Elemental sulfur-driven autotrophic denitrification process for effective removal of nitrate in mariculture wastewater: Performance, kinetics and microbial community. Chemosphere 337, 139354. https://doi.org/10.1016/j.chemosphere.2023.139354

Wang, R., Zheng, P., Ding, A. Qiang, Zhang, M., Ghulam, A., Yang, C., Zhao, H.P., 2016. Effects of inorganic salts on denitrifying granular sludge: The acute toxicity and working mechanisms. Bioresource Technology 204, 65–70. https://doi.org/10.1016/j.biortech.2015.12.062

Wang, T., Wang, H., Ran, X., Wang, Y., 2024. Salt stimulates sulfide−driven autotrophic denitrification: Microbial network and metagenomics analyses. Water Research 257, 121742. https://doi.org/10.1016/j.watres.2024.121742

Wang, Y., Bott, C., Nerenberg, R., 2016. Sulfur-based denitrification: Effect of biofilm development on denitrification fluxes. Water Research 100, 184–193. https://doi.org/10.1016/j.watres.2016.05.020

Wei, C., He, W., Wei, L., Ma, J., Li, C., 2017. The performance and microbial communities of biodegradation-electron transfer with sulfur metabolism integrated process for flue gas desulfurization wastewater treatment. Bioprocess and Biosystems Engineering 40, 1543–1553. https://doi.org/10.1007/s00449-017-1810-2

Wu, G., Yang, G., Sun, X., Li, B., Tian, Z., Niu, X., Cheng, J., Feng, L., 2023. Simultaneous denitrification and organics removal by denitrifying bacteria inoculum in a multistage biofilm process for treating desulfuration and denitration wastewater. Bioresource Technology 388, 129757. https://doi.org/10.1016/j.biortech.2023.129757

Wu, L., Wei, W., Xu, J., Chen, X., Liu, Y., Peng, L., Wang, D., Ni, B.-J., 2021. Denitrifying biofilm processes for wastewater treatment: developments and perspectives. Environ. Sci.: Water Res. Technol. 7, 40–67. https://doi.org/10.1039/D0EW00576B

Xiang, Z., Chen, X., Bai, J., Li, B., Li, H., Huang, X., 2023. Bioaugmentation performance for moving bed biofilm reactor (MBBR) treating mariculture wastewater by an isolated novel halophilic heterotrophic nitrification aerobic denitrification (HNAD) strain (*Zobellella B307*). Journal of Environmental Management 325, 116566. https://doi.org/10.1016/j.jenvman.2022.116566

Yan, J., Yuan, W., Liu, J., Ye, W., Lin, J., Xie, Jiahao, Huang, X., Gao, S., Xie, Jiehui, Liu, S., Chen, W., Zhang, H., 2019. An integrated process of chemical precipitation and sulfate reduction for treatment of flue gas desulphurization

wastewater from coal-fired power plant. Journal of Cleaner Production 228, 63–72. https://doi.org/10.1016/J.JCLEPRO.2019.04.227

Yang, P.Y., Nitisoravut, S., Wu, J.S., 1995. Nitrate removal using a mixed-culture entrapped microbial cell immobilization process under high salt conditions. Water Research 29, 1525–1532. https://doi.org/10.1016/0043-1354(94)00296-J

Ytreberg, E., Hansson, K., Hermansson, A.L., Parsmo, R., Lagerström, M., Jalkanen, J.-P., Hassellöv, I.-M., 2022. Metal and PAH loads from ships and boats, relative other sources, in the Baltic Sea. Marine Pollution Bulletin 182, 113904. https://doi.org/10.1016/j.marpolbul.2022.113904

Yuan, Q., Wang, H., Hang, Q., Deng, Y., Liu, K., Li, C., Zheng, S., 2015. Comparison of the MBBR denitrification carriers for advanced nitrogen removal of wastewater treatment plant effluent. Environ Sci Pollut Res 22, 13970–13979. https://doi.org/10.1007/s11356-015-4546-z

Zan, F., Ma, H., Xiao, C., Chen, G., Wu, D., 2022. Moving-bed biofilm reactor for saline wastewater treatment: Different types of carriers, versatile nitrifying reactions, and functional microbial groups. Journal of Water Process Engineering 50, 103274. https://doi.org/10.1016/j.jwpe.2022.103274

Zeng, D., Liang, K., Guo, F., Wu, Y., Wu, G., 2020. Denitrification performance and microbial community under salinity and MIT stresses for reverse osmosis concentrate treatment. Separation and Purification Technology 242, 116799. https://doi.org/10.1016/j.seppur.2020.116799

Zhai, S., Ji, M., Zhao, Y., Pavlostathis, S.G., Zhao, Q., 2018. Effects of salinity and COD/N on denitrification and bacterial community in dicyclic-type electrode based biofilm reactor. Chemosphere 192, 328–336. https://doi.org/10.1016/j.chemosphere.2017.10.108

Zhai, S., Ji, M., Zhao, Y., Su, X., 2020. Shift of bacterial community and denitrification functional genes in biofilm electrode reactor in response to high salinity. Environmental Research 184, 109007. https://doi.org/10.1016/j.envres.2019.109007

Zhang, T.C., Fu, Y.C., Bishop, P.L., Kupferle, M., FitzGerald, S., Jiang, H.H., Harmer, C., 1995. Transport and biodegradation of toxic organics in biofilms. Journal of Hazardous Materials, Selected papers presented at the Conference on Hazardous Waste Remediation 41, 267–285. https://doi.org/10.1016/0304-3894(94)00118-Z

Zhang, Z., Guo, Y., Guo, L., Hu, F., Zhao, Y., Jin, C., She, Z., Gao, M., Wang, G., 2020. Elucidating salinity adaptation and shock loading on denitrification performance: Focusing on microbial community shift and carbon source evaluation. Bioresource Technology 305, 123030. https://doi.org/10.1016/j.biortech.2020.123030

Zhang, Zhenya, Lei, Z., He, X., Zhang, Zhiyin, Yang, Y., Sugiura, N., 2009. Nitrate removal by *Thiobacillus denitrificans* immobilized on poly(vinyl alcohol) carriers. Journal of Hazardous Materials 163, 1090–1095. https://doi.org/10.1016/j.jhazmat.2008.07.062

Zhao, H., 2005. Effect of ions and other compatible solutes on enzyme activity, and its implication for biocatalysis using ionic liquids. Journal of Molecular Catalysis B: Enzymatic 37, 16–25. https://doi.org/10.1016/j.molcatb.2005.08.007

Zhao, J., Wei, Q., Wang, S., Ren, X., 2021. Progress of ship exhaust gas control technology. Science of The Total Environment 799, 149437. https://doi.org/10.1016/J.SCITOTENV.2021.149437

Zhao, M., Xue, P., Liu, J., Liao, J., Guo, J., 2021. A review of removing SO_2 and NO_x by wet scrubbing. Sustainable Energy Technologies and Assessments 47, 101451. https://doi.org/10.1016/j.seta.2021.101451

Zhao, W., Wang, Y., Liu, S., Pan, M., Yang, J., Chen, S., 2013. Denitrification activities and N_2O production under salt stress with varying COD/N ratios and terminal electron acceptors. Chemical Engineering Journal 215–216, 252–260. https://doi.org/10.1016/j.cej.2012.10.084

Zhao, Y., Liu, D., Huang, W., Yang, Y., Ji, M., Nghiem, L.D., Trinh, Q.T., Tran, N.H., 2019. Insights into biofilm carriers for biological wastewater treatment processes: Current state-of-the-art, challenges, and opportunities. Bioresource Technology 288, 121619. https://doi.org/10.1016/j.biortech.2019.121619

Zhao, Z., Qiu, W., Koenig, A., Fan, X., Gu, J.D., 2004. Nitrate removal from saline water using autotrophic denitrification by the bacterium *Thiobacillus denitrificans* MP-1. Environmental Technology 25, 1201–1210. https://doi.org/10.1080/09593332508618387

Zhou, W., Hao, J., Guo, Y., Zhao, C., Zhang, M., Zhang, S., Han, F., 2024. Revealing bioresponses of biofilm and flocs to salinity gradient in halophilic biofilm reactor. Bioresource Technology 401, 130727. https://doi.org/10.1016/j.biortech.2024.130727

Zhu, S.-M., Deng, Y.-L., Ruan, Y.-J., Guo, X.-S., Shi, M.-M., Shen, J.-Z., 2015. Biological denitrification using poly(butylene succinate) as carbon source and biofilm carrier for recirculating aquaculture system effluent treatment. Bioresource Technology 192, 603–610. https://doi.org/10.1016/j.biortech.2015.06.021

Zou, G., Papirio, S., Lakaniemi, A.-M., Ahoranta, S.H., Puhakka, J.A., 2016. High rate autotrophic denitrification in fluidized-bed biofilm reactors. Chemical Engineering Journal 284, 1287–1294. https://doi.org/10.1016/j.cej.2015.09.074

Zumft, W.G., 1997. Cell biology and molecular basis of denitrification. Microbiology and Molecular Biology Reviews 61, 533–616. https://doi.org/10.1128/mmbr.61.4.533-616.1997

Zuo, L., Yao, H., Li, H., Jia, F., Wei, W., Liu, Y., Ni, B.-J., Chen, X., 2021. Modeling of completely autotrophic nitrogen removal process with salt and glycine betaine addition. Chemosphere 264, 128474. https://doi.org/10.1016/j.chemosphere.2020.128474

PUBLICATION I

Effects of inorganic ions on autotrophic denitrification by *Thiobacillus denitrificans* and on heterotrophic denitrification by an enrichment culture

Alessio D'Aquino, Niko Kalinainen, Hannele Auvinen, Gianni Andreottola, Jaakko A. Puhakka and Marja R.T. Palmroth

Science of the Total Environment, 901 (2023), 165940
https://doi.org/10.1016/j.scitotenv.2023.165940

Science of the Total Environment 901 (2023) 165940

Contents lists available at ScienceDirect

Science of the Total Environment

journal homepage: www.elsevier.com/locate/scitotenv

Effects of inorganic ions on autotrophic denitrification by *Thiobacillus denitrificans* and on heterotrophic denitrification by an enrichment culture

Alessio D'Aquino [a,*], Niko Kalinainen [b], Hannele Auvinen [a], Gianni Andreottola [c], Jaakko A. Puhakka [a], Marja R.T. Palmroth [a]

[a] Tampere University, Faculty of Engineering and Natural Sciences, Bio- and Circular Economy Unit, Korkeakoulunkatu 8, P.O. Box 541, 33014 Tampere, Finland
[b] Valmet Technologies Oy, Lentokentänkatu 11, 33900 Tampere, Finland
[c] University of Trento, Department of Civil, Environmental and Mechanical Engineering, via Mesiano 77, 38123 Trento, Italy

HIGHLIGHTS

- High content of ions in industrial wastewaters pose a challenge for denitrification.
- Batch assays were run with Na^+, Cl^-, K^+, SO_4^{2-} and NO_x-SO_2 scrubber wastewater.
- Single ions inhibited autotrophic and heterotrophic denitrification.
- Cl^- had the most important role in decreasing denitrification rate.
- Denitrification has potential for treatment of NO_x-SO_2 scrubber wastewater.

GRAPHICAL ABSTRACT

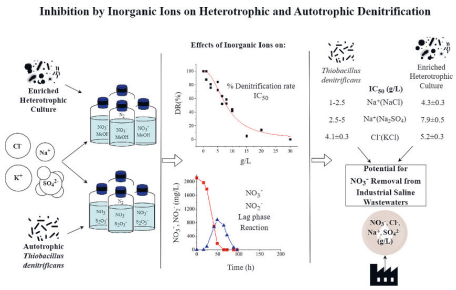

ARTICLE INFO

Editor: Qilin Wang

Keywords:
Biological nitrate removal
Chloride
IC_{50}
Inhibition by ions
Salinity
Scrubber wastewater

ABSTRACT

Salinity of nitrate-laden wastewaters, such as those produced by metal industries, tanneries, and wet flue gas cleaning systems may affect their treatment by denitrification. Salt inhibition of denitrification has been reported, while impacts of individual ions remain poorly understood whilst being relevant for wastewaters where often the concentration of a single ion rather than the salts varies. The aim of this study was to determine the inhibition by inorganic ions (Na^+, Cl^-, SO_4^{2-} and K^+) commonly present in saline wastewaters on denitrification and reveal its potential for the treatment of such waste streams, like those produced by NO_x-SO_x removal scrubbers. The inhibitory effects were investigated for both heterotrophic (enrichment culture) and autotrophic (*T. denitrificans*) denitrification in batch assays, by using NaCl, Na_2SO_4, KCl and K_2SO_4 salts at increasing concentrations. The half inhibition concentrations (IC_{50}) of Na^+ (as NaCl), Na^+ (as Na_2SO_4) and Cl^- (as KCl) were: 4.3 ± 0.3, 7.9 ± 0.5 and 5.2 ± 0.3 g/L for heterotrophic, and 1–2.5, 2.5–5 and 4.1 ± 0.3 g/L for autotrophic denitrification, respectively. Heterotrophic denitrification was completely inhibited at 20 g/L Na^+ (as NaCl), 30 g/L Na^+ (as Na_2SO_4) and 30 g/L Cl^- (as KCl), while autotrophic at 8 g/L Na^+ (as NaCl), 10 g/L Na^+ (as Na_2SO_4) and 15 g/L Cl^- (as KCl). In both cases, Cl^- addition had the most important role in decreasing denitrification rate, while Na^+ at 1 g/L stimulated autotrophic denitrification but rapidly inhibited the rate at higher concentrations. Nitrite reduction was less inhibited by the ions than nitrate reduction and both the osmotic pressure and

* Corresponding author.
E-mail address: alessio.daquino@tuni.fi (A. D'Aquino).

https://doi.org/10.1016/j.scitotenv.2023.165940
Received 16 May 2023; Received in revised form 11 July 2023; Accepted 29 July 2023
Available online 2 August 2023

the toxicity of the single ions played key roles in the overall inhibition of denitrification. Eventually, both autotrophic and heterotrophic denitrification showed potential for the treatment of a saline wastewater from a NO_x-SO_2 removal scrubber from a pulp mill.

1. Introduction

Nitrate discharge has detrimental impacts on the environment (e.g., eutrophication) as well as on human health, and, hence, requires control. Biological nitrate removal is an effective treatment widely employed, for example, in wastewater treatment plants and in groundwater remediation (Chan-Pacheco et al., 2021; Rivett et al., 2008). Biological treatment represents a cost-efficient management of secondary pollution and, thus, has potential also for denitrification of industrial wastewaters (Park and Yoo, 2009). However, industrial wastewaters, like those produced in tanning and food industries (Lefebvre and Moletta, 2006), metal industries (Luo et al., 2021), as well as coal-fired power plants (Koenig and Liu, 2004), often present challenging conditions for denitrifying microorganisms, such as high concentrations of nitrate, metals, and high salinity. For instance, wet scrubbers simultaneously removing NO_x and SO_x from industrial flue gases transfer the pollutants from the gaseous to the liquid phase, thus generating nitrogen and sulphur laden liquid waste streams (Gholami et al., 2020) that need to be treated. Moreover, the chemicals used in the scrubbing process (for a review see Chen et al. (2021)) result in variable concentrations of chloride and sodium ions in the generated wastewater.

Both heterotrophic and autotrophic denitrification have been studied for industrial application, such as for wastewaters from agrifood industry (De Lucas et al., 2005), mining industry (Di Capua et al., 2017b), fishery industry (Mariángel et al., 2008) and flue gas desulphurization (FGD) scrubbers (Vredenbregt et al., 1997; Wei et al., 2017). On one hand, heterotrophic denitrification of industrial wastewaters often requires supplementation of organic electron and carbon sources, therefore increasing the costs of the treatment (Park and Yoo, 2009). However, many industries produce large quantities of organic waste streams that represent potential low-cost carbon and electron sources for heterotrophic denitrification. For instance, in kraft pulp mills, evaporator condensates contain methanol (MeOH) and other organic compounds (Meyer and Edwards, 2014) that can be utilised as carbon and electron sources. Methanol supports heterotrophic denitrification (C/N = 0.93 g/g) according to the following reaction (1) (Foglar and Briški, 2003):

$$1.09\ CH_3OH + NO_3^- + H^+ \rightarrow 0.074\ C_5H_7O_2N + 0.463\ N_2 + 0.72\ CO_2 + 2.421\ H_2O \quad (1)$$

On the other hand, autotrophic denitrification obtains electrons for nitrate reduction from reduced inorganic sulphurous compounds, and does not require addition of organic substrate (Di Capua et al., 2019). For instance, the chemolithoautotrophic *Thiobacillus denitrificans* reduces nitrate to nitrogen gas by oxidizing thiosulphate (S/N = 3.92 g/g) according to reaction (2) (Mora et al., 2014):

$$S_2O_3^{2-} + 1.16NO_3^- + 0.035CO_2 + 0.519HCO_3^- + 0.11NH_4^+ + 0.124H_2O \rightarrow 0.11C_5H_7O_2N + 0.578\ N_2 + 0.435H^+ + 2SO_4^{2-} \quad (2)$$

Salinity of industrial wastewaters, which can reach 150 g/L (Lin et al., 2021), poses a challenge for both autotrophic and heterotrophic denitrification. In a saline environment, Na^+ cations interfere with the enzyme activity (Lin et al., 2021; Wang et al., 2016) and at high concentrations they increase internal osmotic pressure of microbial cells, leading to the breakage of the cell membrane (Yang et al., 2013). In addition, specific toxicity of other ions and their interactions may affect the inhibitory effect (Lin et al., 2021; Macêdo et al., 2019).

Inhibition by salts has been reported for heterotrophic denitrification in batch (Macêdo et al., 2019; Mariángel et al., 2008; Wang et al., 2016; Zhao et al., 2013) and continuous reactor studies (Dinçer and Kargi, 1999; Glass and Silverstein, 1999; Luo et al., 2021; Panswad and Anan, 1999), as well as for autotrophic denitrification in some batch studies (Chen et al., 2022a; Claus and Kutzner, 1985a; Koenig and Liu, 2004). Most of these studies focus on the inhibition caused by NaCl and only few consider the impacts of other salts (e.g., Na_2SO_4, Na_3PO_4, $MgCl_2$, $CaCl_2$). Therefore, the effects of the single ions, such as Cl^- in absence of Na^+, have not been delineated for denitrification. Since in industrial processes other chemicals than NaCl are often present in variable ratios, Na^+ and Cl^- ions concentrations can vary independently from each other in the wastewater. For this reason, the focus on the inhibition by the single ion is of importance, in view, for example, of a biological nitrogen removal process to treat the wastewater from wet flue gas cleaning systems. Moreover, to the best of the authors knowledge, the potential of autotrophic and heterotrophic denitrification to treat high ions content wastewaters from NO_x-SO_2 removal scrubber has so far not been reported. This becomes relevant especially for industries producing nitrogenous waste streams, such as pulp mills, where both inorganic and organic electron donors for their denitrification would be available.

The aim of this work was to reveal the effects of inorganic ions (Na^+, Cl^-, SO_4^{2-} and K^+) on both heterotrophic (enrichment culture) and autotrophic denitrification (*T. denitrificans*), to better understand the limits and the potential of these biological processes for nitrogen removal from high ion content wastewaters. *T. denitrificans* was selected as the model microorganism for autotrophic denitrification as also used in earlier studies (Di Capua et al., 2017a, 2017b; Zhao et al., 2004; Zou et al., 2016). Pair of ions were added as model compounds (NaCl, Na_2SO_4, KCl and K_2SO_4) in batch tests and the inhibitory effects were evaluated on denitrification rate, nitrite accumulation and duration of lag phase. The order of importance of the ions in decreasing denitrification rate was identified with statistical analysis of the data. Moreover, denitrification potential was demonstrated with real NO_x-SO_2 removal scrubber wastewater from a pulp mill.

2. Materials and methods

2.1. Denitrifying microorganisms: source, cultivation, and growth media

A heterotrophic denitrifying culture was enriched from a denitrifying activated sludge of a municipal wastewater treatment plant (WWTP) located in Helsinki (Finland). The most abundant bacterial genera in the sludge were identified by Kruglova et al. (2020) as *Candidatus Microthrix, Trichococcus, Rhodobacter, Hyphomicrobium* and *Geothrix*. During the enrichment period of three months the culture was regularly transferred to fresh medium after NO_3^- and NO_2^- were removed. The final growth medium (Table S1) was modified from Zou et al. (2014) by addition of ammonia, iron, and yeast extract at pH 7, to overcome nutrient limitation (Fig. S1). Nitrate concentration was increased to 2 g/L to simulate a high-nitrate content wastewater. Methanol was supplemented in excess as electron donor (C/N = 1.3 g/g). During the first two months of the enrichment, the pH of the medium was initially buffered by Na_2HPO_4/NaH_2PO_4 buffer solution and $NaNO_3$ was used as nitrate source. Later, KNO_3 and K_2HPO_4/KH_2PO_4 were used to control the sodium concentration in the medium (Table S1).

Autotrophic denitrifying microorganism *Thiobacillus denitrificans* (DSM 12475) was acquired from Leibniz-Institute DSMZ (Germany). The pure culture was aseptically incubated for three weeks using the growth medium recommended by DSMZ (Leibniz-Institute DSMZ, n.d.), to obtain an active culture. Subsequently, the final medium was modified to minimize the concentration of sodium and increase nitrate

concentration to 2 g/L to simulate a high-nitrate content wastewater (Table S1). Thiosulphate and bicarbonate were added in excess to obtain a S/N ratio of 4.62 g/g and a C/N ratio of 0.86 g/g, and achieve sufficient denitrification and alkalinity, respectively. The pH of final medium was around 7.5. Nutrient solution was autoclaved at 121 °C for 20 min while the other solutions were sterilized by filtration through polyethersulfone (PES) membrane (pore size 0.2 μm). *T. denitrificans* culture was maintained by regular transfers to fresh media, once NO_3^- and NO_2^- were removed and to avoid $S_2O_3^{2-}$ and SO_4^{2-} accumulation. *T. denitrificans* was cultivated in the final medium for three months prior to the experiments.

Both cultures were incubated in 117 mL glass serum bottles with 60 mL liquid volume, the one with heterotrophs in non-aseptic and the *T. denitrificans* in aseptic conditions. After the addition of the respective growth medium, the bottles were sealed with butyl rubber stoppers and aluminium crimps and purged for 20 min with N_2 to create anoxic conditions. After the inoculation (10 % *v*/v), the heterotrophic denitrifying enrichment culture and *T. denitrificans* culture were incubated (150 rpm) at 35 °C and 30 °C, respectively. Incubation temperature for *T. denitrificans* was set to 30 °C as at 35 °C no growth was observed in three weeks of incubation (results not shown).

2.2. Denitrification inhibition by ions: batch assays with model compounds

The effect of chloride and sodium concentrations on both autotrophic and heterotrophic denitrification was studied in batch tests in serum bottles (total number of assays: 134) with addition of NaCl, Na_2SO_4 and KCl. Each salt was tested at final concentrations of Cl^- (as KCl) or Na^+ (as NaCl or Na_2SO_4) in the range 1–30 g/L, corresponding to molar concentrations of 0.02–1.3 mol/L and to salinity of 0.2–9.2 % (*w*/w). Growth medium and incubation were as reported in Table S1 and Section 2.1. If needed, pH was adjusted to around 7 with 10 M KOH. The final working volume of each bottle was 60 mL with 10 % (*v*/v) inoculum. Both tests with autotrophic and heterotrophic denitrification were started between 5 and 7 days after the last culture transfer.

Positive controls (no addition of salt solution) were used in both autotrophic and heterotrophic tests. All the incubations were performed in duplicates and sampled until no NO_3^- and NO_2^- were detected (<100 mg/L) or until 42 days (1000 h) if NO_3^- had not been removed. The sampling frequency was increased when the turbidity of the medium increased visually. From the start to the end of the incubation, the pH remained in the range 6.7–7.8 and 8.2–7.0 for heterotrophic and autotrophic denitrification, respectively.

Since high concentrations of K^+ and SO_4^{2-} were present in the Cl^- and Na^+ tests (Fig. 1), their possible inhibitory effects were studied in a complementary batch test with K_2SO_4 addition, following the same procedures as above. The concentrations tested for heterotrophic denitrification were 15 and 35 g/L K^+, while for autotrophic denitrification were 15 and 20 g/L K^+, taking into account the potassium already present in the media.

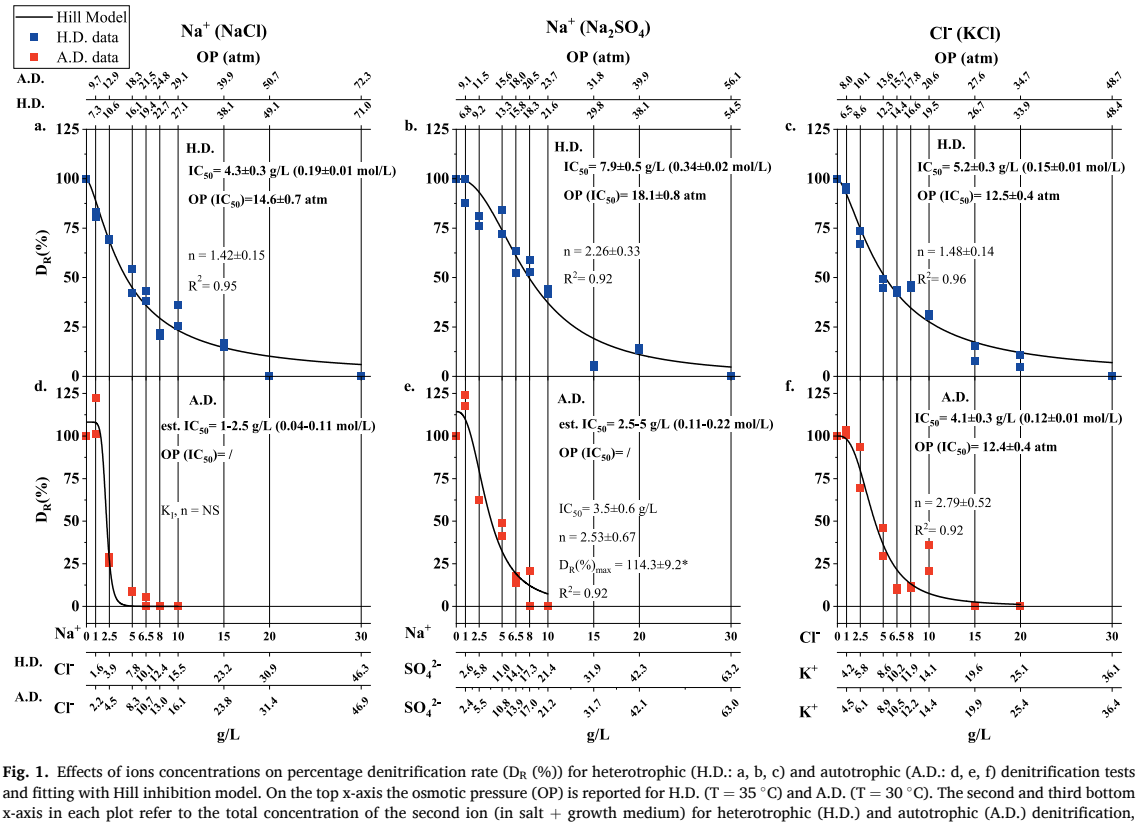

Fig. 1. Effects of ions concentrations on percentage denitrification rate (D_R (%)) for heterotrophic (H.D.: a, b, c) and autotrophic (A.D.: d, e, f) denitrification tests and fitting with Hill inhibition model. On the top x-axis the osmotic pressure (OP) is reported for H.D. (T = 35 °C) and A.D. (T = 30 °C). The second and third bottom x-axis in each plot refer to the total concentration of the second ion (in salt + growth medium) for heterotrophic (H.D.) and autotrophic (A.D.) denitrification, respectively. Two data points (duplicates) are shown for each ion's concentrations. NS: not significant. * Fitted value.

2.3. Source and composition of saline wastewater produced by a simultaneous NO_X-SO_2 removal scrubber system

Wastewater from a wet cleaning system removing NO_x-SO_2 from flue gases produced in two recovery boilers was obtained from a pulp mill. In the NO_x-SO_2 removal scrubber, NaOH is used as scrubbing agent, while ClO_2 and sulphurous compounds are added to increase NO_x solubility. Prior to the scrubber, an electrostatic precipitator is used at the plant to remove particles from the flue gases. A wastewater sample (2 L), collected from the first of the three stages of the scrubber, was stored in a plastic container (prewashed with 1 M nitric acid) for several months at 4 °C. During this period, analysis of samples taken at different frequencies showed that concentrations of anions did not change (results not shown).

The composition of the wastewater sample is presented in Table 1.

2.4. Denitrification batch assays on wastewater produced by a simultaneous NO_x-SO_2 removal scrubber system

Heterotrophic and autotrophic denitrification of real NO_x-SO_2 removal scrubber wastewater was studied in batch assays under non-aseptic conditions. Prior to the experiment, the pH of the wastewater was adjusted to 7 with 10 M KOH and solids were removed by settling. The wastewater supernatant was then added (88 % v/v) to serum bottles (60 mL working volume), together with addition (2 % v/v) of additive solution. The additive solution contained electron donor in excess (MeOH for heterotrophic denitrification (C/N = 1.3 g/g) and $S_2O_3^{2-}$ for autotrophic denitrification (S/N = 4.64 g/g)), and HCO_3^- (C/N = 0.86 g/g) in the test with *T. denitrificans*. The bottles with the wastewater and amendments were purged with N_2 for 20 min before inoculation (10 % v/v) with heterotrophic enrichment culture or *T. denitrificans*. Inoculated bottles with growth medium were incubated as positive controls. The experiment was run in duplicates. Denitrification was monitored by sampling every 24–72 h.

2.5. Analytical methods and calculations

2.5.1. Sampling and analyses

At every sampling time, 1 mL liquid sample was taken and filtered through 0.2 μm Chromafil Xtra syringe filters (Macherey-Nagel, Germany). Before the filtration, samples from the bottles with Cl^- concentration above 10 g/L were pre-treated with chloride elimination set (Hach LCW925) to reduce the Cl^- interference with the nitrite measurement (Glass and Silverstein, 1999). Samples from the heterotrophic denitrification test were stored at −20 °C, while the ones from the autotrophic denitrification test were stored at +4 °C, since at −20 °C excessive formation of precipitate was observed for samples from cultivation after being melted. An additional 0.5 mL sample was taken at the beginning and the end of the incubation for pH measurement with WTW pH-meter 330i. Concentrations of anions (Cl^-, NO_2^-, NO_3^-, SO_4^{2-}, $S_2O_3^{2-}$) in all the filtered samples from the batch tests were analysed via ion chromatograph as reported by Hajdu-Rahkama and Puhakka (2022). Concentration of MeOH was measured in the samples from the heterotrophic denitrification tests via gas chromatograph equipped with a flame ionization detector according to Kokko et al. (2018).

Table 1
Characterization of the wastewater produced from a full-scale simultaneous NO_x-SO_2 removal scrubber system treating the flue gases produced in two recovery boilers of a pulp mill.

Analyte	Concentration (mg/L)	Analyte	Concentration (mg/L)
Cl^-	3 400	Al	1.14
NO_2^-	<100	As	<0.01
NO_3^-	1 100	B	24.70
SO_4^{2-}	13 500	Co	<0.01
$S_2O_3^{2-}$	<100	Cr	0.21
		Cu	0.01
		Fe	7.60
DOC[a]	13	K	22.16
DIC[b]	/	Mg	2.64
		Mn	0.08
pH	1.8	Mo	0.02
T (°C)	64.5	Na	5 200.00
		Ni	0.12
		P	0.29
		Pb	<0.01
		Se	0.02
		V	<0.01
		Zn	0.19

[a] Dissolved Organic Carbon.
[b] Dissolved Inorganic Carbon.

2.5.2. Calculations

Inhibitory effects of the ions on autotrophic and heterotrophic denitrification were monitored as denitrification rate, lag phase and nitrite accumulation. Denitrification rates (mg/L h^{-1}) were estimated by the linear regression tool in Origin 2019b software (100 interpolations with $R^2 > 90$, 4 with $72 < R^2 \leq 90$), considering the part with maximum slope in the plot of NO_3^- concentration vs. time. Percentage denitrification rates (D_R (%)) with respect to the average of positive controls were calculated. If D_R (%) > 0, the time (h) before the steepest part of the NO_3^- concentration curve, approximatively corresponding to the inflection point, was considered as the lag phase of denitrification. Stoichiometry of denitrification reactions was verified by comparing measured concentrations of consumed methanol and consumed/produced thiosulphate/sulphate with theoretical values obtained from Eqs. (1), (2).

The osmotic pressure (OP) and the ionic strength of the solution, due to the main ions in the growth media (Table S1) and the added inhibitory salts, were estimated as described by Fritzmann et al. (2007) and Belessiotis et al. (2016).

Modified non-competitive Hill model was adopted to describe the effect of sodium and chloride ions concentrations on the percentage denitrification rate (D_R (%)), as described by Lin et al. (2021) for Anammox process. The model was expressed with Eq. (3):

$$D_R(\%) = \frac{D_R(\%)_{max} \bullet K_I^n}{K_I^n + I^n} \quad (3)$$

where $D_R(\%)_{max}$ is the maximum percentage denitrification rate (100 %) related to the positive control, K_I (=IC_{50}) is the half-inhibition constant (g/L) corresponding to the ion concentration that results in 50 % inhibition, I is the independent variable representing the concentration of the ion (g/L) and n is the tuning parameter. The model was implemented and fitted to the experimental calculated percentage denitrification rates with the "Non-linear curve fit" tool in Origin 2019b software. R^2 and *p*-value for *t*-test (set at 0.05) were used to evaluate the goodness of the fit and the significance of the parameters (K_I, n). If the fitting of the data returned non-significant parameters, IC_{50} was expressed as a range based on the experimental data.

To identify the ion with the highest effect on denitrification rate, a statistical analysis was performed on the experimental data, separately for heterotrophic and autotrophic denitrification. Concentrations (mol/L) of the ions (Na^+, Cl^-, SO_4^{2-} and K^+) were considered as the independent variables, while D_R(%) was the response variable (see supplementary materials). Partial Least Square Regression (PLSR), previously used for analysis of denitrification studies by Pan et al. (2023), and Random Forest Regression (RF) (Song et al., 2020) were implemented with Minitab software and Python "RandomForestRegressor" function, respectively, to analyse data characterized by strong collinearity. Eventually, standardized coefficients and variable importance values returned by PLSR and RF, respectively, were examined to determine which ion had the highest importance in decreasing denitrification rate.

3. Results

The effects of inorganic ions on percentage denitrification rates (D_R(%)), nitrite accumulation and lag phase for both heterotrophic and autotrophic denitrification are summarized in Figs. 1 and 2. Increasing concentration of the single ions inhibited autotrophic and heterotrophic denitrification to different extents. Despite the partial inhibition of denitrification, when $D_R(\%) > 0$, over 95 % of the initial nitrate concentration was removed (Fig. S2-S7). Moreover, at almost all the studied ion concentrations, >95 % of the accumulated NO_2^- was eventually removed (Fig. S2-S7).

3.1. Effects of inorganic ions on heterotrophic denitrification by enrichment culture

For heterotrophic denitrification (Fig. 1a, b, c), the fitting of the experimental data with the modified Hill inhibition model, showed that 50 % rate inhibition (IC_{50}) with Na^+ (as NaCl), Na^+ (as Na_2SO_4) and Cl^- (as KCl) was obtained at 4.3 ± 0.3, 7.9 ± 0.5 and 5.2 ± 0.3 g/L, with the corresponding osmotic pressures ($OP(IC_{50})$) of 14.6 ± 0.7, 18.1 ± 0.8 and 12.5 ± 0.4 atm, respectively. At the same concentration of Cl^- (5.2 g/L), rate inhibition and cation concentration with NaCl and KCl were 42 % and 3.5 g/L Na^+, and 50 % and 8.8 g/L K^+ (also considering K^+ in the growth medium), respectively. Lower inhibition was observed by K^+ and SO_4^{2-} (as K_2SO_4) as the rate decreased by about 40 % at 15 g/L K^+ and 15 g/L SO_4^{2-}, while co-presence of 35 g/L K^+ and 40 g/L SO_4^{2-} (OP≈ 36 atm) resulted in partial inhibition only (Fig. 3). By expressing the IC_{50} in molar units (mol/L), in accordance with the results in g/L, Cl^- was more inhibitory than SO_4^{2-} when paired with Na^+ as 50 % inhibition was reached at 0.19 ± 0.01 mol/L Na^+ (as NaCl) and 0.34 ± 0.02 mol/L Na^+ (as Na_2SO_4), respectively. This was also seen by plotting OP vs D_R(%) (Fig. S11), since at similar OP, denitrification with addition of Na_2SO_4 had higher rates than with addition of NaCl, while with KCl it had the lowest rates. Also, Na^+ was more inhibitory than K^+ when paired with SO_4^{2-}, as about 40 % inhibition was reached at 0.28 mol/L Na^+ with 0.14 mol/L SO_4^{2-} (as Na_2SO_4) and 0.38 mol/L K^+ with 0.16 mol/L SO_4^{2-} (as K_2SO_4). On the other hand, IC_{50} of Cl^- as KCl (0.15 ± 0.01 mol/L) was lower than that of Na^+ as NaCl (0.19 ± 0.01 mol/L). Eventually, denitrification was completely inhibited at 20 g/L (0.87 mol/L) Na^+ as NaCl, 30 g/L (1.3 mol/L) Na^+ as Na_2SO_4 and 30 g/L (0.85 mol/L) Cl^- as KCl. Denitrification rate decreased with increasing OP and no denitrification activity was observed above OP of 40 atm (Fig. 1 and S11). When plotting D_R(%) with ionic strength (Fig. S12), large variations of the denitrification rates were observed at similar ionic strengths of the solution, further confirming that the type of the ions added had a key role in denitrification inhibition.

Inhibition by the ions was further characterized as increase in lag phase and variation in nitrite accumulation during denitrification (Fig. 2). For heterotrophic denitrification (Fig. 2c), lag phase was not clearly present at the lower Cl^- and Na^+ concentrations but started to increase from 8 g/L Na^+ and 15 g/L Cl^-. With K_2SO_4, the lag phase in the presence of 35 g/L K^+ was between 15 and 22 days. Longer lag phases was seen in the presence of Na^+ (as NaCl and Na_2SO_4) than of Cl^- (as KCl). For instance, at 20 g/L of the ion, lag phase was around 35 days for Na^+ (as Na_2SO_4) while around 10 days for Cl^- (as KCl).

In denitrification, nitrite (NO_2^-) can accumulate as an intermediate during nitrate reduction to nitrogen gas. In this study, in heterotrophic denitrification without salt addition, approximatively 1000 mg/L NO_2^- accumulated (Fig. 2a) and was followed by over 95 % removal within 120 h (Fig. S8). Starting from 5 g/L Na^+ (Fig. 2a), NO_2^- accumulation decreased, with the lowest accumulation for Na^+ (as NaCl). On the other hand, in the presence of Cl^- (as KCl), nitrite steadily accumulated up to 10 g/L Cl^-. No nitrite accumulated in the presence of and above 10 g/L Na^+ (as NaCl), 20 g/L Na^+ (as Na_2SO_4) and 20 g/L Cl^- (as KCl). With K_2SO_4, accumulation of NO_2^- decreased from around 1100 mg/L in the positive controls to around 800 mg/L at 15 g/L K^+ and was eventually removed by over 95 % (Fig. 3). Therefore, Cl^- had a higher effect than SO_4^{2-} while Na^+ higher than K^+ in decreasing nitrite accumulation. Moreover, NO_2^- accumulation was less affected than denitrification rate in the increase in OP and ionic strength (Fig. S12).

In summary, increasing Na^+ concentration resulted in longer lag phase than with increasing Cl^-, and nitrite accumulation (and

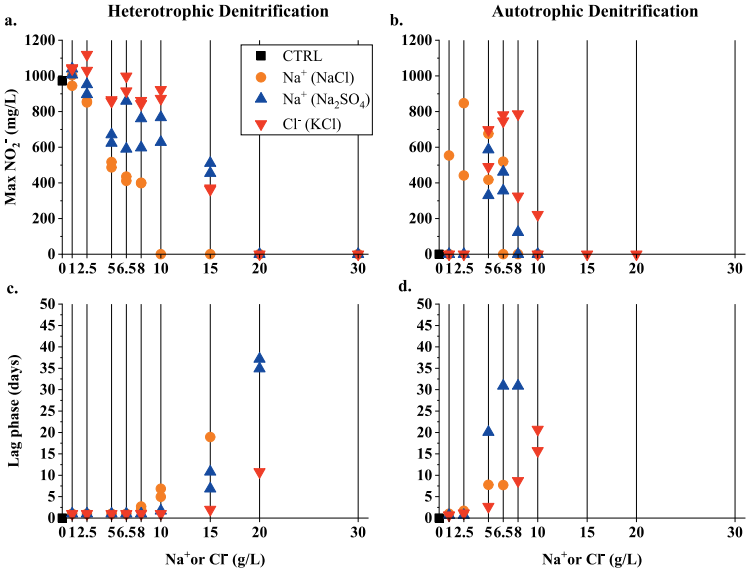

Fig. 2. Effects of ions' inhibition of heterotrophic (on the left) and autotrophic (on the right) denitrification on highest nitrite concentration accumulation during the incubation (a. and b.) and lag phase (c. and d.). Two data points (duplicates) are shown for each ion. Positive controls are indicated as "CTRL" and are represented by average values ($n = 6$) (plot c: standard error < 5 %).

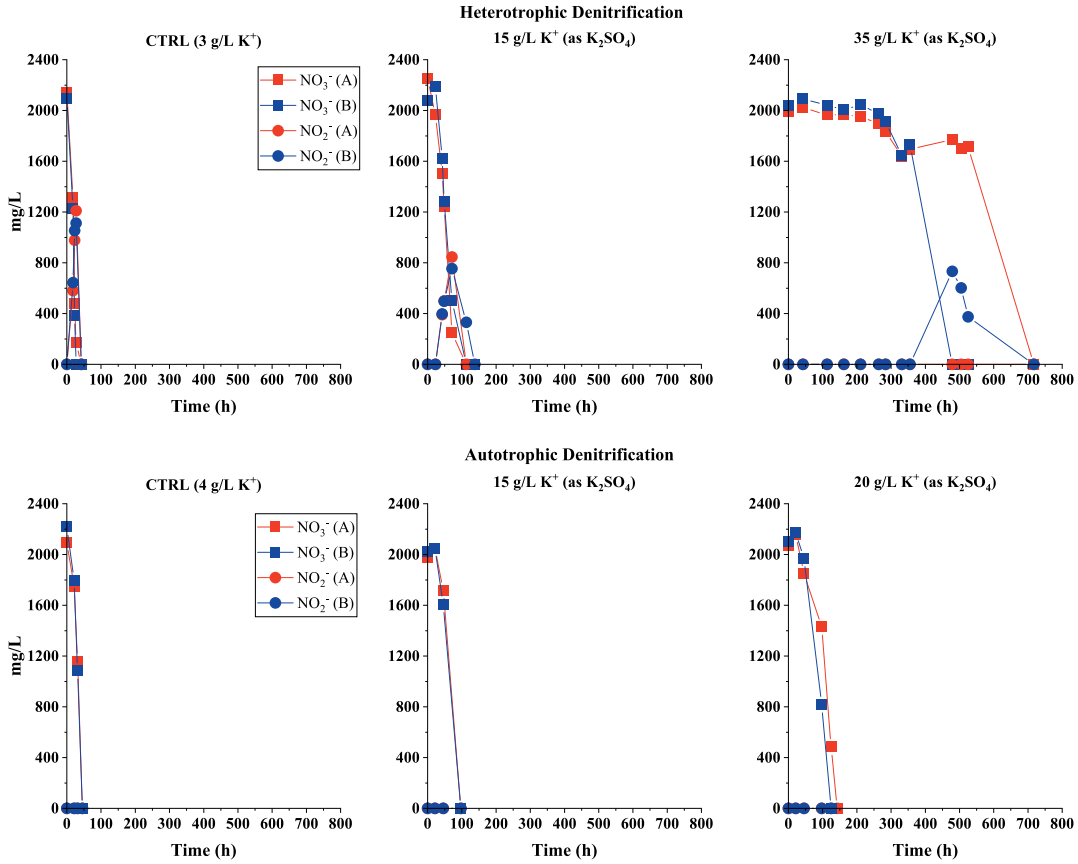

Fig. 3. Nitrate and nitrite concentrations plotted against time at different concentrations of K^+ (as K_2SO_4) for heterotrophic denitrification (first row) and autotrophic denitrification (second row). Two data points (duplicates) are shown for each concentration. CTRL plot refers to the positive control with the only inoculated growth medium in absence of salt addition.

subsequent removal) indicated that nitrite removal was less inhibited than nitrate removal by Cl^- and Na^+ and was less affected by K^+ and SO_4^{2-} than Na^+ and Cl^-.

At the end of the incubations, MeOH removal in heterotrophic denitrification (Fig. S10a) was in line with the stoichiometry and no clear correlation between electron donor consumption and increasing concentration of the ions was apparent. Eventually, after extending the incubation time by additional 30 days, nitrate was not removed at the highest concentrations of Cl^- and Na^+.

Eventually, since all the experiments were conducted with an anion paired with a cation, a statistical analysis of the data was conducted to better discern the effect of the single ions on denitrification rate. Based on the analysis of standardized coefficients for PLSR and variables importance for RF, Cl^- resulted to have the most important role in decreasing denitrification rate (Fig. S13), supporting the observations made. Further considerations on the order of inhibition of the other studied ions could not be made from the statistical analysis, as their ability in predicting the decrease in denitrification rate varied with the two methods.

3.2. *Effects of inorganic ions on autotrophic denitrification by T. denitrificans*

For autotrophic denitrification by *T. denitrificans*, D_R(%) increased at 1 g/L Na^+ (as NaCl and Na_2SO_4) (Fig. 1d, e, c), showing that low concentrations of sodium stimulated denitrification in comparison to the conditions in the positive controls. However, starting from 2.5 g/L Na^+ as NaCl and Na_2SO_4, denitrification rate started to decrease rapidly. Fitting of the experimental data with the Hill inhibition model, returned significant ($p < 0.05$) parameters for Cl^- (as KCl): $IC_{50} = 4.1 \pm 0.3$ g/L and calculated $OP(IC_{50}) = 12.4 \pm 0.4$ atm. Hill inhibition equation (Eq. (3)) did not adequately model Na^+ inhibition, thus, IC_{50} were taken as ranges from the experimental data for Na^+ (as NaCl) and Na^+ (as Na_2SO_4) and were 1–2.5 and 2.5–5 g/L, respectively. In molar units, the values of IC_{50} for Na^+ (as NaCl), Na^+ (as Na_2SO_4) and Cl^- (as KCl) were 0.04–0.11, 0.11–0.22 and 0.12 ± 0.01 mol/L, respectively. Moreover, since duplicates for autotrophic denitrification presented noticeable variation at certain concentrations of Cl^- and Na^+, these assays were rerun. The results of the rerun (Fig. S5, S6, S7), not included in Fig. 1, differed to some extent from the previous tests, which was attributed to sensitivity of *T. denitrificans* under close to fully inhibitory salt conditions. K^+ and SO_4^{2-} had lower inhibitory effects than Cl^- and Na^+ also on autotrophic denitrification rate as it decreased by around 60 % in the co-

presence of 20 g/L (0.51 mol/L) K^+ and 20 g/L (0.21 mol/L) SO_4^{2-} (Fig. 3). Also, at similar OP, denitrification with K_2SO_4 had higher D_R(%) than with the other salts (Fig. S11). Complete inhibition was observed at 8 g/L (0.35 mol/L) Na^+ as NaCl, at 10 g/L (0.44 mol/L) Na^+ as Na_2SO_4 and at 15 g/L (0.43 mol/L) Cl^- as KCl. Total inhibition was reached at similar molar concentrations of both Cl^- and Na^+.

For autotrophic denitrification (Fig. 2d), lag phase increased starting from 5 g/L Na^+ and Cl^-, in the range 3–20 days, and showed longer lag phases in the presence of Na^+ (as NaCl and Na_2SO_4) than of Cl^- (as KCl). With K_2SO_4, the lag phase was between 2 and 4 days at 20 g/L K^+ (Fig. 3).

In the autotrophic denitrification test, no nitrite accumulated in the positive controls (Fig. 2b). With increasing concentrations of Na^+ and Cl^-, NO_2^- accumulation initially increased but then, for the highest concentrations of the ions tested, decreased to below 100 mg/L. Nitrite accumulation started at 1 g/L Na^+ (as NaCl), while it accumulated at 5 g/L Na^+ (as Na_2SO_4) and Cl^- (as KCl). No nitrate accumulated during autotrophic denitrification at any of K^+ (as K_2SO_4) concentrations tested (Fig. 3). Cl^- and Na^+ affected nitrite accumulation more than SO_4^{2-} and K^+, and nitrite removal was less inhibited than nitrate removal, similarly to what observed for heterotrophic denitrification.

For autotrophic denitrification, thiosulphate consumption and sulphate production decreased with increasing concentrations of Na^+ (Fig. S10b and S10c) with respect to the stoichiometry, while Cl^- (as KCl) had a lower effect.

Also, for autotrophic denitrification by *T. denitrificans*, both PLSR and RF returned that Cl^- had the most important role in decreasing denitrification rate (Fig. S13), similarly to what seen for heterotrophic denitrification.

3.3. Denitrification of real wastewater from simultaneous NO_x-SO_2 removal scrubber

The potential of heterotrophic and autotrophic denitrification of real scrubber wastewater was studied in batch tests. In all the tests with inoculated wastewater and electron donor/carbon supplementation, nitrate removal was slower than in positive controls (<50 h for 95 % removal) but it was eventually over 95 % (Fig. 4). Initial nitrate (around 800 mg/L) was removed over 95 % in <80 h by autotrophic denitrification (Fig. 4b) and within 150 h by heterotrophic denitrification (Fig. 4a), at Cl^-, Na^+ and SO_4^{2-} concentrations in the wastewater (OP around 10 atm) of 3 g/L, 4.5 g/L and 12 g/L, respectively (considering dilution caused by culture conditions). Electron donors and products were in line with the stoichiometries of nitrate removal (Fig. 4d and e). Nitrite did not accumulate in batch tests.

In summary, both heterotrophic and autotrophic denitrification removed nitrate from the scrubber wastewater.

4. Discussion

This study revealed the inhibitory effects of chloride, sodium, potassium, and sulphate ions on autotrophic and heterotrophic denitrification as determined by nitrate removal rate, nitrite accumulation and lag phase of the batch incubations. Also, nitrate was successfully removed from real NO_x-SO_2 scrubber wastewater.

4.1. Effects of the ions on heterotrophic and autotrophic denitrification

The effects of single ions on denitrification have not been delineated in detail in previous studies, which have focused mainly on the salts (Table 2). For instance, Cl^- inhibition has been reported for heterotrophic denitrification as NaCl (Holm Kristensen and Jepsen, 1991; Panswad and Anan, 1999) but not as KCl, thus including also Na^+ inhibition. Also, denitrification inhibition by K^+ (as K_2SO_4) has not been described by others, and shows, when compared with other salts in Table 2, the lowest effect in almost all the cases. The results for Na^+ (both Na_2SO_4 and NaCl) inhibition on heterotrophic denitrification rate were similar to those reported by Wang et al. (2016) and Zhao et al. (2013), showing

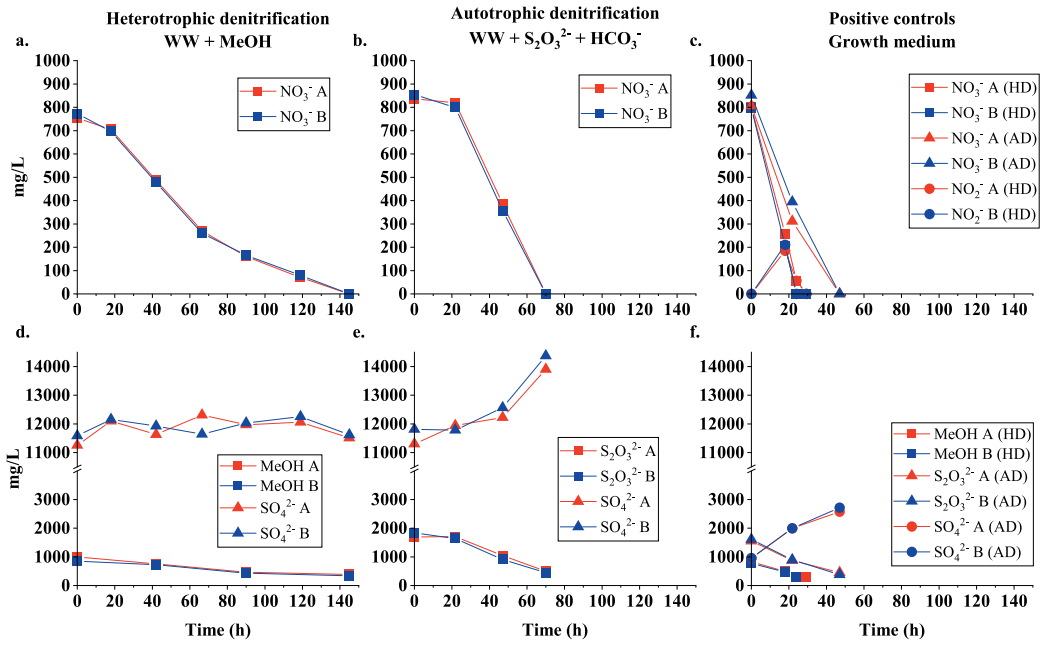

Fig. 4. Nitrate and nitrite concentrations (a, b, c) and MeOH, thiosulphate and sulphate concentrations (d, e, f) vs. time for heterotrophic and autotrophic denitrification of simultaneous NO_x-SO_2 removal scrubber wastewater (WW) with electron/carbon source supplementation. Duplicates (A and B) are shown in each plot.

Table 2
Comparison of studies investigating salinity inhibition on heterotrophic and autotrophic denitrification. All the results refer to batch studies conducted at temperatures ranging from 22 to 37 °C. The concentrations of the added salt reported in the references have been converted into concentration of the added ion for the comparison with this study.

Denitrification	Microorganisms and source	Initial NO_3^- (g/L)	Energy source	Denit. activity inhibition %	Ion concentration (g/L)		Reference
Heterotrophic	Enrichment culture from a denitrifying compartment of a WWTP	2	Methanol	50 % 50 % 50 % ~40 %	4.3 ± 0.3 7.9 ± 0.5 5.2 ± 0.3 15	Na^+ (as NaCl) Na^+ (as Na_2SO_4) Cl^- (as KCl) K^+ (as K_2SO_4)	This study
	Granular sludge from a lab-scale denitrifying reactor	0.44	Acetate	50 % 50 % 50 %	4.54 7.03 3.14	Na^+ (as NaCl) Na^+ (as Na_2SO_4) Na^+ (as Na_3PO_4)	Wang et al. (2016)
	Biomass adapted at 24 g/L NaCl for a year in a batch reactor	0.44	Fish blood water	50 %	18	Na^+ (as NaCl)	Mariángel et al. (2008)
	Inoculum from lab-scale partial denitrification system	0.26	Acetate	71 %	~4	Na^+ (as NaCl)	Ji et al. (2018)
	Seed from lab-scale sequencing batch reactor	0.18	Methanol	31 % ~60 %	~4 ~8	Na^+ (as NaCl) Na^+ (as NaCl)	Zhao et al. (2013)
Autotrophic	*T. denitrificans* (DSM 12475)	2	Thiosulphate	50 % 50 % 50 % ~60 %	1–2.5 2.5–5 4.1 ± 0.3 20	Na^+ (as NaCl) Na^+ (as Na_2SO_4) Cl^- (as KCl) K^+ (as K_2SO_4)	This study
	T. denitrificans enriched from soil	0.92	Thiosulphate	~35 % ~60 %	12 ~5	Na^+ (as NaCl) Na^+ (as Na_2SO_4)	Claus and Kutzner (1985a)
	Enrichment culture from tidal flats	0.44	Elemental sulphur	10 %	8 12	Na^+ (as NaCl) Na^+ (as Na_2SO_4)	Koenig and Liu (2004)
	Enrichment culture from fish cannery wastewater treatment	0.44	Thiosulphate	10 %	4	Na^+ (as NaCl)	Campos et al. (2008)
	Enrichment culture from an anoxic tank of a WWTP	0.11	Sulphide	50 %	26	Na^+ (as NaCl)	Chen et al. (2022a)

higher inhibition by the co-presence of Na^+ and Cl^- rather than Na^+ and SO_4^{2-}. On the other hand, higher tolerance to Na^+ paired with Cl^- was observed by Mariángel et al. (2008) by using denitrifying biomass after a long-term enrichment under saline conditions.

Inhibitory effects on denitrification were also observed in nitrite accumulation and in the increase in lag phase duration. Nitrite accumulation during denitrification depends on many factors, such as nitrate and phosphate concentrations, pH, dissolved oxygen, temperature (Philips et al., 2002). In our study, without ions addition, heterotrophic denitrification accumulated around 1000 mg/L NO_2^- (70 % of the initial nitrogen) and reduced it further (>95 %) with no clear inhibition. In comparison, Glass et al. (1997) reported that heterotrophic denitrification at pH 8 removed 6500 mg/L NO_2^- and was not completely inhibited. With increasing concentrations of the ions, especially Na^+, nitrite accumulation decreased, similarly to what reported by Zhao et al. (2013).

Increasing concentrations of the inorganic ions rapidly decreased autotrophic denitrification rates by *T. denitrificans*. Furthermore, low concentrations of sodium (up to 1 g/L in this study), enhanced the rates, indicating that *T. denitrificans* requires Na^+ for optimal growth. Therefore, Hill inhibition model as written in Eq. (3) did not consider the initial increase in denitrification rate and, thus, did not comprehensively model the sodium effects on autotrophic denitrification. For this reason, IC_{50} were estimated as a range from the experimental data. In our study, Na^+ (as NaCl) had the lowest inhibitory concentration reported for autotrophic denitrification if compared to other reports (Table 2). Moreover, the co-presence of Na^+ and Cl^- resulted more inhibitory than Na^+ and SO_4^{2-}, as also reported by Koenig and Liu (2004). Inhibition by Na^+ as Na_2SO_4 was close to that reported by Claus and Kutzner (1985a) (Table 2), who attributed the inhibitory role to SO_4^{2-}. Contrarily, 20 g/L SO_4^{2-} at the beginning of incubation did not completely inhibit autotrophic denitrification in our study, similarly to the observations of Chung et al. (2014). The different tolerances to ions were likely due to the origin of autotrophic as well as heterotrophic denitrifying microorganisms (different in all the studies as reported in Table 2). As for Cl^- inhibition in absence of Na^+ of autotrophic denitrification, which has not been previously reported, our study showed IC_{50} at 4.1 ± 0.3 g/L Cl^- (as KCl).

For autotrophic denitrification, no nitrite was detected in the positive controls. Hence, salinity also inhibited nitrite reduction and NO_2^- accumulated with increasing concentration of the ions. Claus and Kutzner (1985a) reported 70 % denitrification inhibition on *T. denitrificans* at 1000 mg/L NO_2^-. In our study, the highest NO_2^- accumulation for autotrophic denitrification was around 850 mg/L, and, hence, nitrite inhibition on *T. denitrificans* could not be completely excluded. However, in almost all the cases, nitrite was removed by >95 % and its accumulation decreased with the increase in the ions' concentrations once the nitrate removal become slower. Therefore, despite an initial inhibition of nitrite reduction for autotrophic denitrification, denitritation seemed to be less inhibited by the inorganic ions than

denitratation, as also reported by others for heterotrophs (Mariángel et al., 2008; Zhao et al., 2013) and autotrophs (Chen et al., 2022a).

Eventually, autotrophic denitrification reaction showed to be more affected by Na^+ than the other ions. Consumption of $S_2O_3^{2-}$-S by *T. denitrificans* in the presence of 2.5 g/L Na^+ and above was lower than the stoichiometry (Fig. S10b), indicating that NO_3^- and NO_2^- were not completely reduced to N_2 and other intermediates (not measured in this study) could have possibly accumulated. For instance, Chen et al. (2023) reported accumulation of N_2O with autotrophic NO_2^- removal at increasing NaCl concentrations, indicating that nitrous oxide reduction was the limiting step. Moreover, SO_4^{2-}-S production was lower than $S_2O_3^{2-}$-S consumption (Fig. S10c), suggesting that inhibitory concentrations of Na^+ could also affect the sulphur end products of denitrification reaction.

4.2. Sensitivity of denitrification activity to the single ions

As shown above, the studied ions affected denitrification activity to different extents. Na^+ is toxic at high intracellular levels and can disrupt the cell membrane because of unbalanced osmotic pressure (Yang et al., 2013). Moreover, also anions can affect the activity and stability of many enzymes (for a review, see Zhao (2005)), such as Cl^- and SO_4^{2-} (Lin et al., 2021). Different explanations for the mechanisms of ions and salts inhibition on denitrification have been reported in the literature. For instance, Zhao et al. (2013) reported that osmotic stress played a primary role in the inhibition of denitrification by NaCl and that Na^+ could affect the activity of denitrification enzymes. Moreover, Koenig and Liu (2004) reported for an autotrophic culture enriched from tidal flats that the decrease in denitrification rate was dependent on OP but independent of the type of the salt when studying the effect of a single salt (NaCl or Na_2SO_4) on denitrification. They showed that inhibition started above 20 atm, while in our study at that OP autotrophic denitrification rates were already below IC_{50} for cultures not originally enriched from a saline environment. On the other hand, with multi-ions solution (NaCl, $MgCl_2$ and $CaCl_2$), Macêdo et al. (2019) reported for a heterotrophic culture not cultivated in saline environment that the specific toxicity and the interactions between the salts were the key factors, regardless of the osmotic pressure applied. In the range 11–13 atm, their denitrification rates were inhibited over 70 % against the 50 % observed with KCl in our study. Considering that in our study at the same OP the pairs of ions decreased denitrification rate at different extents, the inhibition by ions was likely due to both the osmotic stress and the toxicity of the single ions. However, the exact mechanisms of ions' inhibition in this study cannot be further disclosed.

As for the order of inhibition of anions and cations, based on the results of our study in mol/L, Cl^- was more inhibitory than SO_4^{2-}, while Na^+ more than K^+. However, Cl^- as KCl had lower IC_{50} than as NaCl. This could indicate that K^+ was more inhibitory than Na^+ when paired with Cl^-, but, as shown in the test with K_2SO_4 in terms of denitrification rate and nitrite accumulation, and as reported by others (Chen et al., 2022b; Fang et al., 2011), bacterial cells seem to be less affected by potassium than sodium ions. Hence, despite more investigations on possible combined inhibition by K^+ and Cl^- are required, in this study, the major inhibitory anion and cation were attributed to Cl^- and Na^+. Furthermore, to better understand the effects of the single ions, the available data were analysed with two different statistical methods both returning Cl^- as the ion with the most important effect on denitrification rate. However, by using salts to study ions' inhibition, only pair of ions can be tested and not all the combinations are possible without adding a third ion (e.g., Na^+-K^+ and Cl^--SO_4^{2-}), which can affect the outcomes of the statistical analysis. Eventually, considering also that the OP associated to the salt at IC_{50} was lower for KCl and NaCl than Na_2SO_4, it can be concluded that Cl^- had very likely the highest toxic effect on both autotrophic and heterotrophic denitrification.

In general, heterotrophic enrichment culture showed higher tolerance to the ions than *T. denitrificans*. Even though composition of microbial community was not characterized, it was very likely that species tolerant to salinity became selectively enriched in the heterotrophic culture. Such selective enrichment has been reported as microbial community change with increasing salinity (Ji et al., 2018; Macêdo et al., 2019; Wang et al., 2018). On the other hand, *T. denitrificans* was the sole denitrifying species in the autotrophic tests, and more sensitive to the ions. The microorganism-based tolerance for ions in nitrogen removal processes, can also be observed for freshwater Anammox bacteria (Lin et al., 2021) and *Acinetobacter* sp. (heterotrophic nitrification and aerobic denitrification) (Chen et al., 2022b), as the former was more sensitive to K^+ rather than Na^+, while the latter was more inhibited by Na^+ than K^+, but for both SO_4^{2-} had the main inhibitory role. Therefore, the source of microorganisms needs to be properly selected for biological nitrogen removal from saline industrial wastewaters based not only on the substrate and the salinity, but also on the inorganic ions present.

4.3. Potential of biological denitrification for the treatment of high-ion-content industrial wastewaters: example of NO_x-SO_2 removal scrubber

Wet scrubbing is a common technology used to treat flue gases emitted by industries as well as vessels (Córdoba, 2015; Deng et al., 2021), which generates a liquid waste. The characteristics of this wastewater depend mainly on the flue gas composition and the type of scrubbing process. In the case of NO_x-SO_x removal scrubbers, ClO_2 and sodium based sulphurous compounds are used to enhance NO_x solubility (Schmid et al., 2022), while NaOH is used as a scrubbing agent (Chen et al., 2021), resulting in high and variable concentrations in the wastewater of not only nitrogenous and sulphurous compounds, but also chloride and sodium, as reported in Table 1 and Table S3 for a system treating flue gases from a pulp mill. To complete the NO_x removal and reduce the overall impact of emissions on water and air, denitrification can represent an effective solution to be implemented along with air emission control. Therefore, in this study, a first investigation on the potential of denitrification to treat wastewater from NO_x-SO_x removal scrubbers was made, starting from the possible inhibitory effects given by the main ions present.

According to the results of the tests with the model compounds, heterotrophic denitrification removed 2 g/L NO_3^- at Cl^-, Na^+ and SO_4^{2-} concentrations higher than those present in the real wastewater samples (Table 1 and Table S3), while *T. denitrificans* (DSM 12475) was more inhibited. Nitrite accumulated and was removed in both autotrophic and heterotrophic denitrification in the presence of the ions, showing promising results to avoid harmful discharge of NO_2^-. However, accumulation of other intermediates, such as N_2O, needs to be carefully considered for the environment. On the other hand, in the test with real wastewater, autotrophic denitrification was faster than heterotrophic denitrification in removing 800 mg/L NO_3^- and no NO_2^- accumulated at 3 g/L Cl^-, 4.5 g/L Na^+ and 12 g/L SO_4^{2-}, showing lower inhibition even in the presence of multiple ions. This could be due, for instance, to the presence of several metals (Table 1), to which autotrophic denitrification seem to have higher tolerance (Claus and Kutzner, 1985b); to other unidentified inhibitors for heterotrophic denitrification and boosters for autotrophic denitrification; or to lack of nutrients as NH_4^+ that has been reported as not essential for *T. denitrificans* (Koenig and Liu, 2001). Thus, the most likely inhibitory factor in the NO_x-SO_2 removal scrubber wastewater for *T. denitrificans* was salinity, similarly to what reported for flue gas desulphurization scrubber wastewater by Koenig and Liu (2004). Nevertheless, salinity tolerance seem to be enhanced in continuous flow reactors, where heterotrophic denitrification has been reported at 71.2 g/L NaCl (Glass and Silverstein, 1999) and 45 g/L Cl^- (Vredenbregt et al., 1997), and autotrophic denitrification at 33 g/L NaCl (Zhao et al., 2004), combined with biofilm systems, which present higher tolerance to toxicity (Liu et al., 2022).

The application of autotrophic denitrification to wastewaters from NO_x-SO_2 removal scrubber represents an interesting solution, as the electron donors could come from the scrubbing process, where large

amounts of $S_2O_3^{2-}$ and SO_3^{2-} are employed (Schmid et al., 2022). Moreover, autotrophic denitrification is reported to have lower N_2O gas production than heterotrophic (Cui et al., 2019), which tends to increase with increasing salinity (Zhao et al., 2013). However, one of the disadvantages of autotrophic denitrification is the large production of SO_4^{2-} (Di Capua et al., 2019), which is already present at high concentrations in the scrubber wastewaters (Table 1). A partial solution to this problem could be the application of mixotrophic denitrification that decreases sulphate production (Sahinkaya et al., 2011). Furthermore, also the variability in composition of NO_x-SO_2 removal scrubber wastewaters (Table 1 and S3) needs to be considered for the development of biological treatments.

Overall, the presence of organic waste streams (Meyer and Edwards, 2014) and the use of $S_2O_3^{2-}$ and SO_3^{2-} in the scrubbing process of flue gases highlight the attractiveness of pulp industry for the application of both autotrophic and heterotrophic denitrification. Therefore, denitrification could represent a potential solution for nitrate removal from NO_x-SO_2 removal scrubber wastewaters, as well as other saline industrial wastewaters, requiring further investigations in larger scale bioreactors.

5. Conclusions

In this study, inhibition by inorganic ions commonly present in saline wastewaters was investigated in batch assays on heterotrophic (enrichment culture) and autotrophic (*T. denitrificans*) denitrification. Moreover, real saline industrial wastewater from a NO_x-SO_2 removal scrubber was used to test denitrification potential. The main conclusions of this study are:

- Cl^- shows to be more inhibitory than Na^+, K^+ and SO_4^{2-} for heterotrophic and autotrophic denitrification rates. Autotrophic denitrification rate by *T. denitrificans* is increased by low Na^+ but at higher concentrations is rapidly inhibited.
- In both autotrophic and heterotrophic denitrification, nitrate removal is more inhibited than nitrite removal by the increasing concentrations of the ions.
- *T. denitrificans* (DSM 12475) shows lower IC_{50} than the heterotrophic enrichment culture and requires further considerations in view of a possible industrial application.
- Both autotrophic and heterotrophic denitrification efficiency is over 95 % for real NO_x-SO_2 removal scrubber wastewater, with autotrophic being faster than heterotrophic, showing the potential of autotrophic denitrification for this saline wastewater.

Declaration of competing interest

The authors declare the following financial interests/personal relationships which may be considered as potential competing interests: Niko Kalinainen reports a relationship with Valmet Technologies Oy that includes employment.

Data availability

Data will be made available on request.

Acknowledgments

Funding: This work was supported by Maa- ja vesitekniikan tuki ry and Emil Aaltosen Säätiö. Also, the collaboration between Tampere University and University of Trento for the project "Sustainable biological management of nitrogenous liquid streams from air emission control" has received funding from the SMART-ER project, funded by the European Union's Horizon 2020 research and innovation programme under Grant Agreement #101016888. The authors would like to thank the laboratory trainees Markku Makkonen, Heini Laine, and Saija Kaukinen for helping in the sampling and analyses during the experiments. Also, the authors would like to thank Valmet Technologies Oy for providing the scrubber wastewater samples, Ph.D. Harri Ali-Löytty (Surface Science Group, Photonics Laboratory, Tampere University) for the ICP-MS analysis of the scrubber wastewater and M.Sc. Nicolò Merzi for the assistance with the statistical analyses.

Appendix A. Supplementary data

Supplementary data to this article can be found online at https://doi.org/10.1016/j.scitotenv.2023.165940.

References

Belessiotis, V., Kalogirou, S., Delyannis, E., 2016. Chapter two-water, the raw material for desalination. In: Belessiotis, V., Kalogirou, S., Delyannis, E. (Eds.), Thermal Solar Desalination. Academic Press, pp. 21–102. https://doi.org/10.1016/B978-0-12-809656-7.00002-7.

Campos, J.L., Carvalho, S., Portela, R., Mosquera-Corral, A., Méndez, R., 2008. Kinetics of denitrification using Sulphur compounds: effects of S/N ratio, endogenous and exogenous compounds. Bioresour. Technol. 99, 1293–1299. https://doi.org/10.1016/j.biortech.2007.02.007.

Chan-Pacheco, C.R., Valenzuela, E.I., Cervantes, F.J., Quijano, G., 2021. Novel biotechnologies for nitrogen removal and their coupling with gas emissions abatement in wastewater treatment facilities. Sci. Total Environ. 797, 149228 https://doi.org/10.1016/j.scitotenv.2021.149228.

Chen, R., Zhang, T., Guo, Y., Wang, J., Wei, J., Yu, Q., 2021. Recent advances in simultaneous removal of SO2 and NOx from exhaust gases: removal process, mechanism and kinetics. Chem. Eng. J. 420 https://doi.org/10.1016/j.cej.2020.127588.

Chen, B., Qaisar, M., Wang, K., Li, W., Cai, J., 2022a. Response of simultaneous sulfide and nitrate removal process on acute toxicity of substrate concentration and salinity: single toxicity and combined toxicity. Sci. Total Environ. 836, 155639 https://doi.org/10.1016/j.scitotenv.2022.155639.

Chen, A.-L., Su, X., Xing, Z.-L., Xu, F.-Q., Chen, S.-J., Xiang, J.-X., Li, J., Liu, H., Zhao, T.-T., 2022b. Effect mechanism of individual and combined salinity on the nitrogen removal yield of heterotrophic nitrification-aerobic denitrification bacteria. Environ. Res. 214, 113834 https://doi.org/10.1016/j.envres.2022.113834.

Chen, B., Qaisar, M., Xiao, J., Li, W., Li, J., Cai, J., 2023. Combined acute effect of salinity and substrate concentration on simultaneous sulfide and nitrite removal process. Sep. Purif. Technol. 305, 122544 https://doi.org/10.1016/j.seppur.2022.122544.

Chung, J., Amin, K., Kim, S., Yoon, S., Kwon, K., Bae, W., 2014. Autotrophic denitrification of nitrate and nitrite using thiosulfate as an electron donor. Water Res. 58, 169–178. https://doi.org/10.1016/j.watres.2014.03.071.

Claus, G., Kutzner, H., 1985a. Physiology and kinetics of autotrophic denitrification by Thiobacillus denitrificans. Appl. Microbiol. Biotechnol. 22, 283–288. https://doi.org/10.1007/BF00252031.

Claus, G., Kutzner, H., 1985b. Autotrophic denitrification by Thiobacillus denitrificans in a packed bed reactor. Appl. Microbiol. Biotechnol. 22, 289–296. https://doi.org/10.1007/BF00252032.

Córdoba, P., 2015. Status of flue gas desulphurisation (FGD) systems from coal-fired power plants: overview of the physic-chemical control processes of wet limestone FGDs. Fuel 144, 274–286. https://doi.org/10.1016/J.FUEL.2014.12.065.

Cui, Y.-X., Biswal, B.K., Guo, G., Deng, Y.-F., Huang, H., Chen, G.-H., Wu, D., 2019. Biological nitrogen removal from wastewater using Sulphur-driven autotrophic denitrification. Appl. Microbiol. Biotechnol. 103, 6023–6039. https://doi.org/10.1007/s00253-019-09935-4.

De Lucas, A., Rodríguez, L., Villaseñor, J., Fernández, F.J., 2005. Denitrification potential of industrial wastewaters. Water Res. 39, 3715–3726. https://doi.org/10.1016/j.watres.2005.06.024.

Deng, J., Wang, X., Wei, Z., Wang, L., Wang, C., Chen, Z., 2021. A review of NOx and SOx emission reduction technologies for marine diesel engines and the potential evaluation of liquefied natural gas fuelled vessels. Sci. Total Environ. 766, 144319 https://doi.org/10.1016/j.scitotenv.2020.144319.

Di Capua, F., Lakaniemi, A.-M., Puhakka, J.A., Lens, P.N.L., Esposito, G., 2017a. High-rate thiosulfate-driven denitrification at pH lower than 5 in fluidized-bed reactor. Chem. Eng. J. 310, 282–291. https://doi.org/10.1016/j.cej.2016.10.117.

Di Capua, F., Milone, I., Lakaniemi, A.-M., Lens, P.N.L., Esposito, G., 2017b. High-rate autotrophic denitrification in a fluidized-bed reactor at psychrophilic temperatures. Chem. Eng. J. 313, 591–598. https://doi.org/10.1016/j.cej.2016.12.106.

Di Capua, F., Pirozzi, F., Lens, P.N.L., Esposito, G., 2019. Electron donors for autotrophic denitrification. Chem. Eng. J. 362, 922–937. https://doi.org/10.1016/j.cej.2019.01.069.

Dinçer, A.R., Kargi, F., 1999. Salt inhibition of nitrification and denitrification in saline wastewater. Environ. Tech. UK 20, 1147–1153. https://doi.org/10.1080/09593332008616912.

Fang, C., Boe, K., Angelidaki, I., 2011. Anaerobic co-digestion of desugared molasses with cow manure; focusing on sodium and potassium inhibition. Bioresour. Technol. 102, 1005–1011. https://doi.org/10.1016/j.biortech.2010.09.077.

Foglar, L., Briški, F., 2003. Wastewater denitrification process - the influence of methanol and kinetic analysis. Process Biochem. 39, 95–103. https://doi.org/10.1016/S0032-9592(02)00318-7.

Fritzmann, C., Löwenberg, J., Wintgens, T., Melin, T., 2007. State-of-the-art of reverse osmosis desalination. Desalination 216, 1–76. https://doi.org/10.1016/J.DESAL.2006.12.009.

Gholami, F., Tomas, M., Gholami, Z., Vakili, M., 2020. Technologies for the nitrogen oxides reduction from flue gas: a review. Sci. Total Environ. 714, 136712 https://doi.org/10.1016/j.scitotenv.2020.136712.

Glass, C., Silverstein, J., 1999. Denitrification of high-nitrate, high-salinity wastewater. Water Res. 33, 223–229. https://doi.org/10.1016/S0043-1354(98)00177-8.

Glass, C., Silverstein, J., Oh, J., 1997. Inhibition of denitrification in activated sludge by nitrite. Water Environ. Res. 69, 1086–1093. https://doi.org/10.2175/106143097X125803.

Hajdu-Rahkama, R., Puhakka, J.A., 2022. High tolerance of chemolithoautotrophic Sulphur oxidizing bacteria towards pulp and paper mill wastewaters and their organic constituents supporting Sulphur recovery in alkaline conditions. Chem. Eng. J. 450, 137972 https://doi.org/10.1016/J.CEJ.2022.137972.

Holm Kristensen, G., Jepsen, S.E., 1991. Biological denitrification of waste water from wet lime–gypsum flue gas desulphurization plants. Water Sci. Technol. 23, 691–700. https://doi.org/10.2166/WST.1991.0519.

Ji, J., Peng, Y., Wang, B., Mai, W., Li, X., Zhang, Q., Wang, S., 2018. Effects of salinity build-up on the performance and microbial community of partial-denitrification granular sludge with high nitrite accumulation. Chemosphere 209, 53–60. https://doi.org/10.1016/j.chemosphere.2018.05.193.

Koenig, A., Liu, L.H., 2001. Kinetic model of autotrophic denitrification in Sulphur packed-bed reactors. Water Res. 35, 1969–1978. https://doi.org/10.1016/S0043-1354(00)00483-8.

Koenig, A., Liu, L., 2004. Autotrophic denitrification of high-salinity wastewater using elemental sulfur: batch tests. Water Environ. Res. 76, 37–46. https://doi.org/10.2175/106143004x141564.

Kokko, M., Koskue, V., Rintala, J., 2018. Anaerobic digestion of 30−100-year-old boreal lake sedimented fibre from the pulp industry: extrapolating methane production potential to a practical scale. Water Res. 133, 218–226. https://doi.org/10.1016/j.watres.2018.01.041.

Kruglova, A., Kesulahti, J., Minh Le, K., Gonzalez-Martinez, A., Mikola, A., Vahala, R., 2020. Low-temperature adapted nitrifying microbial communities of Finnish wastewater treatment systems. Water 12, 2450. https://doi.org/10.3390/w12092450.

Lefebvre, O., Moletta, R., 2006. Treatment of organic pollution in industrial saline wastewater: a literature review. Water Res. 40, 3671–3682. https://doi.org/10.1016/j.watres.2006.08.027.

Leibniz-Institute DSMZ, n.d. *Thiobacillus denitrificans* Medium [WWW Document]. URL https://www.dsmz.de/microorganisms/medium/pdf/DSMZ_Medium113.pdf (accessed 9.9.22).

Lin, L., Pratt, S., Crick, O., Xia, J., Duan, H., Ye, L., 2021. Salinity effect on freshwater Anammox bacteria: ionic stress and ion composition. Water Res. 188, 116432 https://doi.org/10.1016/j.watres.2020.116432.

Liu, E., Fan, C., Zhao, M., Jiang, S., Wang, Z., Jin, Z., Bei, K., Zheng, X., Wu, S., Zeng, Q., 2022. Effects of heavy metals on denitrification processes in water treatment: a review. Sep. Purif. Technol. 299, 121793 https://doi.org/10.1016/j.seppur.2022.121793.

Luo, L., Zhou, W., Yuan, Y., Zhong, H., Zhong, C., 2021. Effects of salinity shock on simultaneous nitrification and denitrification by a membrane bioreactor: performance, sludge activity, and functional microflora. Sci. Total Environ. 801, 149748 https://doi.org/10.1016/j.scitotenv.2021.149748.

Macêdo, W.V., Sakamoto, I.K., Azevedo, E.B., Damianovic, M.H.R.Z., 2019. The effect of cations (Na+, Mg2+, and Ca2+) on the activity and structure of nitrifying and denitrifying bacterial communities. Sci. Total Environ. 679, 279–287. https://doi.org/10.1016/J.SCITOTENV.2019.04.397.

Mariángel, L., Aspé, E., Cristina Martí, M., Roeckel, M., 2008. The effect of sodium chloride on the denitrification of saline fishery wastewaters. Environ. Technol. 29, 871–879. https://doi.org/10.1080/09593330802015318.

Meyer, T., Edwards, E.A., 2014. Anaerobic digestion of pulp and paper mill wastewater and sludge. Water Res. 65, 321–349. https://doi.org/10.1016/j.watres.2014.07.022.

Mora, M., López, L.R., Gamisans, X., Gabriel, D., 2014. Coupling respirometry and titrimetry for the characterization of the biological activity of a SO-NR consortium. Chem. Eng. J. 251, 111–115. https://doi.org/10.1016/J.CEJ.2014.04.024.

Pan, Y., She, D., Shi, Z., Cao, T., Xia, Y., Shan, J., 2023. Salinity and high pH reduce denitrification rates by inhibiting denitrifying gene abundance in a saline-alkali soil. Sci. Rep. 13, 2155. https://doi.org/10.1038/s41598-023-29311-7.

Panswad, T., Anan, C., 1999. Impact of high chloride wastewater on an anaerobic/anoxic/aerobic process with and without inoculation of chloride acclimated seeds. Water Res. 33, 1165–1172. https://doi.org/10.1016/S0043-1354(98)00314-5.

Park, J.Y., Yoo, Y.J., 2009. Biological nitrate removal in industrial wastewater treatment: which electron donor we can choose. Appl. Microbiol. Biotechnol. 82, 415–429. https://doi.org/10.1007/s00253-008-1799-1.

Philips, S., Laanbroek, H.J., Verstraete, W., 2002. Origin, causes and effects of increased nitrite concentrations in aquatic environments. Rev. Environ. Sci. Biotechnol 1, 115–141. https://doi.org/10.1023/A:1020892826575.

Rivett, M.O., Buss, S.R., Morgan, P., Smith, J.W.N., Bemment, C.D., 2008. Nitrate attenuation in groundwater: a review of biogeochemical controlling processes. Water Res. 42, 4215–4232. https://doi.org/10.1016/j.watres.2008.07.020.

Sahinkaya, E., Dursun, N., Kilic, A., Demirel, S., Uyanik, S., Cinar, O., 2011. Simultaneous heterotrophic and sulfur-oxidizing autotrophic denitrification process for drinking water treatment: control of sulfate production. Water Res. 45, 6661–6667. https://doi.org/10.1016/j.watres.2011.09.056.

Schmid, D., Karlström, O., Kuvaja, V., Vuorinen, I., Paavola, M., Hupa, M., 2022. Role of sulfite oxidation in NO 2 absorption in a pH-neutral scrubber solution. Energy Fuel 36, 2666–2672. https://doi.org/10.1021/acs.energyfuels.1c03914.

Song, M.J., Choi, S., Bae, W.B., Lee, J., Han, H., Kim, D.D., Kwon, M., Myung, J., Kim, Y. M., Yoon, S., 2020. Identification of primary effecters of N2O emissions from full-scale biological nitrogen removal systems using random forest approach. Water Res. 184, 116144 https://doi.org/10.1016/j.watres.2020.116144.

Vredenbregt, L.H.J., Nielsen, K., Potma, A.A., Kristensen, G.H., Sund, C., 1997. Fluid bed biological nitrification and denitrification in high salinity wastewater. Water Sci. Technol. 36, 93–100. https://doi.org/10.1016/S0273-1223(97)00341-7.

Wang, R., Zheng, P., Ding, A.-Qiang, Zhang, M., Ghulam, A., Yang, C., Zhao, H.P., 2016. Effects of inorganic salts on denitrifying granular sludge: the acute toxicity and working mechanisms. Bioresour. Technol. 204, 65–70. https://doi.org/10.1016/j.biortech.2015.12.062.

Wang, H., Gilbert, J.A., Zhu, Y., Yang, X., 2018. Salinity is a key factor driving the nitrogen cycling in the mangrove sediment. Sci. Total Environ. 631–632, 1342–1349. https://doi.org/10.1016/j.scitotenv.2018.03.102.

Wei, C., He, W., Wei, L., Ma, J., Li, C., 2017. The performance and microbial communities of biodegradation-electron transfer with sulfur metabolism integrated process for flue gas desulfurization wastewater treatment. Bioprocess Biosyst. Eng. 40, 1543–1553. https://doi.org/10.1007/s00449-017-1810-2.

Yang, J., Spanjers, H., Jeison, D., Van Lier, J.B., 2013. Impact of Na + on biological wastewater treatment and the potential of anaerobic membrane bioreactors: a review. Crit. Rev. Environ. Sci. Technol. 43, 2722–2746. https://doi.org/10.1080/10643389.2012.694335.

Zhao, H., 2005. Effect of ions and other compatible solutes on enzyme activity, and its implication for biocatalysis using ionic liquids. J. Mol. Catal. B Enzym. 37, 16–25. https://doi.org/10.1016/j.molcatb.2005.08.007.

Zhao, Z., Qiu, W., Koenig, A., Fan, X., Gu, J.D., 2004. Nitrate removal from saline water using autotrophic denitrification by the bacterium Thiobacillus denitrificans MP-1. Environ. Technol. 25, 1201–1210. https://doi.org/10.1080/09593332508618387.

Zhao, W., Wang, Y., Liu, S., Pan, M., Yang, J., Chen, S., 2013. Denitrification activities and N2O production under salt stress with varying COD/N ratios and terminal electron acceptors. Chem. Eng. J. 215–216, 252–260. https://doi.org/10.1016/j.cej.2012.10.084.

Zou, G., Papirio, S., Ylinen, A., Di Capua, F., Lakaniemi, A.M., Puhakka, J.A., 2014. Fluidized-bed denitrification for mine waters. Part II: effects of Ni and co. Biodegradation 25, 417–423. https://doi.org/10.1007/s10532-013-9670-1.

Zou, G., Papirio, S., Lakaniemi, A.-M., Ahoranta, S.H., Puhakka, J.A., 2016. High rate autotrophic denitrification in fluidized-bed biofilm reactors. Chem. Eng. J. 284, 1287–1294. https://doi.org/10.1016/j.cej.2015.09.074.

Effects of Inorganic Ions on Autotrophic Denitrification by *Thiobacillus denitrificans* and on Heterotrophic Denitrification by an Enrichment Culture

Alessio D'Aquino[a*], Niko Kalinainen[b], Hannele Auvinen[a], Gianni Andreottola[c], Jaakko A. Puhakka[a] and Marja R. T. Palmroth[a]

[a] Tampere University, Faculty of Engineering and Natural Sciences, Bio- and Circular Economy Unit, Korkeakoulunkatu 8, P.O. Box 541, 33014 Tampere, Finland

[b] Valmet Technologies Oy, Lentokentänkatu 11, 33900 Tampere, Finland

[c] University of Trento, Department of Civil, Environmental and Mechanical Engineering, via Mesiano 77, 38123 Trento, Italy

*Corresponding author. Email address: alessio.daquino@tuni.fi

Supplementary materials: 13 Figures, 3 Tables.

During the enrichment phase of heterotrophic denitrifiers from the sludge of the wastewater treatment plant, first, ammonia and yeast extract were added to the growth medium described by Zou et al. (2014) to overcome nutrients' limitation (Table S1). Then, after some weeks, addition of Fe(II) further increased the denitrification rate and reduced the length of lag phase (Figure S1).

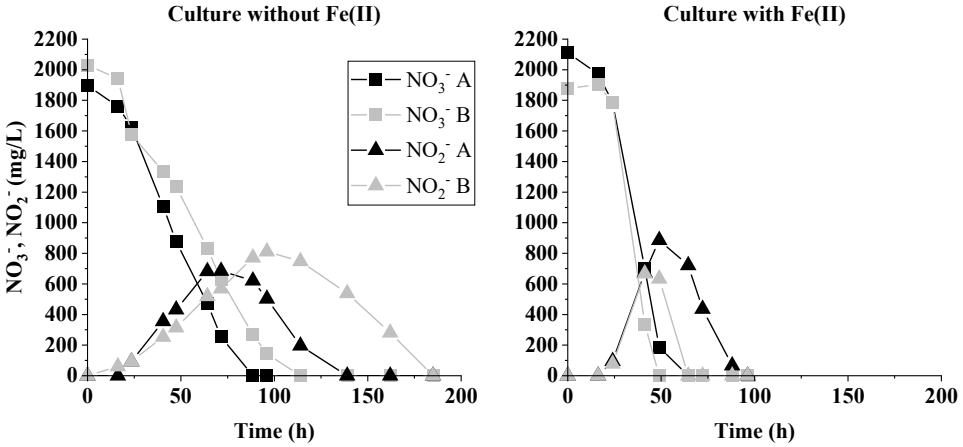

Figure S1. Development of nitrate and nitrite concentrations in the heterotrophic denitrifying enrichment culture using growth medium (with no sodium) without Fe(II) (on the left) and with addition of Fe(II) as 2 mg/L $FeSO_4 \cdot 7H_2O$ (on the right) as two replicates (A and B). Growth medium and incubation conditions were as reported in the Materials and Methods section.

Table S1. Growth media used for the cultivation and experiments for the heterotrophic enrichment culture and autotrophic *Thiobacillus denitrificans*.

Growth medium			
Heterotrophic medium		Autotrophic medium (for *T. denitrificans*)	
	Concentration		Concentration
NO_3^- (KNO_3)	2 g/L	NO_3^- (KNO_3)	2 g/L
MeOH	1.6 g/L	$S_2O_3^{2-}$ ($K_2S_2O_3$)	3.66 g/L
NH_4^+ ($(NH_4)_2SO_4$)	0.2 g/L	$KHCO_3$	3.25 g/L
Yeast extract	5 mg/L	$FeSO_4 \cdot 7H_2O$	2 mg/L
K_2HPO_4	50 mg/L		
K-phosphate buffer solution:		Nutrient solution:	
K_2HPO_4	2.77 gPO_4^{3-} /L	KH_2PO_4	2 g/L
KH_2PO_4	1.73 gPO_4^{3-} /L	NH_4Cl	1 g/L
		$MgSO_4 \cdot 7H_2O$	0.8 g/L
Metals solution:		Trace element solution:	
$FeSO_4 \cdot 7H_2O$	2 mg/L	Na_2EDTA	1 mg/L
$CaCl_2 \cdot 2H_2O$	20 mg/L	$FeSO_4 \cdot 7H_2O$	0.4 mg/L
$MgCl_2 \cdot 6H_2O$	150 mg/L	$ZnSO_4 \cdot 7H_2O$	0.2 mg/L
$Na_2MoO_4 \cdot 2H_2O$	0.1 mg/L	$MnCl_2 \cdot 4H_2O$	0.06 mg/L
$MnCl_2 \cdot 2H_2O$	1.75 mg/L	H_3BO_3	0.06 mg/L
$CoCl_2 \cdot 6H_2O$	0.05 mg/L	$CoCl_2 \cdot 6H_2O$	0.4 mg/L
		$CuCl_2 \cdot 2H_2O$	0.02 mg/L
		$NiCl_2 \cdot 6H_2O$	0.04 mg/L
		$Na_2MoO_4 \cdot 2H_2O$	0.06 mg/L

In the heterotrophic denitrification test with Na^+ and Cl^-, the time for over 95% nitrate removal increased with increasing concentrations of Na^+ as NaCl, Na^+ as Na_2SO_4, Cl^- as KCl (Figure S2, S3, S4). Total inhibition of denitrification was reached at 20 g/L Na^+ (as NaCl), 30 g/L Na^+ (as Na_2SO_4) and 30 g/L Cl^- (as KCl). In all the cases, after nitrite accumulated, it was always removed by more than >95%. Nitrite accumulation stopped at 10 g/L Na^+ (as NaCl), 20 g/L Na^+ (as Na_2SO_4) and 20 g/L Cl^- (as KCl). Lag phases with Cl^- (as KCl) were shorter than with sodium compounds. MeOH consumption was in line with the stoichiometry in all the cases.

Also, in the autotrophic denitrification test with Na^+ and Cl^-, the time for over 95% nitrate removal increased with increasing concentrations of Na^+ as NaCl, Na^+ as Na_2SO_4, Cl^- as KCl (Figure S5, S6, S7). Total inhibition of denitrification was reached between 6 and 7 g/L Na^+ (as NaCl), 10 g/L Na^+ (as Na_2SO_4) and 15 g/L Cl^- (as KCl). Nitrite accumulated starting from 2.5 g/L Na^+ (as NaCl), 5 g/L Na^+ (as Na_2SO_4) and 5 g/L Cl^- (as KCl). In almost all the cases, after nitrite accumulated, it was always removed by more than 95%. Exceptions were made at 5 and 6.5 g/L Na^+, when incubation was interrupted and at 6.5 g/L Cl^-, when accumulated nitrite was not consumed.

Without ions addition, in almost all the cases, both autotrophic and heterotrophic denitrification removed approximatively 2 g/L nitrate within 75 hours, with the only difference that in the former no nitrite accumulation was detected (Figure S8).

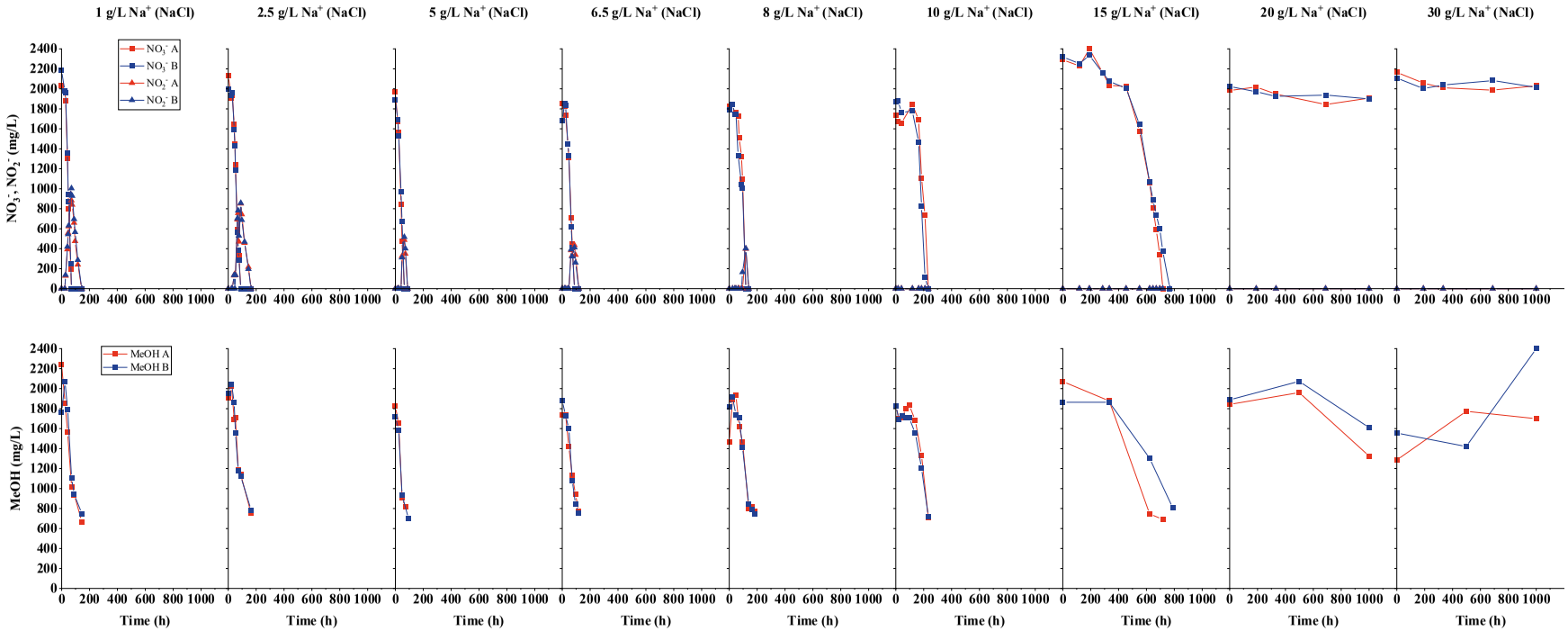

Figure S2. Nitrate and nitrite (first row) and methanol (second row) concentrations plotted against incubation time at increasing concentrations (1-30 g/L) of Na^+ as NaCl in heterotrophic denitrification test for duplicates (A and B).

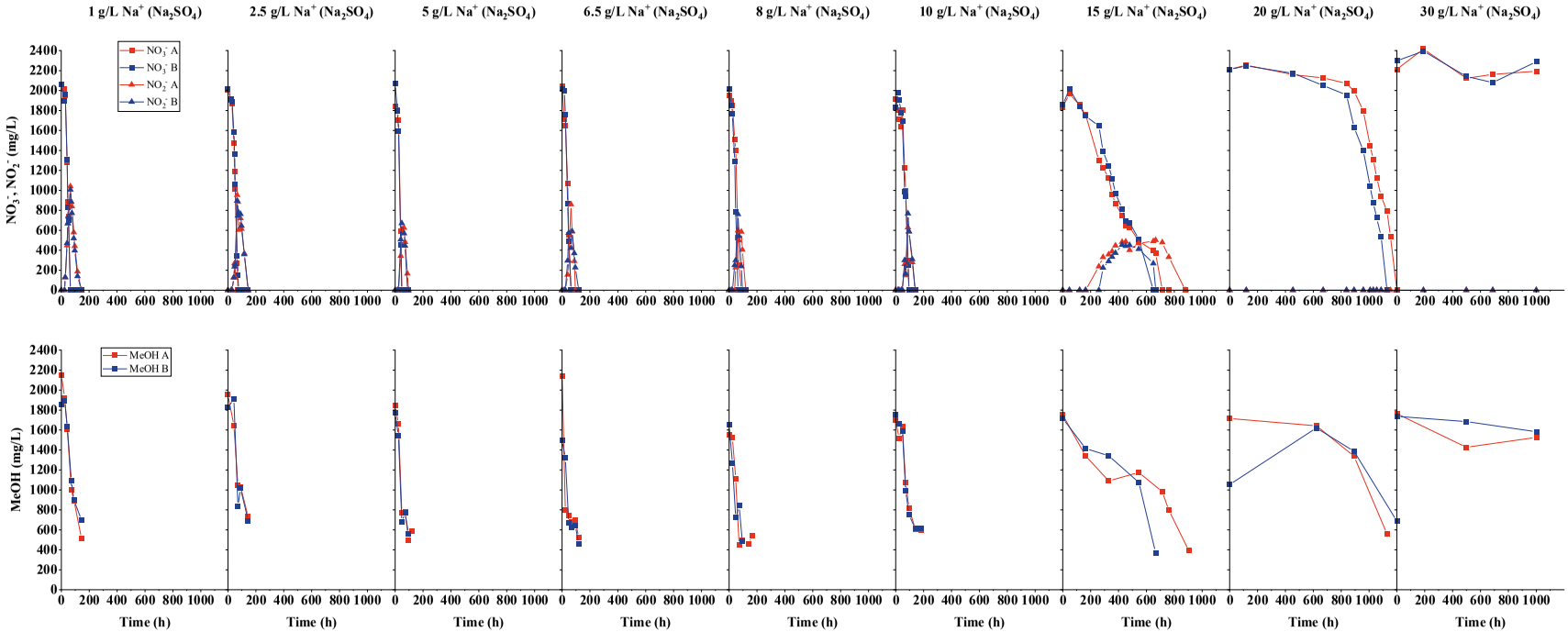

Figure S3. Nitrate and nitrite (first row) and methanol (second row) concentrations plotted against incubation time at increasing concentrations (1-30 g/L) of Na^+ as Na_2SO_4 in heterotrophic denitrification test for duplicates (A and B).

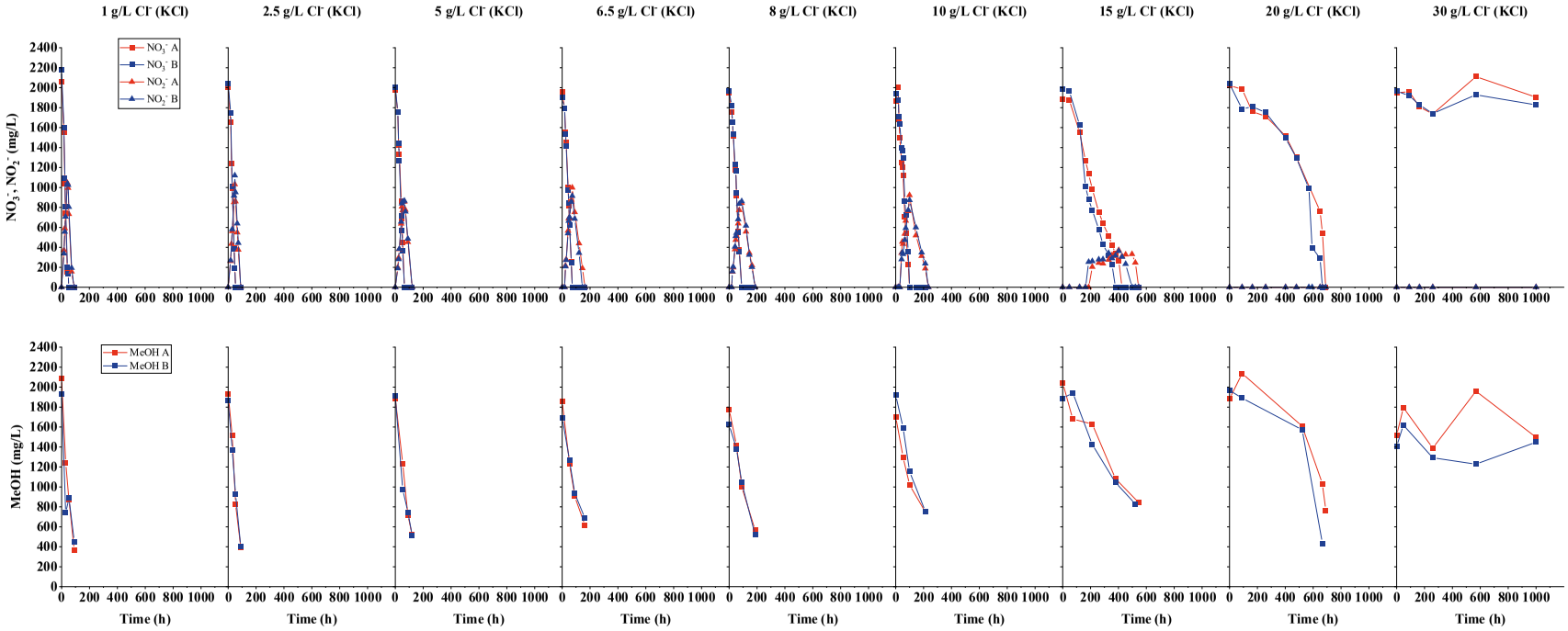

Figure S4. Nitrate and nitrite (first row) and methanol (second row) concentrations plotted against incubation time at increasing concentrations (1-30 g/L) of Cl^- as KCl in heterotrophic denitrification test for duplicates (A and B).

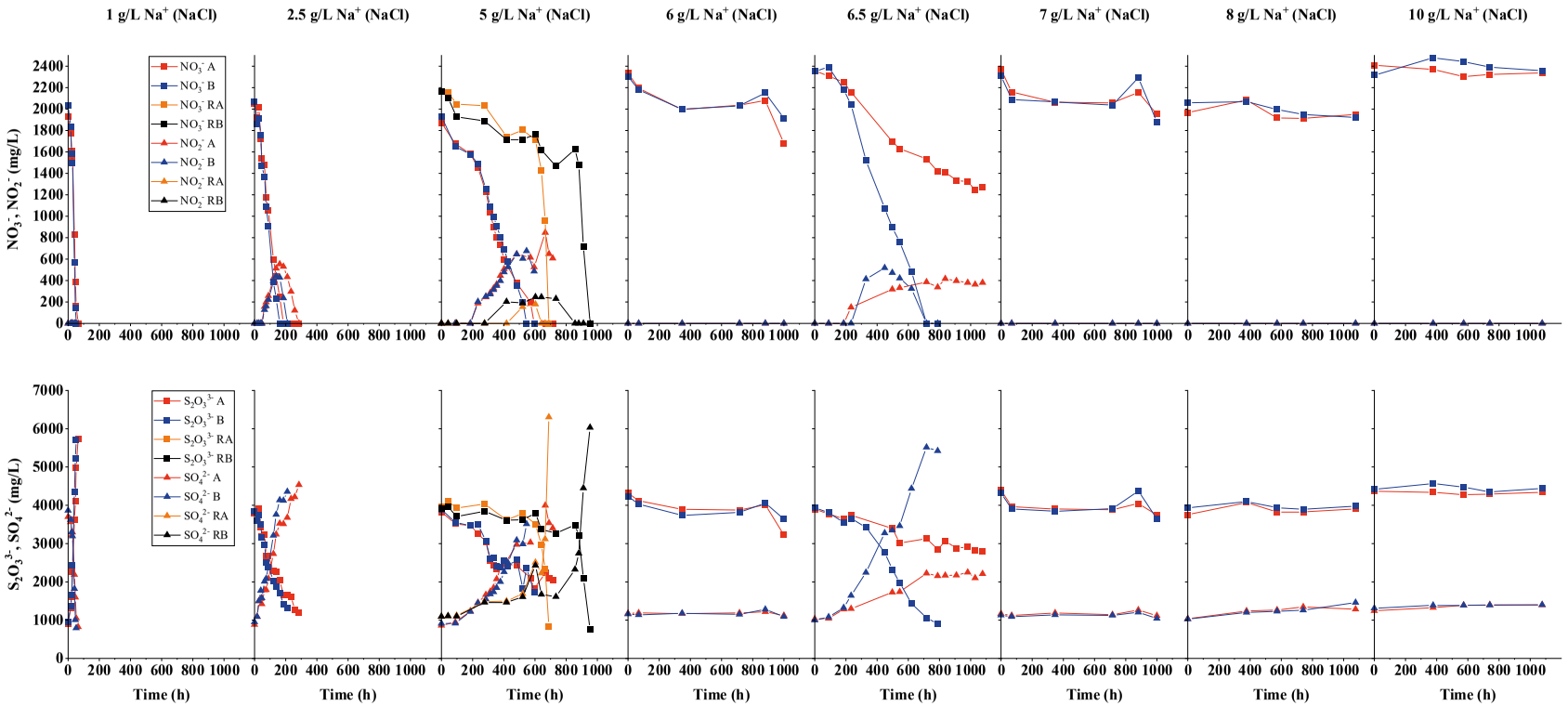

Figure S5. Nitrate and nitrite (first row) and thiosulphate and sulphate (second row) concentrations plotted against incubation time at increasing concentrations (1-10 g/L) of Na^+ as NaCl in autotrophic denitrification test for duplicates (A and B). In the legend, RA and RB refer to duplicates of the rerun test conducted after the main experiments, as mentioned in the results section.

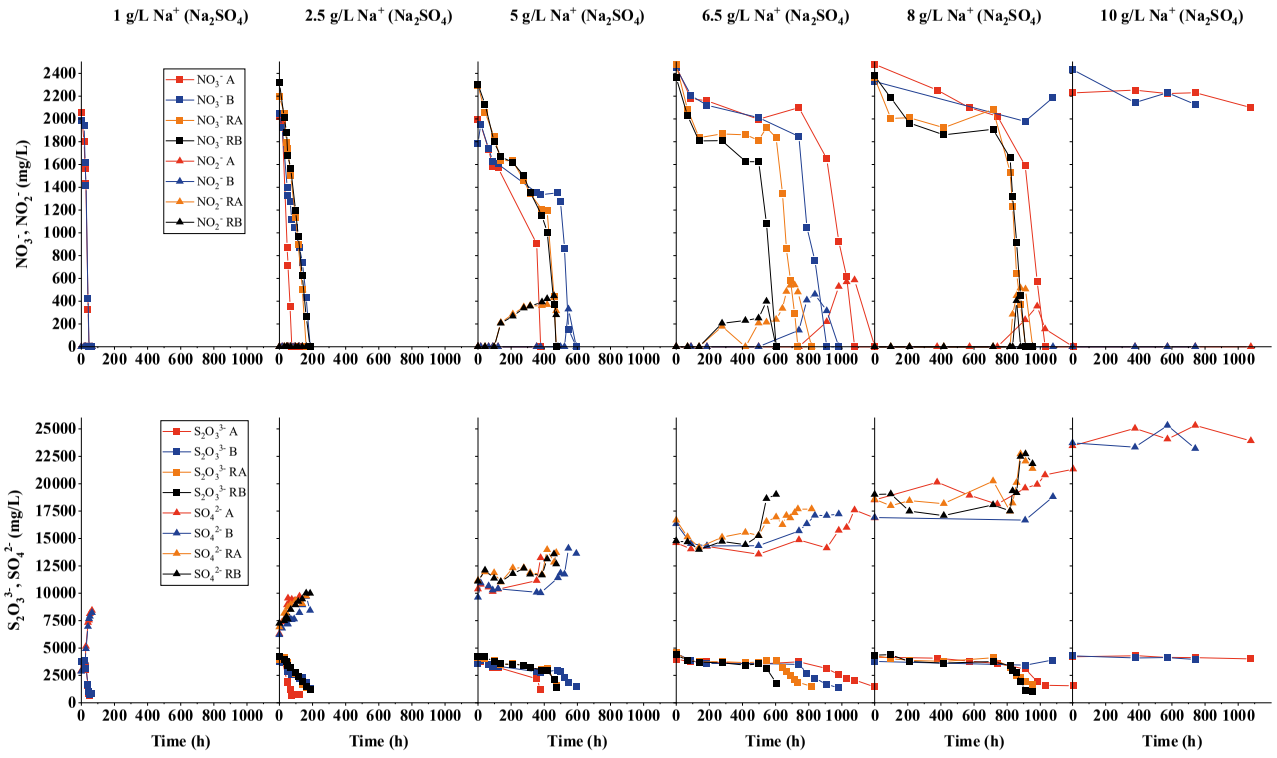

Figure S6. Nitrate and nitrite (first row) and thiosulphate and sulphate (second row) concentrations plotted against incubation time at increasing concentrations (1-10 g/L) of Na^+ as Na_2SO_4 in autotrophic denitrification test for duplicates (A and B). In the legend, RA and RB refer to duplicates of the rerun test conducted after the main experiments, as mentioned in the results section.

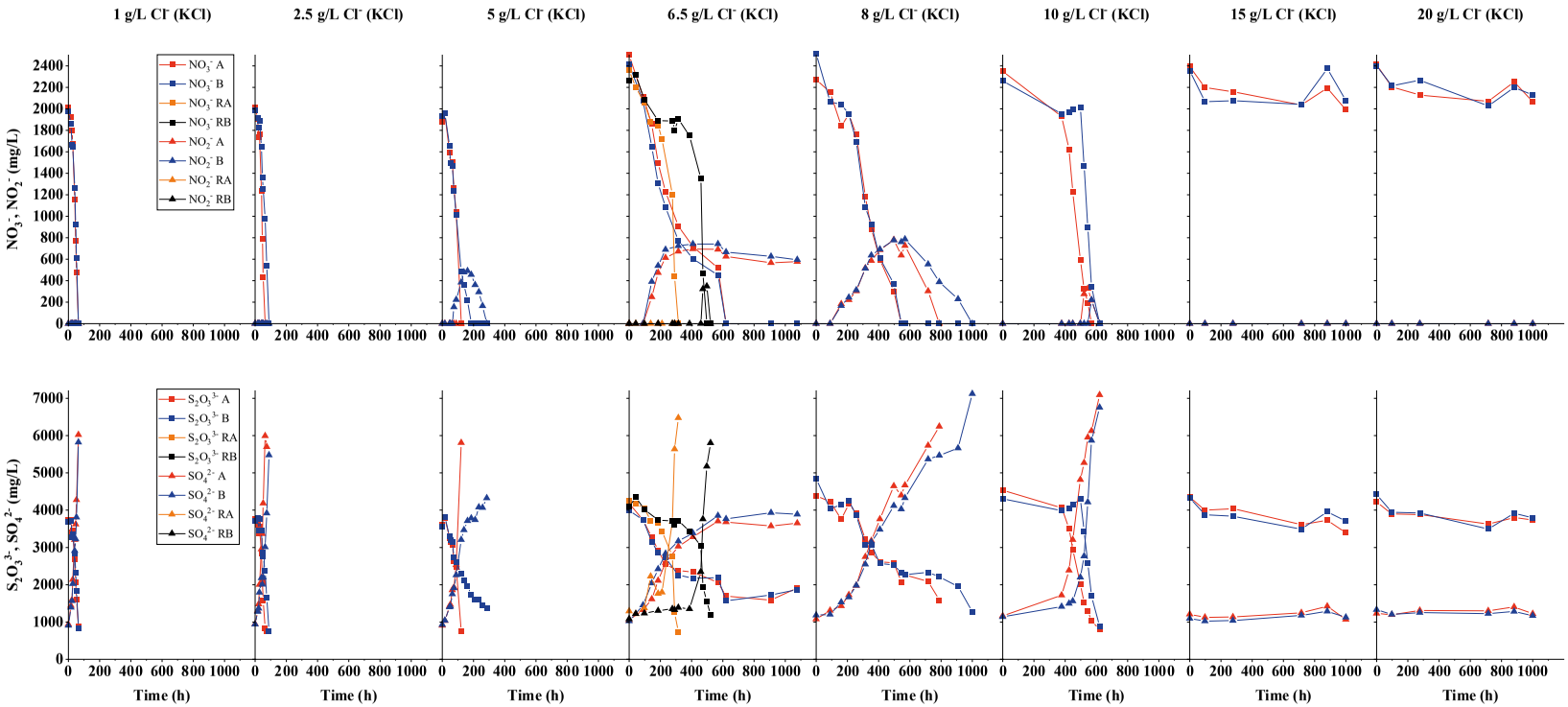

Figure S7. Nitrate and nitrite (first row) and thiosulphate and sulphate (second row) concentrations plotted against incubation time at increasing concentrations (1-20 g/L) of Cl^- as KCl in autotrophic denitrification test for duplicates (A and B). In the legend, RA and RB refer to duplicates of the rerun test conducted after the main experiments, as mentioned in the results section.

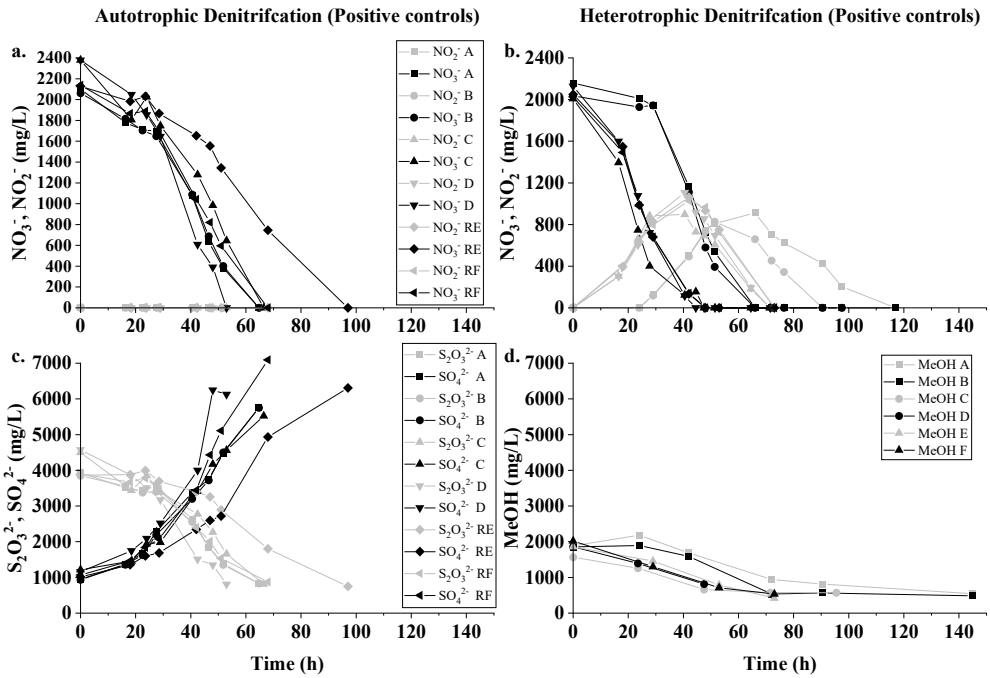

Figure S8. Nitrate and nitrite (a. and b.) and electron donors-product (c. and d,) concentrations plotted against incubation time for positive controls (without salt addition) for autotrophic denitrification tests (on the left) and heterotrophic denitrification test (on the right), for duplicates (A and B). In the legend, RE and RF refer to the rerun test conducted after the main experiments, as mentioned in the Results section.

In the Cl^- and Na^+ inhibition test, by expressing the ions concentrations in mol/L, no changes were observed in lag phase and nitrite accumulation (Figure S9).

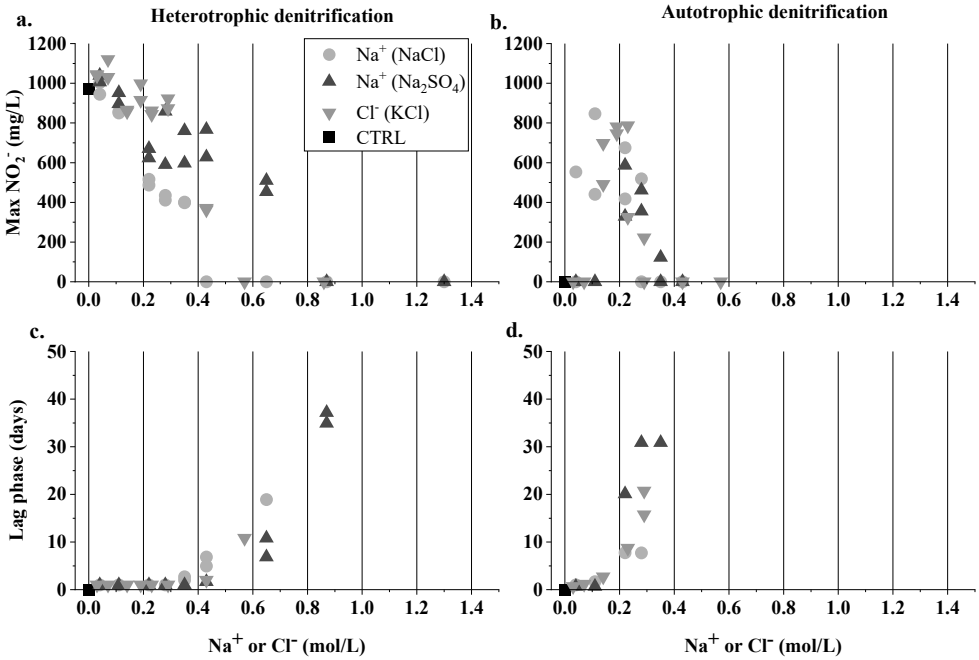

Figure S9. Effects of sodium and chloride inhibition (ions' concentrations in mol/L) of heterotrophic (on the left) and autotrophic (on the right) denitrification on highest nitrite concentration accumulation during the incubation (a. and b.) and lag phase (c. and d.). Two data points (duplicates) are shown for each ion. Positive controls are indicated as "CTRL" and are represented by average values (n=6) (plot c: standard error <5%).

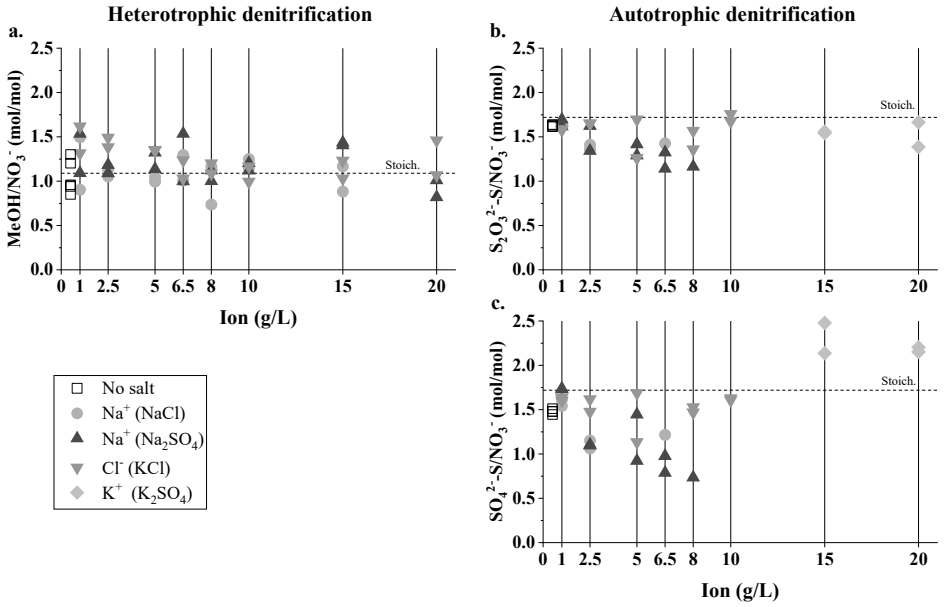

Figure S10. Effects of ions inhibition of heterotrophic (on the left) and autotrophic (on the right) denitrification on: a. Methanol removed-nitrate removed ratio, b. Thiosulphate-sulphur removed - nitrate removed ratio, c. Sulphate-sulphur produced - nitrate removed ratio. Two data points of the same ion at the same concentration represent duplicates. Only cases where nitrate and nitrite were removed over 95% are reported in the plots.

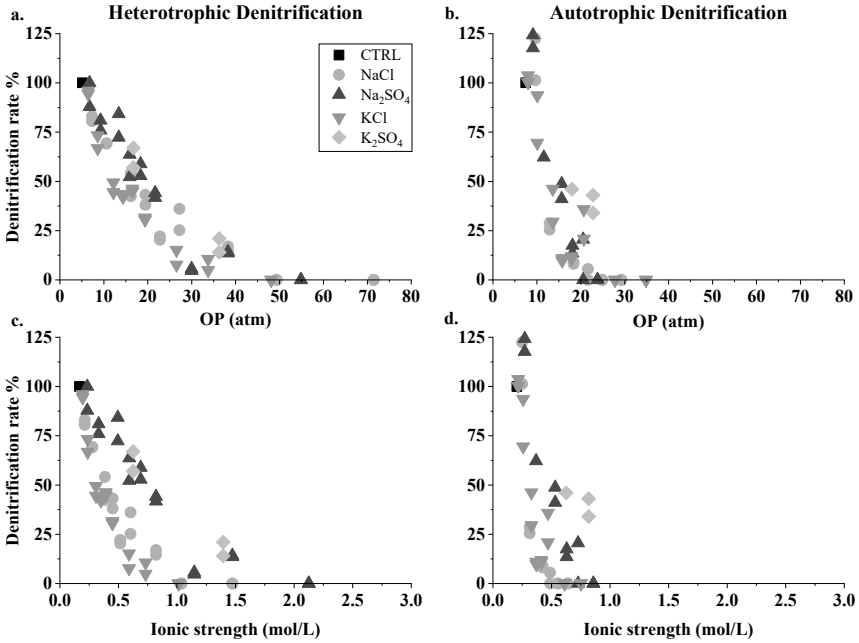

Figure S11. Denitrification rate (%) decrease plotted against osmotic pressure (a. and b.) and Ionic strength (c. and d.) for heterotrophic and autotrophic denitrification.

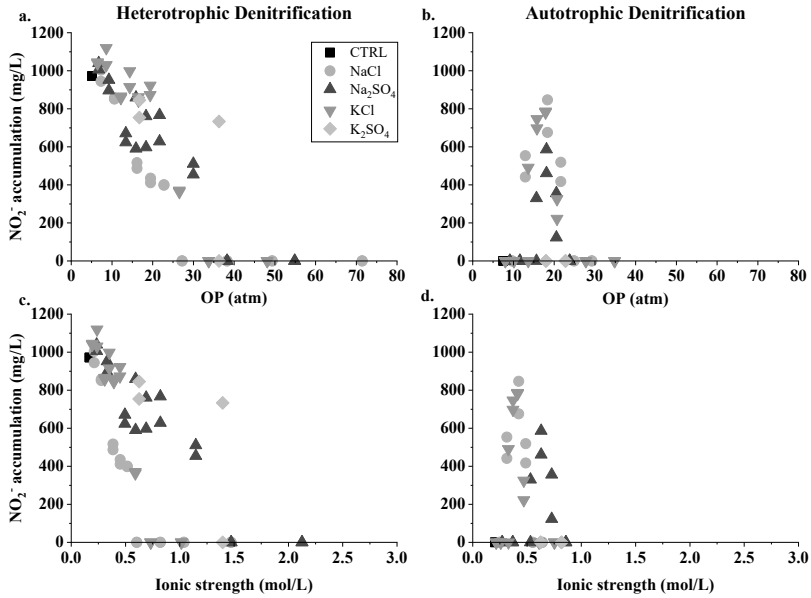

Figure S12. Nitrite accumulation plotted against osmotic pressure (a. and b.) and Ionic strength (c. and d.) for heterotrophic and autotrophic denitrification.

To better understand which ions had the most important roles in decreasing denitrification rate, a statistical analysis of the data was carried out. Two methods, Partial Least Square regression (PLSR) and Random Forest (RF) regression were used to analyze the response of percentage denitrification rate D_R(%) at increasing concentrations of the ions (Na^+, Cl^-, SO_4^{2-} and K^+). The ions were considered as the independent variables characterized by high collinearity, since they were added in pairs as a salt. First, the complete dataset obtained from the experiments was analyzed, separately for heterotrophic and autotrophic denitrification. Then, since the number of conditions for Na^+ and Cl^- was higher than for SO_4^{2-} and K^+, which affects the distribution of the data, the two datasets (heterotrophic and autotrophic) were cut in order to have the same number of conditions for all the ions. Data from the tests with Na_2SO_4 and KCl were left, while data from the test with NaCl were cut to have the same number of conditions as with K_2SO_4. NaCl conditions with similar D_R(%) to K_2SO_4 conditions were selected. A total of 4 datasets were tested (HD complete, HD cut, AD complete, AD cut). The analyzed outputs from the regressions were standardized coefficients for PLSR and Feature Importance for RF. Both describe the ability of each independent variable in predicting the response variable. The higher the absolute value of the standardized coefficient and Feature Importance value, the higher the importance of the variable. For the standardized coefficients of PLSR (see Minitab support), negative sign means that the predictor is negatively correlated with the response variable (i.e., decreases denitrification rate).

Table S2 describes the validation of the model for PLSR of the four datasets, showing that HD datasets were better described by the model than AD. Eventually, for all the datasets and with both the methods (Figure S13), Cl^- resulted to have the highest importance in decreasing the denitrification rate. No considerations on the orders of importance of other ions could be made, as their order varied in the different datasets.

One of the limits of this approach with the available data is that the ions concentrations were always increased in pair since they were added as salts. Moreover, no combinations of K^+- Na^+ and Cl^-- SO_4^{2-} could be studied, due to the nature of the salts. Also, no interactions between the ions were considered in the analysis.

Table S2. Statistics of the PLSR for each condition tested. The p-value was always <0.001 (results of the regression were statistically significant). HD: Heterotrophic denitrification, AD: Autotrophic Denitrification.

	Model Selection and Validation for DR				
	Components	**X Variance**	**Error**	**R-Sq**	**R-Sq (pred)**
HD complete dataset	1	0.315	7261.64	0.75	0.63
	2		6624.85	0.77	0.62
	3		6611.85	0.77	0.62
HD cut dataset	1	0.280	4103.67	0.82	0.77
	2		4008.22	0.82	0.71
	3		3996.69	0.82	0.71
AD complete dataset	1	0.264	11084.1	0.68	0.58
	2		10489.1	0.70	0.57
	3		10455.3	0.70	0.56
AD cut dataset	1	0.278	9214.00	0.64	0.38
	2	0.792	7858.17	0.69	0.47
	3	1.000	7408.18	0.71	0.50

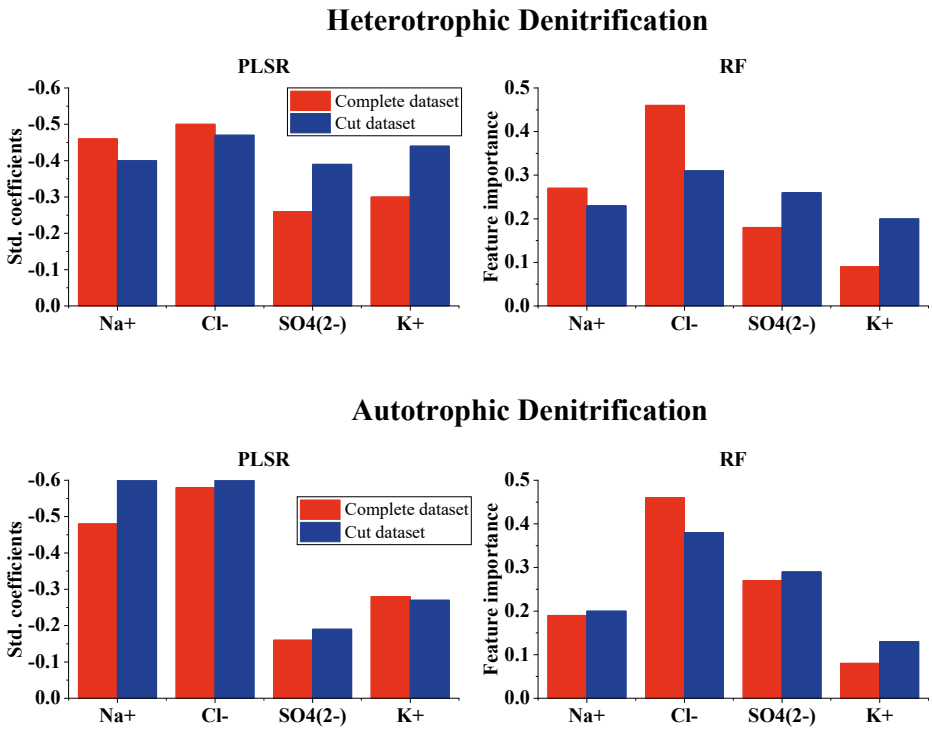

Figure S13. Standardized coefficients and feature importance values of the main inorganic ions tested (independent variables) obtained from PLSR and RF, respectively, for heterotrophic and autotrophic denitrification rates decrease.

Samples from the full-scale simultaneous NO_x-SO_2 removal scrubber system were taken in two different days and characterized. In Table S1 is reported the characterization of a second sample taken on a different day from the one reported in the main manuscript. Sodium concentration was double, thiosulphate and formate were present in terms of g/L and pH was higher than those in the wastewater reported in the materials and methods section of the manuscript. This shows the variability in composition and concentration proper of industrial wastewaters, which, in this case, was mainly due to the different conditions of the scrubbing process. Moreover, the presence of thiosulphate could represent an important energy source for autotrophic denitrification.

Table S3. Characterization of another wastewater sample generated from a full-scale simultaneous NO_x-SO_2 removal scrubber system treating flue gases produced in two recovery boilers of a pulp mill.

Analyte (mg/L)	Concentration	Analyte (mg/L)	Concentration
Cl^-	1800	Al	0.15
NO_2^-	<100	As	<0.01
NO_3^-	400	B	11.50
SO_4^{2-}	17600	Co	<0.01
$S_2O_3^{2-}$	2100	Cr	0.04
$HCOO^-$ (C)	3500 (930)	Cu	0.01
		Fe	0.90
DOC[1]	1440	K	21.00
DIC[2]	/	Mg	0.98
		Mn	0.03
pH	5.2	Mo	0.03
T (°C)	66.5	Na	10900.00
		Ni	0.04
		P	0.58
		Pb	<0.01
		Se	0.01
		V	<0.01
		Zn	0.02

[1] Dissolved Organic Carbon; [2] Dissolved Inorganic Carbon.

REFERENCES

Zou. G., Papirio. S., Ylinen. A., Di Capua. F., Lakaniemi. A.M., Puhakka. J.A., 2014. Fluidized-bed denitrification for mine waters. Part II: Effects of Ni and Co. Biodegradation 25. 417–423. https://doi.org/10.1007/s10532-013-9670-1

PUBLICATION
II

Methanol and thiosulphate from pulp mill waste streams support denitrification under salinity stress

Alessio D'Aquino, Susanna T. Maanoja, Hannele Auvinen, Marja Tiirola, Gianni Andreottola, Jaakko A. Puhakka and Marja R.T. Palmroth

Chemical Engineering Journal, 502 (2024), 158131
https://doi.org/10.1016/j.cej.2024.158131

Chemical Engineering Journal 502 (2024) 158131

Contents lists available at ScienceDirect

Chemical Engineering Journal

journal homepage: www.elsevier.com/locate/cej

Methanol and thiosulphate from pulp mill waste streams support denitrification under salinity stress

Alessio D'Aquino [a,b,*], Susanna T. Maanoja [a], Hannele Auvinen [a], Marja Tiirola [c], Gianni Andreottola [b], Jaakko A. Puhakka [a], Marja R.T. Palmroth [a]

[a] Tampere University, Faculty of Engineering and Natural Sciences, Materials Science and Environmental Engineering Unit, Korkeakoulunkatu 8, P.O. Box 541, 33014 Tampere, Finland
[b] University of Trento, Department of Civil, Environmental and Mechanical Engineering, via Mesiano 77, 38123 Trento, Italy
[c] University of Jyväskylä, Department of Biological and Environmental Sciences, NanoScience Center, Survontie 9C, P.O.Box 35, 40014 Jyväskylä, Finland

ARTICLE INFO

Keywords:
FBBR
Foul Condensate
High-Rate Bioprocess
Ionic Stress
Nitrate Removal
Pulp Mill
Scrubber Wastewater

ABSTRACT

Methanol and thiosulphate are two common compounds found in pulp mill environment. In this study, for the first time, methanol driven, and thiosulphate driven denitrification under salinity stress were studied in fluidized bed bioreactors (FBBR) in a comparative manner. Concentration of salinity, due to Cl^-, Na^+, SO_4^{2-} and K^+ that are present in saline industrial wastewaters, and nitrate loading rate were gradually increased up to 8.1 % and 4.67 ± 0.30 gNO_3^--N/L/d to determine the reactors' resistance and denitrification rate capacity. Moreover, the suitability of real pulp mill methanol-rich foul condensate as alternative electron donor was revealed in the heterotrophic reactor. With foul condensate, heterotrophic denitrification maintained > 97 % nitrate removal at a rate of 2.40 ± 0.10 gNO_3^--N/L/d under 6.8 % salinity, also decreasing nitrite accumulation as compared to pure methanol. Thiosulphate driven autotrophic denitrification showed lower salinity and nitrate loading tolerance than the methanol driven, removing nitrate > 97 % at salinity up to 5.6 % and rate of 1.27 ± 0.10 gNO_3^--N/L/d. Microbial community composition in the heterotrophic reactor remained stable at different salinities, with denitrifying genera *Methylovorus*, *Paracoccus* and *Pseudomonas* playing the major roles. On the other hand, in the thiosulphate driven reactor, inoculated with a pure culture of *Thiobacillus denitrificans*, many other microorganisms, including *Moheibacter*, became enriched. However, nitrate removal was mainly linked with *T. denitrificans* abundance as indicated by decreasing share of the community co-occurring with the decrease of the reactors' performance. In summary, this study showed that thiosulphate and foul condensate supported denitrification under salinity stress, indicating potential for high-rate fluidized bed pre-treatment for nitrate removal from pulp mill NO_x-SO_2 scrubber wastewater prior to direction to subsequent activated sludge process.

1. Introduction

Wastewaters from many industries, such as oil and gas, mariculture, food and pulp-paper are characterized by high salinity (>5%) [1–3] and are often nitrogen-laden [4,5], requiring proper treatments before discharge to the environment. Sustainable and cost-effective handling of industrial saline wastewater combines physico-chemical and biological processes removing specific pollutants, including nitrogen [2,3,6].

High osmotic stress and the presence of multiple inorganic ions (e.g., Cl^-, Na^+, SO_4^{2-}, K^+) in saline wastewaters represent challenging conditions for biological processes [7–10]. To partially overcome this challenge, different types of biofilm reactors have been adopted, since biofilms enhance the tolerance of microorganisms towards inhibitory agents [11,12]. For instance, denitrification under saline conditions has been reported for heterotrophs, among others, in moving bed bioreactor [13,14], expanded granular sludge bed [4,15] and biofilm electrode reactor [16], as well as for autotrophs in packed bed reactors [17–19] and Upflow Anaerobic Sludge Blanket (UASB) [20]. Therefore, a high-rate-biofilm system tolerating the inhibitory conditions is advantageous for the biological treatment of industrial saline wastewaters. Fluidized Bed Bioreactor (FBBR) has the potential of meeting these requirements [21,22]. Both heterotrophic [23–25] and autotrophic [26–28] denitrification in FBBR have been studied under non-saline conditions, whilst the performance of denitrification in FBBR under

* Corresponding author.
E-mail address: alessio.daquino@tuni.fi (A. D'Aquino).

https://doi.org/10.1016/j.cej.2024.158131
Received 26 February 2024; Received in revised form 14 November 2024; Accepted 20 November 2024
Available online 30 November 2024

saline conditions remains to be determined [29]. Furthermore, denitrification in continuous flow reactor under multiple inorganic ions' stress has not been investigated in detail, as many studies have mostly used NaCl to simulate salinity [4,15,17,18,30].

In addition to salinity stress, biological nitrate removal from industrial wastewaters is often limited by the lack of suitable electron donors for denitrification [31], requiring costly chemical supply. Combining different waste streams to provide the necessary substrates for microorganisms would represent a circular and sustainable approach. For instance, effluents from food industries have been used as electron donors for heterotrophic denitrification of metal industry wastewater [32].

Pulp and paper industry represents a significant producer of wastewater worldwide (3 billion m^3 per year) [33]. Its wastewater consists of highly heterogenous waste streams generated by different subprocesses [33,34], some of which contain potential electron donors for denitrification. Among these, evaporator foul condensate is rich in methanol and other non-toxic readily available organics [35,36], whilst wastewater from wet scrubbers removing NO_x and SO_2 from flue gases contains $S_2O_3^{2-}$ and SO_3^{2-} [10,37]. Moreover, overall pulp mill wastewater is usually characterized by high organic content, whilst being deficient in nutrients for activated sludge treatment, requiring ammonium and phosphate supplementations [38,39]. For this reason, most of the wastewater treatments are not optimized for the removal of nitrogen, potentially exceeding the environmental standards in the effluent [40]. When NO_x-SO_2 wet scrubbers are employed to clean the mill's flue gases they generate saline NO_3^-/NO_2^- rich streams (100–300 mg N/L) [10,41] that require treatment. Consequently, it would be beneficial to have a pre-denitrification step for nitrate laden waste streams supported by electron donors generated in the same mill, to reduce nitrogen loading at the main wastewater treatment plant.

Therefore, the aim of this study was to investigate the performance of both thiosulphate driven autotrophic (eqs. S1) and methanol driven heterotrophic (eqs. S2) denitrification in FBBRs under increasing salinities and loading rates, simulating for example the process conditions for the treatment of NO_x-SO_2 scrubber wastewater. Granular activated carbon (GAC) was selected as biofilm carrier for the FBBRs, given its advantageous structure for microbial attachment, adsorption capacity and association with high-rate treatment [26,42,43]. Once inhibition by salinity was met, the FBBRs' performances were recovered by decreasing the salt concentration to a tolerated level. The highest potential denitrification rates were assessed with a kinetic model. Inorganic ions (Cl^-, Na^+, SO_4^{2-} and K^+) in industrial wastewaters were simulated by dosing KCl and Na_2SO_4, while thiosulphate and methanol were selected as electron donors, given their availability in the pulp and paper industry. Then, the suitability of real foul condensate from a pulp mill as electron source for heterotrophic denitrification was investigated for the first time. To our knowledge, foul condensate has been studied for example for the production of volatile fatty acids [44] or methane [36], but not for supporting denitrification under saline conditions, and its potential is still unknown. Furthermore, the microbial community composition and its dynamic response to increasing saline stress and addition of foul condensate were investigated with 16S rRNA gene sequencing. Eventually, based on the results, a potential pre-denitrification step to treat together nitrogen laden streams and foul condensate, and its possible benefits for the pulp mill wastewater treatment plant, are discussed.

2. Materials and methods

2.1. Simulated saline wastewater

Nitrate laden saline wastewater was simulated with tap water amended with 1 g/L NO_3^- (as KNO_3), 2 g/L $S_2O_3^{2-}$ (as $K_2S_2O_3$) and 0.2 g/L NH_4^+ (as NH_4Cl). To simulate the traces of metals present in this type of wastewater [10], a trace element solution was added (Table S1). Potassium phosphate buffer solution (5.1 g/L K_2HPO_4 and 2.5 g/L KH_2PO_4) was used to control pH in the reactor around 7.35 ± 0.45. For the heterotrophic reactor, methanol (0.8 g/L, C/N = 1.3 g/g) or foul condensate was used as organic carbon and electron source, while for the autotrophic, $KHCO_3$ (1.8 g/L, C/N = 0.95 g/g) and $S_2O_3^{2-}$ were used as inorganic carbon and electron sources. The foul condensate was generated from a Finnish pulp mill's evaporator and its composition is reported in Table 1. The condensate was stored at 4 °C and its methanol content remained constant (results not shown).

To determine the salinity resistance to denitrification in a FBBR, concentrations of Cl^-, Na^+, SO_4^{2-} and K^+ were gradually increased in the simulated wastewater, as shown in Table 2, by adding KCl and Na_2SO_4. Before being fed to the reactors, the wastewater was purged with nitrogen gas to reduce the dissolved oxygen concentration.

2.2. Reactors design

Two identical reactor systems were used in this study, one for heterotrophic denitrification and one for autotrophic denitrification, and were fed with the simulated wastewater. The two systems were built as reported by Papirio et al. [23] and consisted of: an FBBR, a peristaltic pump for the recirculation flow, a peristaltic pump pumping the influent from a feed tank to the FBBR and a water level adjustor in the effluent line (Figure S1). The FBBR had a working volume of about 170 mL with a diameter of 4.5 cm, as used by Rasoulnia et al. [43], and was filled with 75 mL of granular activated carbon (GAC) (Filtrasorb 200, Calgon Carbon Corporation, USA) to allow biomass attachment. A 25 mm glass bead was placed at the bottom of the FBBR to retain the GAC and better distribute the recirculation flow in the reactor. Temperature of the FBBR was controlled by an immersed probe and kept at 30 ± 2°C by a heating blanket. The flow rate of the peristaltic pump used for recirculation was continuously adjusted to obtain around 17 % fluidization of the GAC bed and was in the range 380–500 mL/min.

2.3. FBBRs operation

2.3.1. Heterotrophic FBBR (Methanol driven)

The heterotrophic FBBR was operated for 115 days. On day 0, the reactor was inoculated with 10 % v/v of an enrichment culture of denitrifying microorganisms, incubated under non saline conditions at 35 °C with methanol as electron donor, as in our previous study [10]. The FBBR startup (PHASE 0 in Table 2) included 3 days in batch mode, after which continuous flow mode was started at nitrate loading rate (NLR) of 0.44 ± 0.02 g NO_3^--N/L/d (hydraulic retention time (HRT) 12.5 h) and lasted for 13 days to allow biofilm formation. Then, in the next phase (PHASE I), NLR was gradually increased to 0.76 ± 0.08 g NO_3^--N/L/d (HRT 6.7 h). Once the FBBR showed to have stable nitrate removal, the concentrations of inorganic ions, and thus, salinity, were gradually increased to PHASE V to observe the effect on denitrification performance. If no changes in nitrate removal efficiency were observed in 5–7 days, the salinity was increased. Once inhibition of

Table 1
Characterization of the kraft pulp mill foul condensate used in this study as electron donor for heterotrophic denitrification.

Parameter	Value	
Methanol-C	2300	mg/L
DOC	2500	mg/L
NH_4^+	200	mg/L
pH	9.2	
ORP	−380	mV
Ethanol	0–0.19	% (m/v)
Acetone	0–0.19 %	
Turpentine	0–0.09	%
Dimethyl sulphide	0.6	%
H_2S	0–0.09	%
Methanethiol (methyl mercaptan)	0–0.09	%
Dimethyl disulphide	0–0.09	%

Table 2
Inorganic ions' total concentrations, total salinity, and total osmotic pressure (OP) conditions characterizing each phase tested for the heterotrophic (HD) FBBR and the autotrophic (AD) FBBR. PHASE V was not tested for AD.

	Inorganic Ions (g/L)					Total Salinity (%)		Total OP (atm)	
	Cl^-	Na^+	SO_4^{2-}	K^+		HD	AD	HD	AD
				HD	AD				
PHASE 0	0.4	<0.1	<0.1	5.0	5.7	1.3	1.5	5.8	6.7
PHASE I	1.4	2.0	4.2	6.1	6.8	2.1	2.3	10.4	11.3
PHASE II	3.4	5.0	10.4	8.3	9.0	3.5	3.7	18.1	19.0
PHASE III	5.4	10.0	20.9	10.5	11.2	5.5	5.6	29.0	29.9
PHASE IV	7.9	12.5	26.1	13.5	14.2	6.8	6.9	36.6	37.5
PHASE V	10.4	15.0	31.3	16.3	/	8.1	/	44.1	/

denitrification, seen as nitrate accumulation, started to be observed, the salinity was reduced stepwise to avoid incomplete denitrification. Then, from day 79 onwards, foul condensate (FC) was added to the saline wastewater (12–15 % v/v), substituting pure methanol as electron donor. In this phase, called PHASE IV + FC, the NLR was gradually increased to observe the denitrification rate capacity of the system under saline conditions. During this phase, the wastewater feed tank was stored in a cooling box at 10–12 °C, to reduce possible biological activity.

2.3.2. Autotrophic FBBR (Thiosulphate driven)

The autotrophic FBBR was operated for 110 days. On day 0, the reactor was inoculated with 10 % v/v of a *Thiobacillus denitrificans* based culture, incubated under non saline conditions at 30 °C with thiosulphate as electron donor, as in our previous study [10]. The startup phase of the FBBR (PHASE 0 in Table 2) lasted for 46 days, during which batch mode and continuous mode (NLR 0.43 ± 0.06 g NO_3^--N/L/d, HRT 12.5 h) were interchanged, and the reactor was inoculated three more times, before obtaining removal of nitrate > 95 %. On day 47, concentration of inorganic ions was increased to PHASE I and NLR was stepwise increased to 0.78 ± 0.05 g NO_3^--N/L/d (HRT 6.2 h). When denitrification was stable, salinity was gradually increased. When nitrate started to accumulate, indicating inhibition, the salinity was reduced, and NLR decreased to recover the system. Once the reactor's performance recovered, salinity was increased again, and NLR was gradually increased to observe the denitrification rate capacity of the system under saline conditions.

2.4. Analytical methods

2.4.1. Liquid samples

Liquid samples (5 mL) were taken from both feed tank and effluent line for both heterotrophic and autotrophic reactors every 1–3 days. The pH of the samples was measured with WTW pH-meter 330i (WTW GmbH, Germany). Then, the samples were filtered through 0.2 μm Chromafil Xtra syringe filter (Macherey-Nagel, Germany) and stored at −20 °C. Concentrations of anions (NO_2^-, NO_3^-, SO_4^{2-}, $S_2O_3^{2-}$) and methanol in the filtered samples were analysed via ion chromatograph (Dionex Integrion, Thermo Fisher Scientific Inc., USA) and gas chromatograph equipped with a flame ionization detector (GC-2010, Shimadzu Co., Japan), respectively, as done in our previous study [10]. Concentration of NH_4^+ was measured with HACH cuvette test (LCK 303), using a spectrophotometer (HACH LANGE DR 2800, Hach Company, USA). Total dissolved carbon and dissolved inorganic carbon were measured with TOC-VCPH/CPN analyser (Shimadzu Co., Japan), and dissolved organic carbon (DOC) calculated as their difference. Dissolved oxygen in the FBBRs was monitored inside the water level adjustor with HQ40d portable multimeter equipped with an intellical LDO101 probe (Hach Company, USA).

2.4.2. Determination of foul condensate components by HS-GC/MS

The fate of foul condensate components (Table 1) in the heterotrophic FBBR during PHASE IV + FC was studied with headspace gas chromatography/ mass spectrometry (HS-GC/MS; Shimadzu GCMS-QP2020 NX with Nexis GC-2030, Shimadzu Co., Japan). For the analysis, each reactor sample was pipetted (0.5 mL) into two parallel 10-mL-HS vials, which were sealed with crimp-top caps. The HS sampler (Shimadzu HS-20, Shimadzu Co., Japan) was operated with similar parameters reported by Wunder et al. [45]. The GC/MS method was modified from Davoli et al. [46] (for detailed information, see Table S2). Data were acquired on a scan mode for ions with mass-to-charge ratios of 30–150 (α- and β-pinenes considered as representatives of turpentine). The foul condensate components were identified by comparing their mass spectra with the ones in the library software (NIST MS Search 2.4). Consumption of components in the reactor was estimated semi-quantitatively by comparing peak areas in the effluent sample versus in the feed solution.

2.4.3. Biomass estimation

Samples to analyse attached and suspended biomass were taken on days 36, 58, 78, 93 and 106 and on days 58, 71, 86 and 106 from the heterotrophic and autotrophic reactors, respectively, both from the GAC bed and the effluent. Every time, 6 mL effluent and 3.5 mL GAC were collected from the reactor systems. Each GAC sample was weighed, and the cells detached by adding 9 mL washing solution (composition (g/L): 0.1 peptone, 0.38 EGTA, 0.000335 Zwittergent 3–12 and 3.73 KCl), followed by shaking and sonication (5 times at 40 % max amplitude for 60 s with 30 s breaks). Usually, volatile solids (VS) are used for determination of attached biomass in fluidized bed bioreactors [24,26]. In this study, however, during the biomass detachment via sonication, also black carbon powder was detached. Therefore, since part of activated carbon accounts for VS (Figure S5), different methods were adopted. Cells were quantified by 4′, 6-diamidino-2-phenylindole (DAPI) staining technique with epifluorescence microscope (Zeiss Axioskop 2, Carl Zeiss Microscopy GmbH, Germany) and biomass as N content in the cells, as done by Rasoulnia et al. [43] and by Asik et al. [47], respectively. The resulting supernatant from the GAC sample after sonication and the effluent sample were in part stored at −20 °C for DAPI staining and in part collected for microbial population analyses (see section 2.5). The remaining volume of the samples was centrifuged at 4980 rcf at 4 °C for 10 min, the supernatant was discarded, and the cell pellet washed with 1xPBS to remove possible nitrogen other than that contained in the biomass. After centrifugation, the cell pellet was stored at −20 °C for nitrogen measurement.

Liquid samples for the cell counting were diluted 200 times with sterile MQ-water prior to filtration through 0.2 μm on polycarbonate filter and DAPI staining. Afterwards, cells were counted on 20 microscopic fields with epifluorescence microscope and total cells calculated accordingly.

The cell pellet samples for biomass quantification were digested in alkaline (0.15 M NaOH) persulphate (0.15 M $K_2S_2O_8$) solution in a heating block at 120 °C for 60 min, following the protocol of De Borba et al. [48]. After digestion, the samples were let cool down, filtered through 0.45 μm, and NO_3^--N was measured with HACH LCK 339 cuvette test, subtracting the NO_3^--N due to the persulphate solution and present in blank GAC samples. Biomass concentration was then calculated

assuming the formula $C_5H_7O_2N$. Both biomass and cells were then calculated for the whole FBBR system.

2.5. Microbial community analysis

Liquid samples for microbial community analysis from both reactors (both effluent and the carrier), from the initial inocula and the foul condensate were centrifuged at 5000 rcf at 4 °C for 10 min. The supernatant was discarded, and cell pellet stored at −80 °C. While waiting for the analyses, the pellets were stored in DNA/RNA Shield solution. Then, after bead beating of the samples (Omni Bead disruptor, 4500 rpm/40 s, 0.1 mm glass beads 1:1 w/v), DNA was extracted using the Chemagic 360 automated system (PerkinElmer Inc., USA).

The hypervariable region V4 of bacterial and archaeal 16S rRNA gene was amplified using the universal primer pair 515F-Y (GTGYCAGCMGCCGCGGTAA [49]) and 806R (GGACTACNVGGGTWTCTAAT [50]). PCR was done using the Maxima Sybr Green master mix (Thermo Fisher Scientific Inc., USA) with 40 cycles and annealing temperature 53 °C. Secondary PCR with 10 cycles was conducted, now using the primers IonA-barcode-M13: M13-515F-Y (in 10:1 ratio) and P1-806R to attach barcodes and sequencing adaptors to the amplicons, as described by Mäki et al. [51]. PCR-products were purified using the AMPure XP purification system (Beckman Coulter Life Sciences, Indianapolis, USA), analysed using the Qubit dsDNA HS assay (Thermo Fisher Scientific Inc., USA), and pooled in equimolar concentrations. Amplicons were sequenced on the IonTorrent PGM with the Hi-Q View chemistry (Thermo Fisher Scientific Inc., USA).

Sequencing data was processed with CLC Genomics Workbench version 23.0.4 and the Microbial Genomics Module (Qiagen). On average, 26306 ± 2002 (std) sequences were finally obtained per sample after primer trimming and chimera checking, with the average length of 249 bp. Calculations against Silva 138.1 (99 %) database were performed using 99 % taxonomic similarity value in the OTU clustering. Also, a Blast search of the nucleotide sequences was performed to find the closest similarities in NCBI libraries. Total number of genera and Shannon Entropy index were calculated to assess the alpha-diversity of the communities. Beta-diversity was visualized with Principal Component Analysis (PCoA) and non-Metric Multidimensional Scaling (nMDS), using Bray-Curtis distance with R (package "vegan"), to observe the variations in microbial communities under different salinity conditions for both FBBRs. Permutational multivariate analysis of variance (PERMANOVA) test, based on Bray-Curtis distance, was used to evaluate the significance ($\alpha = 0.05$) of the microbial community changes in the FBBRs. Spearman correlation ($\alpha = 0.05$) between the main microbial genera's relative abundance, salinity and nitrate removal was calculated with Python.

2.6. Calculations and kinetics

To evaluate the FBBRs' potential performance in removing nitrogen after recovering from salinity inhibition, modified Stover-Kincannon (S-K) model was fitted to the experimental data under constant salinity condition and at different HRTs. This modified S-K model, which depends on the substrate loading rate and has been used for different biofilm reactor designs and substrates [52–54], also recovering from inhibition, can be written in the linear form as:

$$\frac{HRT}{N_{in} - N_{out}} = \frac{K_B}{U_{max}}\frac{HRT}{N_{in}} + \frac{1}{U_{max}} \quad (1)$$

where the FBBR's HRT was calculated as by Nurmi et al. [55], and U_{max} and K_B are the maximum nitrogen removal rate (g N/L/d) and saturation constant (g N/L/d), respectively. Since nitrite accumulation is a sign of the reactor approaching its loading limit [26], both NO_3^--N and NO_2^--N were considered in the effluent nitrogen (N_{out}). The model was fitted to the experimental data with the Linear Regression Tool in Origin 2019b software, and R^2 and p-value ($\alpha = 0.05$) were used to evaluate the goodness of the fitting and the significance of the parameters.

Nitrate removal efficiency (NRE) was calculated as in Eq. (2), where $NO_{3\,in}^-$ and NO_{3out}^- are the influent and effluent concentrations, respectively:

$$NRE(\%) = \frac{NO_{3\,in}^- - NO_{3\,out}^-}{NO_{3\,in}^-} \cdot 100 \quad (2)$$

The same approach was adopted to also estimate the removal of other compounds ($S_2O_3^{2-}$, methanol, NH_4^+, etc.). Average removal efficiencies, loading rates, concentrations, and related standard deviations during stable conditions under the same HRT or salinity were considered.

Stoichiometric methanol, $S_2O_3^{2-}$ consumption-SO_4^{2-} production and related C/N and S/N ratios were calculated according to the heterotrophic and autotrophic denitrification reactions [10].

3. Results

3.1. Heterotrophic FBBR performance under different salinities and loading rates

In the startup phase (PHASE 0), nitrate removal efficiency (NRE) of > 98 % was obtained after 4 days of operation (Fig. 1). On day 16, salinity in the simulated wastewater was increased to 2.1 % (PHASE I), and nitrate loading rate (NLR) was gradually increased from 0.44 ± 0.02 to 0.76 ± 0.08 g NO_3^--N/L/d (HRT 12.5–6.7 h). NRE was above 98 %, with no nitrite accumulation. Methanol, which was in excess, was completely consumed (C/N = 1.54 ± 0.2 g/g (Figure S6)), likely by other bio-oxidations. During PHASE 0 and I, thiosulphate removal was initially above 98 %, mainly because of adsorption on GAC, and then gradually decreased to 32 ± 13 % in PHASE I. Total biomass and cells in the FBBR (attached + suspended) amounted to 35 mg and $2.77 \bullet 10^{11}$ cells (Fig. 2a), of which more than half was suspended.

Salinity was increased to PHASE II on day 40, followed by PHASE III on day 46, and NRE in the FBBR remained above 98 % (98.7 ± 0.2 %), with no observable changes with respect to PHASE I.

When Cl^-, Na^+, SO_4^{2-} and K^+ concentrations were increased to 10.4, 15, 31.3 and 16.3 g/L (PHASE V: salinity = 8.1 %, OP = 44.1 atm), denitrification was partially inhibited. At a NLR of 0.76 ± 0.08 g NO_3^--N/L/d (HRT 6.7 h), nitrate concentration in the effluent increased and NRE decreased to 64 % (day 58), while nitrite started to accumulate up to 100 mg/L. This indicated that nitrate reduction rate became slower than the loading rate. Similarly, methanol-C consumption decreased from the initial 98 % of previous phases down to 40 %, bringing the consumed C/N closer to the stoichiometric value (Figure S6). Suspended cells decreased 10 times from PHASE I, while attached biomass and cells remained stable (Fig. 2a).

To recover the heterotrophic FBBR from the partial inhibition, Cl^-, Na^+, SO_4^{2-} and K^+ concentrations were decreased to 7.9, 12.5, 26.1 and 13.5 g/L (PHASE IV: salinity = 6.8 %, OP = 36.6 atm) on day 59. After 5 days of operation under this condition, nitrate removal efficiency recovered back to 98 % while some nitrite still accumulated up to 80 mg/L. Methanol-C consumption recovered, bringing C/N to 1.1 ± 0.2 g/g, slightly higher than the stoichiometric value (Figure S6). Also, thiosulphate was removed similarly to PHASE I. Total biomass and cells seemed to recover from PHASE V (Fig. 2a).

Once the FBBR recovered in PHASE IV, real foul condensate was used as electron donor instead of pure methanol from day 79 (PHASE IV + FC), and the denitrification rate capacity of the recovered FBBR investigated. After 15 days at 0.76 ± 0.08 g NO_3^--N/L/d (HRT 6.7 h), NRE was above 98 %, nitrite did not accumulate and methanol in the foul condensate was consumed according to the stoichiometry (C/N = 0.91 ± 0.1 g/g, Figure S6), with no observable inhibition due to the foul condensate. Thus, NLR was increased gradually (days 95–104) to 2.47 ± 0.03 g NO_3^--N/L/d (HRT 2.2 h) and NRE was > 97 %.

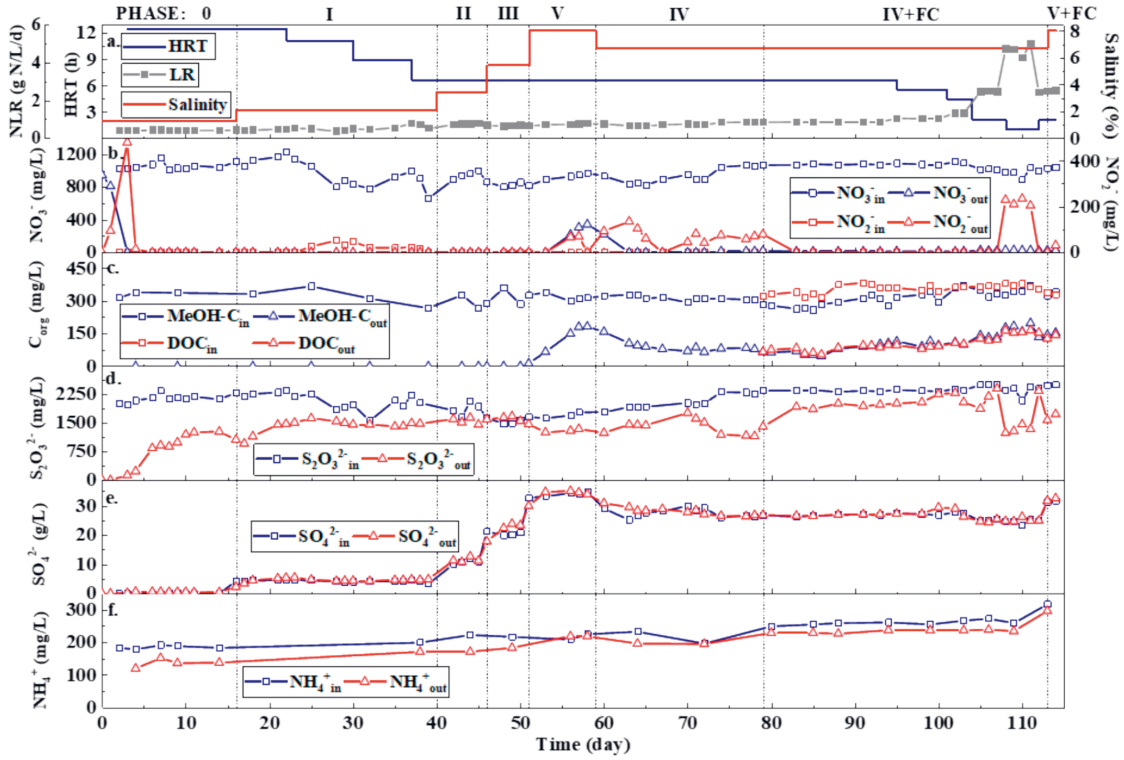

Fig. 1. Concentration-time profiles for different compounds in influent and effluent under different operational conditions in the heterotrophic fluidized bed bioreactor. a.) Operational conditions (loading rate (NLR), hydraulic retention time (HRT) and salinity). b.) nitrate and nitrite c.) Methanol-C (MeOH-C) and dissolved organic C (DOC). d.) Thiosulphate. e.) Sulphate. f.) Ammonium.

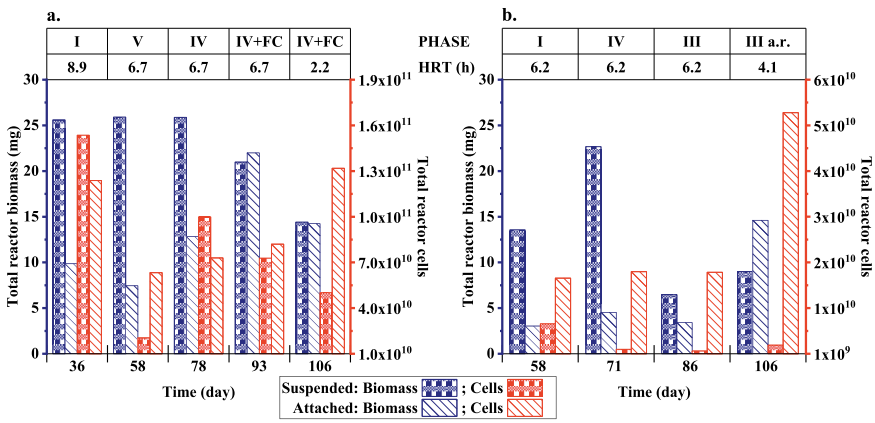

Fig. 2. Total attached and suspended biomass (mg) and total cells for heterotrophic (a.) and autotrophic (b.) fluidized bed bioreactor under the different salinity and HRT conditions.

Approximatively, half of the total biomass was attached in this phase (Fig. 2a). On day 108, NLR was further increased to 4.67 ± 0.30 g NO_3^--N/L/d (HRT 1.1 h) and NO_3^- removal remained > 97 %. Nitrite accumulated and methanol-C consumption decreased (C/N = 0.78 ± 0.1 g/g (Figure S6)), indicating that the reactor was starting to reach its maximum denitrification rate capacity. During PHASE IV + FC, also acetone, dimethyl sulphide, dimethyl disulphide, methanethiol and ethanol present in the foul condensate, which accounted for DOC, were removed by 99 % in the FBBR up to NLR of 2.47 ± 0.03 g NO_3^--N/L/d (HRT 2.2 h) (Figure S3, S4), resulting in methanol-C and DOC having

almost the same concentration in the effluent. Thiosulphate was removed by 13 ± 6 % until day 108, while when NLR was increased to 4.67 ± 0.30 g NO_3^--N/L/d (HRT 1.1 h), $S_2O_3^{2-}$ removal increased to 42 ± 8 %.

Moreover, fitting (R^2 = 0.99, p < 0.05) of modified Stover-Kincannon model with the data of PHASE IV + FC, returned U_{max} = 12.4 ± 2.5 g N/L/d and K_s = 11.6 ± 0.3 g N/L/d (Fig. 3a) and indicated that the maximum denitrification rate capacity of the recovered FBBR was not yet reached at ~ 4.7 g N/L/d (HRT 1.1 h) and salinity of 6.8 %.

Eventually (days 112–114), NLR was decreased back to 2.47 ± 0.03 g NO_3^--N/L/d (HRT 2.2 h) and salinity increased to 8.1 % (PHASE V + FC) for qualitative considerations about the inhibition of the process. However, NRE remained > 97 % and NO_2^- accumulated at around 30 mg/L suggesting that the recovered heterotrophic FBBR could potentially remove nitrate also under this higher salinity stress condition.

During all the conditions tested, sulphate was not reduced or adsorbed, while ammonium was removed by 11 ± 5 %.

3.1.1. Microbial community in the heterotrophic FBBR

At the phylum level, *Bacteirodota* (21–48 %) and *Proteobacteria* (52–79 %) dominated the heterotrophic FBBR (Figure S8). At genus level, after 36 days from the inoculation, in PHASE I, the most abundant genera in the biofilm were *Moheibacter* (43 %), *Methylovorus* (32 %), *Paracoccus* (7 %), *Aquamicrobium* (5 %), *Proteiniphilum* (4 %) and *Castellaniella* (3 %), and alpha diversity and richness were close to those of the original inoculum (Fig. 4a). On the same day, the same main genera were present in the suspended biomass, with *Methylovorus* (61 %) dominating, while richness and diversity were lower than in the biofilm (Fig. 4a). Abundance of genus *Thauera*, which was present in the inoculum, remained below 1 % during the reactor operation.

Once salinity reached 8.1 %, resulting in the accumulation of nitrate and nitrite (Fig. 1b), the microbial community in the biofilm was stable (Day 58), similarly to PHASE IV when FBBR's performance efficiency was recovered. When foul condensate was used as carbon and electron source (Day 93 and 106), the genus *Pseudomonas* become enriched onto the biofilm and *Paracoccus* genus doubled its relative abundance from previous phases.

On the other hand, community change in suspended biomass was more evident than in the biofilm. On PHASE V, relative abundance of *Methylovorus* decreased to 35 %, while the genus *Moheibacter* increased to 29 %, and community's richness and diversity increased. In PHASE IV and IV + FC, the number of genera decreased and became stable, relative abundance of *Moheibacter* decreased back to around 19 %, while abundance of *Paracoccus* and *Pseudomonas* increased to 14 % and 24 % (day 93 and 106), respectively (Fig. 4a).

Overall, the microbial community dynamics did not significantly correlate with salinity changes (Figure S10). Visualization by nMDS and PCoA analyses (Figure S11), also confirmed by PERMANOVA (p = 0.6), showed no significant (p = 0.21) changes in the overall FBBR community throughout the operation due to salinity, while difference between biofilm and suspended communities were significant (PERMANOVA, p = 0.01). Moreover, despite the large number of genera (e.g., *Methylobacillus*, *Curvibacter*, *Rubritepida* etc.) present in the foul condensate (Figure S9), none of them became enriched in the reactor.

3.2. Autotrophic FBBR performance under different salinities and loading rates

In the start-up phase of the autotrophic FBBR (PHASE 0), obtaining NRE > 98 % required 42 days of operation (Fig. 5). After the first 3 days in batch mode, the FBBR was switched to continuous mode for 19 days, but nitrate was not reduced. During this phase thiosulphate was removed by adsorption on the GAC, as no sulphate accumulated. Only after switching the FBBR to batch mode again for extended time (days 24–28 and 32–39) together with reinoculations, nitrate removal via autotrophic denitrification started. Moreover, a complementary batch study (Figure S2), showed that GAC adsorbed thiosulphate and that autotrophic denitrification in the presence of GAC started more than a week later than in the same condition without GAC.

On day 47, salinity level was increased to PHASE I. Since NRE was above 98 %, nitrite did not accumulate and S/N of thiosulphate oxidation-sulphate production were close to the stoichiometry (Figure S7), the NLR was gradually increased to 0.78 ± 0.05 g NO_3^--N/L/d (HRT 6.2 h). Moreover, effluent ammonium was consumed by less than 6 % from the initial concentration (except on days 49 and 100) throughout the whole test. Total biomass and cells in the FBBR (attached + suspended) amounted to 17 mg and $2.51 \bullet 10^{10}$ cells (Fig. 2b).

Salinity was then increased to PHASE II followed by PHASE III (days 59–67), with NRE above 98 % as in PHASE I, while consumed S/N increased to 4.6 ± 0.4 g/g, above the stoichiometry, from that of PHASE I (Figure S7).

When Cl^-, Na^+, SO_4^{2-} and K^+ concentrations were increased to 7.9, 12.5, 26.1 and 14.2 g/L (PHASE IV: salinity = 6.9 %, OP = 37.5 atm) on day 68, inhibition of autotrophic denitrification occurred at NLR of 0.78 ± 0.05 g NO_3^--N/L/d (HRT 6.2 h): nitrate concentration in the effluent

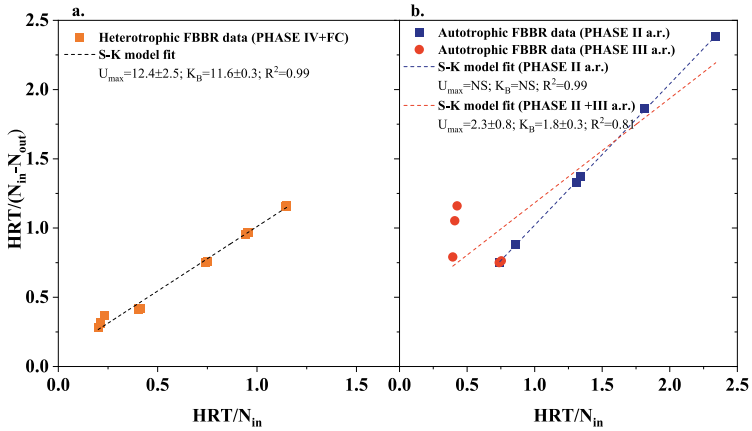

Fig. 3. Modified Stover-Kincannon model fitting with data of loading and denitrification rates of recovered heterotrophic (a.) and autotrophic (b.) fluidized bed bioreactor. U_{max} and K_s are expressed in g N/L/d. a.r.: after recovery.

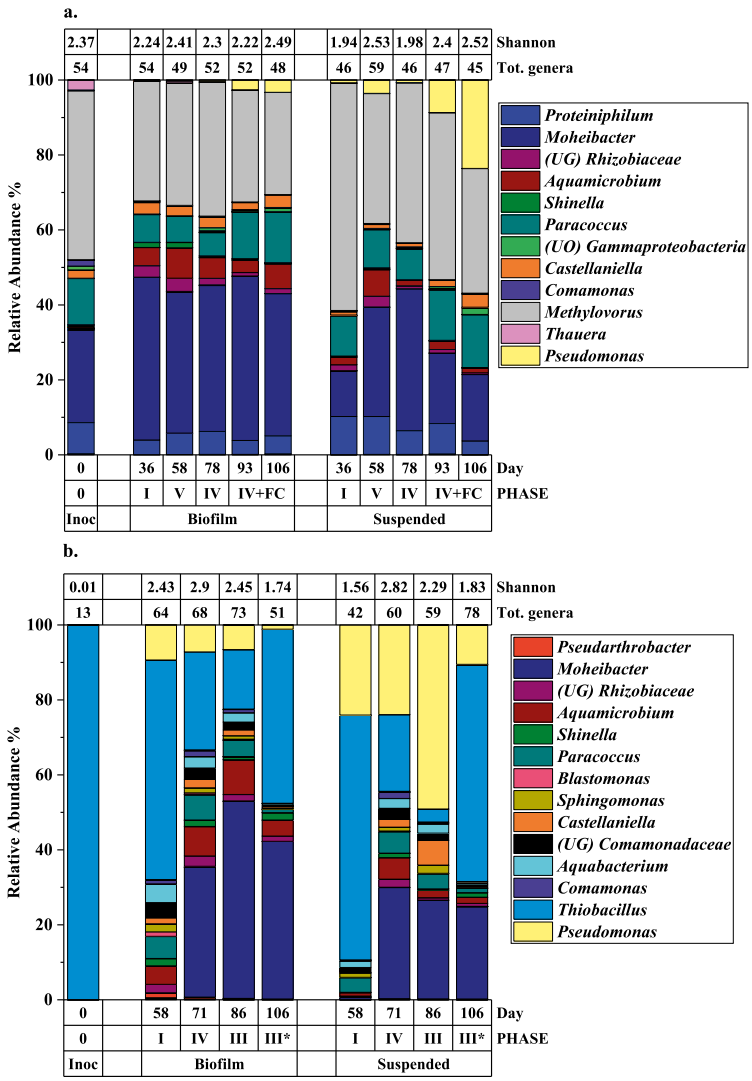

Fig. 4. Relative abundance, total number (Tot. genera), and Shannon entropy (Shannon) of microbial community at genera level in heterotrophic (a.) and autotrophic (b.) fluidized bed bioreactor, for both biofilm and suspension. Other genera not reported here were overall ≤ 1 %. UG = Unknown Genera; UO = Unknown Order; * after recovery.

increased up to 760 mg/L and NRE decreased to 11 % (day 77). Nitrite slightly accumulated up to 46 mg/L, only on days 70 and 71, and was then consumed. Also, thiosulphate concentration in the effluent increased above 1000 mg/L (days 70–91) but was consumed more than stoichiometrically (Figure S7). A decrease in suspended cells was observed, while attached biomass remained quite stable (Fig. 2b).

To recover the autotrophic FBBR, salinity level was decreased to PHASE III (day 77), but NRE did not recover in 7 days and total biomass and cells in the reactor were at their lowest value (Fig. 2b). Therefore, salinity was further decreased to PHASE II on day 87. Since the FBBR did not recover in 5 more days, NLR was gradually decreased. Only when bringing the NLR to 0.44 g NO_3^--N/L/d (HRT 10.3 h), nitrate removal started again via autotrophic denitrification on day 94.

In PHASE II after recovery, NLR was gradually increased to 1.30 ± 0.19 g NO_3^--N/L/d (HRT 4.1 h), and NRE was > 97 % without nitrite accumulation. Consumed S/N (4.3 ± 0.4 g/g) was similar to PHASE II before the inhibition and above the stoichiometry, while average produced S/N (2.9 ± 1.5 g/g) was below the stoichiometric value (Figure S7). On day 105, salinity was increased to PHASE III, corresponding to Cl^-, Na^+, SO_4^{2-} and K^+ concentrations of 5.4, 10, 21 and 11.2 g/L, and nitrate removal was not affected at NLR of 1.30 ± 0.19 g NO_3^--N/L/d (HRT 4.1 h). Both total biomass and cells increased from the previous phase, and more than 60 % of biomass was attached (Fig. 2b). Eventually, in the last days of the FBBR operation, NLR was brought to 2.45 ± 0.10 g NO_3^--N/L/d (HRT 2.1 h) but nitrate accumulated and NRE decreased to around 50 %, indicating that the maximum denitrification rate capacity of the reactor was close.

Modified Stover-Kincannon model to estimate the denitrification

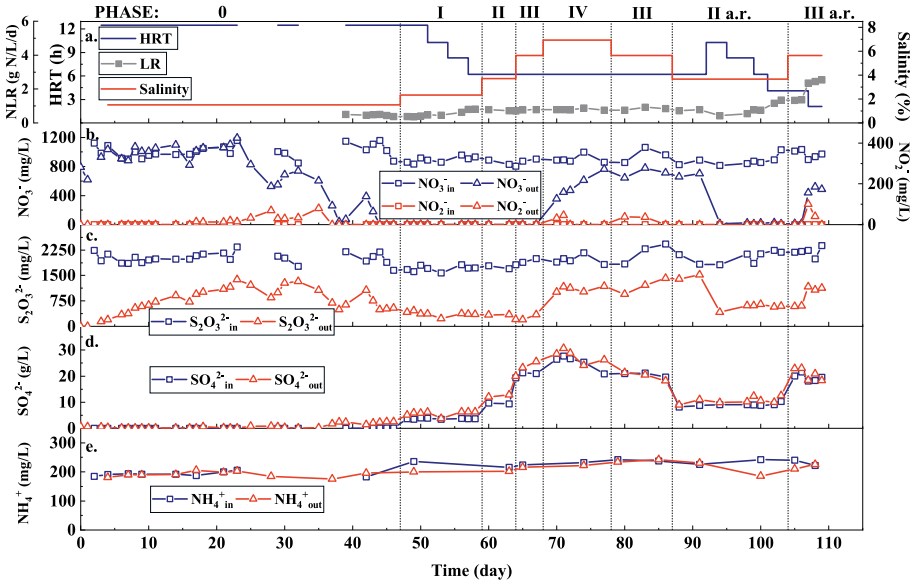

Fig. 5. Concentration-time profiles for different compounds in influent and effluent under different operational conditions in the autotrophic fluidized bed bioreactor. a.) Operational conditions (loading rate (NLR), hydraulic retention time (HRT) and salinity). b.) nitrate and nitrite c.) Thiosulphate. d.) Sulphate. e.) Ammonium. Missing HRT lines between day 0 and 50 indicate batch mode. a.r.: after recovery.

capacity of the FBBR in PHASE II after recovery did not return significant ($p > 0.05$) parameters but suggested that the maximum denitrification rate capacity was not yet reached at NLR of ~ 1.3 g N/L/d (HRT 4.1 h) and 3.7 % salinity. A second fitting including the data from both PHASE II and III was performed (Fig. 3b) with $R^2 = 0.8$. Nevertheless, the maximum nitrogen removal rate ($U_{max} = 2.3 \pm 0.8$ g N/L/d) was close to the one observed of ~ 1.2 g N/L/d (HRT 2.1 h), indicating that maximum denitrification rate capacity of the reactor at salinity of 5.6 % was being reached.

3.2.1. *Microbial community in the autotrophic FBBR*

In the start-up phase, the autotrophic FBBR was repeatedly inoculated with a pure culture of *Thiobacillus denitrificans*. During the reactor operation, several microorganisms became enriched in the FBBR (Fig. 4b). At the phylum level, *Bacteirodota* (1–25 %) and *Proteobacteria* (47–99 %) were dominant (Figure S8). At genus level, on Day 58 of PHASE I, *Thiobacillus* (59 %), *Pseudomonas* (9 %), *Paracoccus* (6 %), *Aquabacterium* (5 %), *Aquamicrobium* (5 %), *Castellaniella* (2 %) and *Sphingomonas* (2 %) were dominant in the biofilm, showing that microbial community had higher diversity than the inoculum. On the same day, *Thiobacillus* (65 %) and *Pseudomonas* (24 %) were dominant in the suspended biomass.

In PHASE IV and III (Day 71 and 86), when denitrification was inhibited, resulting in nitrate accumulation, relative abundance of *Thiobacillus* on the biofilm decreased to 16 %, while *Moheibacter* (53 %) became enriched in the FBBR. Shannon index on Day 71 was the highest of the whole FBBR operation. NRE recovered when *Thiobacillus* relative abundance increased back to 46 %, similar to PHASE I, *Moheibacter* decreased to 42 %, and community's diversity decreased (Day 106) (Fig. 4b).

Salinity inhibition on *Thiobacillus* was more visible in the suspended biomass than in the biofilm, as its abundance decreased to 3 % on day 86, while *Pseudomonas* became the dominant genus. Abundance of *Moheibacter* remained stable between Day 71 and 106. Once the FBBR recovered from the salinity shock, abundance of *Thiobacillus* was similar to PHASE I, while *Pseudomonas* decreased from 49 % to 10 %, together with the richness of the community (Fig. 4b).

The relative abundance of genus *Thiobacillus* was significantly negatively correlated with salinity and positively correlated with NRE (Figure S10), indicating its main role in denitrification. Contrarily, *Moheibacter* was negatively correlated with NRE (Figure S10). Overall, as visualized by PCoA and nMDS plots (Figure S11), salinity had a significant ($p = 0.005$) role for the microbial community changes in the autotrophic FBBR.

4. Discussion

This work delineated for the first time in a comparative manner heterotrophic and autotrophic denitrification under salinity stress in continuous flow biofilm reactors, including biomass quantification and dynamic changes in microbial communities, by using real pulp mill foul condensate and thiosulphate as electron donors. The foul condensate supported and promoted heterotrophic denitrification, demonstrating potential for practical application. Moreover, this study showed denitrification tolerance to salinity among the highest in literature, considering the non-saline history of the cultures used. The complex microbial communities developed in the FBBRs were resilient to the salinity changes, with the heterotrophic community tolerating higher salinity than the autotrophic. Eventually, this study contributes to an engineered solution for the pre-denitrification, supported by electron donors internal to the industrial plant, of nitrate laden saline streams in pulp mills produced by NO_x-SO_2 air pollution control systems, as described in the next paragraphs.

4.1. *Performance of denitrifying FBBRs under saline conditions*

Overall, high-rate denitrification was demonstrated in the FBBRs under saline conditions (Table 3), as also confirmed by modified Stover-Kincannon model (Fig. 3), which was used to evaluate the denitrification rate capacity. According to the model, the heterotrophic FBBR could

Table 3
Denitrification performance under saline conditions for different reactor systems. The table reports only studies using methanol and $S^0/S^{2-}/S_2O_3^{2-}$ as electron donors for heterotrophic (HD) and autotrophic (AD) denitrification, respectively. If not reported, reactor operational parameters were estimated from the data available in the references.

	Microorganisms' source, influent	Reactor type	Salinity %	HRT (h)	Loading Rate (gN/L/d)	Removal %	Ref.
HD	WWTP sludge, synthetic	FBBR	6.8	2.2	2.5	>97 (NO_3^-)	This study
	WWTP sludge, synthetic	CSTR	≤3; 4	48	0.75	99 (NO_x^-); inhib.	[56]
	Seawater, marine mesocosm wastewater	MBBR	2.8	>24	1.5	88 (NO_x^-)	[13]
	WWTP sludge + soil, synthetic	Polymeric carrier bed	3	3	8.4	60 (NO_3^-)	[58]
	Saline enrichment of sludge, synthetic	SBBR	6	24	0.11	<80 (TN)	[59]
	WWTP sludge, synthetic	Biofilm Electrode	3.5	8	0.06	55 (NO_3^-)	[16]
	Seawater, marine mesocosm wastewater	MBBR	2.8	1.6	3.5	75 (NO_x^-)	[60]
AD	*T. denitrificans* culture, synthetic	FBBR	5.6	4.1	1.2	>97 (NO_3^-)	This study
	WWTP sludge, synthetic	S packed bed	3	1	0.6	~80 (NO_3^-)	[18]
	WWTP sludge, synthetic	UASB	3.2	8	0.3	56 (NO_3^-)	[20]
	marine sediments, mariculture tank and anaerobic sludge, synthetic	upflow packed column	3.1	1–4	1	55 (NO_3^-)	[19]

WWTP: Wastewater Treatment Plant; FBBR: Fluidized Bed Bioreactor; CSTR: Continuous Stirred Tank Reactor; MBBR: Moving Bed Biofilm Reactor; SBBR: Sequencing Batch Biofilm Reactor; UASB: Upflow Anaerobic Sludge Blanket.

have withstood higher loading rates at salinity of 6.8 %, showing promising results for the treatment of nitrate laden wastewaters also at higher salinity (Days 112–114, Fig. 1). In general, an increase in salinity leads to a decrease in the denitrification rate, until complete inhibition is reached [9,10]. Therefore, increasing the HRT could improve the removal performance of the reactor.

Despite the high denitrification rate, attached and suspended biomass and cells in both FBBRs remained relatively low (highest: 26 mg and $1.5 \bullet 10^{11}$ in heterotrophic FBBR under non-inhibitory conditions) in comparison to other studies. Only Shelly et al. [14] reported comparable values (31 mg attached biomass protein in a 250 mL moving bed bioreactor) for denitrification at 1.4 % salinity. The reasons for the low biomass/cells value could be due to fact that detachment of biofilm from activated carbon pores is challenging, as well as the difference in the experimental conditions. Eventually, the consistency of the two methods (biomass N and DAPI counting) was verified (Table S4), confirming that the reactors had low biomass production and that heterotrophic had a higher biomass yield than the autotrophic FBBR.

Denitrification performance was higher in heterotrophic FBBR than autotrophic FBBR, possibly because the salinity tolerance limit of *T. denitrificans* was reached. Heterotrophic FBBR in this study could withstand the highest reported salinity concentration for methanol driven denitrification without reducing its nitrate removal efficiency, even outperforming systems using microorganisms from saline environments (Table 3). On the other hand, acetate driven denitrification has been reported to obtain 99 % NRE at 10–14 % salinity [56,57], but longer HRTs (24–48 h) were used. Moreover, this was the first reactor study about $S_2O_3^{2-}$ driven denitrification under saline conditions, and autotrophic FBBR showed the highest salinity tolerance and loading rate capacity among the autotrophic reactor studies in Table 3, considering that NO_2^- accumulation was not observed.

4.2. Dynamics of microbial communities and denitrification efficiency under salinity stress

4.2.1. Heterotrophic FBBR

In the heterotrophic FBBR, microbial community showed its resiliency to increasing salinity, promptly recovering from inhibitory concentrations when the ionic concentrations were decreased. No significant changes were apparent overall in the FBBR's community and NRE was > 97 % at 6.8 % salinity. In previous studies, loss in community's richness and diversity and the enrichment of salt tolerant bacteria has been reported at increasing salinity stress [4,18], as also by Zhai et al. [16] in a methanol driven denitrifying community above 2.5 % NaCl. Contrarily, no major changes in their methanol driven denitrification community were reported between 0 and 4 % NaCl by Osaka et al. [56], even though denitrification was inhibited. The salinity tolerance in our study was likely due to a mix of Cl^-, Na^+, SO_4^{2-} and K^+ ions. Thus, since the toxicity is dependent on the type of ions in saline environment [10,61], and Cl^- and Na^+ were present in lower amount than by using only NaCl, inhibition by ions was lower in our study than in Osaka et al. [56]. Furthermore, high surface GAC provided a protective environment for the biofilm against salinity stress, as suggested not only by the attached cells decreasing less than suspended ones during the FBBR operation but also by the same biofilm microbial community remaining stable. Such community stability at increasing salinities is positive for the stability of the denitrification efficiency.

In the heterotrophic FBBR, the most abundant methanol using genus was identified as *Methylovorus*, found also in other methanol fed denitrifying communities [62]. The most similar sequence was that of species MM2, capable of dissimilatory nitrite reduction [63], which also showed salinity tolerance in our study. Other common genera found in wastewater treatments, including *Paracoccus* and *Pseudomonas* that are capable of complete denitrification and have been reported to tolerate saline conditions [4,15,56,64], were also present in the heterotrophic FBBR.

Nitrite accumulation from the first denitrification step (eq. S2a) was not detected in the effluent until denitrification was partially inhibited at 8.1 % salinity (PHASE V), when NRE decreased to around 60 %. Accumulation of NO_2^- has been reported under salinity stress due to the decrease in *nir* gene responsible of nitrite reduction [15]. However, the inoculum used in this study came from a culture where NO_2^- was seen to accumulate (followed by consumption) under non inhibitory conditions [10]. Therefore, unwanted NO_2^- accumulation was likely due to the overall denitrification reaction slowing down. When foul condensate was used as carbon and electron source after the fast recovery from salinity's partial inhibition, NO_2^- accumulation was not observed (PHASE IV + FC). At the same time, other organic compounds in foul condensate were removed, suggesting that they also served as electron donors for nitrogen removal. Complex mixtures of electron donors have shown their advantages over a single electron donor. For example, Fernàndez-Nava et al. [32] reported up to 57 % higher denitrification rates with organic carbon sources from food industry than with pure compounds. Also, Zhang et al. [64] reported that primary sludge fermentation liquid could enrich communities resistant to higher salinities by increasing the community diversity. In this study, salt tolerant

genera *Pseudomonas* and *Paracoccus*, which is also capable to degrade methylated compounds [65], increased their relative abundances when foul condensate was fed to the FBBR. Therefore, the addition of an industrial side stream like foul condensate was advantageous, as it increased the community's diversity and overall nitrogen removal under salinity stress.

At lower salinities (PHASE I-III), organic C was completely consumed in the FBBR. Likely, microaerobic conditions (measured DO 0.2–0.8 mg/L, results not shown) favoured methanol oxidation by the genus *Shinella* [66], which then disappeared at higher salinities (Fig. 4a). Also, *Moheibacter*, the second most dominant genus during the operation, found in anoxic and aerobic granular sludge [67,68], is strictly aerobic growing up to 4 % NaCl [69]. Hence, it was likely being associated with aerobic methanol oxidation. However, at 6.8 % salinity, C/N ratio was close to the stoichiometry, indicating that methanol driven denitrification was the main organic C removal path, while aerobic oxidation of methanol remained limited. Regardless, *Moheibacter* genus continued to thrive in the FBBR, suggesting that it was possibly growing on organic microbial excretions.

Thiosulphate was removed by adsorption in the first weeks of operation and continued to be removed in later phases, possibly by bio-oxidation. Genera such as *Paracoccus* [70,71] and *Pseudomonas* [72,73] are capable of $S_2O_3^{2-}$ oxidation. In particular, *Pseudomonas* can carry sulphur oxidation in presence of organic carbon [72,73], both aerobically and anaerobically in the presence of N_2O [74], producing S^0 or $S_4O_6^{2-}$ rather than SO_4^{2-}. This could explain why SO_4^{2-} did not vary in the FBBR, while the whitish substance spotted on GAC (Figure S12) could represent S^0.

Ammonium removal remained quite stable trough the FBBR operation, contrarily to what reported by some studies where NH_4^+ increased via dissimilatory nitrate reduction to ammonium (DNRA) during denitrification under saline conditions [16,75,76]. This could be connected to the response to salinity of the main denitrifying genera, different than in this study.

4.2.2. Autotrophic FBBR

At the beginning, a pure culture of *Thiobacillus denitrificans* was inoculated to the autotrophic FBBR followed by a slow start-up, as reported also by Zou et al. [26] in a FBBR with GAC. Then, during the reactor operation, other microbial genera, also potentially capable of autotrophic denitrification, became enriched. Despite this, the key microorganism in autotrophic nitrate removal was *Thiobacillus denitrificans*. When salinity increased to 6.9 % (PHASE IV), *T. denitrificans* was inhibited, its relative abundance drastically decreased and NRE declined to 11 %. This is in line with other studies, where it was strongly inhibited in 5–6.6 % salinity [18,20,77]. When inhibited, relative abundance on biofilm of *Thiobacillus* was at 16 %, while in the suspended biomass it decreased to 3 %. Therefore, GAC partially protected *Thiobacillus* population from salt inhibition and, by retaining the biomass, it allowed the FBBR to recover in 17 days after decreasing salinity and loading rate. Moreover, nitrite accumulation from the first denitrification step (eq. S1a) was lower than in the heterotrophic FBBR, indicating that nitrite reduction was not inhibited in 3.7–6.9 % salinity.

After the recovery (PHASE II a.r.), produced SO_4^{2-}-S /NO_3^--N was lower than stoichiometrically expected, as in our previous study in the presence of inorganic ions [10]. Contrarily, Li et al. [18] reported that produced SO_4^{2-}-S /NO_3^--N was close to the stoichiometry at 6 % salinity, but the key autotrophic microorganisms were different (*Thiogranum*).

From PHASE IV, thiosulphate was removed more than according to the stoichiometric oxidation, which can be attributed to the genera *Paracoccus* and *Pseudomonas*, capable of $S_2O_3^{2-}$ oxidation. These microorganisms became enriched from the tap water used for simulated wastewater as they were present in both FBBRs and have been reported in Finnish drinking water systems together with many others [78]. Their contribution to autotrophic denitrification was minor since nitrate accumulated even though their relative abundance increased. Also, *Moheibacter*, found in other autotrophic denitrification studies [67,79], became enriched in the FBBR likely from tap water. Since *Moheibacter* is strictly aerobic and its abundance was negatively correlated with nitrate removal in our study, it is possible that this genus grew aerobically (measured DO 0.2–1 mg/L) on organic excretions as heterotrophs have been reported in autotrophic systems without added organic carbon sources [80].

Overall, the microbial community in the autotrophic FBBR, started with a pure culture, developed to a more complex community maintaining thiosulphate driven autotrophic denitrification. Complex microbial communities, as discussed for the heterotrophic FBBR, are advantageous for industrial applications as they can increase the resilience of the process to salinity [64].

4.3. Role of scrubber wastewater denitrification in pulp mill wastewater management

Biological processes are established treatment methods for pulp mill wastewaters, being easy to operate and having lower capital costs as compared to physical–chemical methods [33,40,81]. However, since pulp mill wastewaters contains low amounts of nutrients, the activated sludge process is not designed for nitrogen removal [40]. Averagely, pulp mills produce around 10^4-10^5 m^3/day of wastewater [39], while NO_x-SO_2 scrubber wastewater production is about 10^2-10^3 m^3/day. Therefore, a targeted high-rate pre-denitrification system, such as showed in this study, represents a more favourable solution than modifying the existing activated sludge system for denitrification of the overall wastewater of the pulp mill.

Considering a heterotrophic FBBR (maximum denitrification rate of 2.5 g N/L/d) treating NO_x-SO_2 scrubber wastewater (flow: 2 L/s, salinity: 5 %, NO_x^-: 0.15 g N/L), an estimated GAC fluidized bed of around 10 m^3 would remove effectively N at HRT of 1.5 h. Therefore, the FBBR would allow high-rate treatment, but costs related to the bed's fluidization [22] should also be considered.

A further advantage, not only for N laden streams' treatment but also the whole pulp mill, could come from mixing different waste streams in this pre-denitrification treatment. In this study foul condensate demonstrated to be a suitable electron donor for denitrification under salinity stress and, hence, the usual treatment by stripping and burning the non-condensable gases [39] could be reduced, achieving multi-pollutants removal in a biological process. This would also allow to save on electron donor supplementation costs. In addition, foul condensate contains also NH_4^+, which is beneficial for the subsequent activated sludge process of the mill [40]. Therefore, it serves as NH_4^+ source once the waste stream from the scrubber pre-denitrification step is directed to overall wastewater stream for activated sludge treatment. Eventually, further investigations on denitrification with foul condensate under salinity stress should address for example possible N_2O accumulation, a critical environmental factor for denitrification under saline conditions [7].

Similar considerations could be made for a $S_2O_3^{2-}$ driven autotrophic FBBR, since also thiosulphate showed to be a suitable electron donor under salinity stress. In this case, the $S_2O_3^{2-}$ already present in the NO_x-SO_2 scrubber wastewater and potentially harmful for the environment [82], would serve as electron donor and be removed by the denitrification process. However, improvements for the denitrification rate capacity and salinity resistance of autotrophic denitrification are needed. For instance, an engineered exposure of the biofilm to salt stress (priming) before the start-up phase, could improve the process' response to the same stress in the future [83]. Moreover, biological sulphur recovery from the scrubber wastewater and the recirculation of the scrubbing solution might increase the circularity of the approach [84]. Eventually, since heterotrophic denitrification showed higher removal rates than autotrophic denitrification, similarly to other studies [85,86], mixotrophic denitrification [87] could represent a balanced solution not only to improve the loading rate capacity but also to remove both $S_2O_3^{2-}$

from the scrubber wastewater and organic compounds from the foul condensate.

5. Conclusions

This study demonstrates the suitability of methanol and thiosulphate as electron donors for heterotrophic and autotrophic denitrification, respectively, under salinity stress due to Cl^-, Na^+, SO_4^{2-} and K^+. Heterotrophic FBBR removes nitrate by over 97 % at a rate of 2.40 ± 0.10 g NO_3^--N/L/d (HRT 2.2 h) and salinity of 6.8 %, showing its high-rate treatment potential at salinities even higher than NO_x-SO_2 scrubber wastewater. For the first time, it is demonstrated that foul condensate from pulp mill not only supports heterotrophic denitrification, but also enhances nitrogen removal. Moreover, the FBBR's microbial community thrives in biofilm protected environment and remains stable under different salinities. In the autotrophic FBBR, nitrate is removed by over 97 % at a rate of 1.27 ± 0.10 g NO_3^--N/L/d (HRT 4.1 h) and salinity of 5.6 %. *Thiobacillus* remains the key microorganism in thiosulphate driven denitrification and is strongly inhibited at 6.9 % salinity, causing the decrease in the FBBR's nitrate removal efficiency. Overall, methanol driven withstands higher salinity and loading rate than thiosulphate driven denitrification. Eventually, the results show the potential of a high-rate pre-denitrification treatment of scrubber wastewater in pulp mills by using electron donors internal to the mill and, thus, reducing both the organic and nitrate loads on the main wastewater treatment plant.

CRediT authorship contribution statement

Alessio D'Aquino: Writing – review & editing, Writing – original draft, Visualization, Validation, Software, Methodology, Investigation, Funding acquisition, Formal analysis, Data curation, Conceptualization. **Susanna T. Maanoja:** Writing – review & editing, Formal analysis. **Hannele Auvinen:** Writing – review & editing, Visualization, Conceptualization. **Marja Tiirola:** Writing – review & editing, Visualization, Software, Formal analysis, Data curation. **Gianni Andreottola:** Writing – review & editing, Visualization, Supervision, Methodology, Conceptualization. **Jaakko A. Puhakka:** Writing – review & editing, Visualization, Supervision, Methodology, Funding acquisition, Conceptualization. **Marja R.T. Palmroth:** Writing – review & editing, Visualization, Supervision, Resources, Methodology, Funding acquisition, Conceptualization.

Declaration of competing interest

The authors declare that they have no known competing financial interests or personal relationships that could have appeared to influence the work reported in this paper.

Acknowledgments

Funding: This work was supported by Maa- ja vesitekniikan tuki ry (grant number 4301) and Emil Aaltosen Säätiö (grant number 220015 KO). Also, the collaboration between Tampere University and University of Trento for the project "Sustainable biological management of nitrogenous liquid streams from air emission control" has received funding from the SMART-ER project, funded by the European Union's Horizon 2020 research and innovation programme under Grant Agreement #101016888. The authors would like to thank D.Sc. Reka Hajdu-Rahkama for useful suggestions for the FBBRs operation, laboratory trainee Mikko Levàn for helping in the sampling and chemical analyses during the experiments and M.Sc. Nicolò Merzi for the advice with statistical analyses.

Appendix A. Supplementary data

Supplementary data to this article can be found online at https://doi.org/10.1016/j.cej.2024.158131.

Data availability

Data will be made available on request.

References

[1] N.N.R. Ahmad, W.L. Ang, C.P. Leo, A.W. Mohammad, N. Hilal, Current advances in membrane technologies for saline wastewater treatment: A comprehensive review, Desalination 517 (2021) 115170, https://doi.org/10.1016/j.desal.2021.115170.
[2] A. Panagopoulos, Study and evaluation of the characteristics of saline wastewater (brine) produced by desalination and industrial plants, Environ. Sci. Pollut. Res. 29 (2022) 23736–23749, https://doi.org/10.1007/s11356-021-17694-x.
[3] O. Lefebvre, R. Moletta, Treatment of organic pollution in industrial saline wastewater: A literature review, Water Res. 40 (2006) 3671–3682, https://doi.org/10.1016/j.watres.2006.08.027.
[4] S. Miao, C. Jin, R. Liu, Y. Bai, H. Liu, C. Hu, J. Qu, Microbial community structures and functions of hypersaline heterotrophic denitrifying process: Lab-scale and pilot-scale studies, Bioresour. Technol. 310 (2020) 123244, https://doi.org/10.1016/j.biortech.2020.123244.
[5] J. Wang, J. Zhou, Y. Wang, Y. Wen, L. He, Q. He, Efficient nitrogen removal in a modified sequencing batch biofilm reactor treating hypersaline mustard tuber wastewater: The potential multiple pathways and key microorganisms, Water Res. 177 (2020) 115734, https://doi.org/10.1016/j.watres.2020.115734.
[6] Y. Pang, J. Wang, Various electron donors for biological nitrate removal: A review, Sci. Tot. Environ. 794 (2021) 148699, https://doi.org/10.1016/j.scitotenv.2021.148699.
[7] W. Zhao, Y. Wang, S. Liu, M. Pan, J. Yang, S. Chen, Denitrification activities and N_2O production under salt stress with varying COD/N ratios and terminal electron acceptors, Chem. Eng. J. 215–216 (2013) 252–260, https://doi.org/10.1016/j.cej.2012.10.084.
[8] W.V. Macêdo, I.K. Sakamoto, E.B. Azevedo, M.H.R.Z. Damianovic, The effect of cations (Na^+, Mg^{2+}, and Ca^{2+}) on the activity and structure of nitrifying and denitrifying bacterial communities, Sci. Tot. Environ. 679 (2019) 279–287, https://doi.org/10.1016/J.SCITOTENV.2019.04.397.
[9] R. Wang, P. Zheng, A. Qiang Ding, M. Zhang, A. Ghulam, C. Yang, H.P. Zhao, Effects of inorganic salts on denitrifying granular sludge: The acute toxicity and working mechanisms, Bioresour. Technol. 204 (2016) 65–70, https://doi.org/10.1016/j.biortech.2015.12.062.
[10] A. D'Aquino, N. Kalinainen, H. Auvinen, G. Andreottola, J.A. Puhakka, M.R. T. Palmroth, Effects of inorganic ions on autotrophic denitrification by *Thiobacillus denitrificans* and on heterotrophic denitrification by an enrichment culture, Sci. Tot. Environ. 901 (2023) 165940, https://doi.org/10.1016/j.scitotenv.2023.165940.
[11] E. Liu, C. Fan, M. Zhao, S. Jiang, Z. Wang, Z. Jin, K. Bei, X. Zheng, S. Wu, Q. Zeng, Effects of heavy metals on denitrification processes in water treatment: A review, Sep. Purif. Technol. 299 (2022) 121793, https://doi.org/10.1016/j.seppur.2022.121793.
[12] S. Navada, O. Vadstein, A.-K. Tveten, G.C. Verstege, B.F. Terjesen, V.C. Mota, V. Venkataraman, F. Gaumet, Ø. Mikkelsen, A. Kamstra, Influence of rate of salinity increase on nitrifying biofilms, J. Clean. Prod. 238 (2019) 117835, https://doi.org/10.1016/j.jclepro.2019.117835.
[13] M.-A. Labelle, P. Juteau, M. Jolicoeur, R. Villemur, S. Parent, Y. Comeau, Seawater denitrification in a closed mesocosm by a submerged moving bed biofilm reactor, Water Res. 39 (2005) 3409–3417, https://doi.org/10.1016/j.watres.2005.06.001.
[14] Y. Shelly, M. Kuk, O. Menashe, G. Zeira, S. Azerrad, E. Kurzbaum, Nitrate removal from a nitrate-rich reverse osmosis concentrate: Superior efficiency using the bioaugmentation of an Acinetobacter biofilm, J. Water Process Eng. 44 (2021) 102425, https://doi.org/10.1016/j.jwpe.2021.102425.
[15] Y. Miao, R. Liao, X.-X. Zhang, B. Liu, Y. Li, B. Wu, A. Li, Metagenomic insights into salinity effect on diversity and abundance of denitrifying bacteria and genes in an expanded granular sludge bed reactor treating high-nitrate wastewater, Chem. Eng. J. 277 (2015) 116–123, https://doi.org/10.1016/j.cej.2015.04.125.
[16] S. Zhai, M. Ji, Y. Zhao, X. Su, Shift of bacterial community and denitrification functional genes in biofilm electrode reactor in response to high salinity, Environ. Res. 184 (2020) 109007, https://doi.org/10.1016/j.envres.2019.109007.
[17] Z. Zhao, W. Qiu, A. Koenig, X. Fan, J.D. Gu, Nitrate removal from saline water using autotrophic denitrification by the bacterium *Thiobacillus denitrificans* MP-1, Environ. Technol. 25 (2004) 1201–1210, https://doi.org/10.1080/09593332508618387.
[18] Z.-R. Li, X.-N. Zhang, H.-C. Wang, H.-Y. Cheng, A.-J. Wang, Y.-Q. Zhang, C.-W. Cui, Y.-L. Sun, Effects of salinity on sulfur-dominated autotrophic denitrification microorganisms: Microbial community succession, key microorganisms and response mechanisms, Chem. Eng. J. 478 (2023) 147308, https://doi.org/10.1016/j.cej.2023.147308.
[19] L. Wang, J. Liu, Y. Li, Z. Liu, L. Zhang, H. Che, H. Cui, Y. Zhang, Elemental sulfur-driven autotrophic denitrification process for effective removal of nitrate in mariculture wastewater: Performance, kinetics and microbial community,

Chemosphere 337 (2023) 139354, https://doi.org/10.1016/j.chemosphere.2023.139354.
[20] B. Chen, M. Qaisar, J. Xiao, W. Li, J. Li, J. Cai, Strategy to mitigate salinization of sulfide-autotrophic denitrification: Sodium ion uptake from the environment and mutualistic symbiosis among microorganisms, Desalination 573 (2024) 117228, https://doi.org/10.1016/j.desal.2023.117228.
[21] B. Özkaya, A.H. Kaksonen, E. Sahinkaya, J.A. Puhakka, Fluidized bed bioreactor for multiple environmental engineering solutions, Water Res. 150 (2019) 452–465, https://doi.org/10.1016/j.watres.2018.11.061.
[22] F. Di Capua, S. Papirio, P.N.L. Lens, G. Esposito, Chemolithotrophic denitrification in biofilm reactors, Chem. Eng. J. 280 (2015) 643–657, https://doi.org/10.1016/j.cej.2015.05.131.
[23] S. Papirio, A. Ylinen, G. Zou, M. Peltola, G. Esposito, J.A. Puhakka, Fluidized-bed denitrification for mine waters, Part i: Low pH and Temperature Operation, Biodegrad. 25 (2014) 425–435, https://doi.org/10.1007/s10532-013-9671-0.
[24] A. Eldyasti, G. Nakhla, J. Zhu, Impact of calcium on biofilm morphology, structure, detachment and performance in denitrifying fluidized bed bioreactors (DFBBRs), Chem. Eng. J. 232 (2013) 183–195, https://doi.org/10.1016/j.cej.2013.07.084.
[25] F.K.J. Rabah, M.F. Dahab, Nitrate removal characteristics of high performance fluidized-bed biofilm reactors, Water Res. 38 (2004) 3719–3728, https://doi.org/10.1016/j.watres.2004.07.002.
[26] G. Zou, S. Papirio, A.-M. Lakaniemi, S.H. Ahoranta, J.A. Puhakka, High rate autotrophic denitrification in fluidized-bed biofilm reactors, Chem. Eng. J. 284 (2016) 1287–1294, https://doi.org/10.1016/j.cej.2015.09.074.
[27] H.-R. Kim, I.-S. Lee, J.-H. Bae, Performance of a sulphur-utilizing fluidized bed reactor for post-denitrification, Process Biochem. 39 (2004) 1591–1597, https://doi.org/10.1016/j.procbio.2003.07.004.
[28] Z. Gu, Z. Liu, Y. Cheng, Z. Zhu, J. Tian, C. Hu, J. Qu, Intensified denitrification in a fluidized-bed reactor with suspended sulfur autotrophic microbial fillers, Bioresour. Technol. 391 (2024) 129965, https://doi.org/10.1016/j.biortech.2023.129965.
[29] L.H.J. Vredenbregt, K. Nielsen, A.A. Potma, G.H. Kristensen, C. Sund, Fluid bed biological nitrification and denitrification in high salinity wastewater, Water Sci. Technol. 36 (1997) 93–100, https://doi.org/10.1016/S0273-1223(97)00341-7.
[30] S.J. Jafari, G. Moussavi, K. Yaghmaeian, High-rate biological denitrification in the cyclic rotating-bed biological reactor: Effect of COD/NO_3, nitrate concentration and salinity and the phylogenetic analysis of denitrifiers, Bioresour. Technol. 197 (2015) 482–488, https://doi.org/10.1016/J.BIORTECH.2015.08.047.
[31] J.Y. Park, Y.J. Yoo, Biological nitrate removal in industrial wastewater treatment: Which electron donor we can choose, Appl. Microbiol. Biotechnol. 82 (2009) 415–429, https://doi.org/10.1007/s00253-008-1799-1.
[32] Y. Fernández-Nava, E. Marañón, J. Soons, L. Castrillón, Denitrification of high nitrate concentration wastewater using alternative carbon sources, J. Haz. Mat. 173 (2010) 682–688, https://doi.org/10.1016/j.jhazmat.2009.08.140.
[33] R. Toczyłowska-Mamińska, Limits and perspectives of pulp and paper industry wastewater treatment – A review, Renew. Sustain. Energy Rev. 78 (2017) 764–772, https://doi.org/10.1016/j.rser.2017.05.021.
[34] T. Meyer, E.A. Edwards, Anaerobic digestion of pulp and paper mill wastewater and sludge, Water Res. 65 (2014) 321–349, https://doi.org/10.1016/j.watres.2014.07.022.
[35] J.A. Rintala, J.A. Puhakka, Anaerobic treatment in pulp- and paper-mill waste management: A review, Bioresour. Technol. 47 (1994) 1–18, https://doi.org/10.1016/0960-8524(94)90022-1.
[36] M. Badshah, W. Parawira, B. Mattiasson, Anaerobic treatment of methanol condensate from pulp mill compared with anaerobic treatment of methanol using mesophilic UASB reactors, Bioresour. Technol. 125 (2012) 318–327, https://doi.org/10.1016/j.biortech.2012.08.109.
[37] D. Schmid, O. Karlström, V. Kuvaja, I. Vuorinen, M. Paavola, M. Hupa, Role of Sulfite Oxidation in NO_2 Absorption in a pH-Neutral Scrubber Solution, Energy Fuels 36 (2022) 2666–2672, https://doi.org/10.1021/acs.energyfuels.1c03914.
[38] A.H. Slade, R.J. Ellis, M. van den Heuvel, T.R. Stuthridge, Nutrient minimisation in the pulp and paper industry: an overview, Water Sci. Technol. 50 (2004) 111–122, https://doi.org/10.2166/wst.2004.0175.
[39] M. Suhr, G. Klein, I. Kourti, Miguel Rodrigo Gonzalo, Germán Giner Santonja, Serge Roudier, Luis Delgado Sancho, Best Available Techniques (BAT) reference document for the production of pulp, paper and board, European Commission, LU, 2015 https://data.europa.eu/doi/10.2791/370629 (accessed February 1, 2024.
[40] O. Ashrafi, L. Yerushalmi, F. Haghighat, Wastewater treatment in the pulp-and-paper industry: A review of treatment processes and the associated greenhouse gas emission, J. Environ. Manag. 158 (2015) 146–157, https://doi.org/10.1016/j.jenvman.2015.05.010.
[41] A. Koenig, L. Liu, Autotrophic Denitrification of High-Salinity Wastewater Using Elemental Sulfur: Batch Tests, Water Environ. Res. 76 (2004) 37–46, https://doi.org/10.2175/106143004x141564.
[42] W. Gu, L. Wang, Y. Liu, P. Liang, X. Zhang, Y. Li, X. Huang, Anammox bacteria enrichment and denitrification in moving bed biofilm reactors packed with different buoyant carriers: Performances and mechanisms, Sci. Tot. Env. 719 (2020) 137277, https://doi.org/10.1016/j.scitotenv.2020.137277.
[43] P. Rasoulnia, R. Hajdu-Rahkama, J.A. Puhakka, High-rate and -yield continuous fluidized-bed bioconversion of glucose-to-gluconic acid for enhanced metal leaching, Chem. Eng. J. 462 (2023) 142088, https://doi.org/10.1016/j.cej.2023.142088.
[44] T. Eregowda, M.E. Kokko, E.R. Rene, J. Rintala, P.N.L. Lens, Volatile fatty acid production from Kraft mill foul condensate in upflow anaerobic sludge blanket reactors, Environ. Technol. 42 (2021) 2447–2460, https://doi.org/10.1080/09593330.2019.1703823.
[45] C. Wunder, W. Pogoda, A. Paulke, S.W. Toennes, Assay of ethanol and congener alcohols in serum and beverages by headspace gas chromatography/mass spectrometry, MethodsX 8 (2021) 101563, https://doi.org/10.1016/j.mex.2021.101563.
[46] E. Davoli, M.L. Gangai, L. Morselli, D. Tonelli, Characterisation of odorants emissions from landfills by SPME and GC/MS, Chemosphere 51 (2003) 357–368, https://doi.org/10.1016/S0045-6535(02)00845-7.
[47] G. Asik, T. Yilmaz, F. Di Capua, D. Ucar, G. Esposito, E. Sahinkaya, Sequential sulfur-based denitrification/denitritation and nanofiltration processes for drinking water treatment, J. Environ. Manag. 295 (2021) 113083, https://doi.org/10.1016/j.jenvman.2021.113083.
[48] B.M. De Borba, R.F. Jack, J.S. Rohrer, J. Wirt, D. Wang, Simultaneous determination of total nitrogen and total phosphorus in environmental waters using alkaline persulfate digestion and ion chromatography, J. Chromatogr. A 1369 (2014) 131–137, https://doi.org/10.1016/j.chroma.2014.10.027.
[49] A.E. Parada, D.M. Needham, J.A. Fuhrman, Every base matters: assessing small subunit rRNA primers for marine microbiomes with mock communities, time series and global field samples, Environ. Microbiol. 18 (2016) 1403–1414, https://doi.org/10.1111/1462-2920.13023.
[50] A. Apprill, S. McNally, R. Parsons, L. Weber, Minor revision to V4 region SSU rRNA 806R gene primer greatly increases detection of SAR11 bacterioplankton, Aquatic, Microb. Ecol. 75 (2015) 129–137, https://doi.org/10.3354/ame01753.
[51] A. Mäki, A.J. Rissanen, M. Tiirola, A practical method for barcoding and size-trimming PCR templates for amplicon sequencing, Biotech 60 (2016) 88–90, https://doi.org/10.2144/000114380.
[52] R.-C. Jin, P. Zheng, Kinetics of nitrogen removal in high rate anammox upflow filter, J. Haz. Mat. 170 (2009) 652–656, https://doi.org/10.1016/j.jhazmat.2009.05.016.
[53] G.-F. Yang, W.-M. Ni, K. Wu, H. Wang, B.-E. Yang, X.-Y. Jia, R.-C. Jin, The effect of Cu(II) stress on the activity, performance and recovery on the Anaerobic Ammonium-Oxidizing (Anammox) process, Chem. Eng. J. 226 (2013) 39–45, https://doi.org/10.1016/j.cej.2013.04.019.
[54] Ö.S. Kuşçu, D.T. Sponza, Kinetics of para-nitrophenol and chemical oxygen demand removal from synthetic wastewater in an anaerobic migrating blanket reactor, J. Haz. Mat. 161 (2009) 787–799, https://doi.org/10.1016/j.jhazmat.2008.04.039.
[55] P. Nurmi, B. Özkaya, A.H. Kaksonen, O.H. Tuovinen, M.-L. Riekkola-Vanhanen, J. A. Puhakka, Process for biological oxidation and control of dissolved iron in bioleach liquors, Process Biochem. 44 (2009) 1315–1322, https://doi.org/10.1016/j.procbio.2009.07.004.
[56] T. Osaka, K. Shirotani, S. Yoshie, S. Tsuneda, Effects of carbon source on denitrification efficiency and microbial community structure in a saline wastewater treatment process, Water Res. 42 (2008) 3709–3718, https://doi.org/10.1016/j.watres.2008.06.007.
[57] R. Liao, K. Shen, A.-M. Li, P. Shi, Y. Li, Q. Shi, Z. Wang, High-nitrate wastewater treatment in an expanded granular sludge bed reactor and microbial diversity using 454 pyrosequencing analysis, Bioresour. Technol. 134 (2013) 190–197, https://doi.org/10.1016/j.biortech.2012.12.057.
[58] P.Y. Yang, S. Nitisoravut, J.S. Wu, Nitrate removal using a mixed-culture entrapped microbial cell immobilization process under high salt conditions, Water Res. 29 (1995) 1525–1532, https://doi.org/10.1016/0043-1354(94)00296-J.
[59] L. Feng, G. Wu, Z. Zhang, Z. Tian, B. Li, J. Cheng, G. Yang, Improving denitrification performance of biofilm technology with salt-tolerant denitrifying bacteria agent for treating high-strength nitrate and sulfate wastewater from lab-scale to pilot-scale, Bioresour. Technol. 387 (2023) 129696, https://doi.org/10.1016/j.biortech.2023.129696.
[60] M. Dupla, Y. Comeau, S. Parent, R. Villemur, M. Jolicoeur, Design optimization of a self-cleaning moving-bed bioreactor for seawater denitrification, Water Res. 40 (2006) 249–258, https://doi.org/10.1016/j.watres.2005.10.029.
[61] X. Jiang, H. Wang, P. Wu, Y. Lei, L. Deng, W. Wang, Enhanced narH gene expression contributing to nitrite accumulation in simultaneous nitrification and denitrification under Na^+ stress instead of K^+ stress, Chem. Eng. J. 479 (2024) 147637, https://doi.org/10.1016/j.cej.2023.147637.
[62] M.P. Ginige, P. Hugenholtz, H. Daims, M. Wagner, J. Keller, L.L. Blackall, Use of Stable-Isotope Probing, Full-Cycle rRNA Analysis, and Fluorescence In Situ Hybridization-Microautoradiography To Study a Methanol-Fed Denitrifying Microbial Community, Appl. Environ. Microbiol. 70 (2004) 588–596, https://doi.org/10.1128/AEM.70.1.588-596.2004.
[63] M.C. Macey, J. Pratscher, A. Crombie, J.C. Murrell, Draft Genome Sequences of Obligate Methylotrophs *Methylovorus sp.* Strain MM2 and *Methylobacillus sp.* Strain MM3, Isolated from Grassland Soil, Microbiol. Resour. Announc. 7 (2018) 10.1128/mra.00824-18, https://doi.org/10.1128/mra.00824-18.
[64] Z. Zhang, Y. Guo, L. Guo, F. Hu, Y. Zhao, C. Jin, Z. She, M. Gao, G. Wang, Elucidating salinity adaptation and shock loading on denitrification performance: Focusing on microbial community shift and carbon source evaluation, Bioresour. Technol. 305 (2020) 123030, https://doi.org/10.1016/j.biortech.2020.123030.
[65] J. Wang, X. Liu, X. Jiang, L. Zhang, C. Hou, G. Su, L. Wang, Y. Mu, J. Shen, Facilitated bio-mineralization of N,N-dimethylformamide in anoxic denitrification system: Long-term performance and biological mechanism, Water Res. 186 (2020) 116306, https://doi.org/10.1016/j.watres.2020.116306.
[66] M. Lee, S.-G. Woo, L.N. Ten, *Shinella daejeonensis sp. nov.*, a nitrate-reducing bacterium isolated from sludge of a leachate treatment plant, Int. J. Syst. Evol. Microbiol. 61 (2011) 2123–2128, https://doi.org/10.1099/ijs.0.026435-0.
[67] N. Fernández, R. Sierra-Alvarez, R. Amils, J.A. Field, J.L. Sanz, Compared microbiology of granular sludge under autotrophic, mixotrophic and heterotrophic

denitrification conditions, Water Sci. Technol. 59 (2009) 1227–1236, https://doi.org/10.2166/wst.2009.092.
[68] Y.-C. Juang, S.S. Adav, D.-J. Lee, J.-H. Tay, Stable aerobic granules for continuous-flow reactors: Precipitating calcium and iron salts in granular interiors, Bioresour. Technol. 101 (2010) 8051–8057, https://doi.org/10.1016/j.biortech.2010.05.078.
[69] R.-G. Zhang, X. Tan, X.-M. Zhao, J. Deng, J. Lv, *Moheibacter sediminis gen. nov., sp. nov.*, a member of the family Flavobacteriaceae isolated from sediment, and emended descriptions of *Empedobacter brevis*, *Wautersiella falsenii* and *Weeksella virosa*, Int. J. Syst. Evol. Microbiol. 64 (2014) 1481–1487, https://doi.org/10.1099/ijs.0.060178-0.
[70] Y.-X. Cui, B.K. Biswal, M.C.M. van Loosdrecht, G.-H. Chen, D. Wu, Long term performance and dynamics of microbial biofilm communities performing sulfur-oxidizing autotrophic denitrification in a moving-bed biofilm reactor, Water Res. 166 (2019) 115038, https://doi.org/10.1016/j.watres.2019.115038.
[71] M.J. Rameez, P. Pyne, S. Mandal, S. Chatterjee, M. Alam, S. Bhattacharya, N. Mondal, J. Sarkar, W. Ghosh, Two pathways for thiosulfate oxidation in the alphaproteobacterial chemolithotroph *Paracoccus thiocyanatus* SST, Microbiol. Res. 230 (2020) 126345, https://doi.org/10.1016/j.micres.2019.126345.
[72] R.-C. Zhang, C. Chen, X.-J. Xu, D.-J. Lee, N.-Q. Ren, The interaction between *Pseudomonas* C27 and *Thiobacillus denitrificans* in the integrated autotrophic and heterotrophic denitrification process, Sci. Tot. Environ. 811 (2022) 152360, https://doi.org/10.1016/j.scitotenv.2021.152360.
[73] C. Chen, K.-L. Ho, F.-C. Liu, M. Ho, A. Wang, N. Ren, D.-J. Lee, Autotrophic and heterotrophic denitrification by a newly isolated strain *Pseudomonas sp.* C27, Bioresour. Technol. 145 (2013) 351–356, https://doi.org/10.1016/j.biortech.2012.12.027.
[74] D.Y. Sorokin, A. Teske, L.A. Robertson, J.G. Kuenen, Anaerobic oxidation of thiosulfate to tetrathionate by obligately heterotrophic bacteria, belonging to the *Pseudomonas stutzeri* group, FEMS Microbiol. Ecol. 30 (1999) 113–123, https://doi.org/10.1016/S0168-6496(99)00045-8.
[75] S. Zhai, M. Ji, Y. Zhao, S.G. Pavlostathis, Q. Zhao, Effects of salinity and COD/N on denitrification and bacterial community in dicyclic-type electrode based biofilm reactor, Chemosphere 192 (2018) 328–336, https://doi.org/10.1016/j.chemosphere.2017.10.108.
[76] X. Ma, K. Wang, X. Li, G. Liu, H. Chen, C. Piao, S. You, Elucidating the elevated salinity effect on removal of carbon and nitrogen in coupling aromatic degradation to anaerobic denitrification, Chem. Eng. J. 471 (2023) 143999, https://doi.org/10.1016/j.cej.2023.143999.
[77] Z. Shen, L. Xie, C. Lyu, P. Xu, Y. Yuan, X. Li, Y. Huang, W. Li, M. Zhang, M. Shi, Effects of salinity on nitrite and elemental sulfur accumulation in a double short-cut sulfur autotrophic denitrification process, Bioresour. Technol. 369 (2023) 128432, https://doi.org/10.1016/j.biortech.2022.128432.
[78] V. Gomez-Alvarez, S. Siponen, A. Kauppinen, A.-M. Hokajärvi, A. Tiwari, A. Sarekoski, I.T. Miettinen, E. Torvinen, T. Pitkänen, A comparative analysis employing a gene- and genome-centric metagenomic approach reveals changes in composition, function, and activity in waterworks with different treatment processes and source water in Finland, Water Res. 229 (2023) 119495, https://doi.org/10.1016/j.watres.2022.119495.
[79] A. Kostrytsia, S. Papirio, L. Morrison, U.Z. Ijaz, G. Collins, P.N.L. Lens, G. Esposito, Biokinetics of microbial consortia using biogenic sulfur as a novel electron donor for sustainable denitrification, Bioresour. Technol. 270 (2018) 359–367, https://doi.org/10.1016/j.biortech.2018.09.044.
[80] F. Di Capua, A.-M. Lakaniemi, J.A. Puhakka, P.N.L. Lens, G. Esposito, High-rate thiosulfate-driven denitrification at pH lower than 5 in fluidized-bed reactor, Chem. Eng. J. 310 (2017) 282–291, https://doi.org/10.1016/j.cej.2016.10.117.
[81] A. Esmaeeli, M.-H. Sarrafzadeh, S. Zeighami, M. Kalantar, S.G. Bariki, A. Fallahi, H. Asgharnejad, S.-B. Ghaffari, A Comprehensive Review on Pulp and Paper Industries Wastewater Treatment Advances, Ind. Eng. Chem. Res. 62 (2023) 8119–8145, https://doi.org/10.1021/acs.iecr.2c04393.
[82] J.C. Miranda-Trevino, M. Pappoe, K. Hawboldt, C. Bottaro, The Importance of Thiosalts Speciation: Review of Analytical Methods, Kinetics, and Treatment, Crit. Rev. Environ. Sci. Technol. 43 (2013) 2013–2070, https://doi.org/10.1080/10643389.2012.672047.
[83] S. Navada, O. Vadstein, F. Gaumet, A.-K. Tveten, C. Spanu, Ø. Mikkelsen, J. Kolarevic, Biofilms remember: Osmotic stress priming as a microbial management strategy for improving salinity acclimation in nitrifying biofilms, Water Res. 176 (2020) 115732, https://doi.org/10.1016/j.watres.2020.115732.
[84] X. Guimerà, M. Mora, A.D. Dorado, A. Bonsfills, D. Gabriel, X. Gamisans, Optimization of SO_2 and NO_x sequential wet absorption in a two-stage bioscrubber for elemental sulphur valorisation, Environ. Sci. Pollut. Res. 28 (2021) 24605–24617, https://doi.org/10.1007/s11356-020-09607-1.
[85] K. Tang, S. An, M. Nemati, Evaluation of autotrophic and heterotrophic processes in biofilm reactors used for removal of sulphide, nitrate and COD, Bioresour. Technol. 101 (2010) 8109–8118, https://doi.org/10.1016/j.biortech.2010.06.037.
[86] C. Fan, P. Wang, W. Zhou, S. Wu, S. He, J. Huang, L. Cao, The influence of phosphorus on the autotrophic and mixotrophic denitrification, Sci. Tot. Environ. 643 (2018) 127–133, https://doi.org/10.1016/j.scitotenv.2018.06.185.
[87] E. Sahinkaya, N. Dursun, A. Kilic, S. Demirel, S. Uyanik, O. Cinar, Simultaneous heterotrophic and sulfur-oxidizing autotrophic denitrification process for drinking water treatment: Control of sulfate production, Water Res. 45 (2011) 6661–6667, https://doi.org/10.1016/j.watres.2011.09.056.

Methanol and thiosulphate from pulp mill waste streams support denitrification under salinity stress

Alessio D'Aquino[a, b*], Susanna T. Maanoja[a], Hannele Auvinen[a], Marja Tiirola[c], Gianni Andreottola[b], Jaakko A. Puhakka[a] and Marja R. T. Palmroth[a]

[a] Tampere University, Faculty of Engineering and Natural Sciences, Materials Science and Environmental Engineering Unit, Korkeakoulunkatu 8, P.O. Box 541, 33014 Tampere, Finland

[b] University of Trento, Department of Civil, Environmental and Mechanical Engineering, via Mesiano 77, 38123 Trento, Italy

[c] University of Jyväskylä, Department of Biological and Environmental Sciences, NanoScience Center, Survontie 9C, P.O.Box 35, 40014 Jyväskylä, Finland

*Corresponding author. Email address: alessio.daquino@tuni.fi

Supplementary materials

Table S1. Trace element solution added to the simulated wastewater fed to the reactors.

Compound	Concentration
Na_2EDTA	1 mg/L
$FeSO_4 \cdot 7H_2O$	2.4 mg/L
$ZnSO_4 \cdot 7H_2O$	0.2 mg/L
$MnCl_2 \cdot 4H_2O$	0.06 mg/L
H_3BO_3	0.06 mg/L
$CoCl_2 \cdot 6H_2O$	0.4 mg/L
$CuCl_2 \cdot 2H_2O$	0.02 mg/L
$NiCl_2 \cdot 6H_2O$	0.04 mg/L
$Na_2MoO_4 \cdot 2H_2O$	0.06 mg/L
$MgCl_2 \cdot 6H_2O$	35 mg/L
$CaCl_2 \cdot 2H_2O$	0.7 mg/L

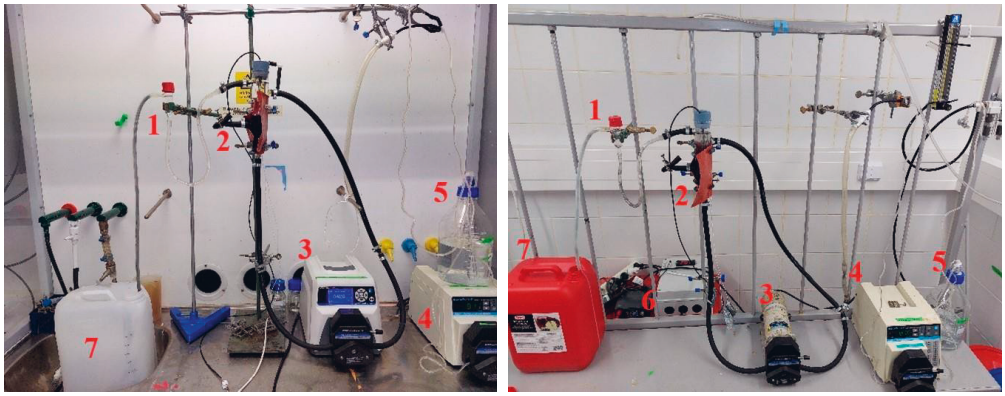

Figure S1. Autotrophic (on the left) and heterotrophic (on the right) fluidized bed bioreactor (FBBR) systems. The two system were identical and as described in the Materials & Methods Section. 1. Water level adjustor; 2. FBBR covered by a heating blanket; 3. Recirculation pump; 4. Feed Pump; 5. Feed tank; 6. Temperature control system; 7. Effluent tank.

Table S2. Headspace gas chromatography/mass spectrometry (HS-GC/MS) method parameters for determination of foul condensate components (modified from Davoli et al. 2003 [1], Wunder et al. 2021 [2]).

Headspace sampler	
Headspace pressure	57 kPa
Oven temperature	70°C
Sample line temperature	90°C
Transfer line temperature	100°C
Shaking level	2
Equilibration time	15 min
Pressurizing time	2 min
Pressure equilibration time	0.1 min
Load time	0.5 min
Load equilibration time	0.1 min
Injection time	1 min
Needle flush time	15 min
Gas chromatograph	
Injection mode	Split
Carrier gas	Helium
Pressure	28.3 kPa
Total flow	83.8 mL/min
Column flow	0.80 mL/min
Linear velocity	32.0 cm/s
Purge flow	3 mL/min
Split ratio	100
Column	ZB-5MSi, 30 m x 0.25 mm ID x 0.25 µm film thickness
Column oven program	25°C hold 3.50 min to 130°C at 5°C/min, hold 0 min to 220°C at 40°C/min, hold 3.25 min
Total run time	30 min
Mass spectrometer	
Ion source temperature	200°C
Interface temperature	250°C
Solvent cut time	0.5 min
Scan time	0.6-30 min
Scan range	m/z 30-150

Batch test: effect of GAC on autotrophic denitrification

During the startup phase of the reactors in the present study, autotrophic fluidized bed bioreactor (FBBR) obtained nitrate removal >95% in 42 days, against the 3 days of heterotrophic FBBR. This was in contrast with the results obtained in our previous study [3], where autotrophic denitrification by *Thiobacillus denitrificans* (DSM 12475) and heterotrophic denitrification by an enrichment culture, which were the same cultures used in the present study, had similar denitrification activities in their respective growth media. Therefore, a batch test to observe possible interference of granular activated carbon (GAC) and of the simulated wastewater with autotrophic denitrification startup was conducted.

The test was run in 117 mL serum bottles (60 mL liquid volume) and five conditions were tested in duplicates, as reported in Table S3. When present, GAC was added to the batch assays in the same volumetric ratio as in the FBBR (V_{GAC}/V_{FBBR}=0.44). Thiosulphate and bicarbonate were added in excess. After the addition of the liquid media (90% v/v) and the GAC, the bottles were sealed with butyl rubber stoppers and aluminum crimps and purged for 20 minutes with N_2 to create anoxic conditions. Then, a *Thiobacillus denitrificans* (DSM 12475) culture, cultivated as described in our previous study [3], was added as inoculum (10% v/v), and the assays incubated at 150 rpm and 30 °C.

The test was monitored for 3 weeks by taking 1 mL liquid sample, filtered through 0.2 µm Chromafil Xtra syringe filters (Macherey-Nagel, Germany). Samples were stored at -20°C. Concentrations of anions (Cl^-, NO_2^-, NO_3^-, SO_4^{2-}, $S_2O_3^{2-}$) were analyzed via ion chromatograph, see Materials & Methods section.

Table S3. Conditions tested in the batch assay for autotrophic denitrification. See Materials & Methods section for the composition of the simulated wastewater in PHASE 0.

Condition's name	Medium	Inoculum	GAC
Growth Control	Growth medium as reported in our previous work [3]	Yes	No
Abiotic FBBR Feed	Simulated wastewater in PHASE 0	No	No
Inoculated FBBR Feed	Simulated wastewater in PHASE 0	Yes	No
GAC + Abiotic FBBR Feed	Simulated wastewater in PHASE 0	No	Yes
GAC + Inoculated FBBR Feed	Simulated wastewater in PHASE 0	Yes	Yes

The results of the batch tests are shown in Figure S2. In the Growth Control and the Inoculated FBBR Feed assays, autotrophic denitrification removed nitrate above 97%, and consumed thiosulphate accordingly, in 48 h, indicating that the simulated wastewater did not inhibit denitrification. In the Abiotic FBBR Feed assays, concentration of NO_3^-, NO_2^-, $S_2O_3^{2-}$ and SO_4^{2-} remained stable during the experiment, and, hence, no apparent chemical transformations were observed. Similar behavior was observed in the GAC + Abiotic FBBR Feed assays, except for $S_2O_3^{2-}$ which decreased below 1000 mg/L in 48 h, suggesting that it was adsorbed onto GAC. Similarly, also $S_2O_3^{2-}$ in the GAC + Inoculated FBBR Feed condition, decreased, indicating adsorption, but NO_3^- was still not removed at 168 h in contrast to the Inoculated FBBR Feed condition. Only between 2 and 3 weeks after the start of the batch test, when a last sample was taken from the GAC + Inoculated FBBR Feed condition, NO_3^- was removed above 97%, and $S_2O_3^{2-}$ consumed. NO_2^- was not detected in any conditions tested.

These results indicated that GAC interfered with the startup of autotrophic denitrification by *Thiobacillus denitrificans* (DSM 12475), also in the autotrophic FBBR, explaining the longer startup

time when compared to heterotrophic FBBR. However, the reasons cannot be disclosed from this test. A possible explanation could be linked to the sequestration of thiosulphate by GAC, which decreased $S_2O_3^{2-}$ concentration in the liquid below the stoichiometric value needed for denitrification. On the other hand, the thiosulphate left in solution was used only after 168 h and the substrate adsorbed onto GAC should have been bio-available for microorganisms [4], unless it had reacted with the GAC surface. This interference is important to be considered for the startup of a reactor with GAC.

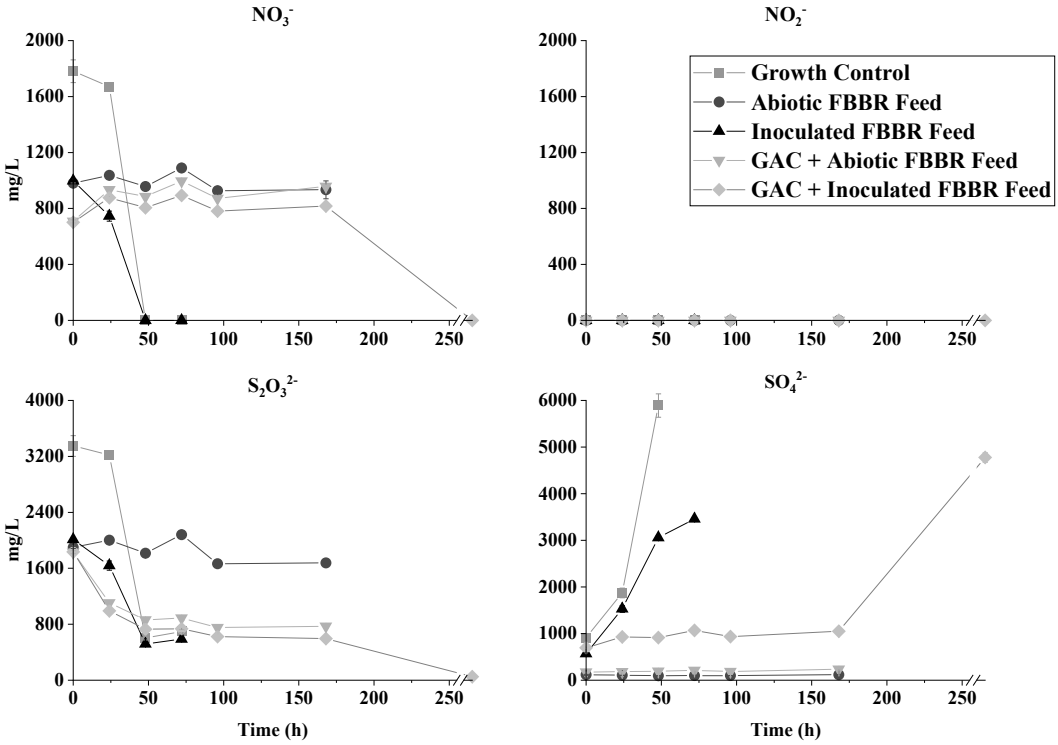

Figure S2. Time profiles of NO_3^-, NO_2^-, $S_2O_3^{2-}$ and SO_4^{2-} concentrations for each condition tested in the autotrophic denitrification batch test. Error bars represent standard deviation of duplicates. The last point after 250 h for the GAC + Inoculated FBBR Feed was taken between 2 and 3 weeks after the start of the experiment (day 0).

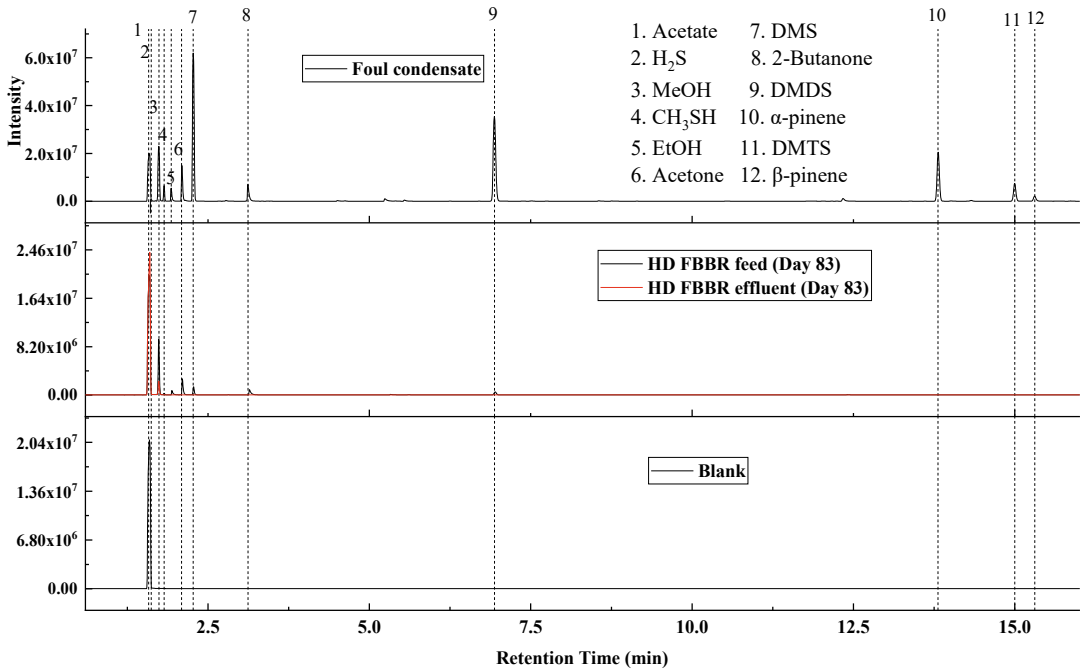

Figure S3. Chromatograms from HS-GC/MS for a foul condensate sample (first subplot from the top), two samples from the heterotrophic (HD) reactor system: Feed (influent simulated wastewater + foul condensate) and FBBR (effluent of the reactor) on Day 83 (second subplot), and a blank sample (MQ-water, third subplot).

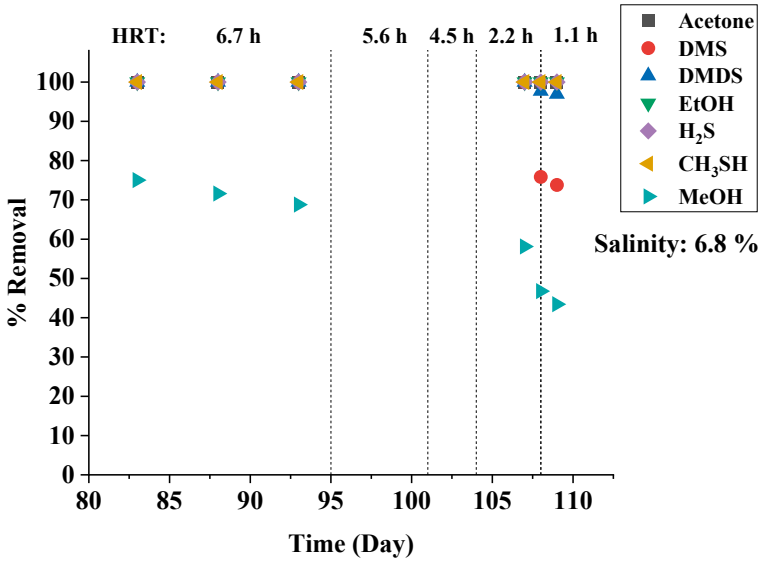

Figure S4. Percentage removal of main compounds (as peak areas from GC/MS) of the foul condensate in the heterotrophic fluidized bed bioreactor.

Figure S5. Granular activated carbon (GAC) after being heated at 105 °C overnight and 550 °C for 2 hours. Weight loss was about 23±2% of the total GAC dry mass (after 105 °C), therefore accounting for volatile solids.

To verify the biomass (suspended and attached) measurements performed as N and as epifluorescence microscopy cell counting, the nitrogen present in the total counted cells in the reactor was estimated for each sample. An average value of $2.35 \cdot 10^{-13}$ g was used for the dry weight of a single bacterial cell for this comparison and was calculated based on values reported in literature [5–8]. The values taken from literature are mainly for a *E. coli* cell in the stationary phase of its growth. Percentage of nitrogen in bacterial cell was assumed 12% according to the formula $C_5H_7NO_2$.

Table S4 shows the comparison between the nitrogen mass measured after digestion of the cell pellet and the nitrogen mass estimated as cells counted multiplied by the N amount of a single bacterial cell. In general, the estimated nitrogen mass was in the same order of magnitude of the measured nitrogen mass, except for the suspended biomass in the autotrophic FBBR, where the estimations were between 10 to 100 times lower than the measurements. This might suggest that the nitrogen measured was due not only to suspended biomass but also to other suspended material, such as EPS. However, an accurate explanation results difficult, especially considering that the calculated total nitrogen comes from a rough estimation, which might include errors from the cell counting as well as from considering the same average value of bacterial cell weight for heterotrophs and autotrophs exposed to different saline concentrations. All in all, the data reported in Table S4 confirm that the results obtained for biomass by DAPI cell counting and nitrogen measurement were consistent.

Table S4. Comparison between measured total nitrogen and estimated total nitrogen masses from the DAPI counting for the total suspended and attached biomass in both heterotrophic and autotrophic fluidized bed bioreactors (FBBR).

(mg)	Sample day	Suspended biomass		Attached biomass	
		Measured Total nitrogen	Estimated Total nitrogen (DAPI)	Measured Total nitrogen	Estimated Total nitrogen (DAPI)
Heterotrophic FBBR	42	3.17	4.34	1.22	3.50
	56	3.21	0.58	0.92	1.79
	76	3.21	2.82	1.59	2.06
	91	2.60	2.06	2.72	2.32
	104	1.78	1.42	1.76	3.72
Autotrophic FBBR	56	1.68	0.21	0.38	0.50
	69	2.81	0.06	0.56	0.54
	84	0.80	0.05	0.42	0.53
	104	1.12	0.08	1.81	1.52

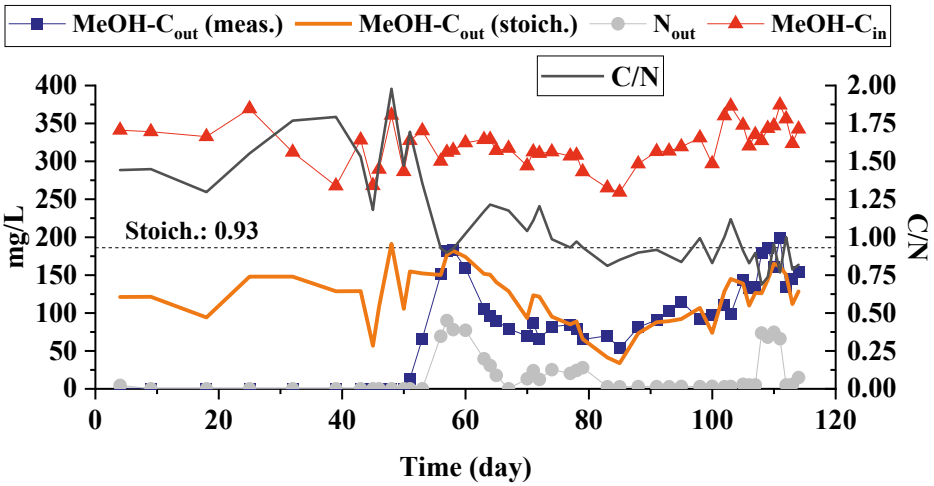

Figure S6. Comparison between measured (meas.) Methanol-C (MeOH-C) and stoichiometric (stoich.) in the effluent of the heterotrophic fluidized bed bioreactor (FBBR). Stoichiometric MeOH-C and C/N were calculated based on the NO_3^- (mg/L) entering the reactor, the NO_3^- in the effluent and considering C/N=0.93 g/g for the complete reduction of NO_3^- to N_2.

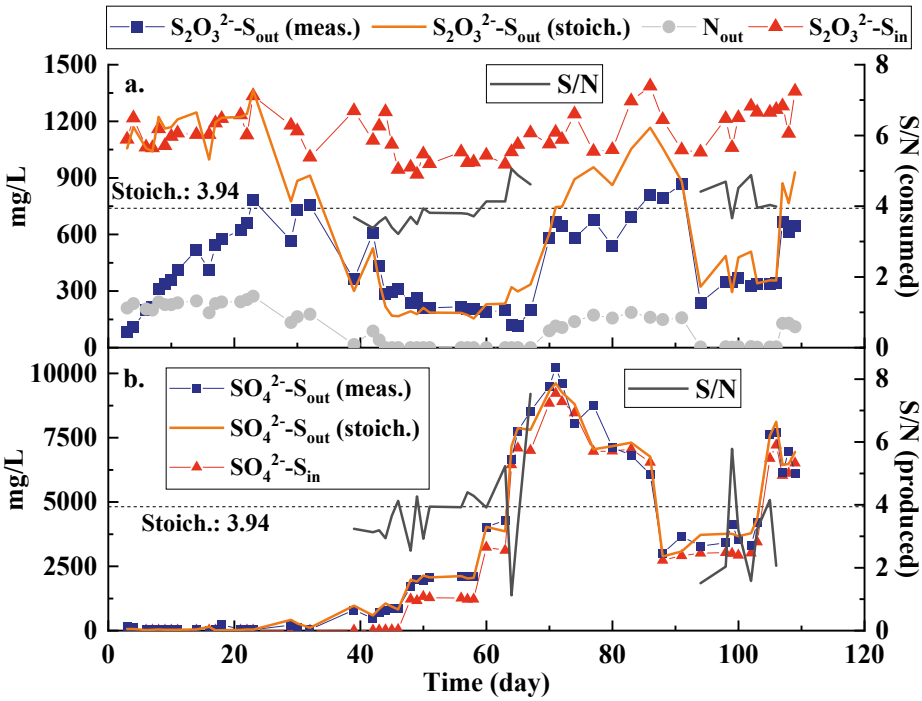

Figure S7. Comparison between measured (meas.) $S_2O_3^{2-}$-S (a.), SO_4^{2-}-S (b.) and stoichiometric (stoich.) $S_2O_3^{2-}$-S (a.), SO_4^{2-}-S (b.) in the effluent of the autotrophic fluidized bed bioreactor (FBBR). Stoichiometric $S_2O_3^{2-}$-S, SO_4^{2-}-S and C/N were calculated based on the NO_3^- (mg/L) entering the reactor, NO_3^- in the effluent and considering S/N =3.94 g/g for the complete reduction of NO_3^- to N_2. S/N is not shown when denitrification was not complete.

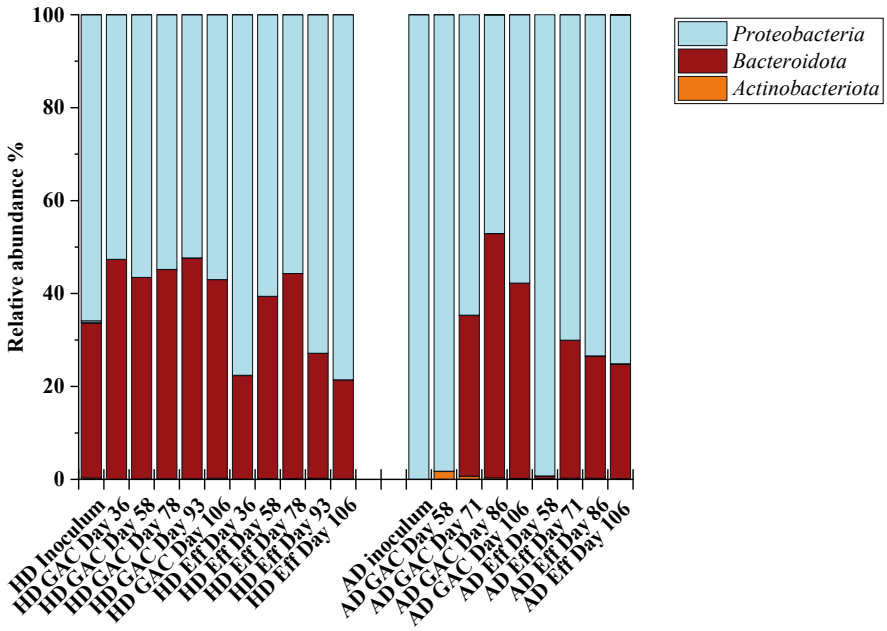

Figure S8. Relative abundance of microbial community at phylum level in both heterotrophic and autotrophic fluidized bed bioreactors (FBBR), for biofilm (GAC) and suspended (Eff) biomass.

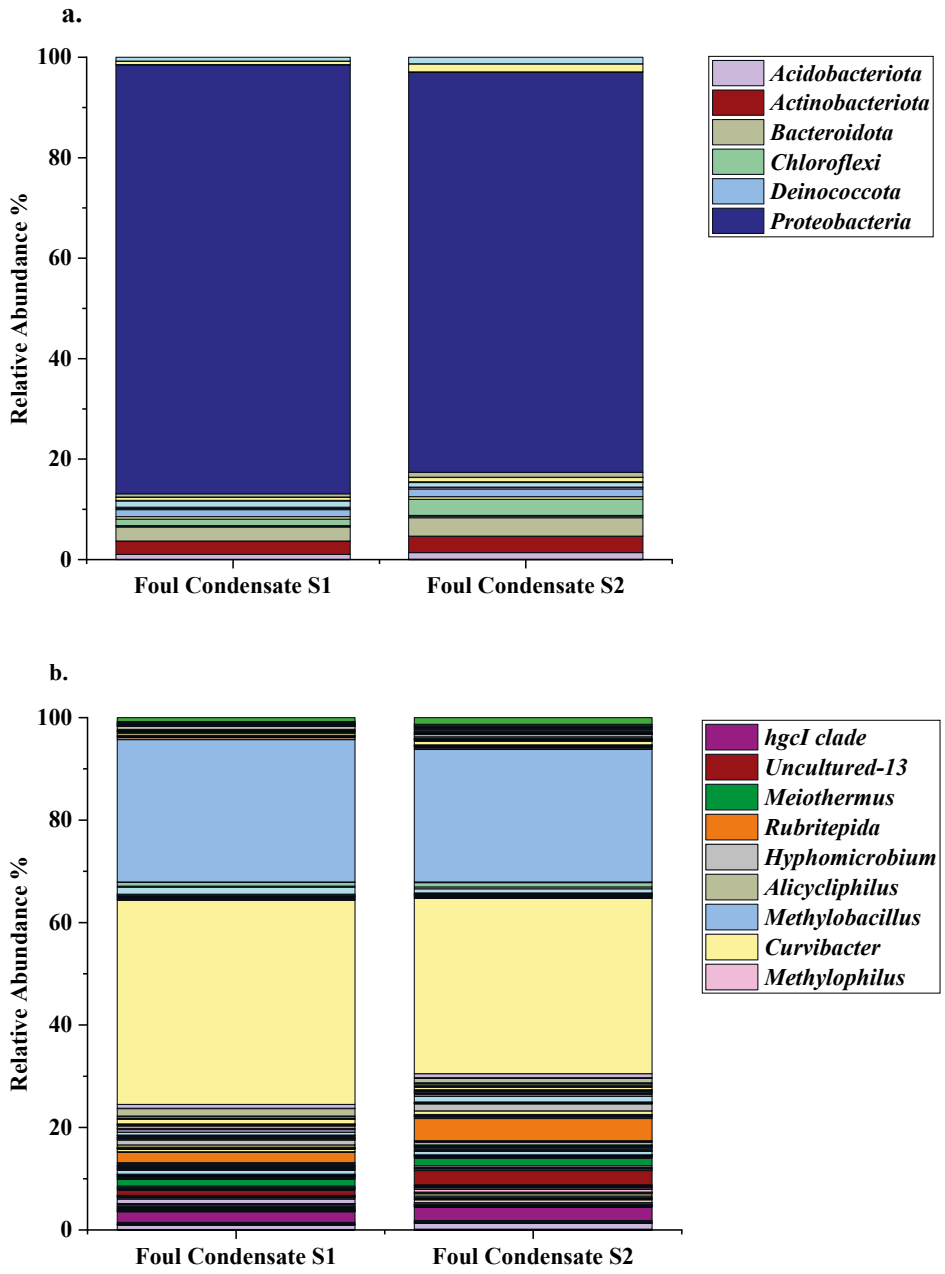

Figure S9. Microbial community composition of the foul condensate samples taken one month apart from the same stock, at phylum level (a.) and genus level (b.).

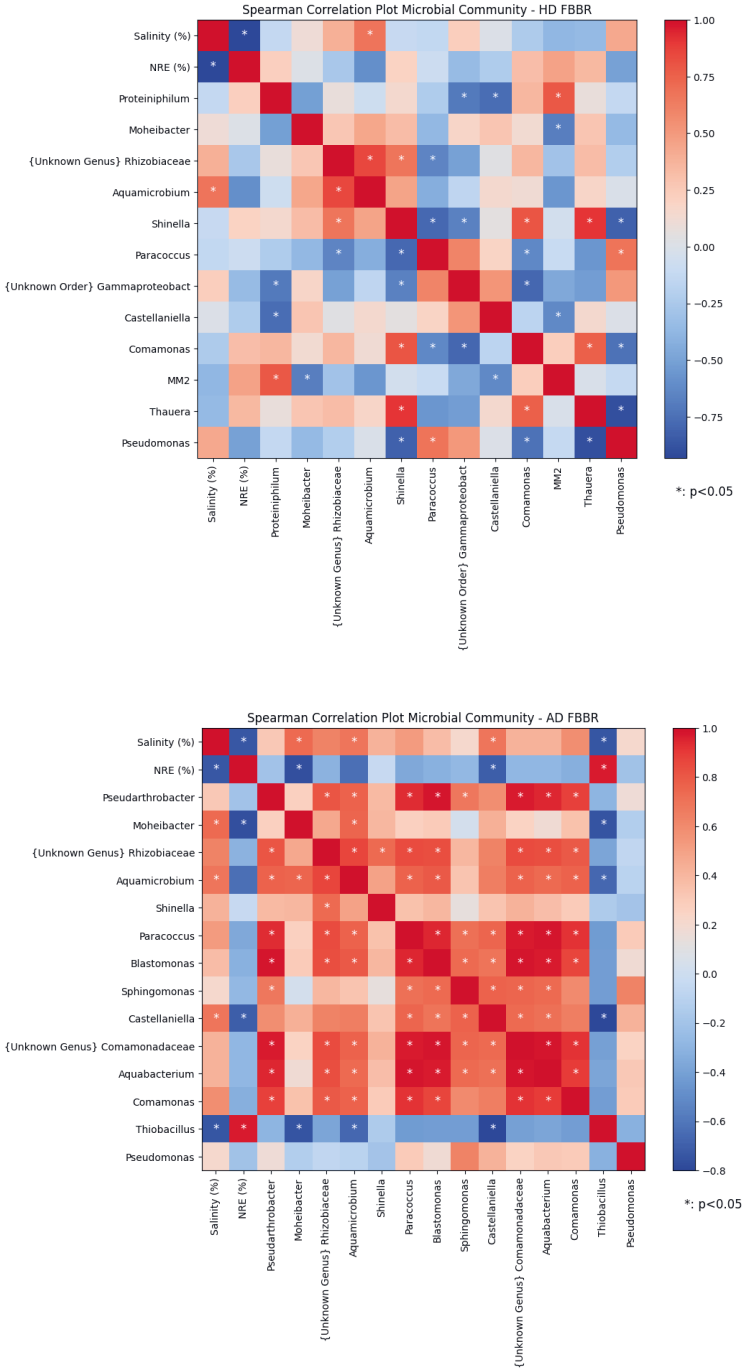

Figure S10. Correlation plots between microbial community at genus level, salinity and nitrate removal efficiency (NRE) in heterotrophic (HD) and autotrophic (AD) fluidized bed bioreactors (FBBR).

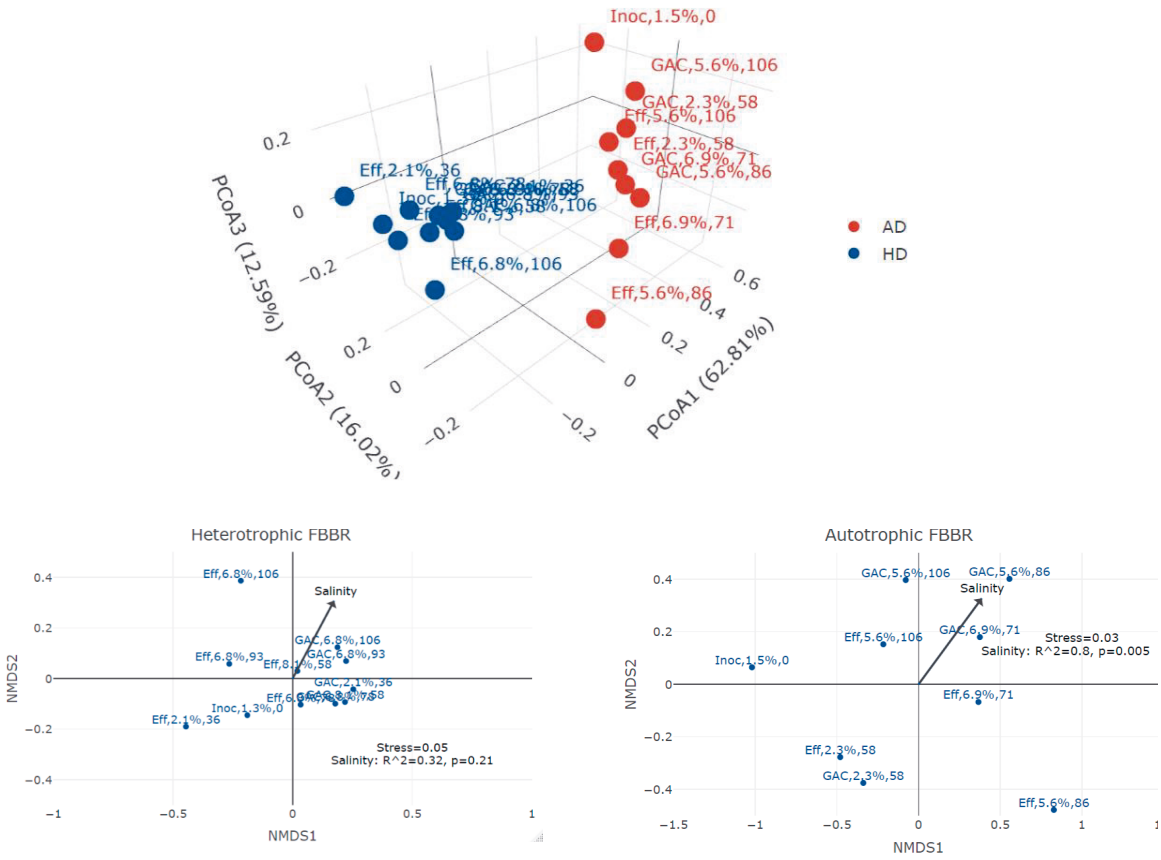

Figure S11. PCoA and nMDS analyses for microbial community relative abundance data at genus level for heterotrophic (HD) and autotrophic (AD) fluidized bed bioreactors (FBBR), by using Bray-Curtis distance method. Each point is described by source of the sample (GAC or Effluent), Salinity %, and Day of the sampling.

Figure S12. Picture of whitish substance spotted on the granular activated carbon (GAC) bed in the heterotrophic fluidized bed bioreactor during PHASE IV+FC that could possibly represent elemental sulphur.

Two step denitrification reactions from nitrate to nitrite and from nitrite to nitrogen gas, for thiosulphate driven autotrophic (eq. S1a and S1b [9]) and methanol driven heterotrophic (eq. S2a, S2b and S2c [10]) denitrification:

$S_2O_3^{2-} + 3.10NO_3^- + 0.73H_2O + 0.45HCO_3^- + 0.09NH_4^+$

$\rightarrow 0.09C_5H_7O_2N + 3.\ 10NO_2^- + 1.64H^+ + 2SO_4^{2-}$ (eq. S1a)

$S_2O_3^{2-} + 2.07NO_2^- + 0.43H^+ + 0.45HCO_3^- + 0.09NH_4^+$

$\rightarrow 0.09C_5H_7O_2N + 1.03N_2 + 0.30H_2O + 2SO_4^{2-}$ (eq. S1b)

$2CH_3OH + 6NO_3^- \rightarrow 6NO_2^- + 2CO_2 + 4H_2O$ (eq S2a)

$3CH_3OH + 6NO_2^- \rightarrow 3N_2 + 3CO_2 + 3H_2O + 6OH^-$ (eq S2b)

Overall, with biomass production:

$1.08\ CH_3OH + NO_3^- + H^+$

$\rightarrow 0.065\ C_5H_7O_2N + 0.468\ N_2 + 0.76\ CO_2 + 2.44\ H_2O$ (eq S2c)

REFERENCES

[1] E. Davoli, M.L. Gangai, L. Morselli, D. Tonelli, Characterisation of odorants emissions from landfills by SPME and GC/MS, Chemosphere 51 (2003) 357–368. https://doi.org/10.1016/S0045-6535(02)00845-7.

[2] C. Wunder, W. Pogoda, A. Paulke, S.W. Toennes, Assay of ethanol and congener alcohols in serum and beverages by headspace gas chromatography/mass spectrometry, MethodsX 8 (2021) 101563. https://doi.org/10.1016/j.mex.2021.101563.

[3] A. D'Aquino, N. Kalinainen, H. Auvinen, G. Andreottola, J.A. Puhakka, M.R.T. Palmroth, Effects of inorganic ions on autotrophic denitrification by *Thiobacillus denitrificans* and on heterotrophic denitrification by an enrichment culture, Sci. Tot. Environ. 901 (2023) 165940. https://doi.org/10.1016/j.scitotenv.2023.165940.

[4] W. Gu, L. Wang, Y. Liu, P. Liang, X. Zhang, Y. Li, X. Huang, Anammox bacteria enrichment and denitrification in moving bed biofilm reactors packed with different buoyant carriers: Performances and mechanisms, Sci. Tot. Environ. 719 (2020) 137277. https://doi.org/10.1016/j.scitotenv.2020.137277.

[5] K. Vrede, M. Heldal, S. Norland, G. Bratbak, Elemental Composition (C, N, P) and Cell Volume of Exponentially Growing and Nutrient-Limited Bacterioplankton, Appl. Environ. Microb. 68 (2002) 2965–2971. https://doi.org/10.1128/AEM.68.6.2965-2971.2002.

[6] K. Fagerbakke, M. Heldal, S. Norland, Content of carbon, nitrogen, oxygen, sulfur and phosphorus in native aquatic and cultured bacteria, Aquat. Microb. Ecol. 10 (1996) 15–27. https://doi.org/10.3354/ame010015.

[7] F.C. Neidhardt, ed., *Escherichia coli* and *Salmonella*: cellular and molecular biology, 2nd ed, ASM Press, Washington, D.C, 1996.

[8] A. Sanz-Jiménez, O. Malvar, J.J. Ruz, S. García-López, P.M. Kosaka, E. Gil-Santos, Á. Cano, D. Papanastasiou, D. Kounadis, J. Mingorance, Á.S. Paulo, M. Calleja, J. Tamayo, High-throughput determination of dry mass of single bacterial cells by ultrathin membrane resonators, Commun. Biol. 5 (2022) 1–10. https://doi.org/10.1038/s42003-022-04147-5.

[9] M. Mora, A. Guisasola, X. Gamisans, D. Gabriel, Examining thiosulfate-driven autotrophic denitrification through respirometry, Chemosphere 113 (2014) 1-8, https://doi.org/10.1016/j.chemosphere.2014.03.083.

[10] F. Rezvani, M.H. Sarrafzadeh, S. Ebrahimi, H.M. Oh, Nitrate removal from drinking water with a focus on biological methods: a review. Environ Sci Pollut Res 26 (2019) 1124-1141, https://doi.org/10.1007/s11356-017-9185-0

PUBLICATION III

Inhibition-level-based carrier selection and kinetic insights for optimised denitrification of saline wastewaters in MBBR

Alessio D'Aquino, Marja Tiirola, Jaakko A. Puhakka, Marja R.T. Palmroth and Gianni Andreottola

Journal of Environmental Management, 394 (2025), 127288
https://doi.org/10.1016/j.jenvman.2025.127288

Journal of Environmental Management 394 (2025) 127288

Contents lists available at ScienceDirect

Journal of Environmental Management

journal homepage: www.elsevier.com/locate/jenvman

Research article

Inhibition-level-based carrier selection and kinetic insights for optimised denitrification of saline wastewaters in MBBR

Alessio D'Aquino [a,b,*], Marja Tiirola [c], Jaakko A. Puhakka [a], Marja R.T. Palmroth [a], Gianni Andreottola [b]

[a] Tampere University, Faculty of Engineering and Natural Sciences, Korkeakoulunkatu 8, P.O. Box 541, 33014, Tampere, Finland
[b] University of Trento, Department of Civil, Environmental and Mechanical Engineering, via Mesiano 77, 38123, Trento, Italy
[c] University of Jyväskylä, Department of Biological and Environmental Sciences, NanoScience Center, Survontie 9C, P.O. Box 35, 40014, Jyväskylä, Finland

ARTICLE INFO

Keywords:
Biofilm
Biological nitrate removal
Bioprocess modelling
Industrial wastewater treatment
Salinity stress
Scrubber wastewater

ABSTRACT

The moving bed biofilm reactor (MBBR) provides a high-rate treatment process for the denitrification of saline industrial wastewaters. The carrier structure regulates the biofilm-liquid contact area and can limit the biofilm exposure not only to substrate but also to inhibitors and thus, affects the process performance. However, the potential for biofilms on different carriers to perform differentially under varying salinities remains unexplored as MBBR optimisation strategy. In this study, the nitrogen removal kinetics and biofilm dynamics of methanol-driven denitrification in two MBBRs with a hollow-body and a porous-body carrier were systematically analysed to assess their best performance at salinities 1–9.5 %. Between 1 and 7.5 % salinity, both MBBRs removed over 90 % nitrogen, with the more exposed biofilm in the hollows resulting in higher removal rates. At 9.5 % salinity, the protected biofilm within the pores resulted in a more stable removal (89.5 ± 1.6 %) than in the more exposed hollows (80.9 ± 6.5 %). In both MBBRs, stable and similar denitrifying communities developed, dominated by *Paracoccus*, *Methylovorus* and *Hyphomicrobium*. Moreover, hypersaline (>3.5 %) wastewater from pulp mill NO_x-SO_2 scrubber was successfully denitrified in MBBRs, showing the potential of biofilm processes for its treatment. Eventually, denitrification kinetics under salinity inhibition in the biofilm was modelled for both carriers by introducing an inhibition factor to the existing Sumo©22 biofilm model. In summary, this study provides the basis for optimising saline industrial wastewater treatment in MBBR through selecting the typology of biofilm carrier based on the inhibition level and for predicting the biofilm process performance with a simplified modelling approach.

1. Introduction

Inhibition by salinity poses a challenge for the biological treatment of many industrial wastewaters, where salt concentration can commonly reach 15 %, given by different inorganic ions (Cl^-, Na^+, SO_4^{2-}, K^+ etc.) (Chen et al., 2024; Panagopoulos, 2022). For example, the wet flue gas scrubbing process generates saline wastewaters rich in NO_x^- and heavy metals (Gingerich et al., 2018). To avoid detrimental effects on the environment and on human health, heavy metals are usually removed via physical-chemical processes (Gingerich et al., 2018), while other dissolved pollutants need specific treatments, such as denitrification for NO_x^- removal.

Bioprocess design and selection are essential to optimise denitrification tolerance against salinity inhibition. Among the reactors, the moving bed biofilm reactor (MBBR), a compact and flexible technology for a high-rate and stable process (Ødegaard, 2006), has been widely used under salinity stress, such as for nitrification (Shitu et al., 2021) and denitrification (Dupla et al., 2006), showing its higher performance than suspended biomass bioreactors also for chemical oxygen demand removal (COD) (Hasanzadeh et al., 2020). To date, possible solutions for its further optimisation have included bioaugmentation with halophiles (Xiang et al., 2023) or enrichment of salt tolerant microorganisms via different startup procedures (Li et al., 2019; Navada et al., 2019). Furthermore, the inhibition-based-selection of the MBBR biofilm carrier would represent a novel and easily implementable optimisation strategy.

The carriers' shape and surface properties and the consequent growing biofilm's thickness and exposed area contribute to the MBBR

* Corresponding author. Tampere University, Faculty of Engineering and Natural Sciences, Korkeakoulunkatu 8, P.O. Box 541, 33014, Tampere, Finland.
E-mail address: alessio.daquino@tuni.fi (A. D'Aquino).

https://doi.org/10.1016/j.jenvman.2025.127288
Received 19 June 2025; Received in revised form 25 August 2025; Accepted 7 September 2025

performance, regulating for example mass transfer processes (Morgan-Sagastume, 2018). Thus, carrier selection plays a key role in the treatment optimisation not only for the specific bioprocess, but also for protection of the forming biofilm against inhibition. Current knowledge about the optimal carrier choice under inhibitory saline conditions remains limited. Different commercial biofilm carriers have been compared for nitrogen removal (Dupla et al., 2006; Tadda et al., 2021; Zan et al., 2022) at constant salinity up to 3 %, while modified sponge biocarriers (ferrous oxalate + activated carbon) have shown improved nitrification performance at salinities up to 3.5 % (Shitu et al., 2021). Thus, according to the state-of-the-art, the carrier selection under saline conditions does not take into account the inhibitor's concentration and would be limited to the best observed removal performance in a salinity range 1–3.5 %. However, many industrial wastewaters are hypersaline (>3.5 %). Moreover, the biofilm exposure to the liquid phase affects not only the mass transfer of substrate, but also that of the inhibitory ions, possibly resulting in carrier-specific optimal performance-salinity ranges. Therefore, the so far unexplored strategy of selecting the carrier based on the salinity concentration needs to be studied as a novel optimisation approach.

Similarly, little is known about salinity inhibition kinetics in biofilms, which is essential for biological models used for the optimisation of bioprocesses (Rittmann et al., 2018). Salinity inhibition on sludge has been modelled with different functions (e.g., Hill's), correlating salt concentration and removal rates (Lin et al., 2021; Mariángel et al., 2008), while only few studies have implemented the inhibitory function in dynamic biological models for activated granular sludge (Carrera et al., 2023) and activated sludge (Zuo et al., 2021). On the contrary, salt inhibition kinetics for biofilm-based reactors has not been reported, often requiring complex models that should consider salt gradients and precipitation and different inhibitory levels along the biofilm depth. Thus, simplified approaches, for example based on the whole reactor bulk phase parameters (Plattes et al., 2006; Wang et al., 2016) that implicitly incorporate diffusion phenomena, could facilitate also salinity inhibition modelling. Moreover, the differences resulting from different biofilm carrier types have not been considered in modelling.

Furthermore, denitrification studies on flue gas wet scrubbing wastewaters have mainly focused on flue gas desulphurisation (FGD) scrubber effluent (Koenig and Liu, 2004; Vredenbregt et al., 1997). The potential of biological nitrogen removal for NO_x-SO_2 scrubber wastewaters, whose composition and process-inhibition differ from the FGD due to the different chemicals used during the scrubbing process (Johansson et al., 2021), needs further investigation. Thus, MBBR could provide a robust technology to improve the process inhibition tolerance.

In this study, optimisation of the MBBR via carrier selection based on the salinity level was explored with a systematic analysis between a hollow-body and a porous-body plastic carrier at salinities up to 9.5 %, using a denitrifying mixed-culture originating from a municipal wastewater treatment plant (MWWTP). Methanol-driven denitrification performance was studied in terms of nitrogen removal performance, biofilm dynamics and microbial community changes, to identify the carrier-specific best performance-salinity ranges. A strategy to model salinity inhibition kinetics by the denitrifying biofilm is proposed, by adding an apparent inhibition factor in Sumo©22 MBBR model and comparing it for the two different carriers. Moreover, the potential of MBBR for the denitrification of real wastewater from a NO_x-SO_2 wet scrubber in pulp mills was investigated.

2. Materials and methods

2.1. MBBR in continuous operation

The reactor system (Fig. S1) consisted of a 3 L (working volume 2.5 L) cylindrical jacketed glass MBBR (Artiglass, Italy) with a sealing cap system (Officine Parisi srl, Italy), a peristaltic pump (Golander, Germany) regulating in/outflows, a mechanical overhead stirrer (Velp, Italy) regulated at 70–140 rpm to keep the carriers mixed by a polyethylene-coated blade, and a thermostatic water bath (Julabo, US) connected to the jacket of the MBBR, controlling its temperature at 30 °C.

The biofilm carriers tested included hollow body disk-shaped AnoxK™ 5 (Veolia Water Technologies-AnoxKaldnes, Sweden) with a protected surface area (PSA) of 800 m^2/m^3, here referred to as K5, and porous paraboloid-shaped Mutag BioChip 30™ (Mutag, Denmark) with a PSA of 5500 m^2/m^3, called M30 (Table S2). A 25 % filling fraction was used with both carriers, corresponding to 191 K5 and 285 M30 pieces. Their denitrification performance was evaluated in continuously fed MBBRs (K5-MBBR and M30-MBBR), by gradually increasing salinity and nitrogen loading rate (NLR).

Both MBBRs were inoculated with a mixed culture originated from the denitrification compartment of a MWWTP (Lavis, Italy). The microbial culture was regularly maintained according to D'Aquino et al. (2023) before inoculation. The MBBRs startup consisted of five weeks semi-batch operation to allow biofilm formation, followed by continuous mode. A nitrogen-laden multi-ionic saline industrial wastewater (Panagopoulos, 2022) fed to the MBBRs was simulated in tap water with 0.225 gNO_3-N/L (as KNO_3), 4 gPO_4^{3-}/L (as K_2HPO_4 and KH_2PO_4), used also as pH buffer, while the salinity was controlled by KCl and Na_2SO_4. Ammonium (0.03 gNH_4^+-N/L as $(NH_4)_2SO_4$) and iron(II) (0.002 g/L $FeSO_4{\cdot}7H_2O$) were added to support microbial activity. Salinity was increased gradually to 9.5 % and increasing NLRs were tested by decreasing hydraulic retention time (HRT) (Table 1). Methanol was added in excess as electron donor (C/N = 1.3 g/g). Before being fed to the reactor, the simulated wastewater was purged with N_2 gas until dissolved oxygen was <1 mg/L.

The performance of MBBRs was monitored by sampling the influent and effluent every 24–72 h. The biofilm and suspended biomass were sampled weekly, at the end of each salinity or NLR condition.

2.2. Denitrification of real NO_x-SO_2 scrubber wastewaters in MBBRs

Two jacketed (working volume 1.5 L) MBBRs were used in semi-batch mode to test denitrification of real scrubber wastewater (Fig. S1) with K5 and M30 carriers, colonised with biofilm as in Section 2.1, at 25 % filling fraction and moved by a magnetic stirrer. Temperature control and purging with N_2 were similar to Section 2.1.

The wastewaters, whose composition is reported in Table S5, were collected from the three stages of a wet scrubber removing NO_x-SO_2 from flue gases generated by recovery boilers in a pulp mill, where the process chemicals include NaOH, ClO_2 and S-compounds. Methanol was chosen as electron donor given its availability in pulp mills (D'Aquino et al., 2024).

The test began with simulated wastewater (Section 2.1) without salinity addition and containing approximately 500 mg/L NO_3^- and was then extended to real wastewaters. Since gradual exposure to inhibitors such as salinity is beneficial for biological processes (Li et al., 2019), the first wastewater tested was the least concentrated (stage III), followed by stage I and, finally, the most concentrated one (stage II), revealing also

Table 1
Salinity, osmotic pressure (OP) and hydraulic retention time (HRT) conditions tested with both K5 and M30 carriers. OP was calculated as in Fritzmann et al. (2007).

Total Salinity (%)	Ions (g/L)				Total OP (atm)	HRTs (h)
	Na^+	Cl^-	SO_4^{2-}	K^+		
1[a]	<0.1	<0.1	0.3	3.3	3.8	12
2.7	5.0	1.0	10.7	4.4	13.3	12
5.5	12.5	3.0	26.4	6.6	28.3	12–4
7.5	17.5	5.0	36.8	8.8	39.2	10–7
9.5	22.5	7.5	47.2	11.5	50.8	10–4

[a] Base salinity in the simulated wastewater.

the different inhibitory levels of the three streams. Between the stage I and stage II tests, the MBBRs were filled with the simulated wastewater to verify the denitrifying activity of the biofilms. For each wastewater tested, denitrification was monitored by pH measurement, and nitrate together with methanol (C/N: 1.3 g/g) were re-supplemented to the reactors to verify nitrogen removal. Then, the wastewater was replaced with the next one via pumps, while the carriers stayed in the reactors. The liquid phase was sampled to monitor NO_x^- removal and dissolved organic carbon (DOC) consumption, while carrier samples (5 pieces) were taken at the beginning of the test (day 6) and at the end (day 66) to measure the total attached solids.

2.3. Specific nitrogen uptake rate tests and salinity inhibition function

Specific nitrogen uptake rate (NUR) test was performed at each salinity concentration for the MBBRs in continuous operations fed with simulated wastewater (K5 and M30). The feeding of the reactor was temporarily stopped, NO_3^--N and methanol in excess were supplemented to the MBBR, and NO_3^--N and NO_2^--N concentrations in the liquid monitored. Then, linear regression was used to calculate the volumetric nitrogen uptake rate (Bassin et al., 2016), which was divided by the total volatile solids' mass (paragraph 2.4.2) (attached + suspended) to obtain the specific denitrification rate DR (mgN/gVS/h) of the whole MBBR at each salinity level.

Salinity inhibition on the DR was assumed to follow the modified non-competitive Hill inhibition function (eq. (1)), as for sludge flocs (Lin et al., 2021; Zuo et al., 2021) and granules (Carrera et al., 2023):

$$DR(mgN/gVS/h) = DR_{max} \cdot \frac{K_I^n}{K_I^n + I^n} \quad \text{(eq. 1)}$$

where DR_{max} is the maximum specific rate (mgN/gVS/h) under non-inhibitory conditions, K_I (=IC_{50}) is the half-inhibition constant (g/L), I is the salt concentration (g/L) and n is the tuning parameter. The function was fitted to the experimental data to find K_I and n in Origin2024b, separately for K5-MBBR and M30-MBBR. Simultaneously to the MBBR NUR tests, nitrogen uptake activity of suspended biomass was measured in batch test (Fig. S3).

2.4. Modelling of MBBR denitrification kinetics under salt inhibition

Time-dependent kinetics of denitrification in MBBR under salt inhibition were modelled in SUMO©22 (Dynamita, France) for K5-MBBR and M30-MBBR. Each MBBR NUR test was simulated with "Sumo 4N", a 4-step denitrification model, for the MBBR biofilm model, where only methanol driven denitrification process was considered. Existing key differential equations were modified to implement the salinity inhibition factor (eq. (1)), resulting in the following expressions for nitrite (eq. (2)) and nitrate concentration (mgN/L) variation in time (eq. (3)):

$$\frac{d(NO_2^-)}{dt} = -\frac{(1\text{-}Y)}{Y \cdot f_{COD,1}} \left(\mu_T \cdot X \cdot \frac{NO_2^-}{K_{NO2} + NO_2^-} \right) - \frac{d(NO_3^-)}{dt} \quad \text{(eq. 2)}$$

$$\frac{d(NO_3^-)}{dt} = -\frac{(1\text{-}Y)}{Y \cdot f_{COD,2}} \left(\mu_{S\text{-}inhib} \cdot X \cdot \frac{NO_3^-}{K_{NO3} + NO_3^-} \cdot \frac{K_{NO2}}{K_{NO2} + NO_2^-} \right) \quad \text{(eq. 3)}$$

$$\text{with } \mu_{S\text{-}inhib} = \mu_T \cdot \frac{K_I^n}{K_I^n + I^n}$$

where μ_T (1/d) is the specific growth rate, X (gCOD/L) is the active biomass, $f_{COD,1}$ and $f_{COD,2}$ are COD-N conversion coefficients for biomass yield (Y), K_{NO3} and K_{NO2} (mgN/L) are the half-saturation constants for nitrate and nitrite, respectively. Salinity inhibition is accounted for with $\mu_{S\text{-}inhib}$, with parameters (K_I and n) changed based on the MBBR tested, while I (salinity concentration) was a new input parameter. Kinetic parameters, biofilm thickness (L), specific surface area (SSA) and other parameters were determined as explained in the supplementary materials (Fig. S9, Tables S3 and S4).

Sensitivity analysis was performed to assess the influence of the model's input parameters (L, SSA, K_I and n) on the output DR, at salinity of 2.7 % and 9.5 %, by varying up to ±50 % their initial estimated/calibrated values at steps of 10 %. μ_T and Y were also considered in the analysis to compare their influence with the abovementioned parameters. To evaluate the model sensitivity for each parameter, the normalised sensitivity coefficient (S) was calculated as in Eldyasti et al. (2012) (eq. S4) for the whole variation range. If $S \leq 0.25$, the parameter was considered not significantly influential, else it was considered influential. The goodness of the model in reproducing the experimental data was evaluated using Thiel's inequality coefficient (TIC), as done by Lanzetta et al. (2024), and coefficient of determination (R^2) as criteria. Values of TIC<0.3 indicated a good reproducibility. To verify the consistency of the model under different biofilm conditions, each salinity level was simulated under the initial conditions of each NUR test, by modifying I and calibrated K_{NO2}, accordingly.

2.5. Analytical methods

2.5.1. Dissolved nitrogen and carbon measurements

Liquid samples were filtered through 0.2 μm Chromafil Xtra syringe filter (Macherey-Nagel, Germany) and stored at −20 °C. NO_3^--N, NO_2^--N and NH_4^+-N were measured with Hach cuvette tests (LCK339, LCK340, LCK343 and LCK303) and DR 3900 spectrophotometer (Zhai et al., 2020) for the continuous flow MBBR experiment, while for the real scrubber wastewater test, NO_3^- and NO_2^- were measured with ion chromatography (Dionex Integrion, Thermo Fisher Scientific Inc., USA). DOC was measured with TOC/TN analyser (FORMACS™ HT-I, Model 2CA17910, Skalar, Netherlands).

2.5.2. Biomass measurement and biofilm observations

In the MBBR, biofilm biomass was measured as attached volatile solids (AVS). Every time, three K5 pieces and five M30 pieces were taken randomly from the MBBR and replaced with new ones. For K5, the carriers were brushed and rinsed with MQ-water and the resulting solutions were measured for attached total solids (ATS) and attached volatile solids (AVS) according to standard methods (APHA, 2017). For M30, given the porous nature of the carrier, some steps (sonication and brushing) were added to the protocol suggested by the supplier to determine AVS and ATS, according to the procedure described in Fig. S5. Total and volatile suspended solids (TSS, VSS) were measured according to standard methods (APHA, 2017).

The biofilm attached to the carriers was observed with optical microscopy (Biostar BM 45, Optech, UK) with Plan 40x/0.65 objective and the biofilm thickness was measured with the software ToupView (ToupTek, China).

2.6. Calculations and removal kinetics

To compare the performance of K5-MBBR and M30-MBBR based on the available surface for the biofilm, nitrogen surface removal rates (NSRR) were calculated as (di Biase et al., 2018):

$$NSRR\ (gNO_x^-\text{-}N/m^2/d) = \frac{Q_{in} \cdot \left(NO_x^-\text{-}N_{inf} - NO_x^-\text{-}N_{eff} \right)}{V_{MBBR} \cdot f \cdot PSA} \quad \text{(eq. 4)}$$

where the nitrogen volumetric removal rate (NVRR) is divided by the filling fraction of the MBBR with the carrier (f), and PSA (m^2/m^3), the protected surface area proper to the carrier.

Statistical significance ($\alpha = 0.05$) of the difference in the nitrogen removal efficiency (NRE) of MBBRs was assessed with Mann-Whitney *U* test. Modified Stover-Kincannon (S-K) equation was fitted to the

experimental data at different salinities and HRTs, similarly to D'Aquino et al. (2024), to compare the volumetric removal rate performance of the MBBR in continuous flow filled with different carriers. The modified S-K model has been used for MBBR (Shitu et al., 2020) and is independent on carrier's surface area as shown in its linearised form (eq. (5)):

$$\frac{HRT}{N_{in}\text{-}N_{out}} = \frac{K_B}{U_{max}}\frac{HRT}{N_{in}} + \frac{1}{U_{max}} \quad \text{(eq. 5)}$$

where the HRT is expressed as volume of the reactor over inflow, and U_{max} and K_B are the maximum nitrogen removal rate (gNO_x^--N/L/d) and saturation constant (gNO_x^--N/L/d), respectively.

To quantify the biofilm detachment, a detachment/attachment index ($\Delta_{biofilm}$) was calculated in terms of AVS detached or attached between two consecutive AVS measurements in time (eq. (6)):

$$\Delta_{biofilm}\ (gAVS/m^2 \text{ or } gAVS/carrier) = gAVS_t - gAVS_{t\text{-}1} \quad \text{(eq. 6)}$$

where $\Delta_{biofilm} < 0$ when biofilm detachment took place.

2.7. Microbial community analysis

To observe the evolution of the microbial community under salinity stress, two carriers and 14 mL liquid were sampled on days 7, 28, 46, 63, 77 for K5-MBBR and on days 7, 14, 32, 49, 60 for M30-MBBR, before increasing the salinity level. The biofilm was manually detached from the carriers aseptically, while in the liquid samples, the cell pellet was separated via centrifugation. Both typologies of samples were stored in DNA/RNA shield solution (Zymo, USA), before DNA extraction and 16S rRNA gene sequencing. The community data was analysed with principal coordinate analysis (PCoA), permutational multivariate analysis of variance (PERMANOVA) and Spearman correlation. The detailed procedure is reported in D'Aquino et (2024).

3. Results and discussion

3.1. MBBRs denitrification performance under hypersaline conditions

3.1.1. Nitrogen removal efficiency

The nitrogen removal performance of the K5-MBBR and M30-MBBR was studied at stepwise increasing salt concentrations and at different HRTs (Fig. 1a).

Between 1 % and 5.5 % salinity, the NREs of the two MBBRs were 98 ± 1 % and not significantly different ($p > 0.05$). At the lowest tested HRT (4 h) and 5.5 % salinity, NRE was 97.7 ± 0.1 % for K5-MBBR and 96.4 ± 1 % for M30-MBBR, with volumetric nitrogen removal rate and surface removal rate 1.2 and 9 times higher in K5-MBBR (7.9 ± 0.6 gN/m^2/d, 1.6 ± 0.1 gN/L_{MBBR}/d) than in M30-MBBR (Fig. 1b and c).

Increasing salinity up to 7.5 % caused temporary nitrate and nitrite accumulation in K5-MBBR (24 mgNO_x^--N/L) and M30-MBBR (55 mgNO_x^--N/L) effluents. M30-MBBR recovered its NRE to 99 % in one day, while nine days were required for K5-MBBR to recover. Overall, NRE were significantly different ($p = 0.01$) at 7.5 % salinity, the highest NVRR were similar (~0.8 gN/L_{MBBR}/d), while NSRR was 6.5 times higher for K5-MBBR.

At 9.5 % salinity, both MBBRs were affected by inhibition as shown by the decrease in NRE, which was significantly different ($p = 0.02$) between the reactors and higher for the M30-MBBR. In M30-MBBR, nitrate and nitrite accumulated (day 50) when salinity was increased, but NRE was fully recovered, contrarily to K5-MBBR, where NRE recovery was not total. When HRT was decreased to 4 h, NRE decreased to 80.9 ± 6.5 % and 89.5 ± 1.6 % in the K5-MBBR and M30-MBBR, respectively. Eventually, when HRT was increased to 7 h, both MBBRs partially recovered in less than three days, as shown by NRE (Fig. 1b). Moreover, increased salinity did not impact DOC and NH_4^+ consumption in MBBRs (Fig. S2).

The U_{max} (gN/L/d) estimated with S-K model (Fig. 2) was higher for K5-MBBR than for M30-MBBR (58.5 ± 15 vs. 31.2 ± 8.7) at 5.5 %

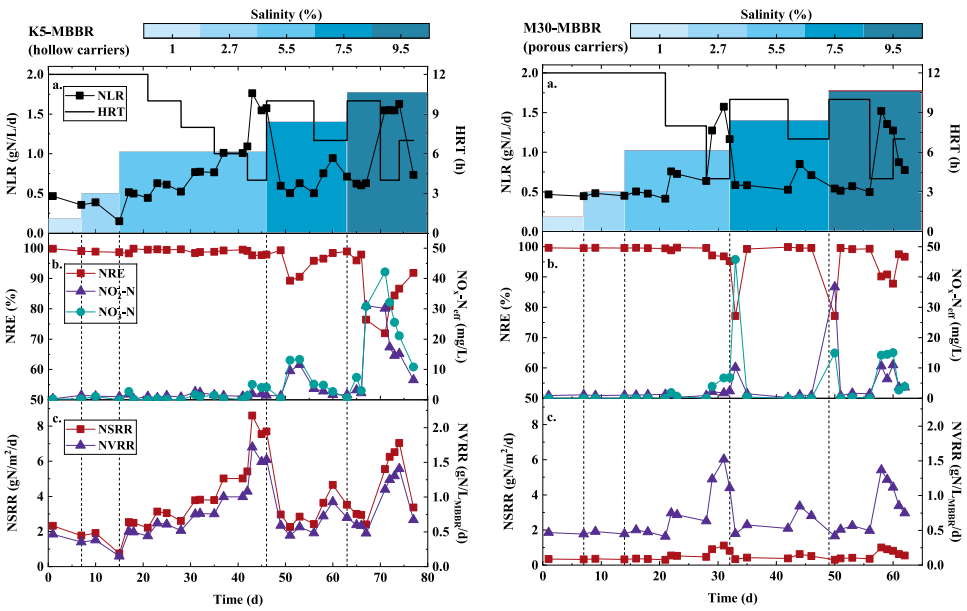

Fig. 1. K5-MBBR (left) and M30-MBBR (right) nitrogen removal performance at increasing salinity. a.) Nitrogen Loading Rate (NLR), salinity and Hydraulic Retention Time (HRT) conditions; b.) Nitrogen Removal Efficiency (NRE) and effluent nitrate and nitrite nitrogen concentrations; c.) Nitrogen Surface Removal Rate (NSRR) and Nitrogen Volumetric Removal Rate (NVRR).

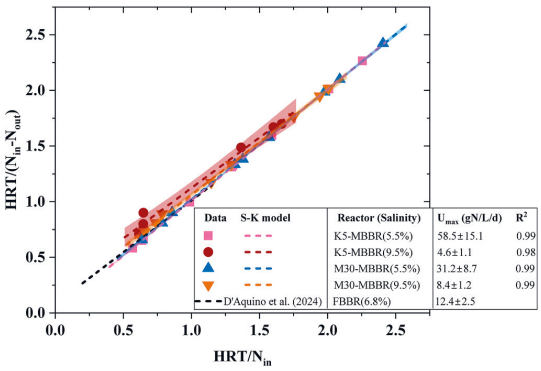

Fig. 2. Fitting of volumetric nitrogen load experimental data with Stover-Kincannon model (dotted lines) for K5-MBBR and M30-MBBR at 5.5 % and 9.5 % salinity. Coloured areas represent upper and lower 95 % confidence intervals for each data set.

salinity, indicating a higher removal rate potential in K5-MBBR. At 9.5 % salinity, U_{max} decreased in both reactors due to salinity inhibition, but was higher in M30-MBBR (8.4 ± 1.2) than in K5-MBBR (4.6 ± 1.1), indicating that K5-MBBR denitrification capacity was more affected by the high salinity.

In the range 1–7.5 % salinity both MBBRs maintained over 90 % NRE and showed prompt responses to salinity changes. Denitrification remained active even at salinity as high as 9.5 % and HRT 4 h, with NREs ≥70 %. Overall, K5-MBBR showed higher nitrogen removal rates when salinity <7.5 %, while M30-MBBR showed a higher NRE and a more stable performance at 7.5 and 9.5 % salinity. Furthermore, the increased water density due to 9.5 % salinity resulted in the carriers' movement upwards, especially in K5-MBBR. A higher density material might guarantee equal distribution of the carriers over the whole reactor volume.

Salinity of 9.5 % is, to our knowledge, one of the highest reported for methanol-driven denitrification (NRE≥70 %) in bioreactors, as summarised in Table S1, considering the non-saline history of the denitrifying community. In comparison, in our previous study in a fluidised bed bioreactor (FBBR) at salinity 8.1 %, the NRE was ≥58 % (D'Aquino et al., 2024). Such tolerance in the MBBRs may be attributed to the higher concentration and thickness of biofilms on the larger plastic carriers than on FBBR's granular activated carbon, where the thickness is controlled by high friction forces (Özkaya et al., 2019). Moreover, U_{max} of the FBBR at 6.8 % salinity was in between U_{max} of the MBBRs at 5.5 % and 9.5 % salinity (Fig. 2) demonstrating not only the decrease in the reactors' volumetric denitrification capacity with increasing salinity, but also that the MBBR provides a high-rate treatment technology for hypersaline industrial wastewaters.

3.1.2. *Biofilm dynamics*

In both MBBRs, AVS quantity increased until the end of the phase with 5.5 % salinity (Fig. 3b). The highest AVS quantity of about 10 g in both MBBRs corresponded to 10 times higher AVS density in K5-MBBR (20.2 gAVS/m^2) than M30-MBBR (2.8 gAVS/m^2). At 7.5 % and 9.5 % salinity, in both MBBRs, the biofilm was partially detached (Fig. 3b and c). In the K5-MBBR, biofilm continued detaching for three consecutive measurements, resulting in a net loss of −15.3 mgVS/carrier (around 30 % of highest value before the detachment) and −5.8 gVS/m^2 in terms of density. When comparing the data points at the same conditions in the M30-MBBR, the detachment was observed only in one measurement at 7.5 % salinity, amounting to a net loss of −7.4 mgVS/carrier (around 20 % of highest value before the detachment) and −0.9 gVS/m^2, followed by an attachment phase. Biofilm detachment due to salinity has also been reported by Wang et al. (2020) for MBBR hollow-body carriers from a MWWTP, where the biofilm coverage almost halved after 96 h at 20 g/L NaCl compared to the initial coverage under non-saline conditions.

Microscopic observations confirmed carrier-specific biofilm detachment. On the K5-MBBR carriers, the biofilm detached as regular fragments (Fig. S8) and settled on the bottom of the reactor, without increasing the effluent VSS (Fig. 3b). The detachment was not as visible in M30-MBBR carriers and likely involved mostly the biofilm layer growing on the external surface (Fig. S7).

The loss of biofilm at 7.5 % salinity did not clearly impact the NRE, suggesting that the detached biofilm fragments in K5-MBBR possibly

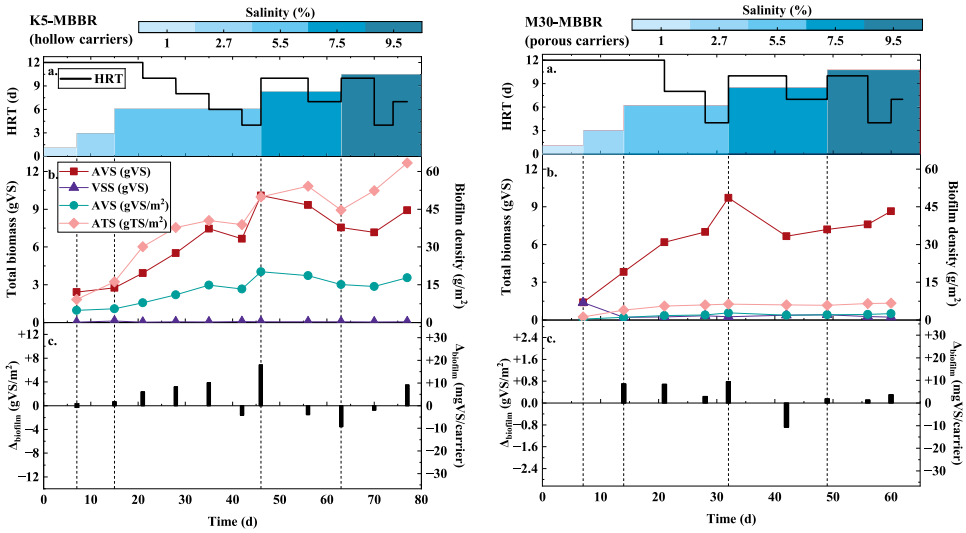

Fig. 3. K5-MBBR (left) and M30-MBBR (right) biofilm development during the reactor operation. a.) Salinity and Hydraulic Retention Time (HRT) conditions; b.) Attached Volatile Solids (AVS), Volatile Suspended Solids (VSS) and Attached Suspended solids (ATS) quantities; c.) Biofilm detachment/attachment index.

contributed to the denitrification activity (Chen and Stewart, 2000; Kragh et al., 2023; Stoodley et al., 2001). However, in-depth understanding on biofilm detachment phenomena due to salinity require further research. This should include disclosing possible mechanisms linked to a) interference (screening of surface charges) with the electrostatic binding interactions between biofilm and the plastic surface due to the dissolved salt ions (Chen and Stewart, 2000); b) variations in osmotic pressure that cause the shrinkage and expansion of the biofilm, resulting in lower resistance to shear stress (Liu et al., 2020).

The presence of large amounts of precipitates on the MBBR carriers' surface was seen as low AVS/ATS ratios during the tests (K5-MBBR: 0.32 ± 0.04 and M30-MBBR: 0.35 ± 0.04), as compared to previously reported values under non-saline conditions (0.80–0.90) (Bassin et al., 2016). Therefore, in hypersaline conditions, it is recommended to discern the AVS and ATS for biofilm quantification to avoid large biomass-overestimation. In the presence of Ca^{2+}, CO_3^{2-}, PO_4^{3-} and NH_4^+ in the liquid phase, common precipitates usually found in heterotrophic MBBRs include calcium carbonate, calcium phosphate and struvite (Gonzalez-Martinez et al., 2015; Goode and Allen, 2011). Their precipitation is mainly mediated by microbial activity that creates favourable concentration-gradient conditions (e.g., CO_2 and OH^- production) in the biofilm (biomineralisation) (Goode and Allen, 2011; Keren-Paz and Kolodkin-Gal, 2020). The formation of inorganic crystals on the biofilm-plastic contact surface should not affect denitrification rate (Dupla et al., 2006), but their role in biofilm adhesion destabilisation under hypersaline conditions remains to be determined.

Eventually, except for the first 15 days of operation when the biofilm was still forming (VSS and AVS comparable), the VSS quantity in both reactors was less than 6 % of the total volatile solids (Fig. 3b). Therefore, the suspended biomass was more exposed to salinity inhibition and the biofilm had the main role in denitrification, as also suggested by the lower denitrification activity of suspended biomass (Fig. S3).

3.1.3. Biofilm carrier selection under salinity stress

At the same filling fraction, K5-MBBR required a lower number of carriers (191) and slower mixing velocity for adequate mobility (80 rpm) than the M30-MBBR (285 carriers, 140 rpm) to obtain similar NVRR, while retaining 10 times more attached biomass per surface unit than M30-MBBR. Thus, a single carrier in K5-MBBR had higher denitrification activity than one in M30-MBBR, as also confirmed in the NUR tests for specific denitrification activity (Fig. 6).

Despite the lower PSA, a single hollow-body carrier retained a larger biofilm quantity than a porous-body one due to the carrier configuration, as also found by Bassin et al. (2016) under non-saline conditions. The large cavities provide mechanical protection from collisions with the other plastic carriers and more volume for biofilm development. On the other hand, the biofilm on the outer surface of the porous carrier is strongly subjected to collisions and higher shear stress, becoming thinner than the biofilm within the large cavities. The biofilm growing in the pores remains more protected, whilst the volume available for biofilm growth is limited.

Moreover, in K5-MBBR, due to the lower shear stress at lower mixing velocities than M30-MBBR, it could be hypothesised that the biofilm was less dense in the large cavities, resulting in higher diffusion of substrate than the biofilm growing on the outer surface of the porous-body carrier, according to the observations made by Loosdrecht et al. (1995) and Horn and Morgenroth (2006). On the other hand, the biofilm growing within the pores remains well protected from the shear stress by the surrounding plastic walls of the carrier, but also less exposed to the liquid phase. Thus, a single K5-MBBR carrier showed higher denitrification rate than a M30-MBBR carrier due to a higher biofilm quantity growing in the non-clogged large cavities that provide better contact with the liquid phase.

Similarly, the carrier configuration played a role also in the resistance to salinity. In general, the biofilm's extracellular polymeric substance (EPS) matrix protects the bacterial cells from salinity stress, for example by hindering diffusion of ions into the biofilm (Siegrist and Gujer, 1985) and by repelling Cl^- anions and adsorbing Na^+ cations (Sudmalis et al., 2020). In this study, the different biofilm structure between the two carriers likely affected also the penetration of saline inorganic ions into the biofilm. Thus, the limited exposed surface for the biofilm within the salt-diffusion controlling pores in M30-MBBR, limited the penetration not only of substrates but also of the inhibitory inorganic salt ions.

Consequently, K5-MBBR hollow carriers' large cavities enabled better biofilm exposure to the liquid phase resulting in higher denitrification rates at salinity <7.5 % (moderately inhibitory), possibly facilitated by less dense biofilm, but also higher exposure to salt ions, becoming more subjected to inhibition and biofilm detachment. Similar results were reported by Dupla et al. (2006) at low (2.8 %) salinity for a cylindrical carrier with wide openings (PSA: 185 m^2/m^3) allowing higher mass transfer than carriers with smaller cavities, reaching 90 % NRE at NSRR of 27 $gN/m^2/d$. In contrast, in M30-MBBR carriers, the biofilm within small, clogged pores was less exposed to the liquid and more protected against highly inhibitory salinities (≥7.5 %), resulting in lower mass transfer but more stable NRE. The use of porous biochip carriers has shown higher process resistance to organic shock loads (Dan and Le Luu, 2021), while this study first reports their resistance under hypersaline conditions.

3.2. Evolution and stability of microbial community in denitrifying biofilm under salinity stress

In both MBBRs, methanol driven denitrifying communities in the biofilm were similar over time, with no significant differences (R^2 = 0.11, $p = 0.06$) caused by increasing salinity. At phylum level, *Bacteroidota* (10–24 %) and *Proteobacteria* (71–90 %) dominated the reactors, while the main genera present were *Paracoccus*, *Methylovorus*, *Hyphomicrobium*, *Moheibacter* and *Proteiniphilum* (Fig. 4). When comparing samples at 1 % and 9.5 % salinity, community richness and diversity (number of genera and Simpson diversity index) decreased in both K5-MBBR and M30-MBBR (Fig. 4). At 5.5 % salinity, some genera, like *Methyloversatilis* and *Azospira* almost disappeared from the community, followed by less evident changes up to 9.5 % salinity. This was also demonstrated by PCoA and PERMANOVA analyses (Fig. 4), showing that salinity increase described to some extent (R^2~0.4, $p < 0.05$) the community changes in each reactor. However, Spearman correlation (Fig. S4) demonstrated that none of the main denitrifying genera was significantly negatively correlated with salinity increase, suggesting that the other less abundant genera were more affected by salinity and caused the main community changes. Therefore, the main selective pressure on the microbial communities was associated with 5.5 % salinity and took place in few weeks of continuous MBBR operation. The methanol-driven denitrifying communities in the reactors survived protected by the biofilm, and remained active and stable even at 9.5 % salinity, regardless of the carrier used. In the liquid phase of both MBBRs, microbial communities were not significantly different (R^2 < 0.09, $p > 0.1$) from the biofilm, showing that the liquid-phase communities originated from the carrier biomass.

Among the main genera present, *Paracoccus* and *Hyphomicrobium*, both capable of complete denitrification (Auclair et al., 2012; Nokhal and Schkegel, 1983), have been reported in methanol fed saline denitrification systems (Labbé et al., 2003; Osaka et al., 2008). Interestingly, *Methylovorus*, identified with the denitrification-capable species MM2 (Macey et al., 2018), and *Moheibacter*, a strictly aerobic microorganism, were also found in a methanol denitrifying FBBR under similar saline conditions (D'Aquino et al., 2024), despite the different origin of the biomass. Thus, based on *Moheibacter*'s metabolic capabilities reported in literature (Zhang et al., 2014), it is suggested that this non-denitrifying genus in the microbial network, likely contributed in maintaining the system anoxic for denitrification by the low-diversity community under salinity stress. Similarly, non-denitrifying *Proteiniphilum*, capable of

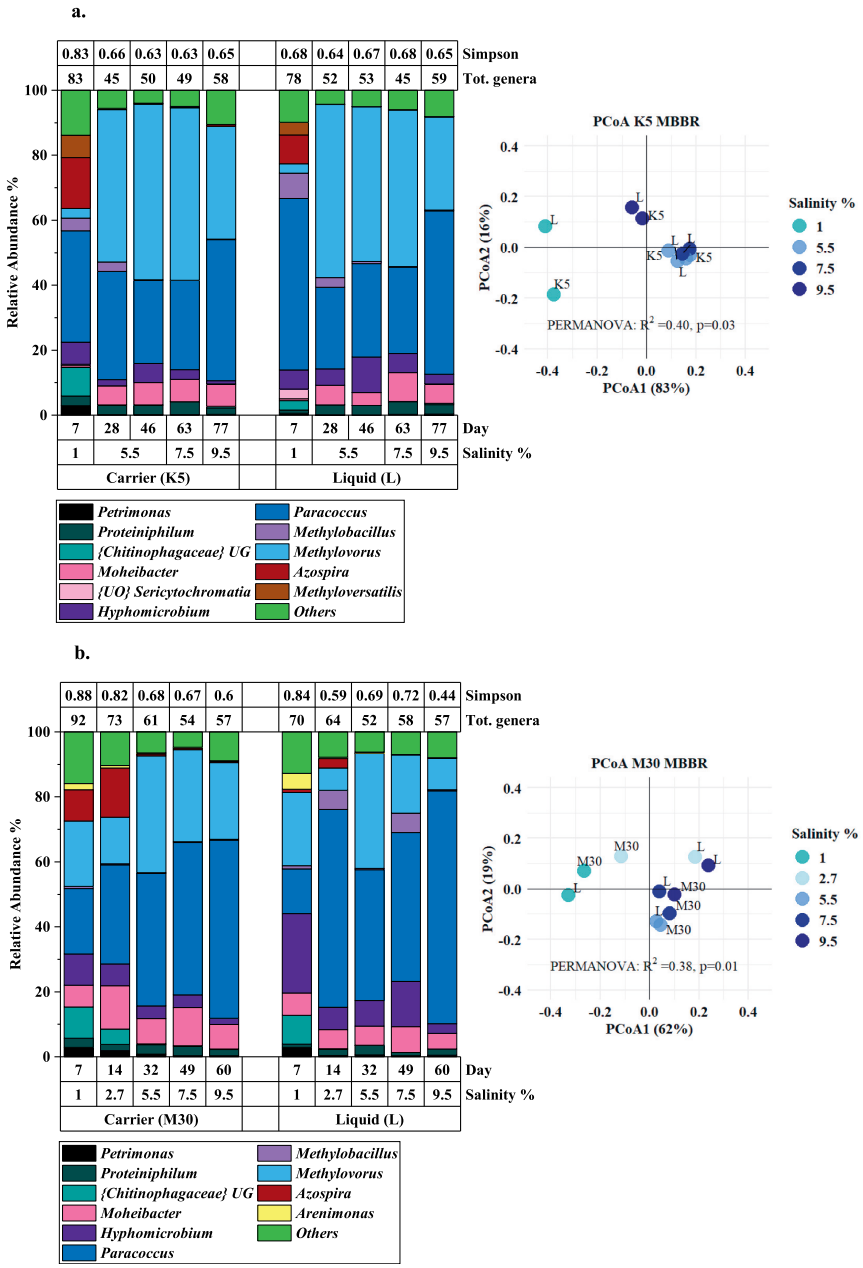

Fig. 4. Microbial community changes in the K5-MBBR (a.) and M30-MBBR (b.) at increasing salinity concentrations for both biofilm and liquid. "Others" represent the sum of single genera below 2.5 % relative abundance.

hydrolysis, fermentation and oxidation of organic compounds under inhibitory conditions (Feng et al., 2023), possibly played a role in the microbial community's stability using metabolic functions other than denitrification. Other studies have also reported the stability of methanol driven denitrifying communities under salinity stress that is likely associated with the low number of denitrifying genera capable of using methanol as electron donor (D'Aquino et al., 2024; Labbé et al., 2003; Osaka et al., 2008).

3.3. Denitrification of NO_x-SO_2 scrubber wastewater in MBBRs

Both MBBRs removed NO_x^- from NO_x-SO_2 scrubber wastewater

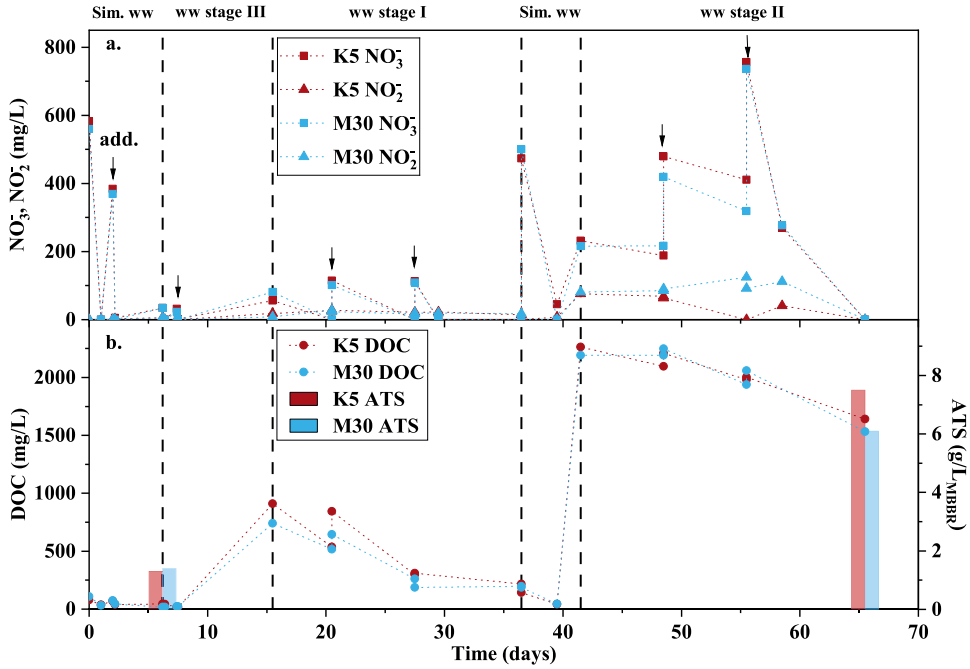

Fig. 5. Denitrification in MBBRs of real NO_x-SO_2 scrubber wastewater with hollow-body carriers (K5) and porous-body carriers (M30). a) Nitrate and nitrite concentrations in time, b) Dissolved Organic Carbon (DOC) and Attached Total Solids (ATS) concentration in time. Arrows indicate nitrate and methanol re-supplementation to the reactors.

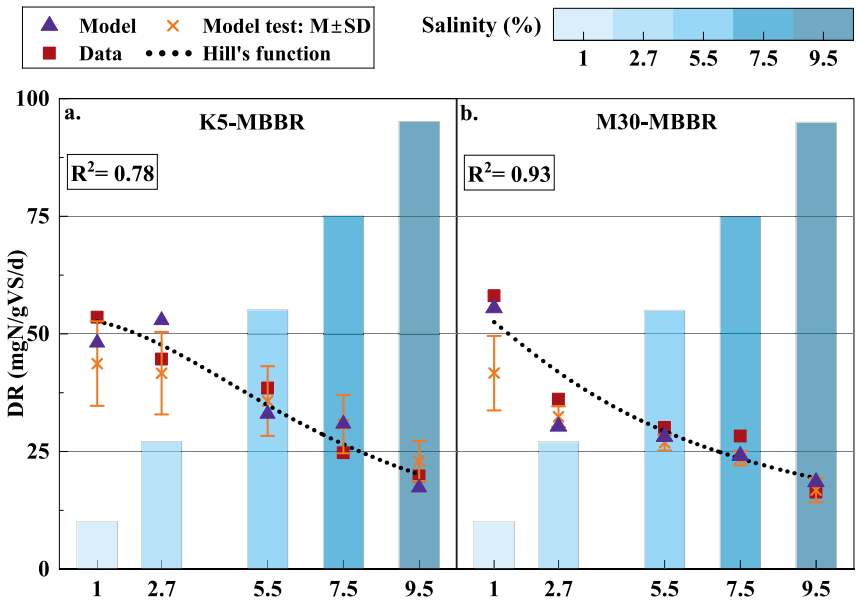

Fig. 6. MBBR kinetics modelling results: specific denitrification rate (DR) for K5-MBBR (a.) and M30-MBBR (b.). "Model" points refer to the modelling of the single NUR test. "Model test" points refer to the test of model consistency run at each biofilm condition of NUR tests under different salinities. Hill's inhibition function is fitted on "Data" points. R^2 is calculated between "Model" and "Data" points.

(Fig. 5a). With stage III and stage I wastewaters, the denitrifying biofilm was able to reduce NO_x^- within two days. With the most concentrated wastewater from stage II (1.9 Cl^-, 27 Na^+, 50 SO_4^{2-}, 0.4 K^+ g/L), inhibition was more evident and resulted in an extended lag phase (around 14 days) for denitrification, followed by NO_x^- removal. Overall, the denitrifying biofilms remained active under the inhibitory NO_x-SO_2 scrubber wastewater conditions and the ATS increased during the operation (Fig. 5b), suggesting that the biofilm was growing on the carriers.

Reports on NO_x-SO_2 scrubber wastewater denitrification are limited. In our previous work (D'Aquino et al., 2023), only wastewater from stage I of the scrubber was successfully denitrified with heterotrophic and autotrophic denitrification with suspended biomass, and the results were confirmed in this study with heterotrophic biofilms. In the wastewater from common FGD scrubbers, Cl^-, which strongly inhibits denitrification (D'Aquino et al., 2023), can reach tens of g/L and toxic metals concentrations, like Hg, Pb and Cr, can be higher than 1 mg/L (Hu et al., 2023). In comparison, the wastewater from NO_x-SO_2 flue gas scrubber in a pulp mill (Table S5) has higher concentrations of sodium and sulphate, but chloride and toxic metals (<0.05 mg/L) are less present, suggesting that the inhibition caused was mainly due to salinity and should be considered as one of the main limiting factors for the scale up and optimisation of the process. In a real treatment, stage II wastewater would account for the majority of the total NO_x-SO_2 scrubber wastewater volume and thus, the outcomes of the current study are promising for its denitrification. Moreover, the gradual exposure of the biofilm to the increasingly concentrated effluents from the different stages, as performed in this study, can represent a possible startup strategy for the MBBR. Also, the ammonium present in the wastewater could serve as nitrogen source for biomass growth, while phosphate addition and pH control are required.

The unexpectedly high concentrations of DOC in stage I and II wastewaters, likely due to the scrubbing chemicals' impurities, were partially removed in the MBBRs (Fig. 5b), as suggested by the consumed C/N molar ratio between 2.5 and 3.2 at complete denitrification (stoich. ~1.1) with stage II wastewater. Possible organic impurities include methanol, formic acid and formaldehyde, which are present in the ClO_2 production when methanol is used as reducing agent in the process (Deshwal and Lee, 2004). The presence of multiple organic compounds in the wastewater could have a positive impact on denitrification under salinity stress, as reported in the studies by Choi et al. (2025) and Zhang et al. (2020), where mixed carbon and electron sources enhanced the adaptation to salinity changes and promoted microbial diversity as compared to a single carbon and electron source.

Considering the denitrification performance under hypersaline conditions, the stability of the methylotrophic denitrifying microbial community enriched from a MWWTP, and the successful denitrification of real scrubber effluent, the MBBR technology shows promise for the management of saline wastewater from NO_x-SO_2 flue gas scrubber in pulp mills, given also its simple design. Used as a pre-denitrification step, it would reduce the nitrogen load on the downstream treatment processes, not optimised for nitrogen removal (Ashrafi et al., 2015) and form an integrated air-water technology to control NO_x emissions to the environment.

3.4. Modelling of denitrification kinetics in MBBRs: effects of salinity and carrier type

3.4.1. Salinity inhibition kinetics

Denitrification kinetics in biofilm under salinity stress was modelled by adding an apparent kinetic inhibition factor ($\mu_{S\text{-}inhib}$) and an apparent half-saturation constant (K_{NO2}) to the existing biofilm model in Sumo©22. The biofilm inhibition kinetic model reproduced well the effect of salinity on denitrification rate obtained from the NUR batch tests of both MBBRs (Fig. 6, S10), especially at salinities ≥5.5 %. At lower salinities (2.7, 5.5 %), K5-MBBR had higher DR than M30-MBBR, while at higher salinities (7.5, 9.5 %) the DR in the two reactors were similar, in accordance with the observations made previously. Nitrite accumulation, due to inhibition, was evident only under 9.5 % salinity. Thus, in almost all the NUR tests, NO_x^--N rate was mostly equal to NO_3^--N rate and no inhibition function for nitrite rate was defined. The same salinity inhibition factor has been used for both nitrate and nitrite reduction rates of granular sludge (Carrera et al., 2023), but this approach was not successful for the biofilm model. Consequently, considering that nitrate and nitrite reduction steps have different inhibition levels (Mariángel et al., 2008), the inhibition factor was applied only to nitrate consumption rate, while nitrite accumulation was controlled with K_{NO2}. This resulted in biofilm K_{NO2} values up to 220 mgN/L and a good fitting between modelled and measured NO_3^--N and NO_2^--N time profiles (Fig. S11). Under non-inhibitory conditions, apparent K_{NO2} for denitrification has been reported of increasing with reactor operational time, due to biofilm thickness and diffusional resistance increase (Wang et al., 2016). Moreover, Regmi et al. (2011) reported low accessibility of nitrite within the biofilm with K_{NO2} for attached nitrite oxidising bacteria over 20-fold that of suspended biomass. Thus, the drastic increase in K_{NO2} is partially due to diffusion limitations in mature biofilms and is likely amplified by the hypersaline inhibitory conditions.

3.4.2. Key parameters and effect of carrier type

The most influential parameters (S > 1) for the biokinetic model of both MBBRs were growth rate (μ_T), similarly to other reports (Eldyasti et al., 2012; Lanzetta et al., 2024) and biomass yield (Y) (Fig. S12). Both parameters were independent of biofilm conditions and salinity, highlighting the importance of their initial estimation.

In the K5-MBBR, at low (2.7 %) salinity, L, SSA and salinity parameters (K_I, n) had low influence (S < 0.15) on DR. Under this condition, biofilm biomass was still growing and suspended biomass significantly contributed to denitrification. At 9.5 % salinity, when biofilm was formed, L and SSA increased their influence (S~0.6), similarly to K_I (S = 0.77). On the other hand, in M30-MBBR, L and SSA had already at 2.7 % salinity significant influence (S = 0.73) on DR, further increasing (S~0.9) at 9.5 % salinity when the biofilm quantity was rather stable. Moreover, at 9.5 % salinity, K_I influence was lower (S = 0.42) than in K5-MBBR. Eventually, in both MBBRs, the model was not significantly affected by changes in the tuning parameter n (S < 0.20).

The differences in the sensitivity analysis results between hollow- and porous-body carriers were mainly due to the difference in SSA. In M30-MBBR, K_I influence on the model was significant but was around half of that in K5-MBBR, while DR was more sensitive to variations in SSA and L. Thus, a decrease in K_I with a hollow-body carrier (e.g., due to microbial community changes as well as biofilm deterioration) would lead to more evident changes in the process' denitrification rate than with a porous-body carrier, according to the sensitivity analysis. Moreover, in the K5-MBBR, where biofilm detachment was more evident, a theoretical decrease by 20–30 % in the SSA or L caused by both salinity and/or shear stress could produce a 12–18 % reduction in denitrification rate. From an operational perspective, such a decrease in DR would result in a higher process HRT required to completely remove nitrogen from the wastewater. This highlights the importance of predicting the biofilm denitrification performance under salinity stress.

3.4.3. Limitations of the simplified modelling approach and future recommendations

The kinetic model reproduced DR more accurately when the biofilm had the main role in denitrification. This was as also observed when testing the model's consistency at different initial biofilm conditions (Fig. 6), which was possible given the stability of the microbial community and assuming that the kinetic parameters (μ_{max}, Y and K_I) did not change among NUR tests. The discrepancy between data and model at salinities <5.5 % was likely due to the limitation of the kinetics in separating biofilm and suspended biomass contributions, as seen for

example in the M30-MBBR at 1 % salinity NUR (Fig. 6b, Fig. S3).

For the model simplification, a single K_I was used for the MBBR system for both attached and suspended biomass and included the effects of biofilm protection and of the carrier configuration on denitrification rates. The limits of such approach include the difficulty in discerning between the inhibition on biofilm and suspended biomass, as well as within the biofilm layers. However, this simplification was considered reasonable, since denitrification in the MBBR was predominantly driven by the biofilm rather than the suspended biomass.

Furthermore, the determination of SSA and L was challenging for the porous carrier, where the active SSA is often lower than the PSA and variable during operation (Rittmann et al., 2018), due to the clogging of the pores by the same biofilm. For the same porous carrier typology used in this study, Bassin et al. (2016) suggested a biofilm thickness <800–1200 μm, but the biofilm grows discontinuously between the pores and the external surface, with consequent challenges in its determination. Therefore, for M30-MBBR, the nominal SSA (or PSA) was assumed, and L was calibrated (Eldyasti et al., 2012), contrarily to the value estimation done for K5-MBBR carriers. Although the model output showed similar sensitivity to variations in SSA or L (Fig. S12), this approximation introduces uncertainty to the modelling and could be overcome by estimating the active SSA with techniques like optical coherence tomography (Li et al., 2016) or magnetic resonance imaging (Caizán-Juanarena et al., 2019).

This study introduces an alternative strategy that allows complex biofilm inhibition kinetics to be modelled based solely on substrate bulk concentration measurements, resulting in an inhibition model dependent only on salinity parameters (K_I, n) related to the whole MBBR system. The factor added to the existing model represents an observed quantification of salinity inhibition on denitrification rate that incorporates implicitly processes proper of biofilm systems, such as diffusion. Hence, this easy-implementable tool has potential for the modelling of wastewater treatment with an established biofilm specialised in denitrification, which can be used to predict the inhibition and to optimise the process accordingly.

Future research should develop the kinetics by adding inhibition functions describing NO_2^- and N_2O accumulation, needed to comprehensively simulate denitrification process in a continuous flow MBBR under salinity stress. Similarly, the implementation of biofilm detachment due to salinity stress is required to reproduce the biofilm quantity and coverage on the carriers that affect the process performance. For example, Dias et al. (2018) calculated the biofilm detachment rate based on the effluent VSS concentration increment, but this approach was not possible in this study, since the VSS did not increase with the biofilm detachment. Thus, new methods, based for example on correlating salinity, shear stress and biofilm quantity should be developed for a comprehensive model.

4. Conclusions

In MBBRs for methanol-driven denitrification under salinity stress with hollow-body or porous-body carriers.

- The biofilm protective environment allows nitrogen removal ≥70 % even at 9.5 % salinity and fast response to changing conditions, demonstrating its potential for hypersaline wastewater treatment.
- At the same filling fraction, similar quantities of biomass are retained, and stable microbial communities develop regardless of the carrier typology, being promising for the stability of the process and its startup with microorganisms from a non-saline source.
- Carrier typology impacts denitrification performance at different salinities. Hollow-body carrier removes N at higher rates at low-moderate salinities (1–5.5 %) due to its exposed biofilm growing in large cavities, while the porous-body carrier provides more stable removal efficiencies at high salinities (7.5–9.5 %) due to salt-diffusion controlling biofilm within the small pores. Therefore, the selection of the carrier based on the salinity concentration range allows the process' optimisation, likely applying also to other inhibitory agents.
- Successful denitrification of NO_x-SO_2 scrubber saline wastewater was achieved in MBBRs, demonstrating the potential of biofilm-based treatment for its management.
- An existing biofilm model incorporated with an inhibition factor reproduces the apparent denitrification biofilm kinetics under various salinities, being promising for wastewater biofilm process modelling.

CRediT authorship contribution statement

Alessio D'Aquino: Writing – original draft, Visualization, Validation, Software, Methodology, Investigation, Funding acquisition, Formal analysis, Data curation, Conceptualization. **Marja Tiirola:** Writing – review & editing, Validation, Methodology, Investigation, Formal analysis. **Jaakko A. Puhakka:** Writing – review & editing, Visualization, Supervision, Methodology, Funding acquisition, Conceptualization. **Marja R.T. Palmroth:** Writing – review & editing, Visualization, Supervision, Methodology, Funding acquisition, Conceptualization. **Gianni Andreottola:** Writing – review & editing, Visualization, Supervision, Resources, Methodology, Funding acquisition, Conceptualization.

Declaration of competing interest

The authors declare the following financial interests/personal relationships which may be considered as potential competing interests:

Alessio D'Aquino reports financial support was provided by Land and Water Technology Foundation. Alessio D'Aquino reports financial support was provided by Walter Ahlström Foundation. Marja Tiirola reports financial support was provided by Research Council of Finland. If there are other authors, they declare that they have no known competing financial interests or personal relationships that could have appeared to influence the work reported in this paper.

Acknowledgments

This work was supported by Maa-ja vesitekniikan tuki ry (grants 4301 and 4758), Tutkijat-Maailmalle-programme (Walter Ahlström Foundation, project 20220036) and the Academy of Finland (project 364081). The authors would like to thank Officine Parisi Srl (Riva del Garda, Italy) for their excellent work in crafting parts for the lab-scale MBBR, Valmet Technologies Oy for providing the scrubber wastewater samples, Simone Cavazzoli and Roberta Villa for their help with the analyses and research material in the laboratory of the University of Trento, Veolia Water Technologies-AnoxKaldnes Sweden and Mutag Denmark for kindly providing the MBBR carriers.

Appendix A. Supplementary data

Supplementary data to this article can be found online at https://doi.org/10.1016/j.jenvman.2025.127288.

Data availability

Data will be made available on request.

References

APHA, 2017. In: Standard Methods for the Examination of Water and Wastewater, 23rd edition. American Public Health Association, Washington, DC.

Ashrafi, O., Yerushalmi, L., Haghighat, F., 2015. Wastewater treatment in the pulp-and-paper industry: a review of treatment processes and the associated greenhouse gas emission. J. Environ. Manag. 158, 146–157. https://doi.org/10.1016/j.jenvman.2015.05.010.

Auclair, J., Parent, S., Villemur, R., 2012. Functional diversity in the denitrifying biofilm of the methanol-Fed Marine denitrification System at the Montreal biodome. Microb. Ecol. 63, 726–735. https://doi.org/10.1007/s00248-011-9960-2.

Bassin, J.P., Dias, I.N., Cao, S.M.S., Senra, E., Laranjeira, Y., Dezotti, M., 2016. Effect of increasing organic loading rates on the performance of moving-bed biofilm reactors filled with different support media: assessing the activity of suspended and attached biomass fractions. Process Saf. Environ. Prot. 100, 131–141. https://doi.org/10.1016/j.psep.2016.01.007.

Caizán-Juanarena, L., Krug, J.R., Vergeldt, F.J., Kleijn, J.M., Velders, A.H., Van As, H., Ter Heijne, A., 2019. 3D biofilm visualization and quantification on granular bioanodes with magnetic resonance imaging. Water Res. 167, 115059. https://doi.org/10.1016/j.watres.2019.115059.

Carrera, P., Strubbe, L., Río, A.V. del, Mosquera-Corral, A., Volcke, E.I.P., 2023. Modelling salinity effects on aerobic granular sludge treating fish-canning wastewater. Environ. Sci.: Water Res. Technol. 9, 747–755. https://doi.org/10.1039/D2EW00874B.

Chen, S., Liu, C., Cao, G., Li, K., Huang, J., 2024. Effect of salinity on biological nitrogen removal from wastewater and its mechanism. Environ. Sci. Pollut. Res. 31, 24713–24723. https://doi.org/10.1007/s11356-024-32417-8.

Chen, X., Stewart, P.S., 2000. Biofilm removal caused by chemical treatments. Water Res. 34, 4229–4233. https://doi.org/10.1016/S0043-1354(00)00187-1.

Choi, M., Jeon, J., Park, S., Choi, D., Kwon, S., Bae, H., 2025. Impact of mixed carbon sources on microbial function and network structure in hypersaline denitrification. Bioresour. Technol. 426, 132366. https://doi.org/10.1016/j.biortech.2025.132366.

Dan, N.H., Le Luu, T., 2021. High organic removal of landfill leachate using a continuous flow sequencing batch biofilm reactor (CF-SBBR) with different biocarriers. Sci. Total Environ. 787, 147680. https://doi.org/10.1016/j.scitotenv.2021.147680.

D'Aquino, A., Kalinainen, N., Auvinen, H., Andreottola, G., Puhakka, J.A., Palmroth, M. R.T., 2023. Effects of inorganic ions on autotrophic denitrification by *Thiobacillus denitrificans* and on heterotrophic denitrification by an enrichment culture. Sci. Total Environ. 901, 165940. https://doi.org/10.1016/j.scitotenv.2023.165940.

D'Aquino, A., Maanoja, S.T., Auvinen, H., Tiirola, M., Andreottola, G., Puhakka, J.A., Palmroth, M.R.T., 2024. Methanol and thiosulphate from pulp mill waste streams support denitrification under salinity stress. Chem. Eng. J. 502, 158131. https://doi.org/10.1016/j.cej.2024.158131.

Deshwal, B.R., Lee, H.-K., 2004. Kinetics and mechanism of chloride based chlorine dioxide generation process from acidic sodium chlorate. J. Hazard. Mater. 108, 173–182. https://doi.org/10.1016/j.jhazmat.2003.12.006.

Dias, J., Bellingham, M., Hassan, J., Barrett, M., Stephenson, T., Soares, A., 2018. Influence of carrier media physical properties on start-up of moving attached growth systems. Bioresour. Technol. 266, 463–471. https://doi.org/10.1016/j.biortech.2018.06.096.

di Biase, A., Devlin, T.R., Kowalski, M., Oleszkiewicz, J.A., 2018. Optimisation of surface area loading rate for an anaerobic moving bed biofilm reactor treating brewery wastewater. J. Clean. Prod. 172, 1121–1127. https://doi.org/10.1016/j.jclepro.2017.10.256.

Dupla, M., Comeau, Y., Parent, S., Villemur, R., Jolicoeur, M., 2006. Design optimisation of a self-cleaning moving-bed bioreactor for seawater denitrification. Water Res. 40, 249–258. https://doi.org/10.1016/j.watres.2005.10.029.

Eldyasti, A., Nakhla, G., Zhu, J., 2012. Development of a calibration protocol and identification of the most sensitive parameters for the particulate biofilm models used in biological wastewater treatment. Bioresour. Technol. 111, 111–121. https://doi.org/10.1016/j.biortech.2012.02.021.

Feng, G., Zeng, Y., Wang, H.-Z., Chen, Y.-T., Tang, Y.-Q., 2023. *Proteiniphilum* and *Methanothrix harundinacea* became dominant acetate utilizers in a methanogenic reactor operated under strong ammonia stress. Front. Microbiol. 13. https://doi.org/10.3389/fmicb.2022.1098814.

Fritzmann, C., Löwenberg, J., Wintgens, T., Melin, T., 2007. State-of-the-art of reverse osmosis desalination. Desalination 216, 1–76. https://doi.org/10.1016/J.DESAL.2006.12.009.

Gingerich, D.B., Grol, E., Mauter, M.S., 2018. Fundamental challenges and engineering opportunities in flue gas desulfurization wastewater treatment at coal fired power plants. Environ. Sci.: Water Res. Technol. 4, 909–925. https://doi.org/10.1039/C8EW00264A.

Gonzalez-Martinez, A., Leyva-Díaz, J.C., Rodriguez-Sanchez, A., Muñoz-Palazon, B., Rivadeneyra, A., Poyatos, J.M., Rivadeneyra, M.A., Martinez-Toledo, M.V., 2015. Isolation and metagenomic characterization of bacteria associated with calcium carbonate and struvite precipitation in a pure moving bed biofilm reactor-membrane bioreactor. Biofouling 31, 333–348. https://doi.org/10.1080/08927014.2015.1040006.

Goode, C., Allen, D.G., 2011. Effect of calcium on moving-bed biofilm reactor biofilms. Water Environ. Res. 83, 220–232. https://doi.org/10.2175/106143010X12780288628255.

Hasanzadeh, R., Abbasi Souraki, B., Pendashteh, A., Khayati, G., Ahmadun, F.-R., 2020. Application of isolated halophilic microorganisms suspended and immobilized on walnut shell as biocarrier for treatment of oilfield produced water. J. Hazard. Mater. 400, 123197. https://doi.org/10.1016/j.jhazmat.2020.123197.

Horn, H., Morgenroth, E., 2006. Transport of oxygen, sodium chloride, and sodium nitrate in biofilms. Chem. Eng. Sci. 61, 1347–1356. https://doi.org/10.1016/j.ces.2005.08.027.

Hu, X., Ji, Z., Gu, S., Ma, Z., Yan, Z., Liang, Y., Chang, H., Liang, H., 2023. Mapping the research on desulfurization wastewater: insights from a bibliometric review (1991–2021). Chemosphere 314, 137678. https://doi.org/10.1016/j.chemosphere.2022.137678.

Johansson, J., Normann, F., Andersson, K., 2021. Techno-Economic evaluation of Co-Removal of NO_x and SO_x species from flue gases via enhanced oxidation of NO by ClO_2—Case studies of implementation at a pulp and paper mill, waste-to-heat plant and a cruise ship. Energies 14, 8512. https://doi.org/10.3390/en14248512.

Keren-Paz, A., Kolodkin-Gal, I., 2020. A brick in the wall: discovering a novel mineral component of the biofilm extracellular matrix. N. Biotech. 56, 9–15. https://doi.org/10.1016/j.nbt.2019.11.002.

Koenig, A., Liu, L., 2004. Autotrophic denitrification of high-salinity wastewater using elemental sulfur: Batch tests. Water Environ. Res. 76, 37–46. https://doi.org/10.2175/106143004x141564.

Kragh, K.N., Tolker-Nielsen, T., Lichtenberg, M., 2023. The non-attached biofilm aggregate. Commun. Biol. 6, 898. https://doi.org/10.1038/s42003-023-05281-4.

Labbé, N., Juteau, P., Parent, S., Villemur, R., 2003. Bacterial diversity in a marine methanol-fed denitrification reactor at the Montreal biodome, Canada. Microb. Ecol. 46, 12–21. https://doi.org/10.1007/s00248-002-1056-6.

Lanzetta, A., Mattioli, D., Di Capua, F., Minieri, V., Papirio, S., Esposito, G., 2024. Modeling complete and shortcut simultaneous nitrification and denitrification coupled to phosphorus removal in moving bed biofilm reactors. J. Water Process Eng. 59, 105022. https://doi.org/10.1016/j.jwpe.2024.105022.

Li, C., Liang, J., Lin, X., Xu, H., Tadda, M.A., Lan, L., Liu, D., 2019. Fast start-up strategies of MBBR for mariculture wastewater treatment. J. Environ. Manag. 248, 109267. https://doi.org/10.1016/j.jenvman.2019.109267.

Li, C., Felz, S., Wagner, M., Lackner, S., Horn, H., 2016. Investigating biofilm structure developing on carriers from lab-scale moving bed biofilm reactors based on light microscopy and optical coherence tomography. Bioresour. Technol. 200, 128–136. https://doi.org/10.1016/j.biortech.2015.10.013.

Lin, L., Pratt, S., Crick, O., Xia, J., Duan, H., Ye, L., 2021. Salinity effect on freshwater anammox bacteria: ionic stress and ion composition. Water Res. 188, 116432. https://doi.org/10.1016/j.watres.2020.116432.

Liu, N., Dopffel, N., Hovland, B., Alagic, E., Vik, B.F., Bødtker, G., 2020. High osmotic stress initiates expansion and detachment of *Thalassospira sp*. biofilms in glass microchannels. J. Environ. Chem. Eng. 8, 104525. https://doi.org/10.1016/j.jece.2020.104525.

Loosdrecht, M.C.M. van, Eikelboom, D., Gjaltema, A., Mulder, A., Tijhuis, L., Heijnen, J. J., 1995. Biofilm structures. Water Sci. Technol. 32, 35–43.

Macey, M.C., Pratscher, J., Crombie, A., Murrell, J.C., 2018. Draft genome sequences of obligate Methylotrophs Methylovorus sp. Strain MM2 and Methylobacillus sp. Strain MM3, isolated from Grassland soil. Microbiol. Resour. Announc. 7. https://doi.org/10.1128/mra.00824-18.

Mariángel, L., Aspé, E., Cristina Martí, M., Roeckel, M., 2008. The effect of sodium chloride on the denitrification of saline fishery wastewaters. Environ. Technol. 29, 871–879. https://doi.org/10.1080/09593330802015318.

Morgan-Sagastume, F., 2018. Biofilm development, activity and the modification of carrier material surface properties in moving-bed biofilm reactors (MBBRs) for wastewater treatment. Crit. Rev. Environ. Sci. Technol. 48, 439–470. https://doi.org/10.1080/10643389.2018.1465759.

Navada, S., Vadstein, O., Tveten, A.-K., Verstege, G.C., Terjesen, B.F., Mota, V.C., Venkataraman, V., Gaumet, F., Mikkelsen, Ø., Kamstra, A., 2019. Influence of rate of salinity increase on nitrifying biofilms. J. Clean. Prod. 238, 117835. https://doi.org/10.1016/j.jclepro.2019.117835.

Nokhal, T.H., Schlegel, H.G., 1983. Taxonomic Study of *Paracoccus denitrificans*. Int. J. Syst. Evol. Microbiol. 33, 26–37. https://doi.org/10.1099/00207713-33-1-26.

Ødegaard, H., 2006. Innovations in wastewater treatment: the moving bed biofilm process. Water Sci. Technol. 53, 17–33. https://doi.org/10.2166/wst.2006.284.

Osaka, T., Shirotani, K., Yoshie, S., Tsuneda, S., 2008. Effects of carbon source on denitrification efficiency and microbial community structure in a saline wastewater treatment process. Water Res. 42, 3709–3718. https://doi.org/10.1016/j.watres.2008.06.007.

Özkaya, B., Kaksonen, A.H., Sahinkaya, E., Puhakka, J.A., 2019. Fluidized bed bioreactor for multiple environmental engineering solutions. Water Res. 150, 452–465. https://doi.org/10.1016/j.watres.2018.11.061.

Panagopoulos, A., 2022. Study and evaluation of the characteristics of saline wastewater (brine) produced by desalination and industrial plants. Environ. Sci. Pollut. Res. 29, 23736–23749. https://doi.org/10.1007/s11356-021-17694-x.

Plattes, M., Henry, E., Schosseler, P.M., Weidenhaupt, A., 2006. Modelling and dynamic simulation of a moving bed bioreactor for the treatment of municipal wastewater. Biochem. Eng. J. 32, 61–68. https://doi.org/10.1016/j.bej.2006.07.009.

Regmi, P., Thomas, W., Schafran, G., Bott, C., Rutherford, B., Waltrip, D., 2011. Nitrogen removal assessment through nitrification rates and media biofilm accumulation in an IFAS process demonstration study. Water Res. 45, 6699–6708. https://doi.org/10.1016/j.watres.2011.10.009.

Rittmann, B.E., Boltz, J.P., Brockmann, D., Daigger, G.T., Morgenroth, E., Sørensen, K.H., Takács, I., van Loosdrecht, M., Vanrolleghem, P.A., 2018. A framework for good biofilm reactor modeling practice (GBRMP). Water Sci. Technol. 77, 1149–1164. https://doi.org/10.2166/wst.2018.021.

Shitu, A., Liu, G., Zhang, Y., Ye, Z., Zhao, J., Zhu, S., Liu, D., 2021. Enhancement of mariculture wastewater treatment using moving bed biofilm reactors filled with modified biocarriers: characterisation, process performance and microbial community evaluation. J. Environ. Manag. 291, 112724. https://doi.org/10.1016/j.jenvman.2021.112724.

Shitu, A., Zhu, S., Qi, W., Tadda, M.A., Liu, D., Ye, Z., 2020. Performance of novel sponge biocarrier in MBBR treating recirculating aquaculture systems wastewater: microbial community and kinetic study. J. Environ. Manag. 275, 111264. https://doi.org/10.1016/j.jenvman.2020.111264.

Siegrist, H., Gujer, W., 1985. Mass transfer mechanisms in a heterotrophic biofilm. Water Res. 19, 1369–1378. https://doi.org/10.1016/0043-1354(85)90303-3.

Stoodley, P., Wilson, S., Hall-Stoodley, L., Boyle, J.D., Lappin-Scott, H.M., Costerton, J. W., 2001. Growth and detachment of cell clusters from mature mixed-species

biofilms. Appl. Environ. Microbiol. 67, 5608–5613. https://doi.org/10.1128/AEM.67.12.5608-5613.2001.

Sudmalis, D., Mubita, T.M., Gagliano, M.C., Dinis, E., Zeeman, G., Rijnaarts, H.H.M., Temmink, H., 2020. Cation exchange membrane behaviour of extracellular polymeric substances (EPS) in salt adapted granular sludge. Water Res. 178, 115855. https://doi.org/10.1016/j.watres.2020.115855.

Tadda, M.A., Altaf, R., Gouda, M., Rout, P.R., Shitu, A., Ye, Z., Zhu, S., Liu, D., 2021. Impact of Saddle-Chips biocarrier on treating mariculture wastewater by moving bed biofilm reactor (MBBR): mechanism and kinetic study. J. Environ. Chem. Eng. 9, 106710. https://doi.org/10.1016/j.jece.2021.106710.

Vredenbregt, L.H.J., Nielsen, K., Potma, A.A., Kristensen, G.H., Sund, C., 1997. Fluid bed biological nitrification and denitrification in high salinity wastewater. Water Sci. Technol. 36, 93–100. https://doi.org/10.1016/S0273-1223(97)00341-7.

Wang, J., Liu, Q., Wu, B., Hu, H., Dong, D., Yin, J., Ren, H., 2020. Effect of salinity on mature wastewater treatment biofilm microbial community assembly and metabolite characteristics. Sci. Total Environ. 711, 134437. https://doi.org/10.1016/j.scitotenv.2019.134437.

Wang, Y., Bott, C., Nerenberg, R., 2016. Sulfur-based denitrification: effect of biofilm development on denitrification fluxes. Water Res. 100, 184–193. https://doi.org/10.1016/j.watres.2016.05.020.

Xiang, Z., Chen, X., Bai, J., Li, B., Li, H., Huang, X., 2023. Bioaugmentation performance for moving bed biofilm reactor (MBBR) treating mariculture wastewater by an isolated novel halophilic heterotrophic nitrification aerobic denitrification (HNAD) strain (*Zobellella B307*). J. Environ. Manag. 325, 116566. https://doi.org/10.1016/j.jenvman.2022.116566.

Zan, F., Ma, H., Xiao, C., Chen, G., Wu, D., 2022. Moving-bed biofilm reactor for saline wastewater treatment: different types of carriers, versatile nitrifying reactions, and functional microbial groups. J. Water Process Eng. 50, 103274. https://doi.org/10.1016/j.jwpe.2022.103274.

Zhai, S., Ji, M., Zhao, Y., Su, X., 2020. Shift of bacterial community and denitrification functional genes in biofilm electrode reactor in response to high salinity. Environ. Res. 184, 109007. https://doi.org/10.1016/j.envres.2019.109007.

Zhang, R.-G., Tan, X., Zhao, X.-M., Deng, J., Lv, J., 2014. *Moheibacter sediminis* gen. nov., sp. Nov., a member of the family *Flavobacteriaceae* isolated from sediment, and emended descriptions of *Empedobacter brevis, Wautersiella falsenii* and *Weeksella virosa*. Int. J. Syst. Evol. Microbiol. 64, 1481–1487. https://doi.org/10.1099/ijs.0.060178-0.

Zhang, Z., Guo, Y., Guo, L., Hu, F., Zhao, Y., Jin, C., She, Z., Gao, M., Wang, G., 2020. Elucidating salinity adaptation and shock loading on denitrification performance: focusing on microbial community shift and carbon source evaluation. Bioresour. Technol. 305, 123030. https://doi.org/10.1016/j.biortech.2020.123030.

Zuo, L., Yao, H., Li, H., Jia, F., Wei, W., Liu, Y., Ni, B.-J., Chen, X., 2021. Modeling of completely autotrophic nitrogen removal process with salt and glycine betaine addition. Chemosphere 264, 128474. https://doi.org/10.1016/j.chemosphere.2020.128474.

Inhibition-level-based carrier selection and kinetic insights for optimised denitrification of saline wastewaters in MBBR

Alessio D'Aquino[a, b*], Marja Tiirola[c], Jaakko A. Puhakka[a], Marja R. T. Palmroth[a] and Gianni Andreottola[b].

[a] Tampere University, Faculty of Engineering and Natural Sciences, Bio- and Circular Economy Unit, Korkeakoulunkatu 8, P.O. Box 541, 33014 Tampere, Finland

[b] University of Trento, Department of Civil, Environmental and Mechanical Engineering, via Mesiano 77, 38123 Trento, Italy

[c] University of Jyväskylä, Department of Biological and Environmental Sciences, NanoScience Center, Survontie 9C, P.O. Box 35, 40014 Jyväskylä, Finland

*Corresponding author. Email address: alessio.daquino@tuni.fi

Supplementary materials

1. Continuous flow MBBRs

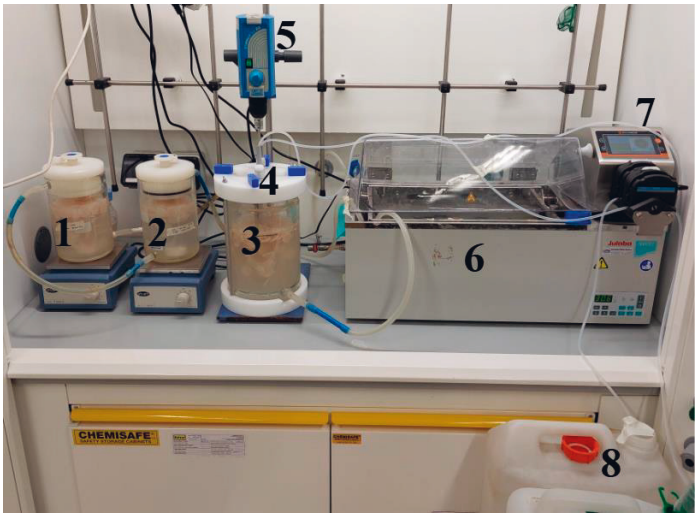

Figure S1. Experimental setup of this study. 1) Moving bed biofilm reactor (MBBR) with K5 carriers on a magnetic stirrer for semi fed-batch test with real scrubber wastewater. 2) MBBR with M30 carriers on a magnetic stirrer for semi fed-batch test with real scrubber wastewater. 3) MBBR for continuous flow tests with K5 and M30 carriers and NUR tests. 4) Airtight reactor cap with ports for influent, effluent, mechanical mixer and sampling. 5) Mechanical mixer. 6) Thermostatic water bath connected to 1, 2 and 3. 7) Peristaltic pump regulating inflow and outflow from 1. 8) Influent and effluent tanks of 3.

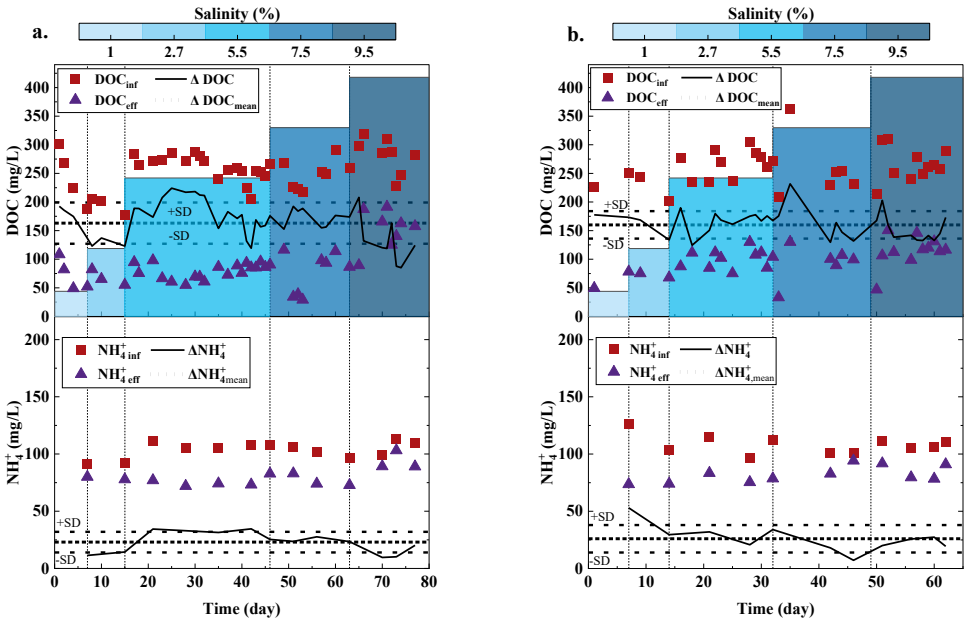

Figure S2. Dissolved organic carbon (DOC) and ammonium ion concentrations time profiles in K5-MBBR (a.) and M30-MBBR (b.), for influent and effluent. Δ represents the difference in concentration between influent and effluent. The average ΔDOC (±SD) for K5-MBBR and M30-MBBR were 163±36 mg/L and 161±24 mg/L. The average ΔNH_4^+ (±SD) for K5-MBBR and M30-MBBR were 23±9 mg/L and 26±12 mg/L. Consumption of DOC and NH_4^+ throughout the entire continuous flow operation were not significantly different (Mann-Whitney test, $p>0.05$) between K5-MBBR and M30-MBBR.

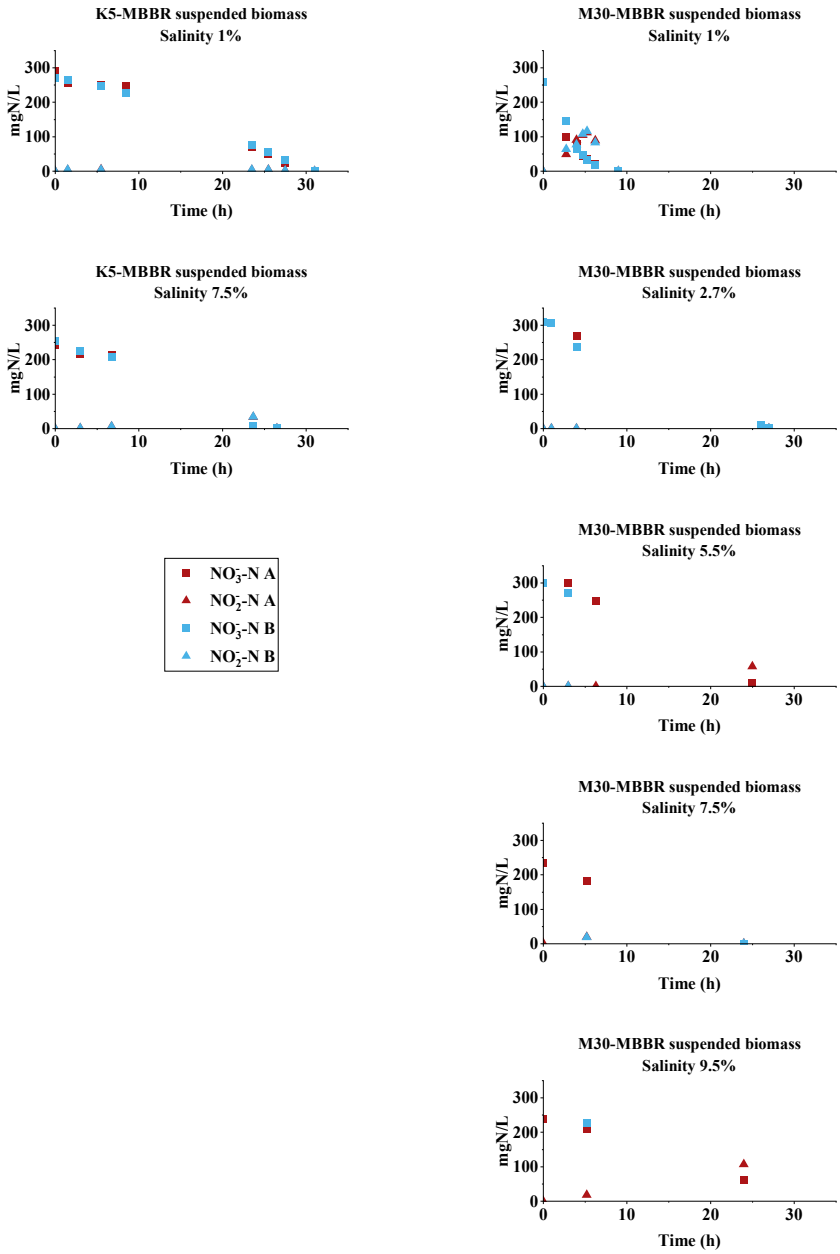

Figure S3. Nitrate- and nitrite- nitrogen time profiles for the suspended biomass in the liquid phase tests. The activity of the suspended biomass was tested at different salinities for K5-MBBR (left column) and M30-MBBR (right column) to observe its contribution to the overall denitrification rate in the MBBR (attached+suspended biomass). Two 50 mL samples were withdrawn from the liquid phase of the MBBR, placed in two sealed glass bottles, spiked with 250 mg/L NO_3^--N and methanol in excess and incubated on a multi-HS-6 magnetic heating stirrer (Velp, Italy) at 30 °C. NO_3^--N and NO_2^--N concentrations were monitored for approximately 24 h.

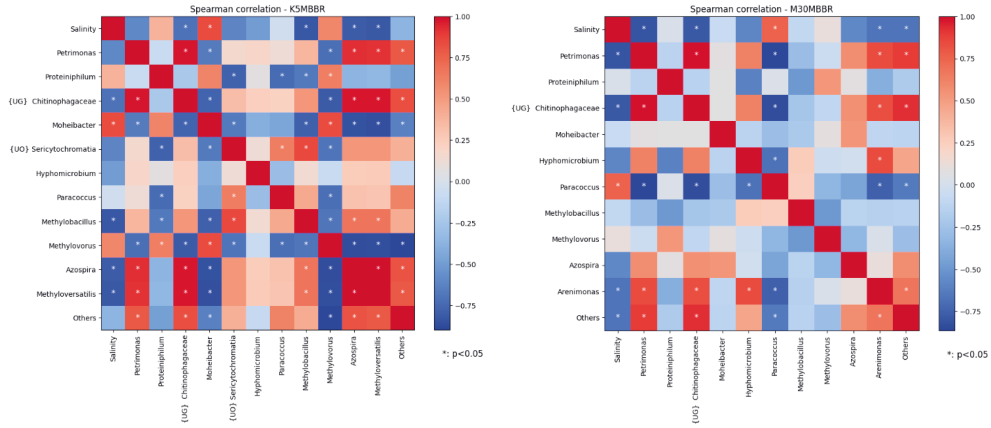

Figure S4. Spearman correlation matrix for the main genera in the K5-MBBR (left) and M30-MBBR (right) reactors and salinity.

Table S1. Methanol driven denitrification performance under saline conditions for different reactor systems. If not reported, reactor operational parameters were estimated from the data available in the references. Modified from (D'Aquino et al., 2024).

Microorganisms' source, influent	Reactor type	Salinity %	HRT (h)	Loading Rate (gN/L/d)	Removal %	Ref.
WWTP sludge, synthetic	MBBR	9.5	4	~1.5	≥70 (NO_x^-)	This study
WWTP sludge, synthetic	FBBR	6.8	2.2	2.5	>97 (NO_x^-)	D'Aquino et al. (2024)
WWTP sludge, synthetic	CSTR	≤3; 4	48	0.75	99 (NO_x^-); inhib.	Osaka et al. (2008)
Seawater, marine mesocosm wastewater	MBBR	2.8	>24	1.5	88 (NO_x^-)	Labelle et al. (2005)
WWTP sludge+soil, synthetic	Polymeric carrier bed	3	3	8.4	60% (NO_3^-)	Yang et al. (1995)
Saline enrichment of sludge, synthetic	SBBR	6	24	0.11	<80 (TN)	Feng et al. (2023)
WWTP sludge, synthetic	Biofilm Electrode	3.5	8	0.06	55 (NO_3^-)	Zhai et al. (2020)
Seawater, marine mesocosm wastewater	MBBR	2.8	1.6	3.5	75 (NO_x^-)	Dupla et al. (2006)

WWTP: Wastewater Treatment Plant; FBBR: Fluidized Bed Bioreactor; CSTR: Continuous Stirred Tank Reactor; MBBR: Moving Bed Biofilm Reactor; SBBR: Sequencing Batch Biofilm Reactor.

2. Biofilm carriers

Table S2. Specifics of K5 and M30 carriers used in the MBBR tests.

	AnoxK™ 5	Mutag BioChip 30™
	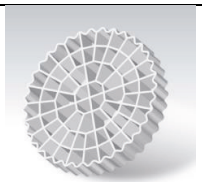	
Protected surface area (m^2/m^3)	800	5500
Nominal diameter (mm)	25	30
Thickness (mm)	3-4.5	1.1
Material	HDPE	PE
Density (kg/dm^3)	0.95	0.95
Bulk weight (kg/m^3)	118	165

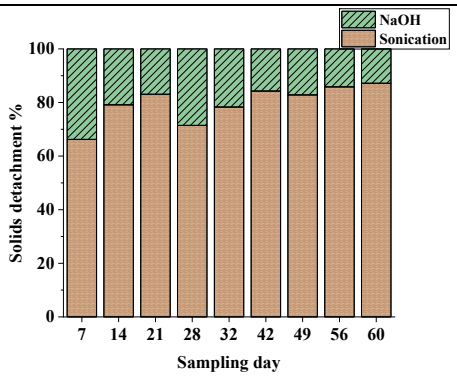

ATS (g) for 5 pieces of M30			
Sampling Day	**sonication+ NaOH**	**Theor.**	**% Recovery**
7	0.075	0.076	0.99
14	0.235	0.266	0.88
21	0.335	0.386	0.89
28	0.361	0.417	0.87
32	0.382	0.485	0.79
42	0.363	0.490	0.74
49	0.354	0.514	0.69
56	0.397	0.533	0.74
60	0.404	0.548	0.74

Figure S5. Percentage of solids mass (mg) detached by sonication and NaOH soaking for M30-MBBR carrier, for each carrier sample (5 pieces). Except for day 7, in all the M30-MBBR samples, sonication detached more than 70% of the total solids detached. The AVS determination procedure was as follows: first, the carriers with biofilm were dried overnight at 70 °C, weighed, immersed in a 30 mL plastic container with MQ-water, and placed in an ultrasonic bath at 50 °C for 15 minutes (Fonseca and Bassin, 2019). After sonication, the vials were manually shaken, the carriers were removed and stored, while the solids in the MQ-water were analysed according to APHA (2017). After the analysis, an AVS/ATS ratio was obtained. The rest of the total attached solids was detached according to the supplier's protocol, by soaking the carriers overnight in 5% NaOH, and measured as weight difference before and after the treatment. The AVS/ATS ratio found above was extended to the total solids detached (sonication+NaOH soaking) to find the AVS. Blank samples of virgin carriers were also analysed to exclude interferences. Considering that sonication detached more than 70% of all the solids detached (Figure S5) for almost all the samples, the possible error committed by extending the AVS/ATS ratio also to the NaOH detached solids was assumed negligible. On the other hand, measuring the AVS in the soaking solution is not reliable due to NaOH possibly reacting with organic substance and resulting in its underestimation (Fonseca and Bassin, 2019). To quantify the

efficiency of the sonication+NaOH soaking method in detaching the solids from the M30 carrier, the ATS quantity measured were compared to the theoretical weight of the solids attached on the carriers. Such weight was calculated as dry carriers with biofilm minus an average weight of the virgin M30 carriers. The average carrier weight was calculated from 25 weight measurement of virgin carriers collected randomly from the stock pack (1 carrier: 0.362±0.016 g). On average, on 9 biofilm measurements, 81±9 % of the ATS was described by the sonication+NaOH soaking method. In the manual detachment method used for K5 carriers, the detachment of the solids was 99%.

a. K5-MBBR at 5.5% salinity **b. K5-MBBR at 7.5% salinity** **c. K5-MBBR at 9.5% salinity**

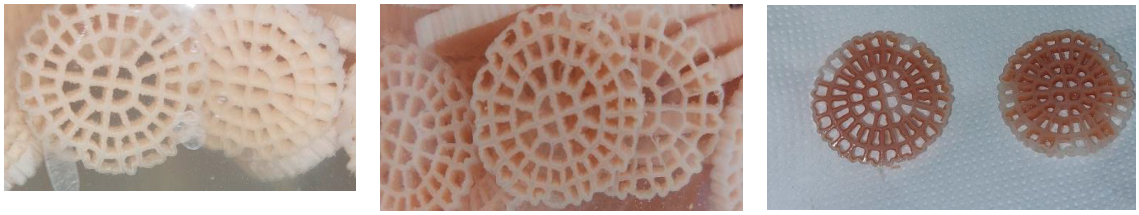

d. M30-MBBR at 5.5% salinity **e. M30-MBBR at 9.5% salinity**

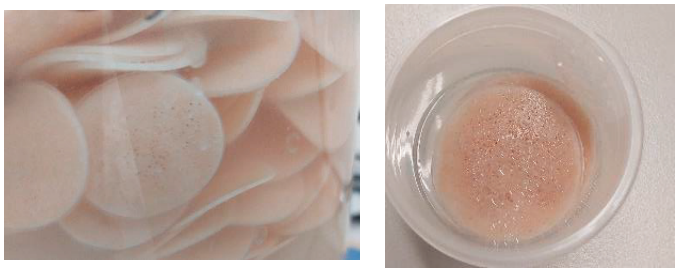

Figure S6. Pictures of colonized K5-MBBR carriers (a, b, c) and M30-MBBR (d, e) carriers at different salinities. For K5-MBBR, at 5.5% salinity (a.) biofilm was growing in all the carrier's cavities. At 7.5% salinity (b.), a first sign of detachment of the biofilm was observed. At 9.5% salinity, biofilm completely detached from many carrier's cavities (c.). For M30-MBBR, the complete detachment was not visually observed (d. and f.).

a. **b.** **c.**

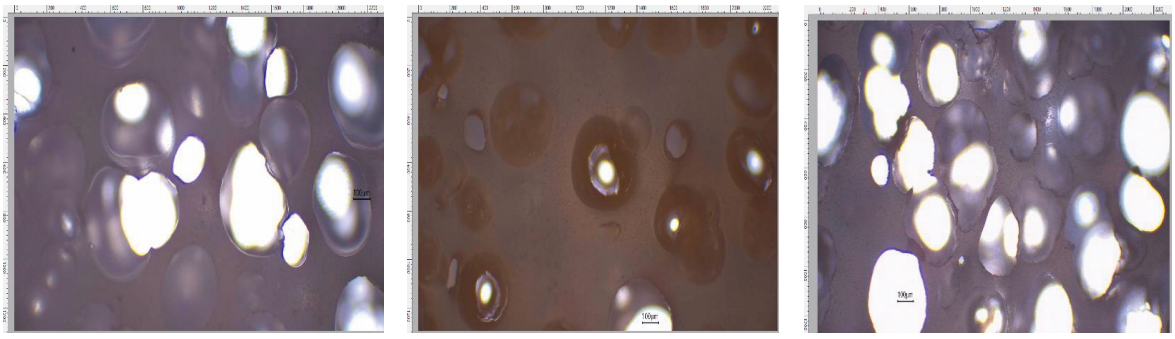

Figure S7. Optical microscopic pictures (magnification 40x) of M30-MBBR carrier before colonization (a), during reactor operation at 7.5% salinity (b), after the biomass detachment procedure (c). Biofilm filled many pores and made the estimation of biofilm thickness challenging (b).

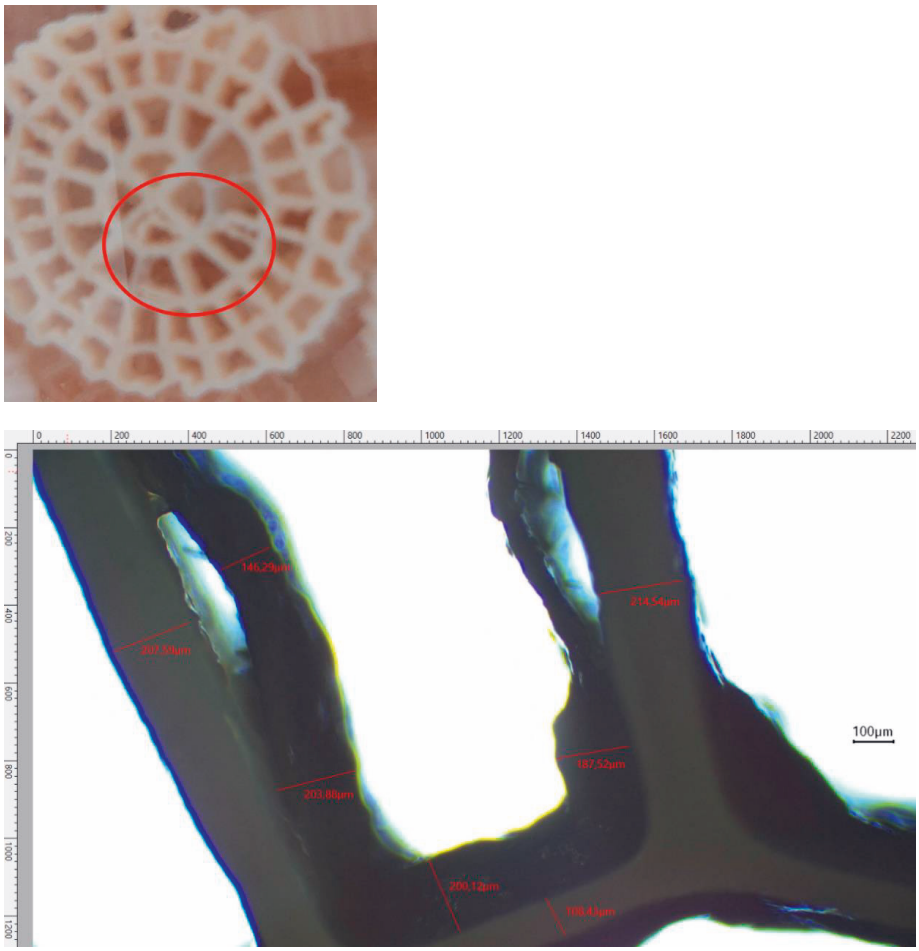

Figure S8. Particular of biofilm detachment from K5-MBBR carrier (optical microscope, 40x magnification) at salinity 7.5%. Approximately, one fourth of the total biofilm detached from the carrier by a visual estimation.

3. Modelling

Specific growth rate (μ_T) and biomass yield (Y) determination

Batch tests were run to determine specific growth rate at 30 °C (μ_T) and biomass yield (Y) of the denitrifying community in the MBBR and used in the SUMO22 model. For both K5-MBBR and M30-MBBR, the tests were run at the end of salinity 1% under non inhibitory conditions (no addition of Na_2SO_4 and KCl). The test was run on the suspended phase, and the set of parameters found extended to the attached biomass, considering that no significant differences between kinetic parameters have been found for suspended and attached biomass (Vannecke and Volcke, 2015). The protocol followed was as suggested by (Dold et al., 2008)

Before starting the MBBR NUR test, four 4.5 mL samples of the liquid phase were taken from the MBBR, and inoculated in four sealed glass bottles (working volume 90 mL, inoculum 5% v/v) containing a growth medium solution (250 mgNO_3^--N/L (as KNO_3), 4 gPO_4^{2-}/L (as K_2HPO_4 and KH_2PO_4), 0.1 gNH_4^+/L (as $(NH_4)_2SO_4$), and 0.002 g/L $FeSO_4 \cdot 7H_2O$, methanol (C/N=1.3 g/g), pH around 7) already purged with N_2. The bottles were incubated on a multi-HS-6 magnetic heating stirrer (Velp, Italy) at 30 °C. The tests were followed for 24-72 hours, until total consumption of NO_x-N. Liquid samples from the experiments were filtered through 0.2 µm Chromafil Xtra syringe filter (Macherey-Nagel, Germany) and NO_3^--N and NO_2^--N were measured with Hach cuvette tests (LCK339, LCK343) in Hach DR 3900 spectrophotometer. Organic carbon used as electron donor was measured as dissolved organic carbon (DOC) with TOC/TN analyser (FORMACS™ HT-I, Model 2CA17910, Skalar, Netherlands). Volatile suspended solids (VSS) were measured according to standard methods (APHA 2005).

Then, NO_3^--N and NO_2^--N data were converted to NO_x-N according to eq. S1, similarly to (Cherchi et al., 2009), where coefficient 0.6 takes into account the denitrification reaction stoichiometry in terms of oxygen equivalents for nitrite and nitrate. Biomass yield was calculated with eq. S2, which depends on the consumed COD/N ratio during the batch test, and which does not affect the estimation of μ_T (Dold et al., 2008). Eventually, the data were fitted in Origin 2024b with eq. S3 (Dold et al., 2008) to find μ_T, where X_0 (mgCOD/L) is the average concentration of biomass in the four bottles and b is the specific death rate (1/d) adjusted at 30 °C (b at 20 °C was taken 0.04 1/d (Dold et al., 2008))

$$NO_x\text{-N (mgN/L)} = NO_3^-\text{-N} + 0.6 \cdot NO_2^-\text{-N} \qquad \text{(eq. S1)}$$

$$Y \ \frac{\text{gCOD}}{\text{gCOD}} = 1 - \frac{2.86}{\Delta\text{COD}/\Delta\text{N}} \qquad \text{(eq. S2)}$$

$$NO_x\text{-N}_t \text{ (mgN/L)} = NO_x\text{-N}_0 + \frac{1-Y}{2.86} \cdot \frac{\mu_T \cdot X_0}{Y \cdot (\mu_T - b)} \cdot \left(e^{(\mu_T - b)\cdot t} - 1\right) \qquad \text{(eq. S3)}$$

The results of the fitting are reported in Figure S9. For both inocula, μ_T was in the range reported in literature (1.3-3.3 1/d in a T range of 20-25 °C (Christensson et al., 1994; Dold et al., 2008; Pan et al., 2023). The difference in the values can be ascribed to the different time of the tests, since the K5-MBBR and M30-MBBR batch tests were run approximatively 3 months apart. Biomass yield, on the other hand, was lower than the values reported in literature for methanol driven denitrification (0.27-0.4 gCOD/gCOD C (Dold et al., 2008; Pan et al., 2023). Eventually, the difference in the time necessary to consume the nitrogen (55 h for K5-MBBR and 30 h for M30-MBBR) was due to the difference in the initial biomass (X_0) in the two tests.

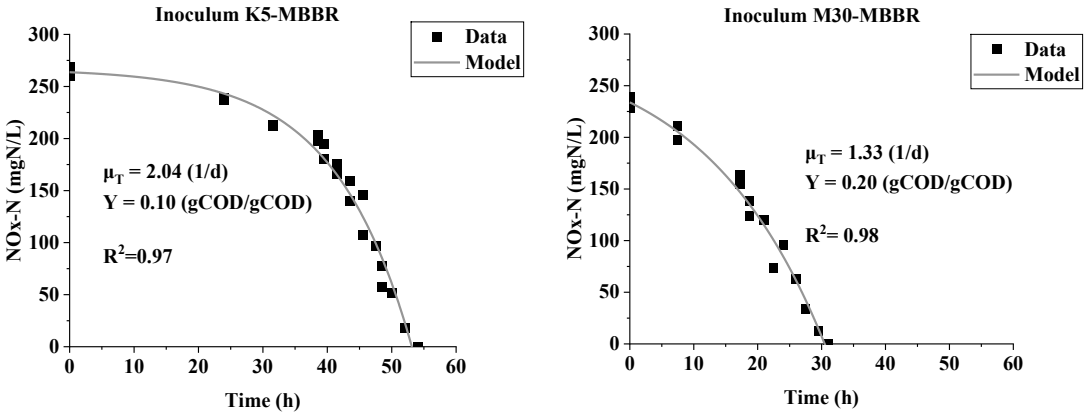

Figure S9. Specific growth rate (μ_T) at 30°C and biomass yield (Y) found for the inoculum taken from K5-MBBR and M30-MBBR. Eq S3 showed a good fitting of the measured data (R^2>0.95) of four replicates. Initial biomass (X_0) was 5.4 mgCOD/L and 40 mgCOD/L for K5-MBBR and M30-MBBR, respectively.

Modelling with SUMO

The main kinetic, stoichiometric and biofilm parameters used in the modelling with Sumo22 for K5-MBBR and M30-MBBR are listed in Table S2 and S3.

Biomass concentration (X) was calculated from volatile solids measurements before each test. Biofilm thickness (L) and specific surface area (SSA) were selected for each test by observing the visible surface occupied by biofilm and the amount of biomass measured on the carriers or calibrated.

Methylotrophic denitrification (MEOLO) was the only active bioprocess considered. In the nitrate and nitrite rate equations pH influence was neglected, since pH was in neutral range in the tests. Inhibition by oxygen was not considered, as DO was below 0.1 mg/L. Also, methanol, NH_4^+, PO_4^{3-}, Na^+, Cl^-, Ca^{2+}, Mg^{2+} (and related half-inhibition constants) were considered not limiting factors for the kinetics being their concentration in excess in the simulated wastewater. Software defaults were used for biofilm diffusion process parameters.

Solid transfer processes, such as detachment and attachment, between biofilm and bulk were not considered in the modelling of the kinetics in batch tests. Biomass decay process and endogenous products consumption were considered but had overall negligible effect.

When comparing the model and data (Figure S10), the model had good fitting with the data especially above 2.7% salinity, when the biofilm had the main role in denitrification. For the K5-MBBR, at 2.7% salinity, due to an interruption of the inflow and outflow in the reactor, the liquid phase remained around 36 h in the reactor before the NUR test. This resulted in a high accumulation of VSS, part of which was already inactive due to the absence of substrate. Therefore, the measured VSS was overestimating the active fraction of suspended biomass. In the model, this resulted in faster denitrification rate than observed in the reactor. However, when considering an active fraction of the total suspended biomass (around 45%), as found by Foladori et al. (2010) for activated sludge, the model could better reproduce the data.

Table S3. K5-MBBR main kinetic, stoichiometric and biofilm parameters used in Sumo22.

K5-MBBR									
Parameter	**Default value SUMO**	**Value in NUR test (Salinity)**					**Determination method**	**Note**	**Reference**
		1.0%	**2.5%**	**5.5%**	**7.5%**	**9.5%**			
Kinetic and stoichiometric									
Maximum specific growth rate of MEOLOs (μ_T) (1/d)	1.30			2.04			Experimental	Value at 30 °C	
Decay rate of MEOLOs (b_T) (1/d)	0.05			0.054			Calculation	Value at 30 °C	(Dold et al., 2008)
Half-saturation of NO_3^- for MEOLOs (AS) (K_{NO3}) (mgN/L)	0.05			0.05			/		
Half-saturation of NO_2^- for MEOLOs (AS) (K_{NO2}) (mgN/L)	0.02	4	4	4	4	250	Calibration	Literature reference value for NO_2^- reduction with methanol: 9.2 mgN/L	(Badia et al., 2021)
Half-inhibition of salinity for MEOLOs (K_I) (gSalt/L)	/			74.4			Experimental		
Tuning parameter of modified Hill's function (n) (/)	/			2.06			Experimental		
Yield of MEOLOs on methanol (Y) (mgCOD/mgCOD)	0.4			0.1			Experimental		
Rate of endogenous decay products conversion (q_{XE}) (1/d)	0.007			0.007			/		
Diffusion factor for half-saturation coefficients ($f_{KS,biofilm}$) (/)	0.4			0.4			/	Multiplies half-saturation coefficients for the biofilm reactions	
Biofilm									
Biofilm thickness (L) (µm)	300	200	200	350	250	275	Calibration/ estimation	Indicative value observed with optical microscopy and then calibrated (increase/decrease) based on the biomass (gAVS) trend. Literature: 280-600 µm	(Arabgol et al., 2022; Li et al., 2016)
Boundary layer thickness (z_{BL}) (µm)	30			30			/	Tested also at 0.3 and 100 µm with no observable difference in the output (results not shown)	
Specific surface of biofilm carrier (SSA) (m^2/m^3)	500	800	800	800	600	600	Calibration/ estimation	Detachment of biofilm due to salinity simulated by decreasing SSA	
n. of biofilm layers (/)	3			3			/		
Mass of attached volatile solids (gAVS)	/	2.4	2.7	9.8	7.35	8.7	Measurement	Used to calculate initial volumetric concentration of anoxic methanol utilizers (X) (mgCOD/L)	

Table S4. M30-MBBR main kinetic, stoichiometric and biofilm parameters used in Sumo22.

		M30-MBBR							
Parameter	**Default value SUMO**	**Value in NUR test (Salinity)**					**Determination method**	**Note**	**Reference**
		1.0%	**2.5%**	**5.5%**	**7.5%**	**9.5%**			
Kinetic and stoichiometric									
Maximum specific growth rate of MEOLOs (μ_T) (1/d)	1.30			1.33			Experimental	Value at 30 °C	
Decay rate of MEOLOs (b_T) (1/d)	0.05			0.054			Calculation	Value at 30 °C	(Dold et al., 2008)
Half-saturation of NO_3^- for MEOLOs (AS) (K_{NO3}) (mgN/L)	0.05			0.05			/		
Half-saturation of NO_2^- for MEOLOs (AS) (K_{NO2}) (mgN/L)	0.02	70	4	20	25	550	Calibration	Literature reference value for NO_2^- reduction with methanol: 9.2 mgN/L	(Badia et al., 2021)
Half-inhibition of salinity for MEOLOs (K_I) (gSalt/L)	/			55.6			Experimental		
Tuning parameter of modified Hill's function (n) (/)	/			1.30			Experimental		
Yield of MEOLOs on methanol (Y) (mgCOD/mgCOD)	0.4			0.2			Experimental		
Rate of endogenous decay products conversion (q_{XE}) (1/d)	0.007			0.007			/		
Diffusion factor for half-saturation coefficients ($f_{KS,biofilm}$) (/)	0.4			0.4			/	Multiplies half-saturation coefficients for the biofilm reactions	
Biofilm									
Biofilm thickness (L) (µm)	300	100	150	200	175	200	Calibration	Calibrated (increase/decrease) based on the biomass (gAVS) trend.	
Boundary layer thickness (z_{BL}) (µm)	30			30			/	Tested also at 0.3 and 300 µm with no observable difference in the output (results not shown)	
Specific surface of biofilm carrier (SSA) (m^2/m^3)	500	5500	5500	5500	5500	5500	Assumption	Constant because detachment was not visually seen	
n. of biofilm layers (/)	3			3			/		
Mass of attached volatile solids (gAVS)	/	1.4	3.7	9.5	7.0	8.4	Measurement	Used to calculate initial volumetric concentration of anoxic methanol utilizers (X) (mgCOD/L)	

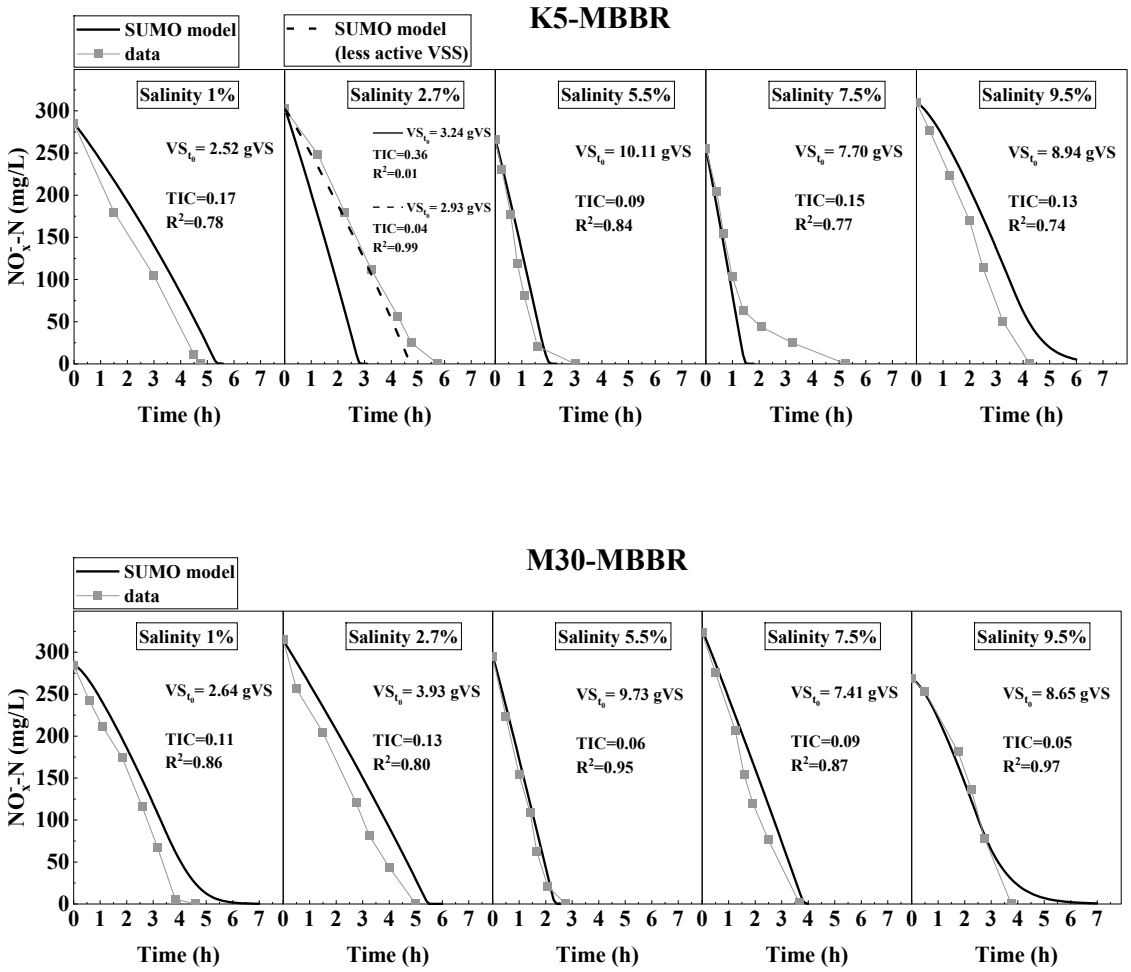

Figure S10. Fitting of the Sumo22 biofilm model modified with the inhibition factor of the NO_x^--N experimental data for each original NUR test for K5-MBBR and M30-MBBR. K5-MBBR NUR test modelling at salinity 2.7% includes also the result considering only 45% of the initial biomass is active. Denitrification rate was calculated with linear regression for each pair (model, data) of curve under the same salinity condition.

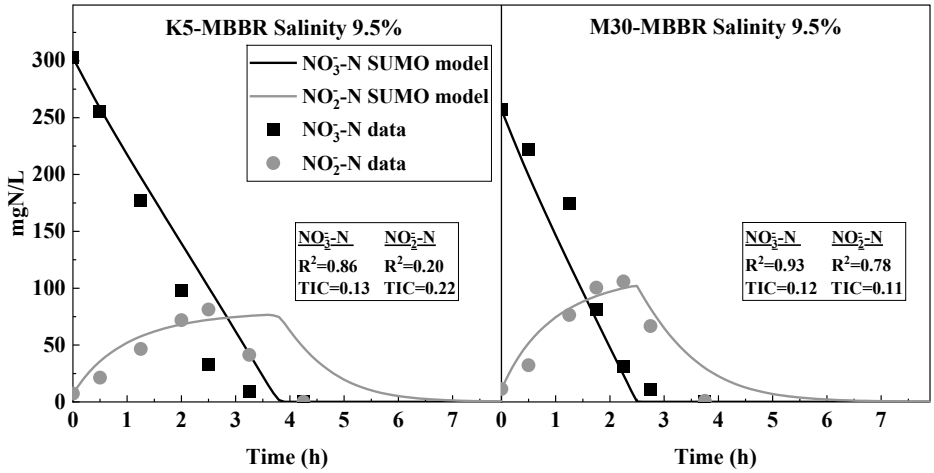

Figure S11. Comparison of the NO_3^--N and NO_2^--N time profiles from the Sumo22 biofilm model modified with the inhibition factor and from the experimental data for K5-MBBR and M30-MBBR at salinity of 9.5%.

Sensitivity Analysis

Sensitivity analysis was conducted for both K5-MBBR and M30-MBBR NUR tests at 2.7% and 9.5% salinity. The parameters tested were biofilm thickness (L), specific surface area (SSA), specific growth rate (μ_T), biomass yield (Y), and salinity inhibition parameters (K_I and n) and were varied by ±50% of their initially estimated values, at steps of 10%. SSA was subjected to negative variations only (up to -70%), if the maximum SSA of the carrier (Table S1) was assumed to be covered by biofilm. To evaluate the model sensitivity of each j-th parameter, the normalized sensitivity coefficient ($S_{i,j}$) was calculated as in (Eldyasti et al., 2012) for each variation step (Eq S4):

$$S_{i,j} = \frac{(y_i - y_0)/y_0}{(x_i - x_0)/x_0} \quad \text{(eq. S4)}$$

where y_i and x_i are the model output (denitrification rate) at the new input variable value and the new input variable, respectively; while y_0 and x_0 are the reference values (calibrated or estimated) of the output and input variables, respectively. To have a unique overall normalized sensitivity coefficient S value for each parameter for comparison purposes, an average of $S_{i,j}$ in the whole variation range was considered. If $S \leq 0.25$, the parameter was considered not significantly influential, else it was considered influential. Also, the most influential parameters were ranked according to their S value.

K5-MBBR

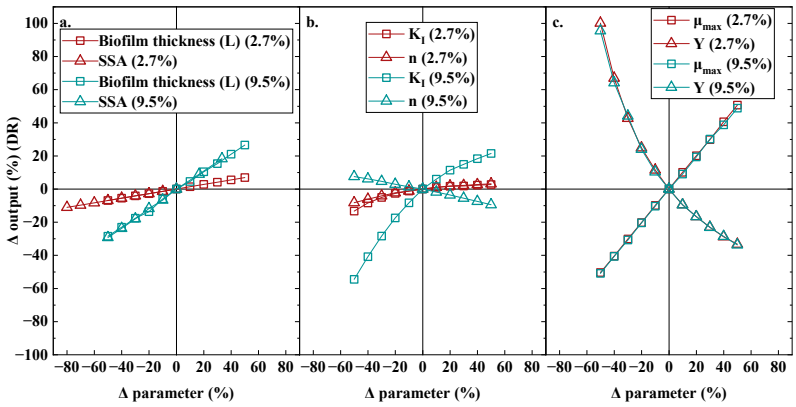

NUR test	S					
Salinity (%)	L	SSA	K_I	n	μ_{max}	Y
2.7	0.14	0.14	0.14	0.11	1.01	1.22
9.5	0.56	0.59	0.77	0.17	1	1.19

M30-MBBR

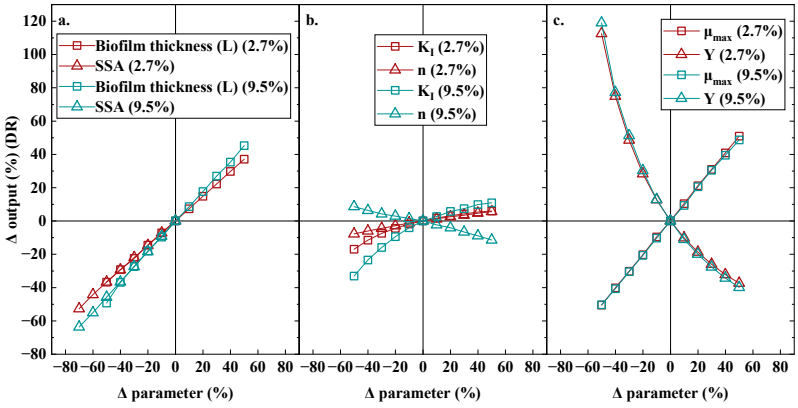

NUR test	S					
Salinity (%)	L	SSA	K_I	n	μ_{max}	Y
2.7	0.73	0.73	0.21	0.13	1.02	1.37
9.5	0.91	0.92	0.42	0.19	1	1.44

Figure S12. Sensitivity analysis for the NUR tests at 2.7% and 9.5% salinities for K5-MBBR and M30-MBBR. In both plots, two parameters are grouped for each salinity level (a. biofilm thickness (L) and specific surface area (SSA), b. salinity parameters, c. specific maximum growth (μ_{max}= μ_T in this study) and biomass yield (Y)) and varied to observe the output percentage variation (denitrification rate (DR) in this study).

4. NO_x-SO_2 scrubber wastewater composition

Table S5. Characterization of the pulp mill NO_x-SO_2 scrubber wastewater collected from the three stages. The wastewaters were analysed by an external laboratory. * adjusted to 7 with KOH for the experiment to exclude pH effect on the process.

mg/L	**Stage I**	**Stage II**	**Stage III**	mg/L	**Stage I**	**Stage II**	**Stage III**
Conductivity at 25°C (µS/cm)	20500	62200	1920	**Ca**	17	18	36
pH (-)	4.6*	6.5	4.8*	**Mg**	7.9	11	3.5
Cl^-	1110	1930	44	**Na**	4850	27000	314
NH_4^+	233	22	41	**K**	194	381	63
NO_3^-	88	230	33	**Al**	1.6	0.45	0.05
NO_2^-	<10	190	<10	**As**	0.03	0.04	<0.01
SO_3^{2-}	43	15	<0.05	**B**	3.9	4.4	0.25
SO_4^{2-}	7300	50000	764	**Co**	<0.01	<0.01	<0.01
$S_2O_3^{2-}$	1790	370	ND	**Cr (VI)**	<0.05	<0.05	<0.05
P_{tot}	1.7	1.9	0.5	**Cr_{tot}**	0.05	0.01	<0.01
DOC	947	2140	45	**Fe**	12	0.58	0.06
				Mn	0.02	0.01	<0.01
				Mo	0.08	0.09	0.01
				Ni	0.02	0.04	<0.01
				Pb	0.02	<0.01	<0.01
				Cu	0.18	0.42	0.02
				Se	0.03	0.06	<0.02
				V	0.06	0.13	0.02
				Zn	0.15	0.02	0.03

5. References

Arabgol, R., Vanrolleghem, P.A., Delatolla, R., 2022. Influence of MBBR carrier geometrical properties and biofilm thickness restraint on biofilm properties, effluent particle size distribution, settling velocity distribution, and settling behaviour. Journal of Environmental Sciences 122, 138–149. https://doi.org/10.1016/j.jes.2021.09.029

Badia, A., Kim, M., Dagnew, M., 2021. Nitrite denitrification using biomass acclimatized with methanol as complementary carbon source: long-term performance and kinetics study. Environ. Sci.: Water Res. Technol. 7, 93–106. https://doi.org/10.1039/D0EW00604A

Cherchi, C., Onnis-Hayden, A., El-Shawabkeh, I., Gu, A.Z., 2009. Implication of Using Different Carbon Sources for Denitrification in Wastewater Treatments. Water Environment Research 81, 788–799. https://doi.org/10.2175/106143009x12465435982610

Christensson, M., Lie, E., Welander, T., 1994. A comparison between ethanol and methanol as carbon sources for denitrification. Water Science and Technology 30, 83–90. https://doi.org/10.2166/wst.1994.0255

D'Aquino, A., Maanoja, S.T., Auvinen, H., Tiirola, M., Andreottola, G., Puhakka, J.A., Palmroth, M.R.T., 2024. Methanol and thiosulphate from pulp mill waste streams support denitrification under salinity stress. Chemical Engineering Journal 502, 158131. https://doi.org/10.1016/j.cej.2024.158131

Dold, P., Takács, I., Mokhayeri, Y., Nichols, A., Hinojosa, J., Riffat, R., Bott, C., Bailey, W., Murthy, S., 2008. Denitrification with Carbon Addition—Kinetic Considerations. Water Environment Research 80, 417–427. https://doi.org/10.2175/106143007X221085

Dupla, M., Comeau, Y., Parent, S., Villemur, R., Jolicoeur, M., 2006. Design optimization of a self-cleaning moving-bed bioreactor for seawater denitrification. Water Research 40, 249–258. https://doi.org/10.1016/j.watres.2005.10.029

Eldyasti, A., Nakhla, G., Zhu, J., 2012. Development of a calibration protocol and identification of the most sensitive parameters for the particulate biofilm models used in biological wastewater treatment. Bioresource Technology 111, 111–121. https://doi.org/10.1016/j.biortech.2012.02.021

Feng, L., Wu, G., Zhang, Z., Tian, Z., Li, B., Cheng, J., Yang, G., 2023. Improving denitrification performance of biofilm technology with salt-tolerant denitrifying bacteria agent for treating high-strength nitrate and sulfate wastewater from lab-scale to pilot-scale. Bioresource Technology 387, 129696. https://doi.org/10.1016/j.biortech.2023.129696

Foladori, P., Bruni, L., Tamburini, S., Ziglio, G., 2010. Direct quantification of bacterial biomass in influent, effluent and activated sludge of wastewater treatment plants by using flow cytometry. Water Research 44, 3807–3818. https://doi.org/10.1016/j.watres.2010.04.027

Fonseca, D.L., Bassin, J.P., 2019. Investigating the most appropriate methods for attached solids determination in moving-bed biofilm reactors. Bioprocess Biosyst Eng 42, 1867–1878. https://doi.org/10.1007/s00449-019-02182-x

Labelle, M.-A., Juteau, P., Jolicoeur, M., Villemur, R., Parent, S., Comeau, Y., 2005. Seawater denitrification in a closed mesocosm by a submerged moving bed biofilm reactor. Water Research 39, 3409–3417. https://doi.org/10.1016/j.watres.2005.06.001

Li, C., Felz, S., Wagner, M., Lackner, S., Horn, H., 2016. Investigating biofilm structure developing on carriers from lab-scale moving bed biofilm reactors based on light microscopy and optical coherence tomography. Bioresource Technology 200, 128–136. https://doi.org/10.1016/j.biortech.2015.10.013

Osaka, T., Shirotani, K., Yoshie, S., Tsuneda, S., 2008. Effects of carbon source on denitrification efficiency and microbial community structure in a saline wastewater treatment process. Water Research 42, 3709–3718. https://doi.org/10.1016/j.watres.2008.06.007

Pan, Y., Sun, R.-Z., Wang, Y., Chen, G.-L., Fu, Y.-Y., Yu, H.-Q., 2023. Carbon source shaped microbial ecology, metabolism and performance in denitrification systems. Water Research 243, 120330. https://doi.org/10.1016/j.watres.2023.120330

Vannecke, T.P.W., Volcke, E.I.P., 2015. Modelling microbial competition in nitrifying biofilm reactors. Biotechnology and Bioengineering 112, 2550–2561. https://doi.org/10.1002/bit.25680

Yang, P.Y., Nitisoravut, S., Wu, J.S., 1995. Nitrate removal using a mixed-culture entrapped microbial cell immobilization process under high salt conditions. Water Research 29, 1525–1532. https://doi.org/10.1016/0043-1354(94)00296-J

Zhai, S., Ji, M., Zhao, Y., Su, X., 2020. Shift of bacterial community and denitrification functional genes in biofilm electrode reactor in response to high salinity. Environmental Research 184, 109007. https://doi.org/10.1016/j.envres.2019.109007